Université Sorbonne Paris Cité

THÈSE DE DOCTORAT DE L'UNIVERSITÉ SORBONNE PARIS CITÉ

École doctorale Bio Sorbonne Paris Cité
Discipline – Immunologie

Présentée par
Francesco ANDREATA

Pour obtenir le titre de
Docteur de l'Université Paris Diderot (Paris VII)

Role of CD31 in neutrophil recruitment and activation during the acute phase of inflammation

Thèse dirigée par Giuseppina CALIGIURI

Soutenue le 21 Septembre 2017 devant le jury composé de :

Pr. Mireille Viguier	Président
Pr. Sabine Steffens	Rapporteur
Pr. Federica Marelli-Berg	Rapporteur
Pr. Matteo Iannacone	Rapporteur
Dr. Véronique Witko-Sarsat	Examinateur
Dr. Margarita Hurtado-Nedelec	Invitée
Dr. Giuseppina Caligiuri	Directeur de thèse

Mes Travaux de thèse ont été menés au sein du laboratoire :

INSERM 1148, Laboratory for Vascular Translational Sciences

Hôpital Universitaire Bichat-Claude Bernard

46 rue Henri Huchard

75016, Paris, France

Titre :
RÔLE DU CD31 DANS LE RECRUTEMENT ET L'ACTIVATION DES NEUTROPHILES PENDANT LA PHASE AIGUË DE L'INFLAMMATION

Résumé :
Les neutrophiles jouent un rôle central dans la première ligne de défense mise en place contre les agents pathogènes. L'une de leur fonction essentielle est caractérisée par la capacité à rejoindre rapidement la circulation sanguine et de migrer vers les sites inflammatoires, où ils seront activés et exerceront des fonctions effectrices extrêmement puissantes. Ces processus doivent être finement contrôlés afin de moduler leur effet dévastateur dans l'organisme. L'hypothèse de travail de ce travail de thèse est que le CD31, un corécepteur ITIM (Immunoreceptor Tyrosine-based Inhibitory Motif), exprimé de manière constitutive à la surface des neutrophiles, joue un rôle essentiel dans la régulation du recrutement et l'activation des neutrophiles au sein des sites inflammatoires.
Nous avons pu mettre en évidence que le CD31 membranaire était clivé lors de l'activation neutrophilaire, et pouvait perdre une grande partie de son domaine extracellulaire, tout en conservant sa portion membranaire. Afin d'étudier le rôle du gain de fonction du CD31 neutrophilaire, nous avons utilisé un peptide synthétique homotypique ayant la capacité de se lier spécifiquement au domaine persistant du CD31 clivé, et permettant le maintien de sa fonction moléculaire. Parallèlement, des souris invalidées pour CD31 ont été utilisées dans divers modèles expérimentaux d'inflammation aiguë afin d'étudier le rôle de sa suppression.
Dans leur ensemble, nos données suggèrent que le CD31 joue un rôle complexe et important dans la régulation du recrutement des neutrophiles au sein des sites d'inflammation aiguë. Nous avons pu montrer que des lymphocytes isolés à partir de souris invalidées pour CD31 adhèrent plus fortement aux cellules endothéliales activées, bien que leur progression hors du vaisseau est retardée. A l'inverse, l'ajout du peptide agoniste CD31 diminue leur adhérence, tout en favorisant leur détachement.
La littérature rapporte que des neutrophiles isolés à partir de souris déficientes en CD31 sont incapables de migrer hors des vaisseaux, ce qui suggère un rôle important du CD31 dans les processus de transmigration. Cependant, les mécanismes sous-jacents restent inconnus. Nous avons pu montrer qu'au sein du front de migration neutrophilaire, le CD31 empêche l'ouverture des intégrines associées en clusters, par le biais du recrutement de phosphatase. Ce processus abouti à un diminution de l'adhérence neutrophilaires à l'endothélium. A l'inverse, la polarisation du CD31 à l'uropode semble être nécessaire à leur détachement. Cette dernière étape implique la fermeture des intégrines et semble être favorisée par la signalisation CD31.
Dans la deuxième partie de ce travail de thèse, nos résultats suggèrent que le CD31 régule également l'activation des neutrophiles au sein des sites inflammatoires. Nous avons tenté de comprendre le rôle du CD31 dans le burst oxydatif et la dégranulation des neutrophiles. SHIP1, une phosphatase impliquée dans la signalisation de CD31, découple l'activation neutrophilaire induite par le récepteur Fc. En utilisant le modèle auto-immun de glomérulonéphrite, nous avons pu montrer que la signalisation du CD31 module les effets délétères causés par les protéases neutrophilaires. Dans ce modèle l'ajout du peptide agoniste CD31 prévient les lésions induites, alors que les souris déficientes en CD31 possèdent des neutrophiles plus activés et des lésions glomérulaires plus importantes.
En conclusion, les résultats des expériences effectuées lors de ce travail de thèse suggèrent (1) que CD31 peut moduler le trafic neutrophilaire en contrôlant les intégrines et (2) que CD31 établit un seuil immunologique impliqué dans l'activation des neutrophiles, limitant leur activation excessive pendant la phase aiguë de l'inflammation.

Mots clefs :
Neutrophiles, Inflammation, CD31, Integrines, Adhésion leucocytaire, Récepteurs ITIM

1 ABSTRACT

Neutrophils play a crucial role in the first line of defense against noxious agents. Central to their function, is their ability to rapidly exit the circulation and migrate to the site of inflammation where they get activated and exert extremely efficient effector functions. A tight regulation of these processes is mandatory to restrict their devastating effects in the organism. The working hypothesis of my thesis was that CD31, an ITIM (Immunoreceptor Tyrosine-based Inhibitory Motif) co-receptor constitutively expressed at the surface of neutrophils, plays a critical role in the regulation of neutrophils functions.

We found that, upon cell activation, the surface CD31 molecules underwent a shedding of a large part of the extracellular portion, leaving a small truncated portion that lingers at the cellular surface. A synthetic homotypic peptide that has the ability to specifically bind and maintain functional CD31 molecular clusters, was used to study the role of CD31 in neutrophils biology by “gain-of-function”. Genetically invalidated mice were used in parallel as a CD31 “loss-of-function” approach both in vitro and in vivo, in experimental mouse models of acute inflammation.

Altogether our data unveil a complex and important role for CD31 in the regulation of the recruitment of the neutrophils at sites of acute inflammation. We show that $CD31^{-/-}$ neutrophils established stronger adhesion on activated endothelial cells but their progression out of the vessel was delayed. At the opposite, the use of the CD31 agonist peptide prevented the attachment while it favored the detachment of the migrating neutrophils.

It was previously observed that $CD31^{-/-}$ neutrophils are unable to migrate out of the vessels and it had been proposed that CD31 is necessary for the transmigration but the underlying mechanism had remained unknown. We show that the phosphatases recruited and activated by CD31, by co-clustering with the integrins at the migration front, prevented their opening and hence inhibited the adhesion of neutrophils on the endothelium. At the opposite, CD31 polarization at the uropod appeared to be crucial for the detachment of the neutrophils. We found that this step, that relies upon the closure of the integrins, was favored by the CD31 signaling.

Furthermore, our findings showed that CD31 not only regulates the recruitment but also the activation of neutrophils at sites of inflammation. Indeed, in the final part of my thesis, I studied the regulatory effect of the engagement of CD31 on the oxidative burst and the degranulation of neutrophils. The identified phosphatase involved in this function of CD31 was SHIP1 (inositol phosphatase) which uncouples the Fc-receptor dependent neutrophil activation. By using an autoimmune glomerulonephritis model, which develops antibody-dependent acute inflammation, we showed that CD31 signaling is crucial for limiting the collateral damage caused by neutrophil-derived proteases: the CD31 agonist peptide prevented the damage whereas the induction of the disease in $CD31^{-/-}$ mice resulted in greater neutrophil activation and glomerular damage.

The results of the experiments performed during my thesis work suggest that, during the acute phase of inflammation, CD31 regulates the integrin-dependent steps involved in neutrophil trafficking and raises the immunologic threshold for neutrophil activation. In conclusion, CD31 exerts an important and unforeseen regulatory function that is critical in order to limit the deleterious side effects of neutrophil activation during the acute phase of inflammation.

Keywords :
Neutrophils, Inflammation, CD31, Integrins, Leukocyte adhesion, ITIM receptors

2 ACKNOWLEDGMENTS

I would like to express my gratitude and sincere thanks to all the committee members that gave me the honor to evaluate my thesis works. I'm sure that the defense will be a memorable moment and your presence will provide a priceless contribution to my training.

A first thanks to Pr. *Mireille Viguier*, for having accepted to be the president of the jury.

A special thanks to the rapporteurs, Pr. *Federica Marelli-Berg,* Pr. *Sabine Steffens* and Pr. *Matteo Iannacone*, for the time spent in reading my manuscript, your interest, the brilliant suggestions and comments in this warm summer.

I am grateful to Dr. *Véronique Witko-Sarsat* for having accepted to be the examiner of the jury and to Dr. *Margarita Hurtado-Nedelec* as a special guest. Your attendance in the jury and the discussion with you are precious for my work.

È difficile esprimere a parole quanto sia grato e riconoscente a *Pina*, la mia direttrice di tesi. In questi anni non solo ti sei presa cura di me e della mia educazione, ma hai saputo credere in me e valorizzarmi sempre, nonostante cominci ad intuire solo ora quanto sia difficile tutto ciò (specialmente con uno studente come il sottoscritto…). Se sono cresciuto durante questo dottorato è merito tuo, del tuo contagioso entusiasmo, della tua infinita energia – ma da dove la prendi?! – e delle responsabilità che hai voluto affidarmi con una fiducia che non pensavo di meritare. Sappi che la mia più grande soddisfazione è renderti fiera, spero di esserci riuscito.

Toni, je suis sûr que je ne trouverai jamais plus un maître comme toi. Cela a été un honneur et un privilège indescriptible d'avoir pu travailler, apprendre et grandir dans ton équipe. Tu as fait un pari sur moi dès le premier instant, tu m'as poussé à aller là où je n'aurais jamais osé et tu m'as toujours et infatigablement soutenu dans cela. L'attention, la gratuité et la paternité que tu m'as démontrées dans toutes ces années est tout simplement émouvante. Je n'oublierai absolument jamais ce que tu as fait pour moi et j'espère un jour pouvoir revenir travailler avec toi.

Je voudrais remercier tout particulièrement les directeurs de l'unité de recherche qui se sont succédé dans ces années. Merci au docteur *Jean-Baptiste Michel* qui m'a accueilli dans ce qui à l'époque s'appelait l'INSERM U698, et merci au docteur *Didier Letourneur*, actuel directeur de l'unité INSERM U1148.

Merci au docteur *Olivier Thaunat* et au docteur *Chien-Chia Chen* qui m'ont permis de collaborer à leur travail extraordinaire, à partir duquel j'ai appris tant de choses.

Un immense merci à *Alexy*. Pharmacien, médecin, anesthésiste et scientifique (mais combien de titres as-tu ?!), souvent nous étions au laboratoire à récolter des échantillons de patients même jusqu'à dix heures du soir ! Ton enthousiasme et ta disponibilité ont été véritablement précieux dans ces années.

Merci à *Marc Clément*, quand je suis arrivé à Paris il y a 5 ans, tu as été mon premier tuteur. Ta passion pour la recherche, à part m'enseigner un grand nombre de choses, a eu un poids fondamental dans la décision d'entreprendre ce doctorat. Je t'en serai pour toujours reconnaissant.

I would like to thank Dr. *Pasquale Maffia* and Dr. *Robert Benson* from the institute of infection of the Glasgow University. Your outstanding expertise and knowledge in intravital microscopy has given the most amazing results that I ever had. I sincerely wish to work with you in the near future!

Merci à *Benoît Ho-Tin-Noé*, expert mondial de plaquettes et de neutrophiles. Les discussions scientifiques et tes conseils précieux ont donné un tournant fondamental à mon travail. Merci pour tout.

Je ne remercierai jamais assez *Corinne* et *Asma*. Vous êtes les vrais fondements de cette unité de recherche, sans vous tout notre travail serait tout simplement impossible.

Merci *Alexia* ! Au cours de ces années, tu as été une grande amie et collègue, nous avons pu nous confronter sur tant de thèmes et l'amitié avec toi m'a enrichi comme peut-être aucune autre. Bon courage pour ta dernière année de thèse !

Comment ne pas remercier mon *Guigui* ! Numéro 1 indiscutable de l'expérimentation animale, sans toi une grande partie de mes expériences n'aurait pas eu lieu. Tu m'as appris beaucoup de choses et ta présence (et surtout tes playlists !) me rendaient toujours heureux.

Merci à *Greg*, scientifique d'excellence et futur papa ! Même si nous nous sommes connus seulement cette année, j'ai pu apprécier ton amitié et tes conseils. Tu es exactement le scientifique que j'aspire à devenir un jour. Bonne chance mec !

Je voudrais remercier de tout cœur *Marie*, avec qui j'ai partagé cette année l'aventure et la responsabilité de l'enseignement en université. Merci du temps que tu m'as consacré pour m'aider à préparer les cours, je suis sûr que bientôt tu deviendras une des meilleurs profs à P7 !

Un remerciement spécial à *Kévin(ou)*, ta sympathie (et surtout ta folie !) ont rendu les congrès de Biarritz et de Boston – et beaucoup d'autres moments – véritablement inoubliables.

Un merci de cœur à *Charlotte*, collègue du CD31 et bientôt docteure de recherche. Grâce à toi, j'ai tant appris (et pas seulement en sciences), malgré les difficultés tu as su tenir dur à tête haute. Tu as été une des personnes que j'ai admiré le plus pour ta ténacité et ta connaissance, aussi à toi je te souhaite bon courage.

Un merci infini à *Varouna*, la meilleure chirurgienne expérimentale que je connaisse et elle aussi collègue du CD31. Tu m'as enseigné beaucoup de techniques *in vivo* et les discussions que nous avons eues ont été un soulagement dans les moments difficiles. Bonne chance pour ta prochaine aventure à Servier !

Grazie *Lele*, amico fidato e instancabile lavoratore, sempre disponibile quando avevo bisogno di una mano. Buona fortuna con il tuo nuovo lavoro. Sono sicuro che eccellerai.

Un remerciement spécial à *Julie*, ma préférée ! Merci pour ton aide indispensable dans les manips de microscopie en flux, ton enthousiasme et ta sympathie ont réussi à me contaminer, même dans les journées les plus difficiles !

Merci à *Aurélie*, la meilleure des anapath. Tu m'as appris l'histologie du rein, grâce à toi j'ai pu m'aventurer dans le projet sur la glomérulonéphrite. Bonne chance pour la soutenance de thèse que tu passeras bientôt !

Sandrine, la reine du porphyromonas gingivalis ! Je n'oublierai jamais ta sympathie et ta disponibilité. Ça a été un grand plaisir de te connaître.

Un grand merci aux « étudiants » qui m'ont été confiés dans ces années, *Etienne* et ensuite *Alice*. J'espère avoir été un bon tuteur. C'est le rapport avec vous qui a suscité mon désir de vouloir enseigner. Je vous souhaite bonne chance et je suis fier que vous ayez réussi à obtenir avec mérite ce que vous ambitionniez.

Un remerciement immense à *Marie-Anne*, les conseils qui avons échangé pendant ces années, le partage de connaissances (et les réactifs !) ils m'ont sauvé la vie bien plus qu'une seule fois. Bonne chance pour ton avenir.

Merci à *Kamel*, qui, outre ayant été un vrai ami, m'a enseigné à faire des western blots et surtout à ne pas s'énerver dans le cas (très fréquent) où ils ne fonctionnaient pas !

Merci à *Anh*, ton soin pour la gestion de l'animalerie a rendu possible la mise en œuvre de la majorité des manips.

Merci *Jamila* ! Tu m'as appris beaucoup de choses sur la culture cellulaire et de ça je t'en suis très reconnaissant.

Un merci à *Marion*, véritable experte des immunomarquages. Sans tes conseils, les images n'auraient jamais été aussi belles.

Merci à *Samira Benadda*, responsable de la plateforme d'imagerie à la fac. Ta contribution et ta disponibilité ont été fondamentales.

Merci à *Véronique Ollivier*, qui a eu de la patience avec moi dès que je suis arrivé au labo et qui m'a appris à faire les manips en flux !

Merci à *Jonathan*, radiopharmacien avec qui nous nous sommes aventurés dans des études pionnières sur le p8RI. Je te souhaite bonne chance pour ta fin de thèse.

Un grazie ai miei "coloc" dell'appa alti livelli! *Deca*, *Andrea* e *Jack*. Vivere con voi in questi anni e condividere questa esperienza è stato un privilegio assoluto. Non dimenticherò mai i birrini e le cene gluten-free, il riscaldamento rotto in gennaio e le degustazioni di champagne! Voi mi avete insegnato che siamo chiamati a fare grandi cose nella vita e mi siete stati compagni in questo. Sempre signori.

Un remerciement spécial à *Devy*, le meilleur producteur de rhum arrangé qui existe ! C'est toi qui m'as appris à analyser les données de l'Orbitrap (comment aurais-je fait sans toi ?!), je suis sûr que tu auras une brillante carrière (et méritée).

Toutes ces années de recherche m'ont permis de rencontrer des gens formidables, passionnés, curieux et désireux de partager leurs connaissances. J'aimerais les remercier pour tout le temps qu'ils ont pu m'accorder : *Jean-Pierre Couty, Jean Sénémaud, Sayah Neila, Abitbol Yael, Martine Jandrot-Perrus, Stéphane Loyau, Marie-Paule Jacob, Mathilde Varret, Karen Aymonnier, Yacinne Boulaftali, Karim Sacré, Adrian Brun, Catherine Deschildre, Ariane Truffier, Christine Choqueux, Jean-Philippe Desilles, Petra El Khoury, Radouane Ghebouli, Reda Hmazzou, Angele Gros, Liliane Louedec, Xavier Norel, Sanae Mkaddem, Thibaut Léger, Camille Garcia, Marien Lenoir, Lamia Lamrani* et malheureusement je sais que j'en oublie d'autres…

Grazie a tutti i gli amici con i quali ho condiviso un pezzetto di strada. Troppi per essere menzionati tutti, ma di cui custodisco nel cuore volti e momenti indimenticabili. Dal *Master de Génétique*, a quelli che sono rimasti in Italia e coloro che ho incontrato qui a Parigi. La vostra amicizia è stata una compagnia grande.

Infine il ringraziamento più sentito va ai miei genitori che, con semplicità, mi hanno insegnato per che cosa vale la pena vivere.

3 TABLE OF CONTENTS

4 List of Figures

5 ABBREVIATIONS

ACR: Albumin to Creatinine Ratio

ADCC: Antibody-Dependent Cell-mediated Cytotoxicity

Btk: Bruton's Tyrosine Kinase

CBA: Cytometric Bead Array

CD: Cluster Differentiation antigen

CG: Cathepsin G

CXCL1: C-X-C motif Ligand 1

CR: Complement Receptor

EC: Endothelial Cell

ECM: Extracellular Membrane

Fc: Fragment Crystallizable

FcRγ: Fragment Crystallizable Receptor gamma

fMLP: formyl Methionine-Leucyl-Phenylalanine

GBM: Glomerular Basement Membrane

G-CSF: Granulocyte-Colony Stimulating Factor

GFP: Green Fluorescent Protein

GPCR: G Protein-Coupled Receptor

GPI: Glycosylphosphatidylinositol

GN: Glomerulonephritis

KO: Knock Out

IC: Immune Complex

Ig:	Immunoglobulin
IHC:	Immunohistochemistry
IL:	Interleukin
ITAM:	Immunoreceptor Tyrosine-based Activation Motif
ITIM:	Immunoreceptor Tyrosine-based Inhibition Motif
LAD:	Leukocyte Adhesion Deficiency
LFA1:	Lymphocyte Function-associated Antigen 1
Ly6G:	Lymphocyte antigen 6 complex locus G
Mac1:	Macrophage-1 antigen
MMP:	Matrix Metalloprotease
MP-IVM:	Multi Photon Intravital Microscopy
MPO:	Myeloperoxidase
MS:	Mass Spectroscopy
NADPHOx:	Nicotinamide Adenine Dinucleotide Phosphate Hydrogen Oxidase
NaSG:	Sodium Stibogluconate
NE:	Neutrophil Elastase
NET:	Neutrophil Extracellular Trap
NIS:	Non-Immune Serum
PBMC:	Peripheral Blood Mononuclear Cells
PECAM-1:	Platelet-Endothelial-Cell Adhesion Molecule 1
PMN:	Polymorphonuclear Cell
PR3:	Proteinase 3
PSGL-1:	P-Selectin Glycoprotein Ligand-1

PTK: Protein Tyrosine Kinase

PTP: Protein Tyrosine Phosphatase

RGD: Arginine-Glycine-Aspartic

ROS: Reactive Oxygen Species

SDS-PAGE: Sodium Dodecyl Sulphate - Poly Acrylamide Gel Electrophoresis

SFK: Src Family Kinases

SH2: Src Homology 2 domain

SHIP1: SH2-containing Phosphatidylinositol- ‘5-phosphatase-1

SHP1/2: SH2-containing Phospho-Tyrosine phosphatase-1/2

SHG: Second Harmonic Generation

Syk: Spleen Tyrosine Kinase

TEM: Trans-Endothelial Migration

TIRF: Total Internal Refraction Fluorescence Microscopy

TNFα: Tumor Necrosis Factor alpha

WB: Western Blot

WT: Wild Type

INTRODUCTION

6 INTRODUCTION

6.1 The Neutrophil

Neutrophils were first recognized as a distinct blood cell-type in the late nineteenth century by Paul Ehrlich when he was performing pioneering studies with new staining techniques. These cells were characterized by a peculiar “polymorphous nucleus” and a tendency to be stained by neutral dyes, thus they were (and they are still) called neutrophils or polymorphonuclear leukocytes (PMN). They belong to the “innate” arm of the immune system because the ability of neutrophils to perform their immunologic functions is immediate and do not depend on previous exposure to microorganisms. Neutrophils represents the largest (almost 60%) population of circulating white blood cells and constitute the very first line of defense against noxious stimuli. They were thought to be just simple soldiers that dye once finish their task, without being decisive for the late stages of the inflammatory response. More recently, new neutrophils unexpected roles are being uncovered: neutrophils play indeed important roles in shaping both innate and adaptive immune responses, and actively contribute, not only to the breakdown, but also to the repair of injured tissue (Nathan, 2006). Another paradigm about neutrophils has also been shifted: it was thought that, upon extravasation, neutrophil are committed to die in the extravascular tissue, but recent studies showed that a small portion of neutrophils can re-enter back to the systemic circulation and disseminate the inflammation to distal organs (Woodfin et al., 2011), indicating that mechanisms controlling neutrophils trafficking are central for the host homeostasis.

Neutrophilopoiesis doubtless accounts for the major effort of the bone marrow, with a production that can reach the incredible amount of 10^{11} cells in just a single day. This tremendous effort can be justified by their important functions as innate first line of defense against pathogens: mature neutrophils spend their entire life in indefatigably scanning every single corner of the host, ready to coordinate a precise and powerful response to find and destroy the menace if they sense the presence of a danger. If unemployed, at the end of

their life are cleared from the circulation mainly by the reticuloendothelial system in the liver, spleen and bone marrow (Saverymuttu et al., 1985). But if any danger is present, they immediately coordinate an accurate response in order to find and destroy it. Considering this vital task, they are equipped with the most brutal, indiscriminate and lethal arsenal of weapons among the entire immune system (Lacy, 2006). Neutrophils are short-lived cells (8-12 hours in humans) and are unceasingly generated from myeloid precursor in the bone marrow (Borregaard, 2010). Although is still unclear the reason why they are established with such a short life, it's tempting to speculate that their continuous turnover may be a mechanism to protect the host by collateral damages, as neutrophil apoptosis and efferocytosis by the reticuloendothelial system would prevents the leakage of their dangerous content (Poon et al., 2014). Indeed, while effective in their devastating ability, these weapons are just as fatal to the host as to their envisioned targets. In contrast to other components of the innate immune system – such as dendritic cells and mast cells that reside in extravascular tissues – neutrophils have to undergo an elaborate migratory process out of the vascular lumen, usually in post-capillary venules, in order to exert their host-defense actions into the peripheral tissues. However, if inappropriately triggered, excessive and/or prolonged, the neutrophils response can also lead to several pathological disorders (Segel et al., 2011).

Even though the neutrophil field is simply immense (a quick research on PubMed results in more than 10^5 scientific works on this cell type), I will focus on what is currently known about neutrophil biology in relation with the experimental work that I have performed during my PhD work. In particular, I will introduce the current knowledge on the following questions: what are the major weapons employed by these cells? How does the neutrophil recognize the presence of a danger within the circulation? How they reach the inflammatory site? What are the mechanisms and consequences of neutrophil activation?

6.1.1 License to kill: the neutrophil cytotoxic arsenal

Neutrophils must transport in the systemic circulation a considerable collection of harmful armaments, ready to be quickly employed at the correct time and in a controlled manner. They are indeed characterized by the intracellular presence of discrete vesicles of storage called granules, which contain all the constituents needed for neutrophil functions. These proteins are packaged during neutrophil maturation (Borregaard, 2010) in at least four types of granules that can be classified depending both the timing of their appearance during neutrophil maturation and the unique features of their content.

(i) Azurophil granules – also known as primary – are the first to be formed during myelopoiesis and contains the most cytotoxic proteins. They are usually not exocytosed and contains for instance the myeloperoxidase (MPO, an important enzyme involved in the respiratory burst), Serprocidins (Elastase, Proteinase 3 and Cathepsin G, which are serine proteases for the hydrolytic degradation of bacteria) and antimicrobial peptides called Defensins (cationic peptides able to disrupt the bacterial membrane).

(ii) Specific granules – also known as secondary –, which also contain antimicrobial constituents like Neutrophil Gelatinase-associated Lipocalin (NGAL), Cathelicidin, Lysozyme and MMP-8 (Faurschou and Borregaard, 2003), but, at variance with azurophil granules, do not contain peroxidase enzymatic activities.

(iii) Gelatinase granules – also known as tertiary –, are less equipped in antimicrobial agents in comparison to the previous two and act as reservoirs of matrix-degrading enzymes (in particular collagenase or MMP-9 from which the name of these granules). They are more easily exocytosed and this is important during neutrophils recruitment at the inflammatory site, since the action of the MMPs help to digest the extracellular matrix and the vascular basement membrane, allowing their transit through the vascular wall and throughout the external tissues (Sengelov et al., 1995).

(iv) The last type is represented by secretory granules. They were discovered as the organelles responsible for the rapid upregulation of CD11b at the neutrophil surface after stimulation with the formyl-Methionyl- Leucyl-Phenylalanine (fMLP) peptide (Borregaard et al., 1987). Secretory vesicles are indeed rich in the β_2-integrin CD11b:CD18 (Sengelov et

al., 1993), the fMLP-receptor (Sengelov et al., 1994a) and the complement receptor 1 (Sengelov et al., 1994b). Moreover, the mobilization of secretory granules is accompanied by shedding of L-selectin from the cellular surface, and all these changes allow the neutrophil to interact with the activated endothelium in order to start the recruitment process to the inflammatory site (Borregaard et al., 1994).

When arrived at their destination, neutrophils have mobilized almost all their secretory vesicles, 40% of their gelatinase granules, 20% of their specific granules and only 5% of their azurophilic granules (Sengelov et al., 1995). Thus, when the neutrophils are finally faced with the noxious agent, their receptors are upregulated at the membrane surface, while most of the bactericidal and proteolytic enzymes are still retained, ready for fusion with the phagocytic vacuole during the microorganism engulfment.

To conclude, granules are far more than just inert containers for dangerous compounds, but rather they represent active players in almost all neutrophil activities during inflammation.

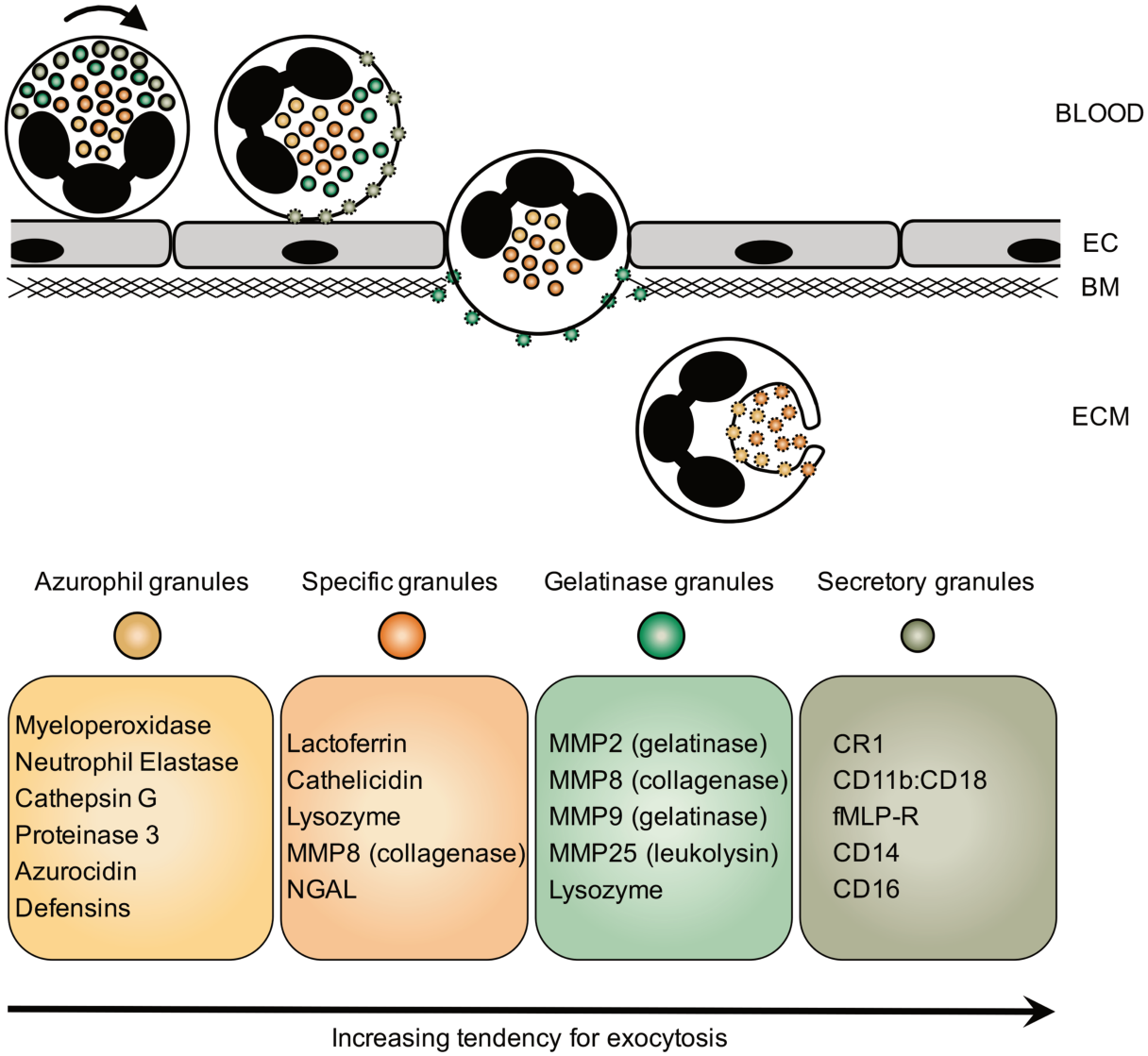

FIGURE 1. NEUTROPHIL GRANULES CONTENT

The constituents of different granules are defined by their content. In addition, granules are also released according to a hierarchy with secretory granules being the most readily exocytosed and azurophil granules only undergoing partial exocytosis. CR, complement receptor; MMP, Matrix Metallo Protease; NGAL, neutrophil gelatinase-associated lipocalin; EC, Endothelial Cell; BM, Basement Membrane; ECM, Extra Cellular Matrix. (Adapted from Pham et al. 2006)

6.1.2 Margination and mobilization of circulating Neutrophils

Experiments performed almost 60 years ago, showed that approximately half of radio-labelled autologous neutrophils disappear from the systemic circulation within seconds when injected in healthy volunteers (Mauer et al., 1960), while, in other experiments, the blood count of circulating neutrophils was drastically increased by the intravenous administration of adrenaline (Athens et al., 1961). These data indicated the existence of a neutrophil pool that could be retained or mobilized if necessary, and this recoverable portion of cells were named “marginated”. Marginated neutrophils reside principally in the bone marrow, spleen, liver and lungs (Peters, 1998). Although the reason why neutrophils are concentrated within these organs remains largely undefined, it is possible that they act as reservoirs of mature neutrophils, which can be rapidly deployed to sites of inflammation in case of necessity. It is also likely that the marginated neutrophils are just patrolling these organs and this would result in a reduction of their input/output ratio across these tissues. Nevertheless, is well known that systemic inflammation is associated with circulating neutrophilia and several inflammatory mediators have been shown to augment neutrophils blood count when injected experimentally into animals (Hsu et al., 2011). Even though the precise mechanisms that control neutrophil mobilization are poorly characterized, recent data suggested that the G-CSF in combination with CXCL1 are able to disrupt the neutrophil retention in the bone marrow (Wengner et al., 2008), but for the other organs remains to be determined.

A successful immune response depends on the capacity of leukocytes to correctly move in the organism. This is particularly important for neutrophil, as demonstrated by the fact that genetic deficiencies of adhesion molecules are associated with recurrent and lethal bacterial infections (Anderson and Springer, 1987), while vicious recruitment might result in severe collateral damages to the host and chronic inflammation (Singbartl et al., 2000). Neutrophil trafficking depends principally by a class of specialized receptors called integrins. These proteins are not constitutively active and their adhesive properties are tightly controlled by multiple signaling pathways.

6.1.3 Integrins: how they work

Integrins are transmembrane heterodimers of non-covalently associated α and β subunits (Hynes, 2002). Nowadays, are known 18 α and 8 β subunits that can be assembled in 24 different receptors with different ligand specificity and with different cellular distribution (**Figure 2a**). Among all, immune cells are the only that express a specific subfamily of integrins composed of a common β_2 subunit associated to one of four distinct, yet highly homologous, alpha subunits (α_L, α_M, α_X, and α_D). In particular, $\alpha_M\beta_2$ is specifically presented by cells belonging to the myeloid lineage and recognizes a multitude of heterogeneous ligands. Ligands include extracellular matrix components such as fibronectin, laminin, collagen and vitronectin (Bohnsack and Zhou, 1992), counter-receptors of the immunoglobulin super-family such as ICAM-1 (Diamond et al., 1991) and ICAM-2 (Xie et al., 1995), MPO (Johansson et al., 1997), elastase (Cai and Wright, 1996) and several others (Podolnikova et al., 2015).

All integrins are characterized by the presence of a short cytoplasmic tail, a single transmembrane domain and several flexible extracellular domains with a headpiece containing the ligand binding site (**Figure 2b**). Considered the high-flexibility of the ectodomains, changes in their conformation dramatically influence the affinity and the avidity for their specific ligand. There are structural and functional evidences for at least three global β_2 integrin conformations: closed/bent, opened headpiece and fully-extended headpiece (Luo et al., 2007). Integrin with a bent headpiece conformation hide the ligand binding-site, whereas different signals can switch the conformation toward an intermediate or fully-opened conformation that display respectively intermediate or high affinity for the ligand. Most of the understanding of integrins conformational changes comes from experiments with “reporter antibodies” whose epitope is inaccessible in the bent configuration, but is exposed when the integrin extends (Stephens et al., 1995). As integrins lack endogenous enzymatic activity, their activation is induced by the molecular assembly of signaling complexes at the site of their cytoplasmic tail (O'Toole et al., 1994) in a process called “inside-out” signaling. The latter is a very complex process in which several proteins are involved (Campbell and Humphries, 2011). One of the most important player implicated in integrin activation is Talin1, a 270kDa soluble protein that exists in an auto-inhibited

conformation in the cytoplasm, but becomes active when docked at the cellular membrane by the interaction with specific phospholipids produced after cellular activation (Critchley, 2009). Engagement of different signaling pathways (GPCR, SFK and ITAM), leads to the local generation of phosphatidylinositol 4,5-bisphosphate. Binding of Talin1 to PtdIns(4,5)P_2 via its FERM (4.1/ezrin/radixin/moesin) domain release it from its inhibited form and permit to the protein to associate to the integrin β subunits (Ye et al., 2016). Membrane-docked Talin1 act as a bridge for integrins, filamentous actin (F-actin) and other actin-binding proteins: the interactions of integrin cytoplasmic tail with this intracellular complex, finally lead to an allosteric rearrangement of the ectodomains that open the headpiece for an optimal orientation of the binding site (Du et al., 1993).

The importance of Talin1/integrins interaction during neutrophil recruitment was recently addressed *in vivo*, with mice in which Talin1 was genetically-modified on residues crucial for its interaction to β_2-integrins (Yago et al., 2015). In this work, an invalidating point mutation of Talin1 in the myeloid lineage protected mice from ischemia-reperfusion injury. Talin-deficient neutrophils were indeed not able to extend the ectodomain of β_2-integrins and hence could not complete the adhesion cascade on the endothelial cell in the vascular lumen and reach the inflammatory site.

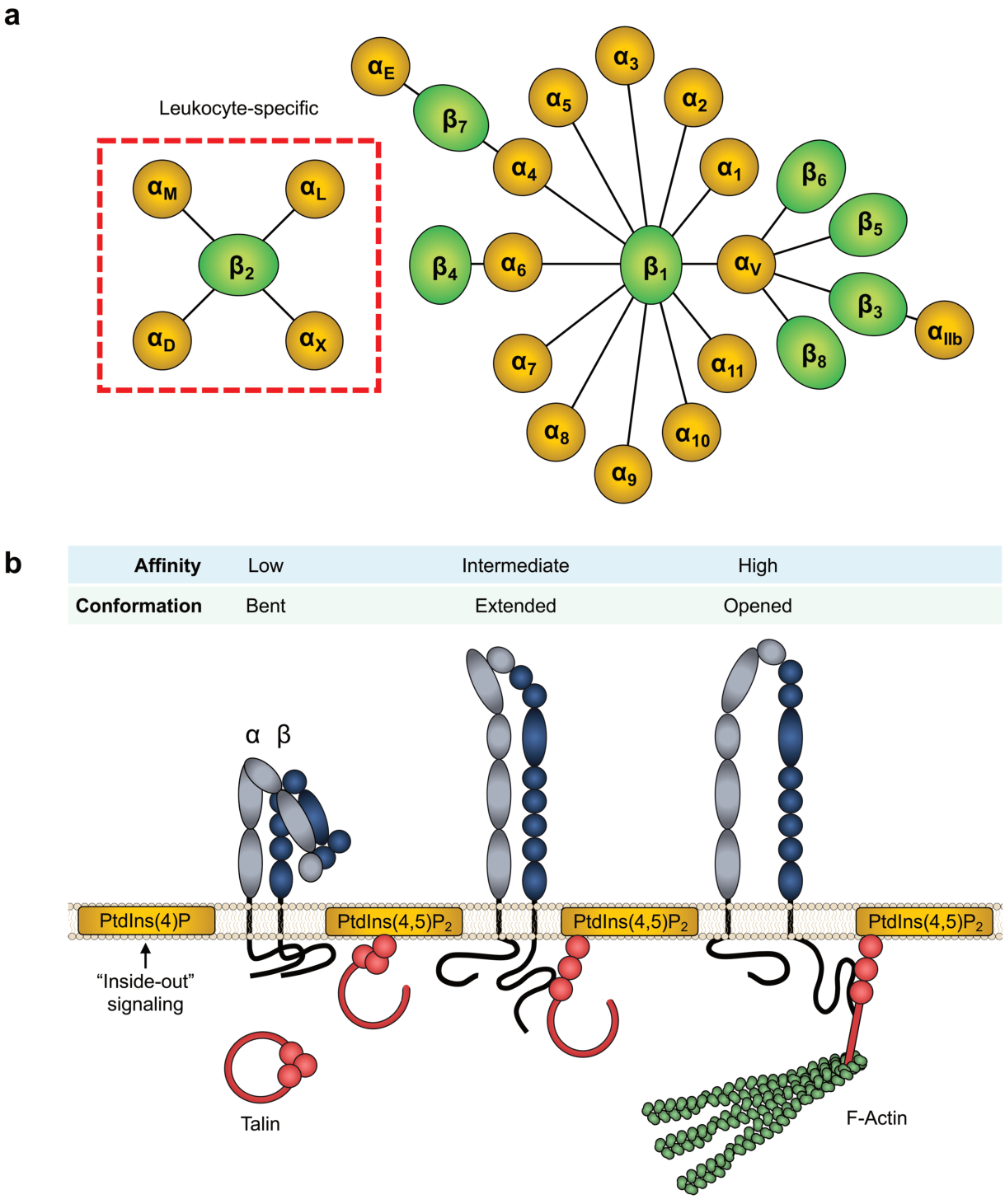

FIGURE 2. THE INTEGRIN SUPERFAMILY: STRUCTURE AND ACTIVATION

(a) *Integrins can be classified according to their beta chain in different α:β heterodimers with different specificity and cellular distribution.* ***(b)*** *Integrin in a closed conformation hide their binding*

site and display poor reactivity for their ligands. Inside-out signaling trigger the local production of PtdIns(4,5)P_2 which recruit Talin1 at the cell membrane. Interaction with PtdIns(4,5)P_2 release Talin1 from its autoinhibited conformation, which allow it to interact with the cytoplasmic tail of the β subunit. Interaction between Talin1 and integrin introduces allosteric changes that alter the ectodomain thereby releasing the headpiece from its bent form. The molecular linking with Talin1 and actin filaments tilts the β subunit leading to further conformational modifications in which the binding site is fully-exposed.

6.1.4 The adhesion cascade

Mature neutrophils continuously circulate in the blood stream, patrolling the vessels in search for inflammatory cues. To do so, they establish weak, transient contacts with the selectins expressed by the vascular endothelium of postcapillary venules. Upon the occurrence of an organ injury, the expression of "danger signals" by the damaged cells lead to the local production and secretion of cytokines and other pro-inflammatory mediators that activate endothelial cells of the nearby microvasculature. These activated endothelial cells communicate the presence of the danger to circulating leukocytes by increasing the expression of selectins and adhesion molecules at their surface. This can occur within seconds, via the rapid mobilization of the Weibel-Palade bodies (Utgaard et al., 1998), and can be sustained within a few hours by a *de novo* synthesis (Kansas, 1996). The increased expression of selectins, allows the tethering (capture) of floating leukocytes, thereby inducing cells to "roll" in the vascular lumen at 20-40 µm/sec with a shear stress that spans from 1 to 10 dynes/cm^2 (Sundd et al., 2011). Under these dynamic conditions, leukocytes are able to rapidly establish and broke adhesive connections by the engagement of their P-Selectin Glycoprotein Ligand-1 (PSGL1). The interaction of leukocyte PSGL1 with endothelial selectins (P- and E-selectin), induces an inside-out signaling pathway that leads to the augmentation of neutrophil adhesion with a consequent reduction of the rolling speed. From a molecular point of view, PSGL1 engagement induces the phosphorylation of immunoreceptor tyrosine-based activation motif (ITAM) adaptors (Fcγ-chain or DAP12), which, in turn, starts an inside-out transduction pathway mediated by the recruitment of the

Spleen Tyrosine Kinase (Syk). All these events finally result in a conformational change of leukocyte β_2-integrins towards an intermediate-affinity form (LFA-1 for all leukocytes and Mac-1 specifically for neutrophils and monocytes), that enable neutrophils to slow further their speed by additional interactions with endothelial cell adhesion molecules like ICAM-1 (Zarbock et al., 2008). This slow rolling phase (≈5µm/sec) permits to increase progressively the efficiency of leukocyte contacts with the chemokines (meanwhile locally produced and secreted) that have been immobilized onto the endothelial glycocalyx. The interaction between the endothelial-bound chemokines with their specific receptor at the surface of the leukocytes, drives a GPCR-dependent integrin full-opening and allows the complete arrest of the neutrophil on the inflamed endothelial cell (Lefort et al., 2012). Once arrested, they start to actively crawl on the endothelial surface (even against the flow direction) probing the inflammatory cues and following the chemokine gradient to reach the correct site for leaving the vessel ("extravasation"). At this stage of their recruitment, neutrophils must hold their integrins in their maximal adhesive state in order to not be pulled away – back in the blood flow – by the hydrodynamic forces present in the vessel.

While the understanding of the mechanisms promoting integrin strengthening and neutrophil adhesion on endothelial cells is increasing (Hogg et al., 2011), the regulatory pathways that control these processes are still not well defined. A recent work has suggested that SH2-containing phosphatases might be important in this setting (Stadtmann et al., 2015).

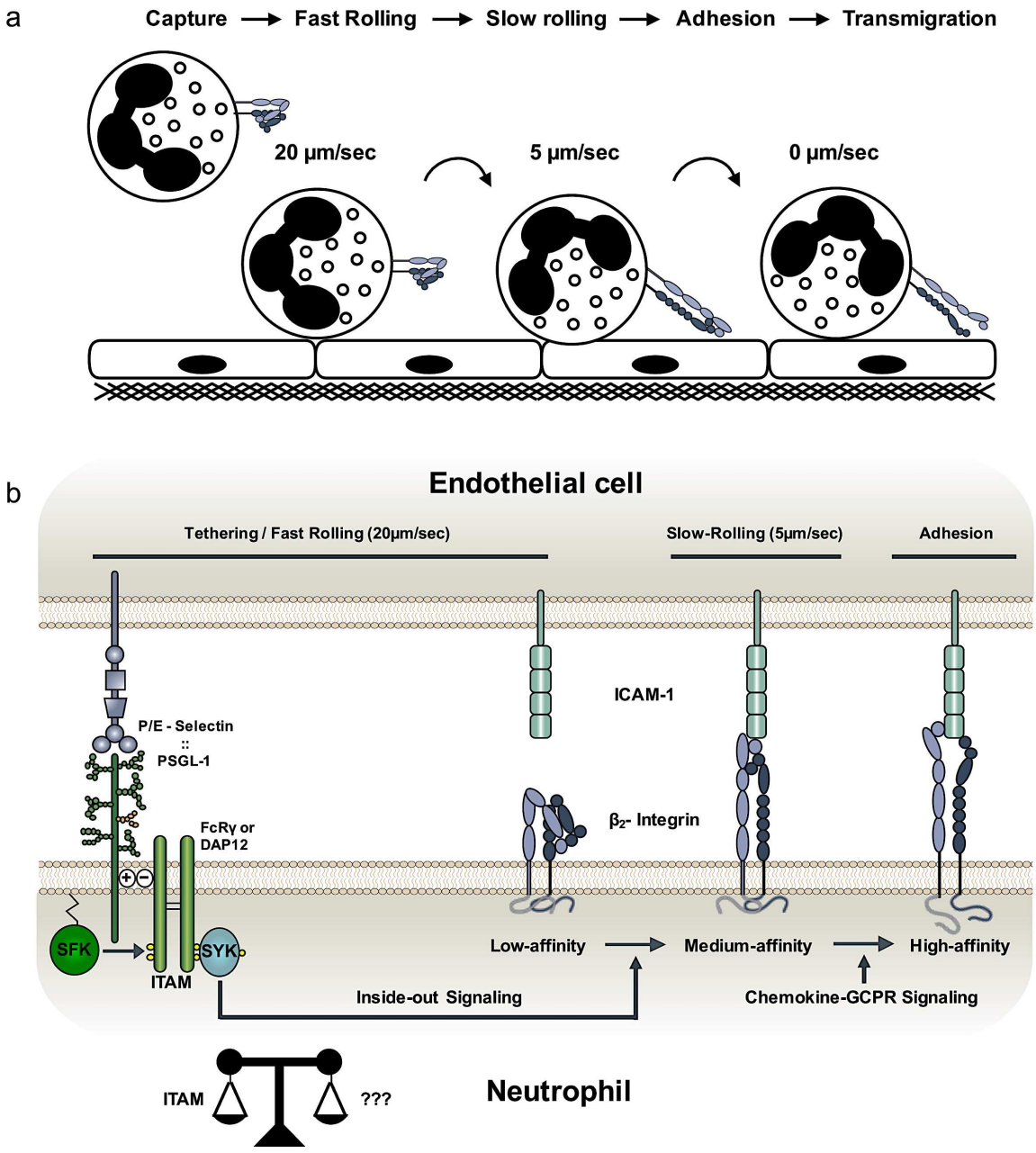

FIGURE 3. NEUTROPHIL INTERACTION WITH ACTIVATED ENDOTHELIAL CELLS

(a) *Close to the inflammatory sites, neutrophils tether along the activated endothelium by transiently and weakly bind to the selectins. This selectin-mediated "fast rolling" is then followed by a reduction of neutrophil speed ("slow rolling"), mediated by the endothelial adhesion molecules, which, in the presence of specific chemokines, turns into a complete arrest.* ***(b)*** *Interaction of neutrophil PSGL-1 with selectins, results in an ITAM-mediated inside-out signaling pathway that modifies the conformational orientation of β_2-integrins. The changed conformation*

augments their affinity for cell adhesion molecules (like ICAM-1). Finally, GCPR-signaling triggered by chemokines immobilized on the endothelial surface, induces the high-affinity conformational state that allow the neutrophil to completely arrest within the vascular lumen.

6.1.5 Breaching the wall: the transendothelial migration

Rolling, adhesion and crawling are consecutive steps of leukocyte-endothelial cell interactions that prepare neutrophils to reach the right exit sites from where they transmigrate through the endothelial barrier (trans-endothelial migration, TEM). When neutrophils interact with the vessel wall, their shape changes noticeably from an almost spherical to a flattened phenotype. These alterations are associated with the reorganization of cytoskeleton and with a cellular polarization: the migrating leukocyte forms a “leading” edge at its front of migration whereas the rear forms the so called “uropod”, a structure characterized by high contractility and a low adhesion state (Hind et al., 2016). Even though neutrophils can occasionally leave cross the endothelial layer by a transcellular way, directly traversing the body of the endothelial cells (Carman and Springer, 2008), the majority of leukocytes actively crawl towards endothelial cell-to-cell junctions and they cross the endothelial barrier in a paracellular way, in between adjacent cells. Once leukocytes are in proximity of the junctions, the local engagement of endothelial ICAM-1 trigger the loosening of endothelial cell contacts and opening of a passage between them (Shaw et al., 2001). More precisely, the endothelial cell activates downstream signaling pathways that induce VE-cadherin to be cleared from the site of transmigration along the junction, in order to release the adherent junctions and allow the passage of the leukocyte (Vestweber, 2015). The latter is predominantly regulated by their interaction with the adhesion molecules on the endothelial cells which extend their apical membrane projections enriched in ICAM-1 which are called ‘transmigratory cups’ (Carman and Springer, 2004).

When a leukocyte engages the TEM process, it establishes several consecutive intimate contacts with the adjacent endothelial cells. These leukocyte-endothelial contacts at the lateral borders of adjacent endothelial cells are crucial for neutrophils to cross the vessel. A

plethora of studies on the signaling pathways that are triggered during the diapedesis have focused on the endothelial side, whereas very little is known about the effects that such interactions generate on the leucocyte counterpart (Vestweber, 2015). The endothelial junctional proteins that are involved in TEM have been identified and characterized by the use of monoclonal antibodies that were able to impair leukocyte transmigration at specific stages of this process. The most important junctional proteins involved in TEM were found to be the “Junctional Adhesion Molecules” (JAM-A/B/C), CD99 and CD31. While CD99 and CD31 establish trans-homotypic interactions, JAM proteins bind with leukocyte β_2-integrins and actively assist the passage of leukocytes through the endothelial barrier. Once the basal side of the endothelial cells is reached, leukocytes need to dissociate from them and cross the underlying basement membrane. This last step of TEM remains largely enigmatic.

6.1.6 Trafficking beyond the endothelial cell and detachment out of the vascular wall

After crossing the endothelial barrier, neutrophils must take their way through another physical obstacle of the vessel wall: the basement membrane (BM). The BM is a thin extracellular matrix structure containing supramolecular organized networks of laminins (mainly isoforms 4 and 5) and collagen type IV which are interconnected by bridges of nidogens and perlecan (Yousif et al., 2013). The assembled BM enclose outside the vessel wall and provides endothelial cells with structural support, while (with a pore size in the order of 50 nm) only small molecules can passively diffuse across it. Although the molecular mechanisms are poorly understood, wild-type neutrophils are able to cross the tight BM barrier without any obvious problem, indicating that they may adopt different strategies to pass through. In this regard, immunohistological observations have highlighted the presence of BM areas with low expression regions (LER) of laminins and collagen IV (Wang et al., 2006) that are permissive sites privileged by leukocytes to leave the vascular wall (Voisin et al., 2010). In addition, subunits of laminins with lower capacity for crosslinking with collagen type IV (notably the short α chain of laminin-4), might provide more penetrable LERs due to

an easier dissociation of the matrix networks during cell migration (Yousif et al., 2013). Indeed, LER are transiently enlarged after the passage of leukocytes and neutrophils that egress into the tissue carry with them laminin fragments, indicating also a local proteolytic digestion of the BM (Voisin et al., 2010).

Different receptors expressed by transmigrating leukocytes have been proposed to support the interactions between neutrophils and the BM. Experiments performed with monoclonal antibodies able to inhibit neutrophil adhesion on laminin *in vitro* and *in vivo* have suggested that specific integrins may govern neutrophil interaction on the BM, such as $\alpha_6\beta_1$ (also known as VLA6). Yet, neutrophil interaction on laminin must also be dependent from β_2-integrins (CD11b:CD18), as suggested by the fact that anti-β_6 and anti-β_1 antibodies are not able to prevent neutrophils adhesion to the BM when used alone, but they concomitantly need a β_2-integrin inhibition (Bohnsack, 1992). The authors of these studies concluded that contribution of VLA6 to neutrophil to adhere to laminin seemed to be weaker than that of CD11b:CD18. In support of this conclusion, recent experiments found that myeloid-specific genetic invalidation for the integrin β_1 subunit in mice, surprisingly, resulted in a four-fold increase of transmigrated neutrophils in a peritonitis model (Sarangi et al., 2012). These observations might therefore indicate that β_1-integrins can even constitute a brake for neutrophil egression into the inflammatory site.

After penetrating the vascular wall and before approaching the parenchyma of inflamed tissue, leukocytes must detach from the outside portion of the endothelial layer and from the basement membrane, a fundamental – and yet largely enigmatic – process. Intravital observations of extravasating neutrophils have shown that, while the leading edge of migrating neutrophils moves forward towards the interstitial tissue, the uropod remains “trapped” at the level of the basolateral part of the endothelial cell junction (Hyun et al., 2012). By this peculiar process, cells became exceptionally elongated (20 to 50µm) and spend several minutes in this state before completely detach. It’s tempting to speculate that uropod retention at the basolateral side of the vessel might be the heritage of the strong adhesive interactions established during the adhesion cascade, when the neutrophils had to face the hemodynamic conditions in the blood stream. In this regard, the step of neutrophils elongation could be needed in order to initiate the closure of the integrins, now that the cells must detach in order to get out, into the static interstitial compartment. Most

notably, in addition to a putative active detachment process, while making their way out of the vessel, the migrating leukocytes can mutilate themselves and leave pieces of their cell membranes, expressing CD11b and chemokines along the vessel wall, which has been suggested to provide additional chemotactic cues to guide other leukocytes to the inflammatory site (Lim et al., 2015).

At the end of the TEM, once they reach the inflamed tissues, the neutrophils exhibit an altered phenotype, enhanced survival, and increased effector functions. Accordingly, the vascular adhesion and breaching steps of extravasating neutrophils not only limit the extent of neutrophil accumulation in inflamed tissue but also represent mandatory steps that will influence neutrophil effector function once they are ready to face the noxious agent at the sites of tissue inflammation.

6.1.7 Neutrophil activation: the end game?

When neutrophils are recruited at an inflammatory site, they must deal with an extremely complex task as they have to stop against the blood flow, move across a changing environment and integrate a plethora of information in order to correctly orchestrate an appropriate immune response. For this purpose, they are equipped with a large number of cell surface receptors for the recognition of the inflammatory milieu (cytokines and chemokines) and the noxious agents (Futosi et al., 2013). Neutrophils can directly recognize pathogen-associated structures or danger signals via the “innate” receptors for PAMP and DAMP or indirectly, via the binding of the specific antibodies that coat the biological target to their Fc-receptors. The latter mechanism provides a link between the adaptive and the innate immune response (**Figure 4**).

Emigrated neutrophils must first follow a hierarchical gradient of interstitial chemokine that guide them through the injured site. Important chemoattractant molecules include IL-8 (the murine orthologue is CXCL1), leukotriene B4 (LTB4) and bacterial peptides containing the N-formyl-Methionyl-Leucyl-Phenylananine (fMLP) motif. Interestingly, although protein

formylation is a specific bacterial signature, host necrotic cells can themselves be a source of fMLP-containing peptides by the release of mitochondrial proteins (Raoof et al., 2010). Within the tissue, chemokines that are associated closer to the site of inflammation (for example fMLP) have higher priority than chemokines released at intermediary sites (like CXCL1 or LTB4) to guide neutrophils (McDonald et al., 2010). Once neutrophils have breached the multiple layers of the vascular wall and entered into the in inflamed extravascular space, they change their intracellular and membrane phenotype for the detection of tissue damages and for optimal microbial clearing (El Benna et al., 2002). Indeed, extravasated leukocytes are more active than blood neutrophils and much more responsive to stimulations, a phenotype that have been called “primed” state (Hallett and Lloyds, 1995). The three main ways by which neutrophils can destroy a noxious agent are (i) the oxidative burst, (ii) employment of antibiotics proteins and (iii) release of neutrophil-extracellular traps (NETs).

G-protein-coupled receptors	Fc-receptors	Adhesion receptors	Cytokine receptors	Innate receptors
Formyl-peptide receptors • FPR1 • FPR2 • FPR3 *Chemoattractant receptors* • BLT1 (LTB4-R) • BLT2 (LTB4-R) • PAF-R • C5a-R *Chemokine receptors* • CXCR1 (human) • CXCR2 • CCR1 • CCR2	*Fcγ-receptors (human)* • *FcγRI (activatory)* • *FcγRIIA (activatory)* • *FcγRIIC (activatory)* • *FcγRIIIA (activatory)* • *FcγRIIIB (activatory)* • *FcγRIIB (inhibitory)* *Fcγ-receptors (mouse)* • *FcγRI (activatory)* • *FcγRIII (activatory)* • *FcγRIV (activatory)* • *FcγRIIB (inhibitory)*	*Selectins and ligands* • *L-selectin* • *PSGL-1* *Integrins* • *LFA-1 ($\alpha_L\beta_2$)* • *Mac-1 ($\alpha_M\beta_2$)* • *VLA-4 ($\alpha_4\beta_1$)*	*Type I cytokine receptors* • *IL-4R* • *IL-6R* • *IL-12R* • *IL-15R* • *G-CSFR* • *GM-CSFR* *Type II cytokine receptors* • *IFNα-R* • *IFNγ-R* *IL-1R family* • *IL-1RI* • *IL-1RII* *TNFR family* • *TNFR1* • *TNFR2* • *Fas*	*Toll-like receptors* • *TLR1* • *TLR2* • *TLR4* • *TLR5* • *TLR6* • *TLR8* • *TLR9* *C-type lectins* • *Dectin-1* • *Mincle* • *CLEC-2* *NOD-like receptors* • *NOD2* • *NLRP3* *RIG-like receptors* • *RIG1* • *MDA5*

FIGURE 4. NEUTROPHIL RECEPTORS

Examples of neutrophils receptors. G-protein-coupled chemokine and chemoattractant receptors, Fc-receptors, adhesion receptors such as selectins and integrins, various cytokine receptors, immune receptors such as Toll-like receptors and C-type lectins. (adapted from Futosi et al. 2013)

The production of reactive oxygen species by the oxidative burst is one of the most formidable weapon with which neutrophils destroy pathogens. The enzymatic system that begins the ROS production is the NADPH oxidase (Bedard and Krause, 2007), a supramolecular machine composed by six different proteins: two transmembrane proteins (p22phox and gp91phow) and four cytoplasmic proteins (p47phox, p67phox, p40phox and Rac1/2). In resting neutrophil, all these components are largely cytosolic, but, upon activation, they assemble together and start to transfer electrons across the membrane in order to transform molecular oxygen (O_2) to superoxide anion (O_2^-), which is immediately dismutated into the more toxic hydrogen peroxide (H_2O_2). Both O_2^- and H_2O_2 can damage a variety of biomolecules, especially DNA, which is believed to be the main way by which ROS kill bacteria (Van Acker and Coenye, 2017).

The second way of neutrophils effector functions is the mobilization of their intracellular granules and their cytotoxic content. As discussed previously, the granules are packed with different constituents and are used for distinct purposes during neutrophil recruitment. Although the content of gelatinase granules and secretory vesicles mainly help neutrophils to interact with the surrounding environment (by the upregulations of receptors and matrix-remodeling enzymes), specific and azurophilic granules contain antimicrobial proteases and peptides that directly destroy pathogens. The latter, are mainly used to kill pathogens intracellularly, as the release of their content into the surrounding tissues can cause severe collateral damages to the host. Granules are prevented from being released until specific receptors signal activate their movement to the cell membrane for secretion of their contents. In this process, membrane phospholipids play an important role, as production of inositol triphosphate (IP_3) was shown to be a pivotal second messenger for the increase of intracellular Ca^{2+} and the mobilization of granules (Fensome et al., 1996). The steps of exocytosis involve granule translocation toward a target site of the cell membrane via actin remodeling and microtubule assembly, and move by tethering and docking along the exocytosis path of the cytoskeleton through the sequential action of the SNARE complex (Mollinedo et al., 2006). Finally, the actin cytoskeletal mesh beneath the cellular membrane must be disassembled in order to allow the fusion of the granule membranes to the inner surface of the cell membrane and release their content (Jog et al., 2007).

Neutrophils are also able, in certain conditions, to release part of their nuclear content through the formation of extracellular networks made of double stranded DNA complexed with citrullinated histones and azurophilic antimicrobial proteins (MPO, NE and CG). This effector function has been called Neutrophil Extracellular Traps (or NET) (Brinkmann et al., 2004). NET networks are called so because they are able to capture bacteria, to prevent their dissemination and to kill them by the close exposure with the cytotoxic proteins with which NETs are complexed. It has been suggested that neutrophils are able to sense microbe size, and – although they prefer phagocyte microbes if are sufficiently small –, neutrophils are stimulated to release NETs specifically in response to microbes that are too large to engulf (Branzk et al., 2014). NET formation is an active process requiring an energy-dependent rearrangement of the nuclear architecture and the decondensation of the heterochromatin by the action of peptidyl arginine deiminase 4 (PAD4) an enzyme that catalyzes the conversion of histone's arginines into citrullines, thereby reducing their strong positive charge and thus weakening the histone-DNA interactions (Li et al., 2010).

Although all neutrophil effector functions are necessary for life, they are just as dangerous to microorganisms as to the host that they are intended to protect. Molecules supposed to kill microbes, such as reactive oxygen species and proteases, if not under control, can leak from live or dying leukocytes and kill self-cells. This is particularly known for sterile injuries (i.e. inflammations without microbe pathogens), in which the inflammatory response mediated by neutrophils may actually do more harm than good. This concept is well illustrated by the ischemia-reperfusion injury, were depletion of neutrophils substantially reduced the extent of acute tissue damages (Romson et al., 1983). Although in those settings would be potentially useful block neutrophil recruitment with pharmacological strategies, a complete immune suppression may not be the best option as it would compromise host defense against infections as well as tissue repair once the acute inflammatory phase is passed.

Upon ending their task, when the triggering stimulus is gone, neutrophils undertake the "resolution" phase of the acute inflammatory process. Neutrophils are indeed active players in clearing tissue cellular debris and – while dying by apoptosis – they secrete soluble mediators that prevent further neutrophil recruitment (Sugimoto et al., 2016). At this stage, resident or infiltrated macrophages eliminate the dead neutrophils, a process called

efferocytosis, which triggers the differentiation of these macrophages toward a reparative (M2) phenotype (Ortega-Gomez et al., 2013). This is a crucial event for the resolution of inflammation as suggested by the fact that chronic pathological conditions occur when neutrophil efferocytosis by macrophages is deregulated (Millet et al., 2015). The physiologic issue of the interaction between apoptotic neutrophils and the macrophages responsible for their efferocytosis may also be tightly controlled by an effective CD31 receptor function, as suggested by the work of Brown et al. (Brown et al., 2002).

In this context, targeting an endogenous protein capable to set a threshold for neutrophil recruitment and activation, as well as for driving the appropriate signals for the resolution of inflammation, should prove to be a fruitful approach to modulating the extent of the inflammatory response as well as the wound healing process.

6.2 The CD31 molecule

CD31 has been implicated since its discovery in numerous biological functions such as leukocyte transmigration, platelet activation and angiogenesis; all features that were attributed to its putative adhesive properties. However, several biochemical and functional studies have shown that CD31 contains two cytoplasmic immunoreceptor tyrosine-based inhibitory motifs (ITIMs), that upon phosphorylation are able to mediate inhibitory signals through the docking and activation of SH2-containing phosphatases. Like other molecule of the Ig-ITIM superfamily, CD31 acts as an inhibitory receptor, serving to moderate tyrosine kinase-dependent pathways and to globally set a threshold for activation in several cell types.

6.2.1 Protein structure and general features

The CD31 molecule was first identified as a protein shared by both platelets and endothelial cells (Goyert et al., 1986) and was then named “Platelet-Endothelial-Cell Adhesion Molecule 1” or PECAM-1. CD31 was cloned almost 30 years ago for human (Newman et al., 1990) and for the murine orthologous (Xie and Muller, 1993). It is constitutively expressed on all hematopoietic cells – with the exclusion of red blood cells – besides on endothelial cells, in which it is particularly enriched at the cell-junctions (Ilan et al., 2001).

CD31 is a single-pass transmembrane protein with the N-terminal exposed to the extracellular space and the C-terminal into the cytoplasm. The mature amino acid sequence includes 574 extracellular residues followed by a 19-hydrophobic sequence – that corresponds to the transmembrane region – and a cytoplasmic tail composed by 118 residues (**Figure 5**). A 27-signal peptide at the N-terminus is further processed and cleaved during the maturation of the protein in the endoplasmic reticulum. The CD31 expected molecular weight is about 83 kDa, but numerous N-linked and O-linked glycosylation

increase the apparent molecular weight up to 130 kDa for the mature protein (Newton et al., 1999). The extracellular region is composed by six Ig-like C2-type domains counted from 1 to 6 from the more distal to the membrane-proximal. Each domain presents two conserved cysteine residues – separated by 55/75 aminoacids – that are covalently linked together resulting in a three-dimensional structure typical of the Ig-fold family, which is organized in seven anti-parallel β-sheets packed against each other in a β-sandwich (Halaby et al., 1999).

At the very beginning of its cytoplasmic tail, CD31 possess a cysteine residue in position 622 that undergo to palmitoylation. This post-translational modification has been shown to be required for CD31 localization in lipid rafts, which seems to be important for CD31-dependent signaling properties (Sardjono et al., 2006). Because of the sequence similarity of its extracellular domains to those of other characterized Ig-CAMs, CD31 was originally assigned to the family of cell adhesion molecules, but after the discovery of two conserved ITIM motifs it was placed into the Ig-ITIM family (Newman, 1999). The cytoplasmic tail contains also several serine/threonine residues that were shown to be functionally phosphorylated and seem to be important for the association with the β-catenin (Ilan et al., 2000).

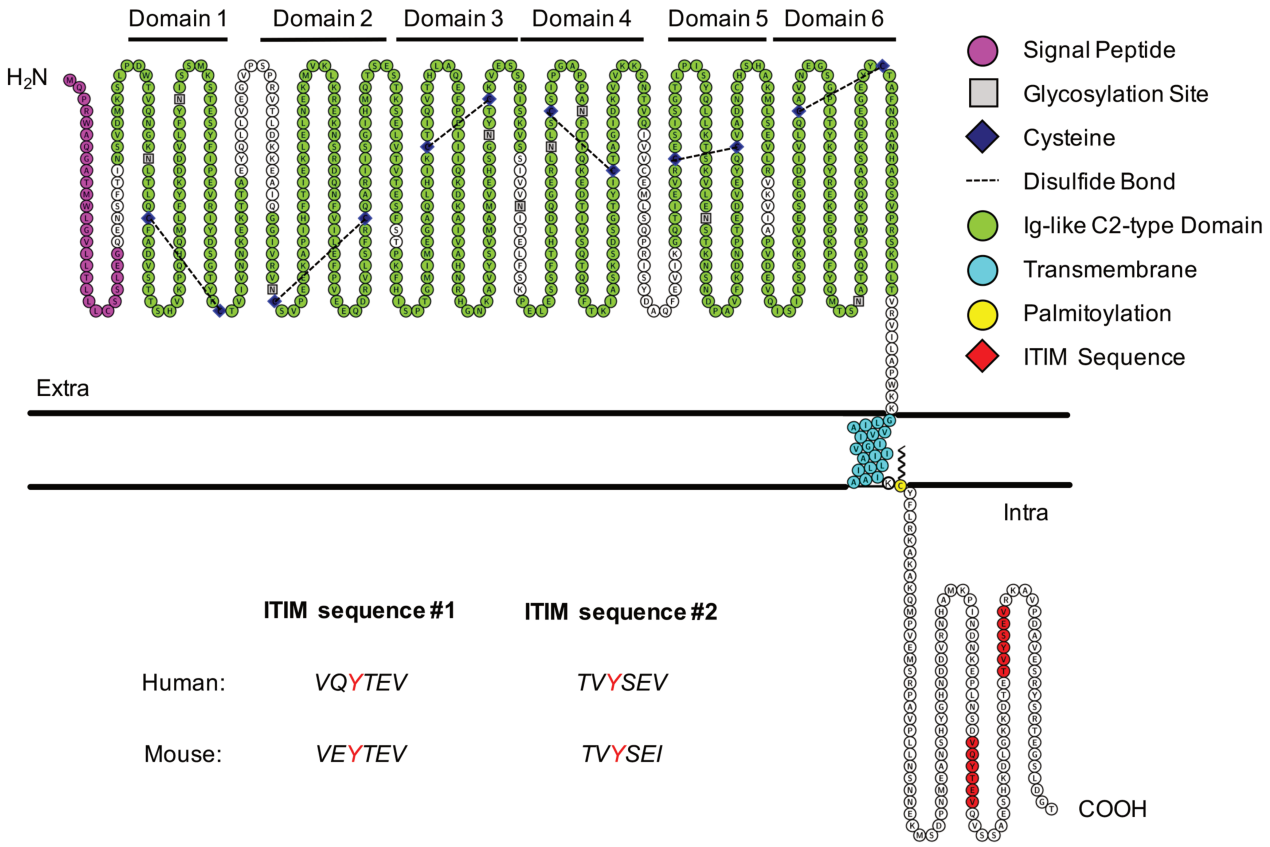

FIGURE 5. CD31 STRUCTURE

Schematic representation of the CD31 molecule with the principal structural and functional domains done with the online opensource Protter software.

6.2.2 *Gene and splicing variants*

The localization of the PECAM-1 gene is found on the chromosome 17 in human (while in mice is located on the chromosome 6) and its open reading frame is composed of 16 exons (**Figure 6**). Exons 1 and 2 encode the 5'-untranslated region and the signal peptide, while the exons from 3 to 8 are translated into the Ig-like extracellular domains from 1 to 6 respectively (Kirschbaum et al., 1994). The transmembrane domain and the cytoplasmic tail

are more complex since they can undergo to several alternative splice variants (Newman and Newman, 2003). Endothelial cells are the only cell type that has been documented to secrete a soluble form of CD31 by an alternative spliced mRNA from which the exon containing the transmembrane domain (exon 9) has been removed (Goldberger et al., 1994). This secreted CD31 molecule is 10 kDa smaller than the transmembrane form and can be detected in human plasma at the level of 10-25 ng/ml in healthy subjects. While all CD31 exons are phase 1 (i.e they end with a nucleotide that become part of the first triplet of the ensuing exon), exon 15 is a phase 0 exon. Splicing out of exon 15 (∆15 CD31), therefore, results not only in loss of the amino acids normally encoded by exon 15 itself, but also outcomes in changing the reading frame of downstream exon 16 with the generation of a new C-terminal sequence (Newman and Newman, 2003). Although this variant retains both the ITIM sequences, endothelial cells transfected with ∆15 CD31 failed to rescue from apoptosis after treatment with a chemotherapy agent, pointing out cytoprotective properties of the C-teminal tail (Bergom et al., 2008). Another variant was documented – at the mRNA level – to lack the exon 14, which codes for one of the two ITIM motif present in the cytoplasmic tail (Wang et al., 2003). Although ∆14 CD31 still contains one of the two ITIM motifs (i.e. the one encoded by the exon 13), CD31/SH2-containing phosphatases interaction seems to require the tyrosine phosphorylation at both ITIM sequences (Jackson et al., 1997). It is reasonable to think that these isoforms may have different biological properties, but the physiological role of ∆14 CD31 has not been fully investigated yet. Finally, as human cells express mostly the full-length CD31 (Wang et al., 2003), it remains to be determined whether differential signaling induced by the various CD31 isoforms may be relevant in humans.

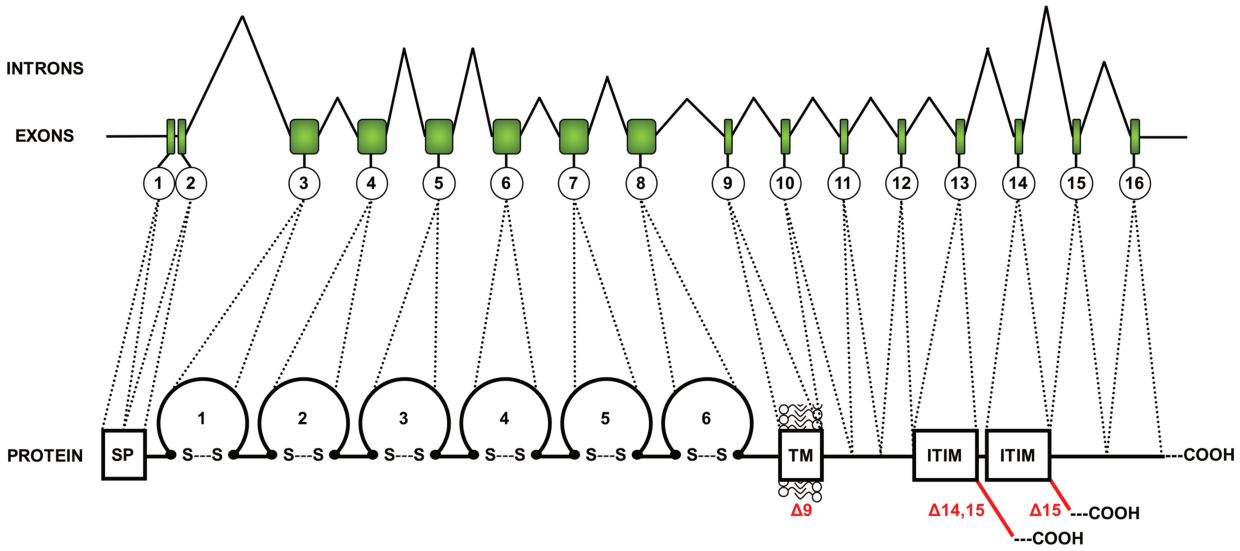

FIGURE 6. SCHEMATIC REPRESENTATION OF THE HUMAN CD31 GENE

Position and relative size of each exons is illustrated by green boxes, while introns are depicted as solid lines. Dotted lines indicate the corresponding encoded protein regions. SP signal peptide, S---S disulfide bond, TM transmembrane region, ITIM Immunoreceptor tyrosine-based inhibition motif. (Adapted from Kirschbaum et al., 1994). Different spliced form can occur, they are depicted in red and some of them can cause a reading frame-shift which lead to new C-terminal sequences.

6.2.3 CD31 activation and signaling pathways

CD31 monomers exhibit surprisingly little affinity for each other and, although has been classified as a cell adhesion molecule, CD31 is unable to mediate sustained cell-cell adhesive interactions (Newton et al., 1999). Instead, are more and more becoming appreciated the immunomodulatory properties delivered by the ITIM motifs present in the cytoplasmic tail (Cheung et al., 2015; Clement et al., 2015; Fornasa et al., 2012; Groyer et al., 2007).

CD31 does not possess intrinsic kinase activity and, to operate, it needs (i) to clustered, (ii) to be phosphorylated on its ITIM motif in order to (iii) became a docking site for SH2-containing phosphatases able to transmit downstream pathways.

CD31 is able to both heterophilic and homophilic interactions with CD31 molecules expressed by adjacent cells (trans-homophilic interactions) and with CD31 molecules on the plane of the same membrane (cis- homophilic interactions). To be engaged, it has been well demonstrated that both the distal Ig domains 1 and 2 are important for the formation of the primary homophilic contacts (Paddock et al., 2016) since cells that lack those domains are not able to bind full-length recombinant CD31 *in vitro* (Sun et al., 1996). The current molecular model proposes that trans-homophilic interactions mediated by the distal domains, induce a primary oligomerization of CD31 proteins on the same membrane plane that are further stabilized by the proximal 6^{th} domain in a zipper-like arrangement (Newton et al., 1997) (**Figure 7**). This model is supported by the experimental findings that mutant CD31 proteins lacking the domain 6 fail to undergo homophilic binding (Fawcett et al., 1995), while monoclonal antibodies mapping this region are able to induce it (Sun et al., 1996). Cis-interaction at the membrane plane would substantially increase total avidity of the complex leading the organization of signaling complexes and the formation of docking points for cytosolic proteins.

Because CD31 does not possess intrinsic enzymatic activities, the identity of kinase able to phosphorylate its tyrosine on the ITIM motifs has been subject of extensive investigation and a large body of evidences support a role for Src family kinase (SFK) Lck, Lyn, Fyn, c-Src and also Csk (Cao et al., 1998; Cicmil et al., 2000; Lu et al., 1997). It happens often that the same tyrosine kinase that phosphorylate ITAM-bearing receptors also phosphorylate an ITIM-bearing receptor in order to control the extent of activation. The characteristic feature of an ITIM motif is a tyrosine residue followed by a Leucine or Valine at the position +3 and generally preceded by a hydrophobic amino acid at -2 (consensus motif L/I/V/S-x-Y-x-x-L/V). Although CD31 possess in total 4 different tyrosine residues (Y_{623}, Y_{663}, Y_{690} and Y_{713}), mutant form of human CD31 in which the tyrosine residues at positions 690 and 713 (i.e. belonging to the ITIM motifs) were replaced with phenylalanine, failed to become tyrosine phosphorylated in transfected HEK293 cells exposed to pervanadate, suggesting that ITIM sequences are the only that can be tyrosine-phosphorylated (Jackson et al., 1997). A

tyrosine residue within this sequence is able, upon phosphorylation, to interact specifically with Src-homology 2 (SH2)-containing phosphatases, leading to their recruitment from the cytosol to the inner layer of the cellular membrane. It has been shown that ITIMs-CD31 can become a docking site for the SH2-containing tyrosine phosphatase SHP-1 and SHP-2 (Henshall et al., 2001), the phosphatidylinositol 5' phosphatase SHIP1 and the PLCγ1 (Pumphrey et al., 1999).

There is growing evidences that CD31 associate both physically and functionally also with cytoskeletal proteins. It would seem that CD31 is able to regulate F-actin assembly, especially during cell migration, likely by the interaction with β-catenin (Ilan et al., 1999). Finally, CD31 serine residues have also been shown to undergo to phosphorylation in platelets (Newman et al., 1992) and endothelial cells (Ilan et al., 2000). Serine phosphorylation on CD31 cytoplasmic tail – conversely to tyrosine phosphorylation – is already detectable in resting cells and its level increase by 2/3 folds upon cellular activation.

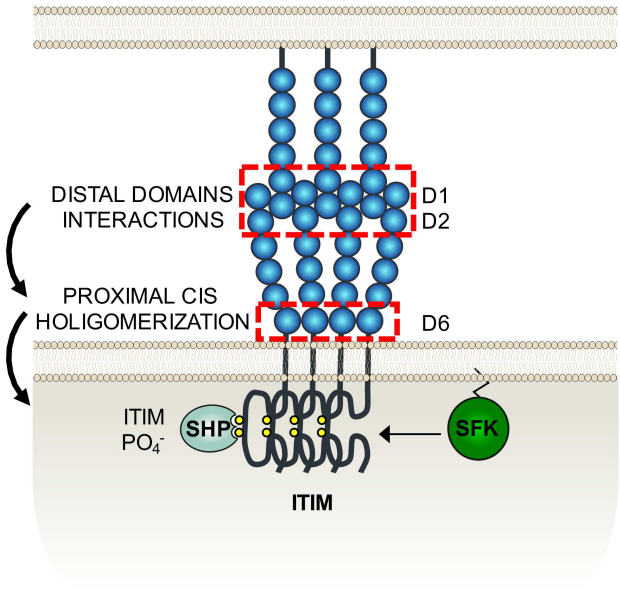

FIGURE 7. ZIPPER MODEL FOR CD31 CLUSTERING AND MOLECULAR ACTIVATION

Interaction of distal D1/D2 domains mediate trans-homotypic binding that are further stabilized by the membrane proximal D6. Clustering of CD31 by member of the Src family kinase (SFK) phosphorylate both ITAM-bearing activator receptors and ITIM-CD31 motifs. Phosphorylated CD31 act as a molecular platform for the recruitment of SH2-containing phosphatases (SHP) that antagonize the effect of SH2-containing tyrosine kinases (PTK) recruited by ITAM receptors.

(Adapted from Newton et al., 1997)

6.2.4 *Interplay between ITAM and ITIM-bearing receptors for the immune response*

A hallmark of the immune system is the ability to maintain an equilibrium between the extremes of reactivity and quiescence, at any moment ready to release an arsenal of cytotoxic weapons yet capable of maintaining control over these potentially lethal functions. Thus, the final outcome of a cellular response is determined by a complex interplay by activating and inhibiting signaling pathways and this balance is important to achieve a correct immune response, while preventing at the same time overwhelming inflammation or autoimmunity. One of the best characterized cellular pathways in immune cells are the Immunoreceptor Tyrosine-based Activation Motif (ITAM) and Immunoreceptor Tyrosine-based Inhibition Motif (ITIM) (Barrow and Trowsdale, 2006).

ITAM motif are found in the cytoplasmic tail of important immunoreceptors (like the CD3 subunits of TCR, Igα/Igβ subunits of BCR, Fc-Receptors and several others) and are characterized by the consensus YxxL/I$(x)_{6\text{-}10}$YxxL/I. In the prototypical immunoreceptor pathway, engagement of those receptors leads to activation of Src-family kinases, which, in turn, phosphorylate immunoreceptor tyrosine-based activation motifs (ITAMs) present on either the receptor itself or on associated subunits (DAP12 or the Fcγ-common chain). In neutrophils, phosphorylated ITAMs become a molecular platform for the recruitment of the SH2-containing tyrosine kinase Syk, while for T-lymphocytes and Natural killer cells the counterpart is represented by ZAP70. Membrane-docked Syk, in turn, phosphorylate several different substrates, which lead to a complex network of interconnecting signaling pathways (**Figure 8**). One of the enzymes activated downstream is the phosphatidylinositol 3-kinase (PI3K), which converts the local pool of phosphatidylinositol(4,5)P_2 in phosphatidylinositol(3,4,5)P_3. The Tec kinases are one of the few tyrosine kinases that have pleckstrin-homology domains (PH) with which can directly bind PIP_3 and be engaged at the cellular membrane (Schwartzberg et al., 2005). One of the Tec kinase is the Bruton's tyrosine kinase (Btk), which activate in turn the PLCγ for the production of soluble IP_3 and the release of intracellular Ca^{2+} by which further downstream signaling events are triggered (Odin et al., 1991).

The immune cells often employ coupled ITIM pathways in order to counterbalance and keep in check the cellular responses mediated by the ITAM signalizations. In some cases, the activating and inhibitory receptors recognize different ligands, whereas, in other circumstances, cells simultaneously express pairs of activating and inhibitory receptors with closely related extracellular domains binding similar ligands. (like the human Fc-receptors CD32A and CD32B). In this context, the simultaneous triggering of an ITIM receptor may lead to a negative feedback inhibition of the ITAM pathway depending on the recruited phosphatase. Recruitment of SHIP1 can interfere with activating signaling pathways by hydrolyzing phosphoinositide intermediates and preventing the recruitment PH-domain-containing enzymes, such as BTK and PLCγ, thereby diminishing downstream events such as the increase in intracellular calcium levels (Ono et al., 1996). Recruitment of SH2-containing tyrosine phosphatase would inhibit as well ITAM pathway, but by the dephosphorylation of functional activating tyrosine phosphorylations on PI3K, PLCγ, Syk and the ITAM motif itself.

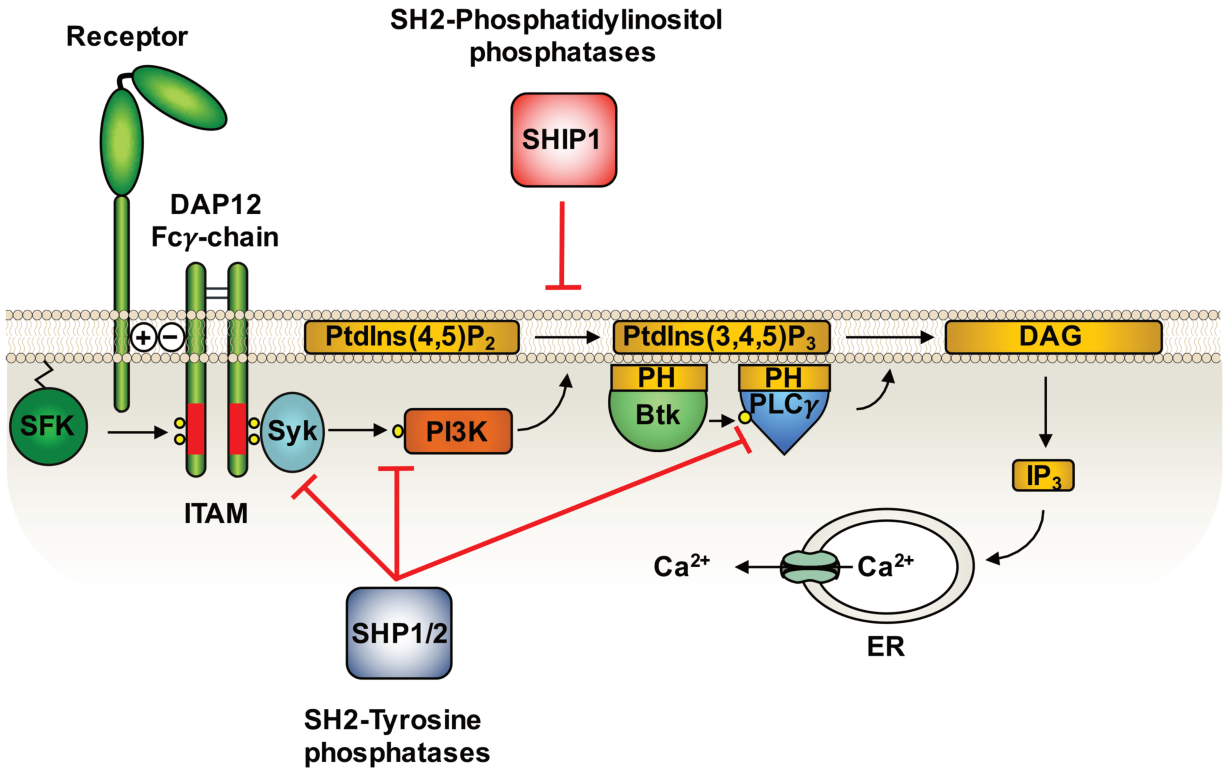

FIGURE 8. INTERPLAY BETWEEN ITAM AND ITIM PATHWAYS

Crosslinking of an ITAM-bearing receptor results in its phosphorylation and in the recruitment of Syk, which in turn activates a number of other signal-transduction molecules. SH2-phosphatases recruited by ITIM-bearing receptor are able to control the activation pathway by different mechanisms. (SFK Src Family Kinase, Syk Spleen Tyrosine Kinase, PI3K phosphatidylinositol 3 kinase, Btk Bruton's Tyrosine Kinase, PH Pleckstrin Homology domain, PLC Phospholipase C, ER Endoplasmic Reticulum, SHP SH2-containing Tyrosine Phosphatase, SHIP SH2-containing Phosphatidylinositol Phosphatase).

6.2.5 CD31 cellular expression and functions

CD31 is expressed constitutively and specifically by the vascular and hematopoietic cells. On endothelial cells, CD31 is expressed at high density at the lateral borders while it is present at a lower density on the surface of hematopoietic and immune cells namely macrophages, neutrophils, monocytes, mast cells, T cells, B cells and platelets. Of note it is not expressed on erythrocytes and mesenchymal cells like fibroblasts, epithelial cells and smooth muscle cells. Thus, given its exclusive expression in the vascular compartment and its signaling features, CD31 presents the criteria to be a major regulator of the homeostasis at the blood/vessel interface.

6.2.5.1 Endothelial cells

Endothelial cells express the highest level of CD31 with approximatively $2*10^6$ copies for each single cell, mostly localized at the lateral junctions (Newman, 1994). Given its abundant expression, CD31 has been demonstrated to be involved in the initial formation and stabilization of cell-cell contacts at junctions between endothelial cells (Albelda et al., 1991), the maintenance of a vascular permeability barrier (Ferrero et al., 1995), and formation of new blood vessels in angiogenesis (DeLisser et al., 1997). Moreover, endothelial cells present a network of intracellular CD31 pool just beneath the plasma membrane which has been shown to actively recycle to the lateral borders when leukocytes are performing the transendothelial migration (Mamdouh et al., 2003). Interestingly, the CD31 trans-homophilic engagement between IL1β-activated endothelial cells and transmigrating leukocytes, results

in a downregulation of NFκB translocation into the nucleus of endothelial cells (Cepinskas et al., 2003). Endothelial CD31 engagement with leukocytes thereby initiate a negative feedback loop that prevents excessive leukocyte recruitment to sites of inflammation by dampening the expression of pro-inflammatory adhesion molecules on the endothelial cell surface.

6.2.5.2 Platelets

Circulating human platelets constitutively express about 10^4 CD31 molecules per cell (Newman, 1994) and the literature largely agree to confer a negative regulatory role for platelet activity. When Platelets are challenged *in vitro* with collagen, the simultaneous crosslinking of CD31 with a monoclonal antibody has been shown to induce CD31 phosphorylation and a subsequent inhibition of platelet aggregation, degranulation and calcium mobilization (Cicmil et al., 2000). *In vivo*, platelets from $CD31^{-/-}$ mice displayed contrariwise enhanced aggregation and α-granules secretion in response to activation (Patil et al., 2001).

6.2.5.3 T cells

On lymphocytes, CD31 is present at $0.5*10^5$ copies per cell and the most studied immunoregulatory function on T cells has been the control of TCR-dependent activation (Newton-Nash and Newman, 1999). Interestingly, CD31 expression is constitutive on this cell type, but peripheral blood T cells with a memory/activated phenotype lack this molecule at their surface (Stockinger et al., 1992). Surprisingly, it has been shown that TCR-mediated activation resulted in the cleavage and shedding of the extracellular T cell CD31 comprising Ig-like domains 1 to 5 with a resulting loss of its inhibitory function, as the necessary trans-homophilic engagement (**FIGURE 7**) cannot be established due to the lack of the distal domains (Fornasa et al., 2010).

6.2.5.4 B cells

In human B lymphocytes, co-ligation of the BCR complex with CD31, inhibits downstream Ca^{2+} efflux (Henshall et al., 2001), while $CD31^{-/-}$ B cells are hyper-responsive upon BCR

engagement (Wilkinson et al., 2002). In relation to these findings, $CD31^{-/-}$ mice have increased titer of circulating IgM and IgG antibodies and are prone to spontaneously develop lupus-like autoimmune diseases with age.

6.2.5.5 Mast cells

CD31 seems to be implicated also in the regulation of mast cells activity, as $CD31^{-/-}$ mice subjected to an experimental type-I hypersensitivity model revealed elevated concentration of serum histamine compared to WT littermates (Wong et al., 2002), suggesting that CD31 may be implicated also in susceptibility to allergic diseases.

6.2.5.6 Macrophages

In macrophages, CD31 has been demonstrated to be implicated in the process of phagocytosis (Brown et al., 2002). The encounter of a viable cell with the phagocyte, leads to the viable cell to actively detach via the homophilic interaction of CD31 on both cell surfaces. During apoptosis, the inside-out signaling of CD31 is somehow disabled so that the apoptotic cell does not actively reject the phagocyte anymore. The lack of CD31 therefore enable the attachment of the apoptotic cell to the macrophage, thus triggering the process of efferocytosis.

6.2.5.7 Neutrophils

Neutrophils are, among the leukocytes, the cell types that express the higher CD31 level (10^5 copies/cell). Nevertheless, very little it is known about its molecular function in this specific cell type. When $CD31^{-/-}$ mice were generated for the first time, neutrophils were surprisingly found trapped at the outside edge of the vascular wall between the endothelial cell layer and the underlying basement membrane in a model of sterile peritonitis (Duncan et al., 1999). The role of CD31 in this process seemed to be dependent from the trans-homophilic engagement between neutrophils and endothelial cell CD31, since chimeric mice with the CD31 genetic invalidation only in hematopoietic cells recapitulate the same phenotype of neutrophil retention found in the complete knockout strain (Dangerfield et al., 2002).This phenomenon has been suggested to be related to an inability of $CD31^{-/-}$ to

upregulate $\alpha_6\beta_2$ integrins with a consequent defect to detach from laminin present on the basement membrane (Dangerfield et al., 2002), even though the molecular mechanism for this phenomenon is currently unknown. In addition, neutrophils derived from $CD31^{-/-}$ mice shown a significant reduction in cell motility and spreading in response to CXCL1, also indicating a possible role for CD31 in modulating neutrophil migration (Wu et al., 2005). The only heterophilic molecular partner found to associate with CD31 in neutrophils is CD177 (Sachs et al., 2007), a neutrophil-specific GPI-anchored glycoprotein for which the function has not been completely elucidated. It has been proposed that CD177 interaction with the CD31 domain 6 is able to destabilize the endothelial cell junctional integrity in such a way as to facilitate the transmigration process (Bayat et al., 2010).

7 AIMS OF MY THESIS

The main commitment of my thesis work has been to evaluate to potential role of CD31 to exert immunoregulatory functions involved in controlling the recruitment and activation of neutrophils during the acute phase of inflammation. By assigning CD31 to the family of adhesion molecules, and based on the studies using genetic deletion or molecules able to block CD31 engagement, it had been previously suggested that CD31 is a yet another molecule involved in neutrophil trans-endothelial migration. Nevertheless, being its ITIM-bearing receptor nature mostly neglected, the signaling functions of CD31 in neutrophil biology have be overlooked so far.

The present work is structured according to the different objectives that I have pursued during my PhD:

(i) The first aim that I had fixed was to investigate the role of CD31 in the biology neutrophils. Nothing is known concerning the dynamic of the expression and distribution of CD31 at the cell membrane, its signaling properties and its molecular partners in neutrophils. All these findings were therefore required in order to proceed the investigations that I have planned.

(ii) The fact that CD31 expression is restricted specifically at the blood/vessel interface, prompted me to considered whether it may play a major role in this compartment. The second aim of my thesis was hence focused in the understanding whether and how CD31 was implicated in controlling neutrophil trafficking from the blood throughout the vascular wall in its way towards an inflammatory site.

(iii) In the third and last part, the experimental works were done in order to investigate whether the CD31 ITIM signaling properties could control neutrophil ITAM-mediated activation in inflammatory conditions in which the effector functions of activated neutrophils can cause severe collateral damages to the host.

My working strategy was based on a complementary approach, using basic science, *in vitro* tools to dissect the putative mechanisms at the cellular/molecular levels and suitable *in vivo* models in order to appropriately test my hypothesis in conditions of experimental acute

inflammation. The function of CD31 has been systematically tested by using two complementary approaches based on the use of $CD31^{-/-}$ mice (loss-of-function) and of a CD31 agonist peptide (gain-of-function). The data obtained in such way allowed us to in-depth dissect the immunoregulatory functions of the CD31 in neutrophils.

The experimental work is structured in three different sections according to the aforesaid aims. Each section is introduced with a description of the context in which the work is placed. The results are then presented in the ensuing paragraphs at the end of which a figure is accompanied by the legend and the material and methods used to generate the related results. Finally, each part is concluded with a summary of the results and a graphical abstract depicting the main findings of the section.

EXPERIMENTAL WORK

8 EXPERIMENTAL WORK

8.1 Aim I: Study of CD31 in the biology of human Neutrophils

8.1.1 Context of Aim I section

CD31 is an ITIM-bearing receptor, constitutively and exclusively expressed by endothelial cells and all cells of hematopoietic origin, with the exception of erythrocytes (Marelli-Berg et al., 2013). Its inhibitory signaling functions have been studied in platelets (Thai le et al., 2003), lymphocytes (Fornasa et al., 2010) and endothelial cells (Cheung et al., 2015). When it comes to neutrophils, however, CD31 has not been comprehensively investigated so far in terms of (i) surface expression, (ii) membrane distribution, (iii) molecular partners, and (iv) signaling functions.

Being essential effectors of the innate arm of the immune system facing noxious agents, neutrophils can undergo deep cellular modifications and change the expression of several membrane proteins in order to react to the specific stimuli (Middelhoven et al., 1997). This phenomenon is rapid and can be accompanied by the modifications of surface receptors through the exocytosis of secretory granules that store ready-made copies of such receptors (Graves et al., 1992) and/or their proteolytical destruction (Zen et al., 2011). The loss of inhibitory molecules caused by the latter process can, however, result in an inappropriate and destructive activation of neutrophils and lead to severe collateral damages to the host.

The aim of the first part of this work was to study the expression and membrane distribution of CD31 in human neutrophil under resting and activated conditions using different experimental approaches. We also sought to study its intracellular signaling properties which, although pivotal for CD31-mediated functions, have never been investigated in this specific cell type. CD31 can indeed be phosphorylated by members of the Src family kinase on its ITIM in order to become a platform for the recruitment of phosphatases (Newman et al., 2001). Consequently, we performed experiments designed to explore the dynamic

phosphorylation of CD31 cytoplasmic ITIM motifs in neutrophils and we developed a molecular tool that was able to sustain its functionality. Finally, we used an unbiased proteomic approach in order to identify putative molecular partners of the CD31 for its role in neutrophil biology.

8.1.2 *The commitment of CD31 into signaling platforms is followed by its shedding in neutrophils*

8.1.2.1 Evaluation of CD31 shedding

With the purpose of studying the dynamics of CD31 expression on purified human neutrophils by flow cytometry, we examined single cell suspensions under resting and activated conditions. Freshly purified human peripheral blood polymorphonuclear cells were first primed with IL-8 and then stimulated with the formyl-Methionyl-Leucyl-Phenylalanine (fMLP) tripeptide, to activate the primed neutrophils (Futosi et al., 2013). Multicolor flow cytometry analysis was then performed in order to evaluate the integrity of CD31 at the cell surface, according to the activation state. To this aim, we used two monoclonal antibodies, each directed against a different portion of the extracellular CD31 molecule (as described in Fornasa et al., 2010), and a third monoclonal antibody directed against CD11b, the signal of which increases in proportion with the extent of cellular activation (Kinhult et al., 2003).

As shown in **Figure 9a**, flow cytometry data demonstrate that at 30 minutes after challenging neutrophils in suspension with fMLP, the MFI corresponding to the most distal extracellular domain (D1) is reduced in an inversely-correlated manner with the MFI of CD11b, which reflected cellular activation (**Figure 9b**). Interestingly, the reduction in the MFI signal corresponding to the membrane-distal domain 1 (D1) of CD31 was not associated with a reduction of the MFI corresponding to a membrane-proximal epitope mapped on the sixth domain (D6), nor with that corresponding to the cytoplasmic tail of the molecule (**Figure 9c**), suggesting that CD31 molecules were truncated and not reduced in their entirety.

To assess whether the truncation (cleavage) of CD31 was due to a neutrophil activation-dependent enzymatic activity, we evaluated the integrity of a recombinant extracellular human CD31 protein sequence (rhCD31, ADP6, R&D Systems), after incubation at different temperatures with the cell-free conditioned supernatants prepared from resting or activated neutrophils. As shown in **Figure 9d**, when incubated with conditioned supernatants at 4°C, rhCD31 was always detectable since at this temperature catalytic activities are largely inhibited. Conversely, when incubated at 37°C, only the addition of conditioned supernatants coming from activated neutrophils resulted in the degradation (decreased detectable amount) of the soluble rhCD31 molecule, suggesting that the reduction of CD31 domain 1, signal assessed by flow cytometry, could be due to the action of an active, temperature-dependent, soluble protease released by activated neutrophils.

8.1.2.2 Analysis of CD31 distribution in membrane microdomains

Many membrane proteins display highly organized yet distinct patterns of distribution which can be further rearranged after specific cellular processes. In this respect, lipid rafts are pivotal membrane micro-domains originally identified as insoluble in the detergent TritonX at 4°C (Brown and Rose, 1992) and implicated in the assembly of transient signaling platforms (Simons and Toomre, 2000).

CD31 has previously been documented to translocate to lipid rafts in collagen-challenged human platelets (Lee et al., 2006). Likewise, we evaluated by Western blot the CD31 dynamic relocation, over the lipid compartments of the cell membrane, after human neutrophil activation. As shown in **Figure 9e**, full-length CD31 gradually disappeared from the TritonX-soluble membrane fraction after fMLP challenging and at 30 minutes it was barely detectable. Interestingly, as soon as 5 minutes, a portion of CD31 translocated to the TritonX-insoluble fraction, while a band of 29 kDa – which was absent in the resting condition – appeared in the raft moiety. In order to understand which segment of CD31 sequence can fit such molecular weight, we performed a computational analysis with the online opensource ExPASy software, searching an amino acid sequence belonging to CD31 with a theoretical mass of 29 kDa and containing a portion of the extracellular domain (since the blot was revealed with a polyclonal antibody directed against the CD31 extracellular portion). As depicted in **Figure 9f**, the sequence spanning from V491 towards the carboxyl-terminal

tail matched those criteria. This was an interesting finding, since it demonstrates that the truncated CD31 that remains at the cell surface of activated neutrophil contains the entire part of the sixth domain, in agreement with previous results in other leukocytes (Fornasa et al., 2010) and in agreement with the flow cytometry characterization (**Figure 9a**).

To resume, when analyzing the dynamics of CD31 molecules at the surface of neutrophil's cell membrane, we found that CD31 is rapidly engaged within lipid rafts upon neutrophil activation and that most of the extracellular portion of the molecule is cleaved, leaving a juxta-membrane fragment lingering at the cellular surface.

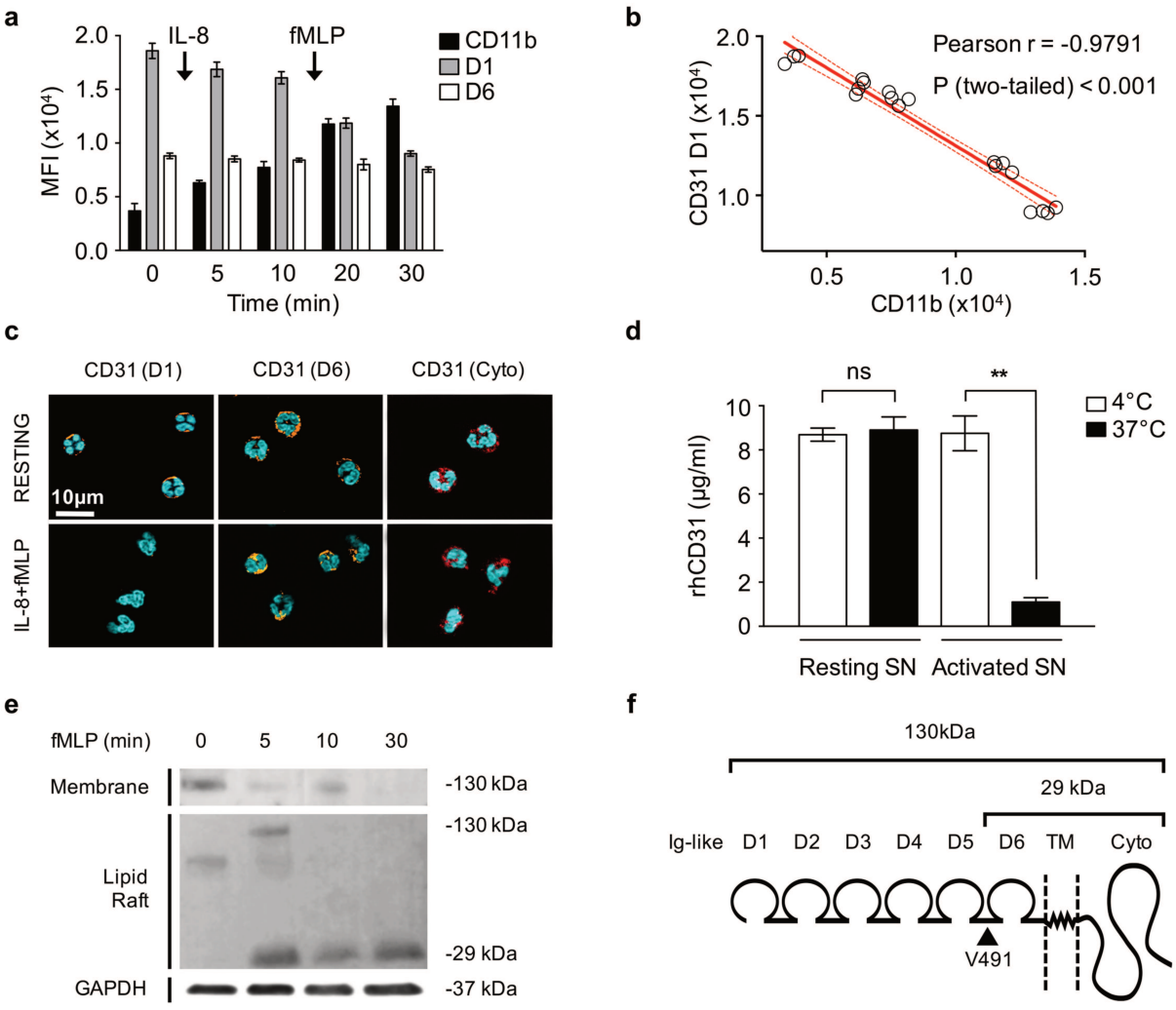

FIGURE 9. NEUTROPHIL'S CD31 IS ENZYMATICALLY SHED UPON CELL ACTIVATION.

(a) *Flow Cytometry analysis of the MFI corresponding to the staining of CD31 domain 1 (D1, clone WM59), CD31 domain 6 (D6, clone MBC78.2) and CD11b (clone D12) expression of freshly isolated human neutrophils challenged with IL-8 (10^{-8}M) and fMLP (10^{-7}M), in suspension, for 30 minutes. At the indicated time points, cells were fixed with 2% PFA, washed, and stained with fluorescent antibody mix for 40 min at 4°C. Flow cytometry analysis was performed using an LSR II flow cytometer (BD Biosciences). Data were analyzed with DIVA 7 (BD Biosciences).* ***(b)*** *Pearson product-moment correlation coefficient of CD31 domain 1 (D1) and CD11b Mean Fluorescent Intensities (MFI).* ***(c)*** *Fluorescent microscopy analysis of CD31 domain 1 (D1), domain 6 (D6) and cytoplasmic tail (Cyto, clone MBC235.1) on cytospin neutrophils activated as described above. Images were captured on a Zeiss Axiovert 200 M inverted microscope equipped with an ApoTome® module.* ***(d)*** *Cell-free conditioned supernatants coming from resting or activated human neutrophils were incubated with 10µg/ml of soluble recombinant human CD31 (rhCD31, R&D Systems # ADP6) for 45 minutes at 37°C or 4°C. The amount of rhCD31 at each time point was measured by cytometric magnetic beads and the BioPlex® technology (Bio-Rad). COOH BioPlex Pro® capture beads were covalently coated with a monoclonal antibody directed against CD31 domain 1 (clone MBC78.3). These beads were added to the biologic fluid containing the rhCD31, washed and incubated with a phycoerythrin (PE)-conjugated monoclonal antibody directed against CD31 sixth domain (clone MBC78.2, Thermofisher #MHCD3104). Data are representative of at least three independent experiment and are expressed as mean ± SD. P *<0.05 **<0.01 ***<0.001 (Unpaired Student's t-test).* **(e)** *Analysis of CD31 membrane distribution by western blot of human neutrophils at indicated times (minutes) after the challenge with fMLP. Stimulated neutrophils were lysed in TritonX-based buffer and detergent-solubilized and insolubilized fractions were separated by SDS-PAGE under non-reducing conditions. Proteins were blotted on a nitrocellulose membrane and stained with a polyclonal antibody directed against extracellular CD31 (Santa Cruz #sc8306). GAPDH was used as internal loading control.* ***(f)*** *Schematic representation of CD31 domains and molecular weights of the different forms identified.*

8.1.3 *The loss of the CD31 signaling due to its cleavage is rescued by a synthetic homophilic peptide that specifically binds the truncated sequence lingering at the cell surface and maintains functional molecular clusters*

As a signaling receptor, CD31 molecules sequentially establish trans-homophilic and cis-homophilic interactions, according to the zipper model proposed by Newton et al. in 1997 (Newton et al., 1997). The membrane-distal domains 1 and 2 (D1/D2) are crucial for establishing the primary trans-homophilic contacts, which in turn are necessary in order to drive, in a second step, the cis-homophilic interactions of the domain 6 (D6) (Paddock et al., 2016). The latter result in the formation of CD31 molecular clusters which allow their proximity to other receptor-associated kinases and the phosphorylation of its Immunoreceptor Tyrosine-based Inhibitory motif (ITIM).

The cleavage of CD31 and shedding of its distal D1/D2 domains invalidates the first, trans-homophilic step of CD31 clustering (**Figure 9a**). However, the since the domain 6 – which is involved in the second, cis-homophilic step of CD31 clustering – remains exposed at the cell surface (**Figure 9c**), we postulated that the engagement of this CD31 fragment could result in the transmission of downstream signals, in spite of its cleavage. This hypothesis was based on the fact that Zehnder and coworkers had shown – more that 20 years ago – that a monoclonal antibody (clone LYP 21) directed against the sixth domain, was the only one (among a panel of five anti-CD31 antibodies) able to inhibit T cell activation in a specific and dose-dependent manner (Zehnder et al., 1995). The same group reported that a CD31 derived 23-mer peptide, corresponding to the epitope of the LYP 21 antibody (Asn-551 to Lys-574), surprisingly exerted the same inhibitory effect of the antibody itself. Zehnder and coworkers could not explain this observation, because they found that the proliferating T cells were “CD31 negative”. Indeed, those cells had most likely undergone an activation-driven cleavage of CD31 (Fornasa et al., 2010) but at that time neither the shedding of CD31 nor the role of domain 6 in the transduction of CD31 receptor signal had been yet reported.

An agent able to rescue CD31 signaling could display an interesting therapeutic potential in pathologic conditions characterized by excessive leukocyte activation. In order to identify a drug-suitable CD31 agonist peptide, we screened two peptide libraries derived from the

human and mouse parent 23-mer sequences (Chen et al., 1997; Zehnder et al., 1995). Functional screening of the peptide libraries was performed by assessing the expression of CD69 on mononuclear cell suspensions (derived from mouse spleen and from human peripheral venous blood) after stimulation by CD3/CD28 crosslinking. The best hit, defined as the sequence that best inhibited both mouse and human T-cell activation (based on CD69 expression), was found within the most membrane-proximal extracellular sequence of the CD31 molecule (**Figure 10a**, 10-mer aa 564-574, sequence NH_2-VRVFLAPVKK-COOH), which is highly conserved between the two species. The aa 564-574 sequence presented unfortunately an inconvenience for its use in aqueous solutions as it displayed very poor solubility in water (**Figure 10b**). Within this conserved sequence, we identified an 8-mer peptide (P8F, L-aminoacids, "forward" sequence NH2-RVFLAPVK-COOH) that was more readily soluble in water as detected by HPLC analysis and that showed minimal aggregated/degraded products (**Figure 10c**). The corresponding 8-mer *retroinverso* peptide (P8RI, D-aminoacids, inverse order sequence NH2-kvpalfvr-COOH) was also synthetized and displayed a very high solubility in water (**Figure 10d**). The double inversion of the P8RI sequence was meant to eventually reproduce the spatial configuration of the P8F sequence, but with the advantage of being resistant to eukaryote peptidases because of the D-enantiomer of its amino acids (Weinstock et al., 2012). Both P8F and P8RI peptides were as effective as the parent 23-mer peptide in reducing the extent of T-lymphocyte activation (data no shown) and we therefore chose the P8RI D-enantiomer (because of its peptidase-resistance) for further development and studies. Since the parent 23-mer peptide had been found to be biologically effective at 2.5mg/Kg subcutaneously (Fornasa et al., 2010), we began with using the same dose-range for pre-clinical studies with this derived sequence.

The subcutaneous injection of this peptide dosage resulted in the peptide being detectable in the plasma up to 8 hours after its injection (**Figure 10e**). In the perspective of pre-clinical studies and drug development, P8RI was subjected to ADME-tox analyses by the evaluation of potassium currents mediated by a transgenic hERG (human ether-a-go-go related gene) channel with using the conventional patch-clamp technique (Yu et al., 2016).

As shown in **Figure 10f**, The IC 50 of P8RI on the hERG potassium tail current amplitude was set at 150 µg/ml, which represents ≈40-fold the maximal detectable concentration of the peak drug concentration (Cmax) in the plasma of mice having received a 2.5mg/kg dose

by subcutaneous injection (Cmax). Of note, at the concentration of 5µg/ml, which is higher than the Cmax, the peptide has no effect on the tail amplitude of the potassium hERG channel.

Based on the physicochemical properties, the adme-tox analysis and its ability to inhibit activated leukocytes, we chose to use the P8RI sequence (patent WO-2013190014), as a pharmacologic molecular tool to target of the lingering CD31 extracellular truncated sequence that remains exposed at the surface of activated neutrophils.

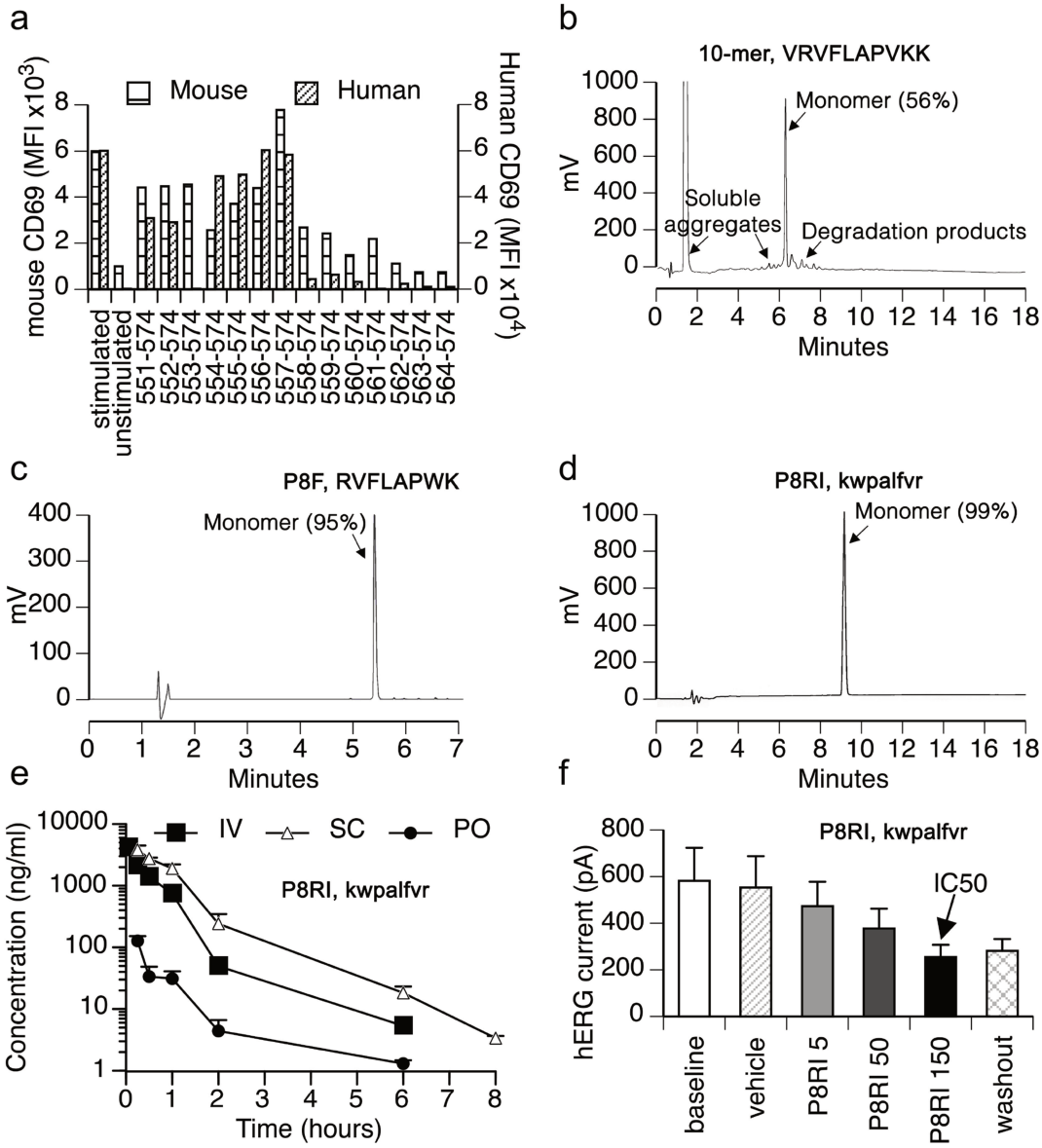

FIGURE 10. IDENTIFICATION OF A DRUG-SUITABLE CD31 AGONIST PEPTIDE

(a) The best hit was selected from a 94 sequences peptide library (obtained by progressive truncation of one amino acid at a time, from the N- or the C- terminal or from both starting from the 23-mer parent human (Zehnder et al., 1995) and mouse (Chen et al., 1997) peptide sequences) on the basis of its ability to reduce both mouse and human leukocyte activation. The best hit following these criteria was a sequence spanning from mouse CD31 sequence aa 564 to 574 (10-mer). ***(b)*** *HPLC analysis of the 10-mer peptide 564 to 574 selected in "a" showed a poor*

water solubility (56% monomer in aqueous solution) and the presence of aggregates and debris of variable size. ***(c)*** *The 8-mer forward (P8F) sequence aa 565-573, fully comprised within the 10-mer sequence but lacking the N-terminal valine and C-terminal lysine, showed an excellent water solubility (95%).* ***(d)*** *The corresponding retro-inverso sequence (P8RI) showed an even greater solubility (99%).* ***(e)*** *Pharmacokinetics, as assessed by plasma concentration time course analysis of P8RI after a bolus administration by intravenous (IV, 1 mg/Kg) or subcutaneous (SC, 2.5mg/Kg) injection, or an oral 2.5mg/Kg dose (per os, PO) in C57Bl/6 mice(n=8/group).* ***(f)*** *In vitro analysis of the hERG tail current amplitude on a stable cell line showed that the IC 50 of P8RI corresponded to the concentration of 150μM (x40 fold the AUC following subcutaneous injection of a 2.5mg/Kg dose in mice).*

As shown in **Figure 11a**, by using a fluorescent-conjugated P8RI version, we found that the peptide did not bind to mouse $CD31^{-/-}$ bone marrow-derived granulocytes, demonstrating that its binding at the cellular surface specifically requires the presence of CD31 (its molecular target). Furthermore, the peptide only bound activated cells, indicating that it may specifically interacts with pre-existing CD31 clusters (i.e. once CD31 is already engaged), rather than forcing CD31 oligomerization on resting cells. This hypothesis was supported by the fact that the peptide gradually increased its the binding to the cellular surface during neutrophil activation and not in a bimodal way (**Figure 11b**).

In order to be defined as an agonist, in addition to binding specifically to the truncated CD31 receptor, P8RI also ought to produce a CD31-mediated biological response. If we consider how the parent CD31 peptides exert their agonist effect on lymphocytes (Fornasa et al., 2010), in order to determine whether P8RI was an agonist for CD31 function on neutrophils, it had to uphold the formation of CD31 clusters and the phosphorylation of the CD31 ITIM motifs. For studying CD31 clusters at the cellular surface, we used Total Internal Refraction Fluorescence microscopy (TIRF), which allows the “en face” appreciation of cell membrane receptor clustering since the excitation of the fluorophores occurs in an extremely thin axial region of the surface over the objective (Fish, 2009). As indicated in **Figure 11c**, TIRF microscopy revealed that resting neutrophils did not present CD31 clusters and no signal of the fluorescent peptide was detectable. When analyzed 30 minutes after neutrophils were challenged with fMLP, when the vast majority of CD31 molecules are shed (**Figure 9c**), no clusters could be observed either, likely because after its cleavage CD31 clusters dissolve,

as it is the case for lymphocytes (Fornasa et al., 2010). However, when neutrophils were activated in the presence of the peptide, CD31 clusters (green staining) were readily detectable even after 30 minutes stimulation, indicating that the peptide was able to hold in place the CD31 clusters in spite of the cleavage and shedding of the surface receptor. Importantly, native CD31 (green) and the fluorescent peptide (red) co-localized together, further supporting the homo-oligomerization of the synthetic sequence with the native receptor within its molecular clusters.

Finally, we investigated the competence of the peptide to sustain CD31 intracellular signaling by performing a Western blot analysis using a monoclonal antibody directed against the phosphorylated form of the CD31 ITIM tyrosine 713 (pY_{713}). As shown in **Figure 11d**, the peptide induced CD31 pY_{713} in a dose-dependent manner. Of note, on resting neutrophils, the Y_{713} ITIM sequence remained unphosphorylated.

Collectively, these data indicate that the homotypic binding of a peptide derived from the juxta-membrane sequence of CD31 can sustain CD31 pathway by holding in place the CD31 clusters that are already established, resulting in the persistence of the downstream CD31 ITIM phosphorylation and functionality. Of note, the peptide had no effect on resting cells. Therefore, I have used this peptide, as a “CD31-agonist” pharmacologic tool, during the subsequent parts of my work in order to study the effect of CD31 “gain of function” in neutrophil biology.

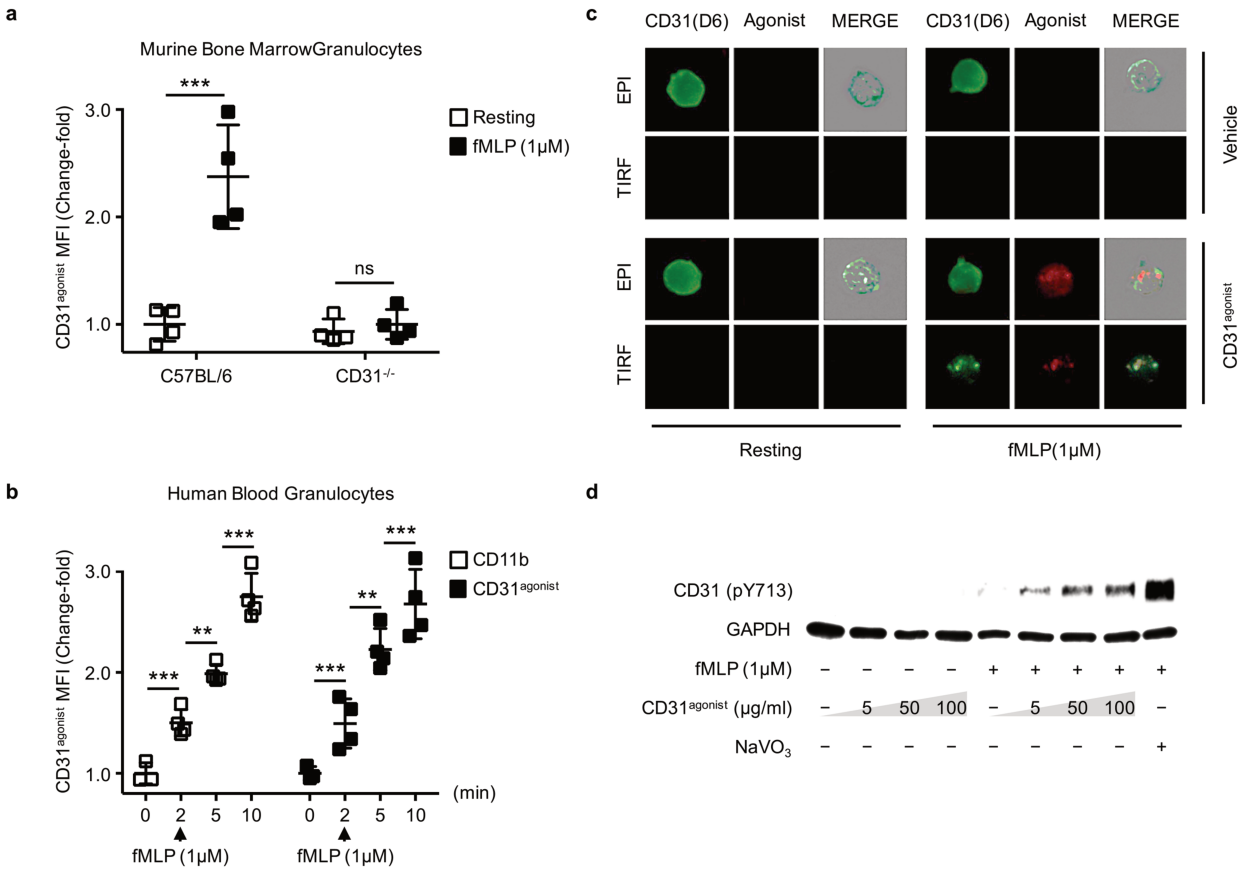

FIGURE 11. CHARACTERIZATION OF THE CD31^{AGONIST} PEPTIDE IN RESTORING CD31 FUNCTIONALITY IN NEUTROPHILS

To restore the CD31 signaling that is lost by its cleavage and shedding, the homophilic octopeptide (CD31^{agonist}) was used to engage the CD31 pathway. ***(a)*** *In order to assess the specificity of the CD31^{agonist} binding to neutrophils, neutrophils were prepared from CD31$^{+/+}$ and CD31$^{-/-}$ mice. Femurs were flushed with ice-cold PBS/EDTA under sterile conditions and filtered through a 70µm cell strainer. Whole bone marrow single cell suspensions were incubated with a fluorescent FITC-conjugated CD31^{agonist} and stimulated or not for 10 minutes with 10^{-7}M fMLP at 37°C. Co-staining of the cells was carried out as described before and analyzed by flow cytometry. CD31^{agonist} intensity was measured from the granulocytes gate established on FSC/SSC morphological parameters. MFI were reported as the fold-change from the basal condition.* ***(b)*** *In order to study the dynamic binding of the CD31^{agonist} on neutrophil under basal and activated conditions, purified cells from healthy donors were incubated with 50µg/ml of the FITC-conjugated CD31^{agonist},*

*stimulated with fMLP, and analyzed at different time points. At each time point, cells were washed and fixed with 2%PFA for 10 minutes at 4°C. Neutrophils were then stained with a monoclonal antibody directed against CD11b (clone D12) and analyzed by flow cytometry using an LSR II flow cytometer (BD Biosciences). Median fluorescent intensities (MFI) were reported as a fold change from the unstimulated, baseline condition (time 0). Data are representative of two independent experiments and are expressed as mean ± SD. P *<0.05 **<0.01 ***<0.001 (Unpaired Student's t-test).* ***(c)*** *Freshly isolated human neutrophils were stained with an A488-conjugated monoclonal antibody directed to CD31 sixth domain (D6, clone MBC78.2) and with or without a rhodamine-conjugated form of the $CD31^{agonist}$. Next, neutrophils were stimulated with fMLP for 30 minutes, washed, fixed and analyzed by TIRF or Epifluorescence (EPI) microscopy. In the presence of the $CD31^{agonist}$ (red), CD31 clusters (green staining) were readily detectable, upon neutrophil activation with fMLP. No clusters could be observed in resting neutrophils, nor on activated neutrophils in the absence of the $CD31^{agonist}$.* ***(d)*** *Primary human neutrophils were isolated from a healthy donor as described above. Cells were pre-treated or not with incremental doses of $CD31^{agonist}$ for 10 minutes and then incubated for additional 10 minutes with fMLP (to provoke activation) or vehicle (to obtain "resting" condition, for comparison) at 37°C. Sodium Pervanadate ($NaVO_3$) condition was used as a positive control for protein phosphorylation. Neutrophils were then lysed in lysis buffer and 20µg of proteins from each condition were separated by electrophoresis and blotted onto a nitrocellulose membrane. A monoclonal antibody against phosphorylated CD31 tyrosine-713 (rabbit monoclonal anti-pY_{713}, Abcam #ab180175) was used to reveal ITIM phosphorylation on the blots. Total protein content was assessed by detection of the GAPDH in each lysate.*

8.1.4 Molecular reshaping of CD31 may influence the CD31/integrin interaction during cell migration

CD31 is an immunologic co-receptor in the sense that it does not possess intrinsic catalytic activities and needs to associate to other receptor proteins in order to acquire its signaling properties (Ilan and Madri, 2003). Indeed, CD31 has been shown to be an important scaffolding molecule for other proteins/receptors in platelets (Lee et al., 2006), macrophages

(Deaglio et al., 1998; Wang et al., 2011) and endothelial cells (Biswas et al., 2005), but little is known about CD31 molecular partners in human neutrophils.

To study this aspect of the CD31 biology in neutrophils, we choose a proteomics approach in order to find CD31 partners in neutrophils without any *a priori* knowledge (Zhang et al., 2013). We performed a co-immunoprecipitation on resting and fMLP-stimulated human neutrophils lysates using magnetic beads covalently-bound with a monoclonal antibody directed against CD31 domain 6 (clone MBC78.2) followed by a mass spectrometry proteomic analysis. For this experiment, the selection of detergent for cell lysis was critical, as we sought to solubilize the lipid rafts in which CD31 was supposed to translocate (**Figure 9e**). Octyl β-D-glucopyranoside was our choice of election because it has a superior solubilizing power (compared to NP-40 and TritonX), while its non-ionic chemistry allows to maintain native protein-protein interactions (Kan et al., 2013).

As indicated in **Figure 12a**, CD31 co-immunoprecipitated with CD177, a putative CD31 molecular partner that was previously reported in the literature (Sachs et al., 2007). CD177 is a GPI-anchored protein that belongs to the Ly-6 superfamily and its function has not been completely elucidated except that it has been proposed to play an important role in neutrophil-endothelial interactions (Bayat et al., 2010). Another CD31-associated protein was PR3 (Proteinase 3 or Myeloblastin), a serine protease whose expression is restricted to polymorphonuclear leukocytes. PR3 has already been found to be associated with CD177 (Bauer et al., 2007; Jerke et al., 2017), but this is the first time that the proximity of PR3 and CD177 is reported in the same molecular complex with CD31. In the light of the cleavage findings, it is tempting to speculate that PR3 may act as the responsible protease on activating neutrophils, although in the present work we did not explore further this possibility. From a functional point of view, the most important finding was that β_2-integrins were major CD31 molecular partners in human neutrophils in our experimental conditions. Strikingly, the association of β_2-integrins with CD31 was dramatically reduced in fMLP-activated neutrophils. On the basis of our previous findings and of this observation, we hypothesized that the engagement of CD31 may modulate the function of β_2-integrins and that cleavage of CD31, which results in the dissolution of its clusters and invalidated of its co-receptor functions, could be a rapid mechanism employed by the activated cell to release integrin from the regulatory CD31 pathway.

In order to visualize the association of CD31 with β_2-integrins in real-time, we realized time-lapse fluorescent microscopy experiments in which purified human neutrophils in suspension were labelled with different monoclonal antibodies and then placed onto a fibronectin-coated surface to allow their adherence and movements. As soon as the cell adhered to the surface, CD31 and CD11b rapidly reorganized at the uropod (**Figure 12b**), but a minor fraction of both molecules remained localized at the opposite, minor pole. Of note, the entire CD31 molecule (positive staining for both domain 6 and domain 1) was present at the uropod, whereas at the minor pole, CD31 molecules appeared to be cleaved (the staining for domain 6 was positive but that for domain 1 was negative) suggesting that the presence of an intact CD31 may be important for preventing integrin activity. Indeed, the adhesion-state is weak at the uropod so as to facilitate rear detachment during forward cellular movements (Hind et al., 2016). Instead, the cleavage of CD31 at the minor pole may be necessary in order to uncouple the integrin-regulatory function of CD31 and allow the integrins to exert their properties for the effective adherence of the neutrophils.

a

Description	Accession Number	∑Coverage	∑#Unique Peptides	Normalized Score (resting)	Normalized Score (fMLP)
CD31	P16284	23.85	14	148.51	144.59
CD177	Q8N6Q3	22.43	2	41.57	62.64
PR3	P24158	37.89	4	13.42	44.78
Integrin beta-2	P05107	28.22	14	128.74	28.34

b

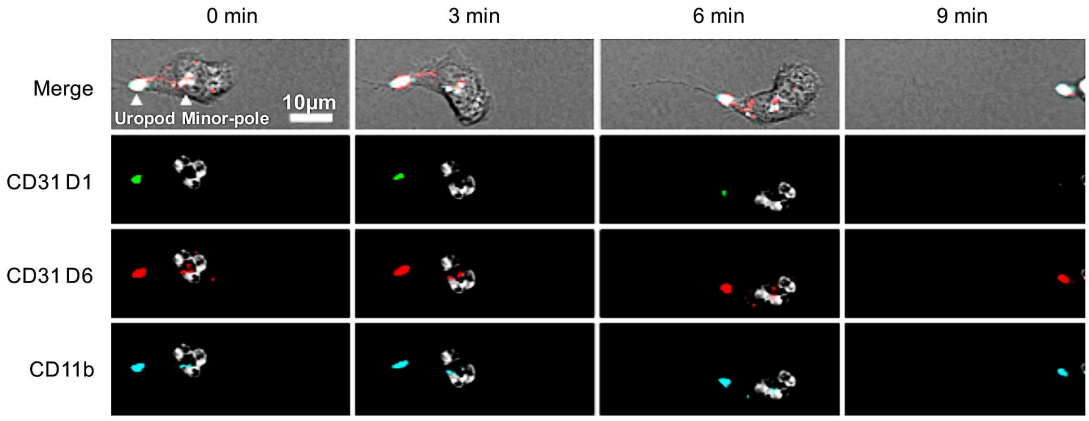

FIGURE 12. CD31 DYNAMICALLY PARTICIPATES TO INTEGRIN MOLECULAR COMPLEXES

(a) *Example of results from shotgun proteomic experiments used for the identification of CD31 partner in human neutrophils. Peripheral blood-derived human granulocytes were treated with or without fMLP (10^{-7}M) for 10 minutes at 37°C, in duplicates. Cells were next lysed in a modified RIPA buffer containing 1% Octyl-beta-d-Glucopyranoside for 30 min on ice. Nuclei and cellular debris were separated from solubilized proteins by centrifugation (14000 g, 10 min at 4°C). Pre-cleared lysates were incubated with magnetic beads covalently bound with a monoclonal antibody directed against CD31 domain 6 (clone MBC78.2) for 2 hours at 4°C. After extensive washing with PBS-Tween (0.5%), bead-captured molecular complexes were digested with trypsin and processed for protein analysis with a LTQ Velos Orbitrap equipped with an EASY-Spray nanoelectrospray ion source coupled to an Easy nano-LC Proxeon 1000 system (Thermo Fisher Scientific). MS data were treated with Mascot® search server for protein identification. Probability thresholds were set greater than 90% probability for protein identifications, based upon at least 2 peptides identified with 80% certainty. The score for each protein was normalized with the score*

of the same protein obtained with a decoy immunoprecipitation in the same conditions using beads coupled with a control isotype antibody (preclearing step). Normalized scores were accepted as significant if greater than 10. ***(b)*** *Time-frames images from a video of neutrophils stained with fluorophore-coupled monoclonal antibodies directed against CD11b (clone D12, APC-conjugated), CD31 domain 1 (D1, clone WM59, FITC-conjugated), and domain 6 (D6, clone MBC78.2, PE-conjugated) for 10 minutes at room temperature. Cells were placed onto a fibronectin-coated surface (ibidi #80823) to allow their adherence/migration. Images were recorded for 10 minutes, starting from the addition of the neutrophil suspension to the ibidi wells, using a Zeiss Axiovert 200 M inverted microscope.*

8.1.5 *CD31 signaling at the uropod may switch β_2-integrin towards inactive forms*

Having described the co-localization of CD31 with β_2-integrins, we hypothesized a role for CD31 in integrin-related signaling. Since integrins are key molecules involved in the process of adherence and detachment of moving neutrophils, we aimed at determining at a sub-cellular scale whether CD31 was phosphorylated (and hence biologically active) at the sites of integrin clusters on the cell membrane.

Purified polymorphonuclear cells from healthy donors were plated onto a polystyrene surface previously coated with ICAM-1 (the optimal ligand for β_2-integrins) and IL-8 (with the aim to favor neutrophils movements and promote the inside-out integrin conformational opening). After fixation, cells were stained with different fluorescent monoclonal antibodies for multicolor confocal microscopy analysis. As shown in **Figure 13**, in agreement with the previous real-time fluorescent microscopy experiments, confocal analysis confirmed that CD31 molecules were mostly concentrated at the uropod of adhering neutrophils. Importantly, these CD31 clusters, at the cell rear, were phosphorylated on their ITIMs, as assessed by concomitant immunofluorescent staining using a monoclonal antibody directed against the phosphorylated CD31 Y_{713} (one of the two ITIM motifs present at the cytoplasmic tail of the protein), indicating that CD31 signaling is functionally engaged at the uropod

(**Figure 13a**). In addition, we found that the SH2-containing Inositol Phosphatase SHIP1 (**Figure 13b**), which is one of the phosphatases that can be recruited and activated by the phosphorylated ITIMs of CD31 (Pumphrey et al., 1999), was also concentrated at the cellular rear, at the same site of the cellular membrane. These observations support our hypothesis that, during cell migration, an intact, functional CD31 is engaged at the uropod of neutrophils.

Previous studies had already attempted to explore the role of CD31 in respect to integrin-driven migration, but the different experimental designs that had been used in the past had led to puzzling and conflicting results. Indeed, by simply counting the number of cells that remain attached to a surface after stimulation followed by a washing step, it had been reported that the ligation of CD31 by specific monoclonal antibodies, augment β_2-integrin-driven adherence of neutrophils (Berman and Muller, 1995), while other experiments have shown, inversely, that CD31 homophilic engagement in human macrophages induced cellular detachment by transmitting “leave-me-alone” signals (Brown et al., 2002).

In order to analyze the role of CD31 in regulating integrin activity during neutrophil migration, we reasoned that it was important to analyze in detail the conformation of the integrin at the site of CD31 localization. Indeed, integrins change their orientation during activation and switch from a low-affinity bent structure to an open state in which they present a high-affinity binding site (Campbell and Humphries, 2011). As shown in **Figure 13c**, the staining of neutrophils with an antibody that binds $\alpha_L\beta_2$ integrins (LFA-1) – regardless their conformation – localized both at the uropod and at the focal zone, while at the lamellipodium the staining was more diffuse. We therefore used the reporter antibodies NKI-L16, the epitope of which is exposed only when this β_2 integrins is extended (Lefort et al., 2012), whereas it is cryptic and not accessible on bent LFA-1. Interestingly, the staining for intact CD31 and for extended β_2-integrins were mutually exclusive: NKI-L16 positive clusters (opened integrins) were localized exclusively at the migrating focal zones, were intact CD31 was absent, whereas the staining with this antibody was absent at the uropod, where most intact CD31 was concentrated. The fact that CD31-positive clusters co-localize with integrin that display no reactivity towards NKI-L16 mAb, indicates that CD31 is enriched at the uropod together with inactive LFA-1, in contrast to activated integrins, which are restricted to the midcell zones.

Altogether, our data suggest that CD31 signaling may play a role in controlling integrin conformation, maintaining them in a closed/bent conformation at the uropod – where the cell needs to detach – during cell migration.

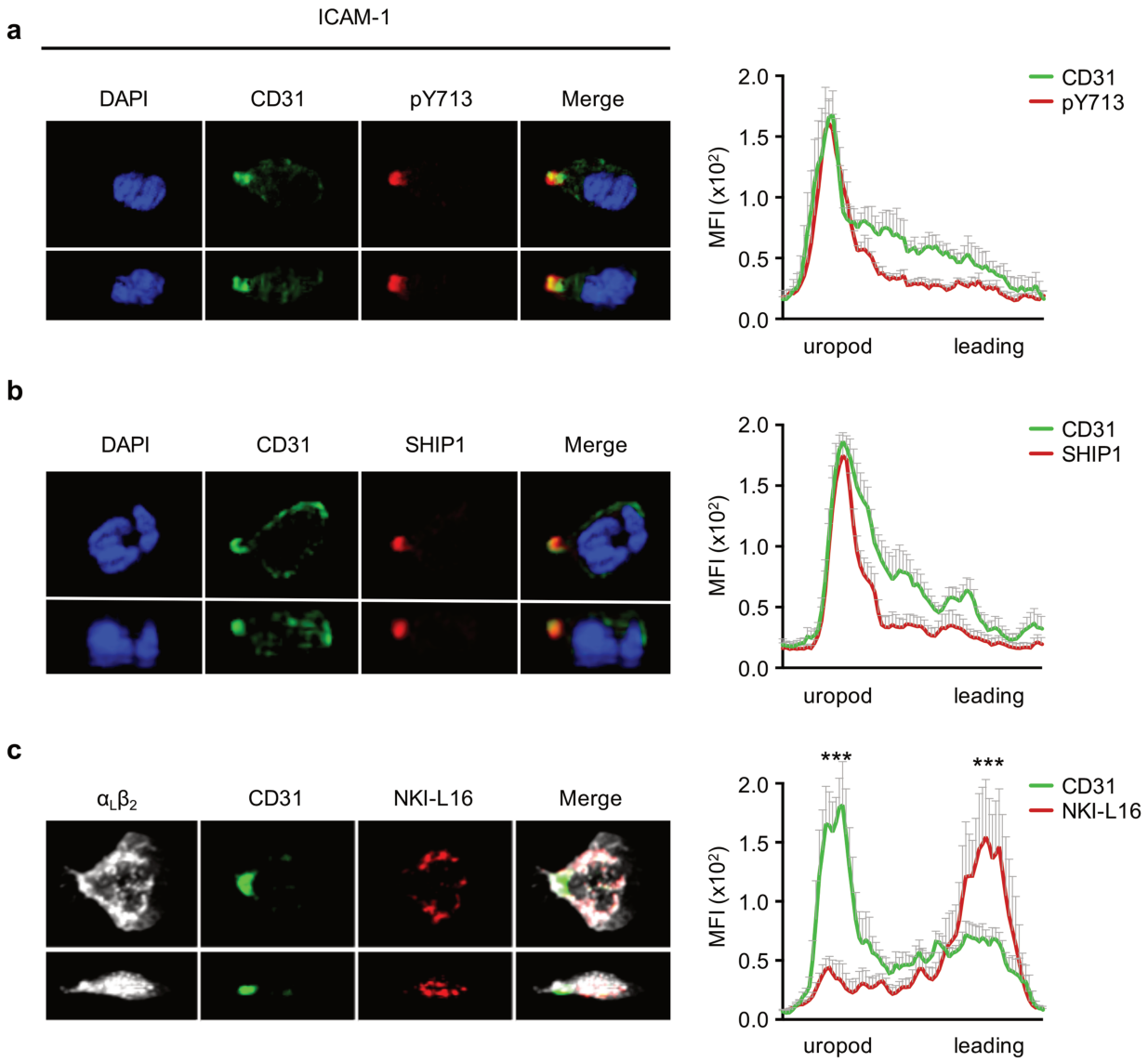

FIGURE 13. CD31 AND INACTIVE BETA 2 INTEGRINS COLOCALIZE IN UROPODS

Polystyrene slides (Ibidi #80826) were coated with recombinant human ICAM-1 (R&D Systems # ADP4) overnight at 20µg/ml. The next day the slides were blocked 1 hour with 1%BSA and IL-8 (R&D Systems # 208-IL-050, 10ng/ml). Freshly-isolated human neutrophils were placed on coated surfaces for 5 minutes at 37°C. Cells were then fixed with 2% PFA for 10 minutes on ice and

stained with fluorescent-labelled monoclonal antibodies directed against CD31 D1/D2 (clone WM59, green) and ***(a)*** *against the phosphorylated CD31 ITIM 713 (pY_{713}, clone EPR8079, red),* ***(b)*** *against SHIP-1 (clone P1C1, red) or* ***(c)*** *against CD11a (clone TS2/4, white) and CD11a active conformation (clone NKI-L16, red). Cells were mounted in ProLong Gold® and Z-stack images were taken with a Zeiss Axiovert 200 M inverted microscope equipped with an ApoTome® module. Representative 3D reconstructions of top and side view are shown. Quantification of mean fluorescence intensities (MFI, gray values range 0-255) of the indicated staining along the cell axis is also shown (mean ± SEM [SEM bars in grey color]; n > 10 cells/staining; statistical comparisons between the 20 first frontal and 20 last posterior measurement points). P *<0.05 **<0.01 ***<0.001 (Unpaired Student's t-test). Images and quantifications are representative of 3 independent experiments with 3 different donors.*

8.1.6 Summary of Aim I section and graphical abstract

The first part of this study was aimed at investigating the biology of CD31 in primary human neutrophils. We found that the CD31 is expressed on resting leukocytes in basal conditions. Nevertheless, after cell activation, the molecule rapidly (<5 min) translocate in detergent-resistant membrane regions where it is enzymatically degraded during neutrophil activation. Surprisingly, the fact that a juxta-membrane portion of the molecule is still at the cellular surface suggests that the engaged CD31 has been subjected to a shedding process rather than being completely degraded. PR3 is a putative for completing the CD31 proteolysis since we found it to be associated with CD31 by MS analysis. This will have to be confirmed by supplementary experiments.

We aimed next at rescuing the functionality of shed CD31 with an homophilic synthetic peptide derived from the first 8 amino acids belonging to the extracellular sequence of the protein. We could demonstrate that this peptide was able to specifically bind to its target and that the binding would be probably influenced by the presence of pre-existing CD31 molecular complexes. Additionally, this peptide was able to maintain both CD31 clusters and CD31 ITIM phosphorylation (even after neutrophil activation), indicating that it is a *bona fide* agonist.

From a functional point of view, we uncovered the fact that CD31 interacts with β_2-integrins and that this partnership is lost upon shedding, suggesting that CD31 might have a role in controlling integrin activity in human neutrophils. Given that integrins are implicated in cellular adhesion, we observed by fluorescence microscopy the dynamic localization of these proteins in motile neutrophils. As a matter of fact, functional CD31 rapidly redistributed at the uropod during cell migration, along with integrins which were in an inactive form. Given that the cellular rear is characterized by a low-adhesion state, as a whole our results suggest that CD31 might restrain integrin activity and thus might have a role in controlling neutrophil trafficking during inflammatory processes.

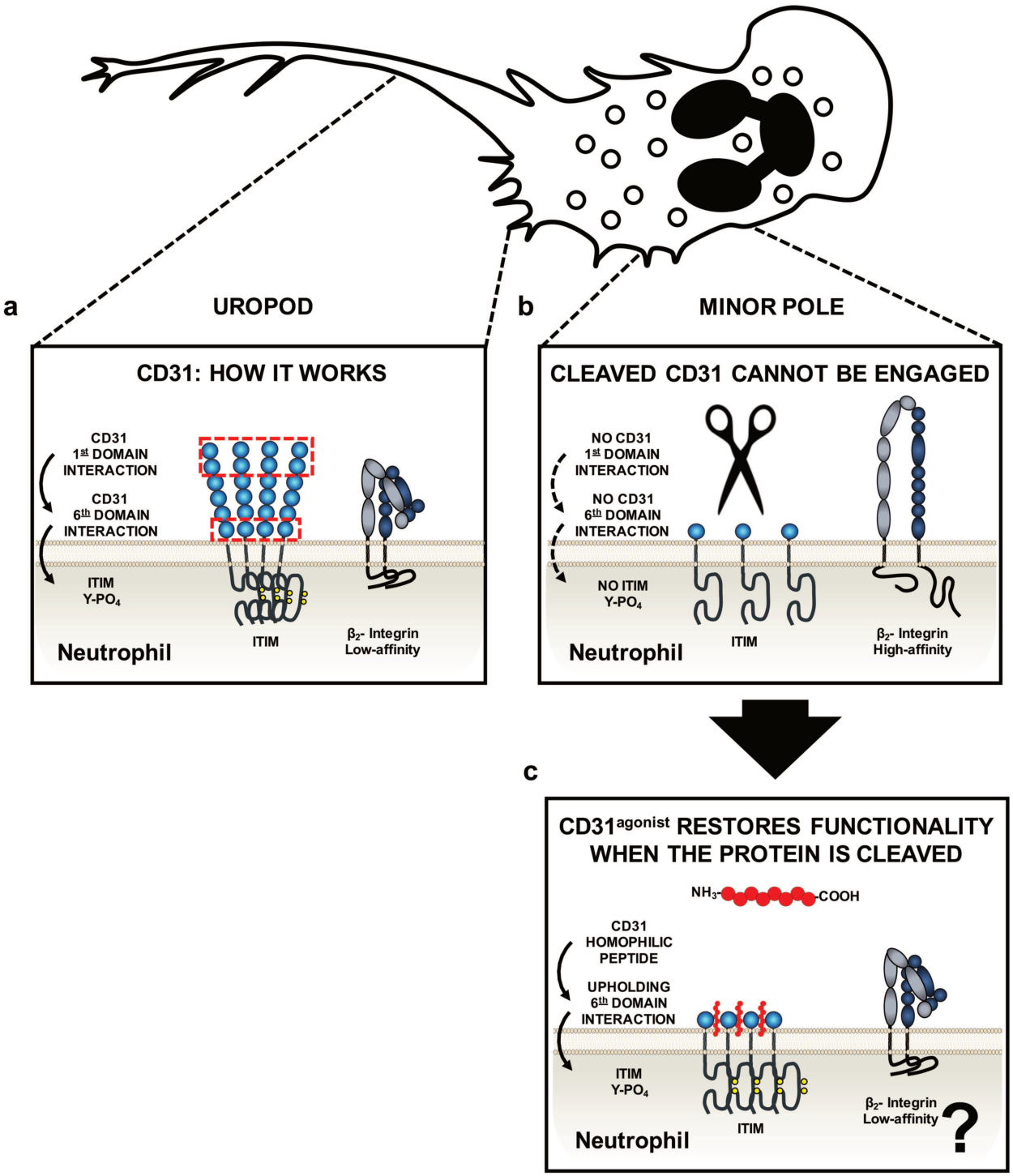
a
UROPOD
b
MINOR POLE
CD31: HOW IT WORKS
CD31
1st DOMAIN
INTERACTION
CD31
6th DOMAIN
INTERACTION
ITIM
Y-PO4
Neutrophil
ITIM
β2- Integrin
Low-affinity
CLEAVED CD31 CANNOT BE ENGAGED
NO CD31
1st DOMAIN
INTERACTION
NO CD31
6th DOMAIN
INTERACTION
NO ITIM
Y-PO4
Neutrophil
ITIM
β2- Integrin
High-affinity
c
CD31agonist RESTORES FUNCTIONALITY
WHEN THE PROTEIN IS CLEAVED
NH3-
-COOH
CD31
HOMOPHILIC
PEPTIDE
UPHOLDING
6th DOMAIN
INTERACTION
ITIM
Y-PO4
Neutrophil
ITIM
β2- Integrin
Low-affinity
?

FIGURE 14. GRAPHICAL ABSTRACT OF AIM I SECTION

(a) *CD31 engagement results in molecular clustering mediated by the first distal domain and it is further stabilized by cis-interactions of the sixth domains. CD31 clusters are phosphorylated on ITIM motifs and co-localize at the uropod with bent/inactive integrins during neutrophil migration.* ***(b)*** *Neutrophil activation results in CD31 shedding that leave the sixth domain at the cell membrane. Proteolytic cleavage provokes CD31 disengagement that shuts down its signaling and dissolves CD31 molecular clusters. Non-functional, cleaved CD31 is present at the minor pole and co-localize with open, active integrins.* ***(c)*** *The binding of the* $CD31^{agonist}$ *on the lingering sixth domain, rescued CD31 signalization and may restore its competence in controlling integrin adhesiveness.*

8.2 Aim II: CD31 and neutrophil recruitment during the acute phase of inflammation

8.2.1 Context of Aim II section

Neutrophils are the most abundant leukocyte population in the blood and crucial immune effectors in the acute phase of inflammation (Kolaczkowska and Kubes, 2013). After their differentiation in the bone marrow, mature neutrophils incessantly patrol and scan endothelial cells in the microvasculature, searching for extravasation signals locally driven by the presence of noxious agents. The ability to establish strong interactions with activated endothelial cells, culminating in the complete arrest and breach across the endothelial barrier, is one of the most important step in neutrophil-mediated acute inflammatory response. The exit of neutrophils from the blood, which occurs primarily at the level of the post-capillaries venules (Muller, 2013), follows an ordered procedure referred to as “neutrophil recruitment”.

The classical multistep cascade of neutrophil recruitment consists in (i) an initial capture of neutrophils onto activated EC, (ii) rolling on the endothelium, (iii) firm arrest, (iv) crawling, (v) transmigration across the endothelial layer, (vi) detachment from the vessel and (vii) migration towards the inflammatory site. During this process, the neutrophil must integrate a multitude and very complex amount of information, since each step provides continuous and overlapping instructions that influence the next one (Nourshargh and Alon, 2014). Neutrophil adhesion is principally mediated by their β_2-integrins in a non-redundant manner, as the genetic deficiency of the β_2 subunit (ITGB2) in humans leads to a severe pathology known as leukocyte adhesion deficiency (LAD), which results in recurrent bacterial infections (Hanna and Etzioni, 2012).

While neutrophils infiltration to injured tissue is needed, their powerful cytotoxic potential, if not kept under check, can be disastrous and it can provoke tissue injury as documented in many inflammatory disorders including ischemia reperfusion (Yago et al., 2015), Alzheimer's disease (Zenaro et al., 2015) and rheumatoid arthritis (Wipke and Allen, 2001).

The present section will show the results we obtained in experimental settings aimed at studying the role of CD31 in controlling neutrophil trafficking towards the inflammatory site.

8.2.2 Genetic deficiency of CD31 endows neutrophils with improved rolling capacities

Mature neutrophils continuously circulate in blood vessels establishing weak, transient contacts with the selectins expressed by the endothelial cells, a process known as “fast rolling” in which the speed of the rolling neutrophils is of about 40 μm/sec in post-capillary venules. Leukocyte velocity is dramatically reduced to approximately 5 μm/sec on inflamed endothelial cells: in these conditions, the inside-out conformational activation of integrins allows the neutrophil to establish additional interactions with cell-adhesion molecules exposed on activated endothelial cells (Kuwano et al., 2010). Indeed, in resting conditions, circulating leukocytes ought not to stick to the healthy endothelium and thus maintain their integrins into an inactive state. When they need to establish strong interactions with the inflamed endothelial cells, they must decrease their speed and eventually stop, resisting against the force exerted on them by the blood flow.

We hypothesized that CD31 could have a role in the control of the leukocyte adhesion on endothelial cells based on the following observations: (i) CD31 is a trans-homophilic receptor constitutively expressed at the surface of both leukocytes and endothelial cells, suggesting that it may play key functions in the regulation of the neutrophil-endothelial cell interactions that take place during the recruitment steps; (ii) CD31-CD31 interactions have previously been shown to actively drive cell-cell detachment of live cells (Brown et al., 2002); (iii) we found – as shown in the experimental part I (**Figure 13**) – that intact and functional CD31 closely associates with closed integrins at the uropod of adherent neutrophils, whereas the CD31 molecules that associate with the active integrins at the migration front are truncated (cleaved, not functional). To test this hypothesis, we have setup an *in vitro* system in which primary microvascular endothelial cells deriving from C57BL/6 mice were seeded in micro-fluidic channels and cultured under pulsatile flow. In order to study the rolling of neutrophils on these EC, we proceeded with an overnight TNF-α stimulation which resulted in the

loosening of the junctional organization (assessed by VE-cadherin expression) thus affecting the EC permeability (**Figure 15a**, left panels). Of note, the TNF-α-stimulation was necessary in order to provide the endothelial cells with suitable adhesive properties allowing to retain neutrophils under physiological venular shear stress (**Figure 15a**, right panels). This setting was therefore suitable to study whether and how the loss of the CD31 signaling pathway could modify the neutrophil adhesion steps.

Experimental neutrophils were purified from WT and $CD31^{-/-}$ mice, stained with distinct fluorescent dyes and mixed together in order to study their behavior in the same experimental condition. To this purpose, the stained cells were placed in the flow chambers and allowed to run over the pre-activated endothelial cells in competition. The flow was set at a speed mimicking the post-capillary flow condition. These assays were performed using an equal number of WT and $CD31^{-/-}$ neutrophils within the same channel, in order to avoid a possible channel-to-channel bias. As shown in **Figure 15b** and **c,** compared with wild type cells, the rolling velocity of CD31 deficient neutrophils was significantly reduced, indicating that the interactions established by neutrophils with endothelial cells are stronger in the absence of CD31. Moreover, the total distance covered by each neutrophil was shorter (**Figure 15d**, **e**), indicating that the absence of CD31 favored the steps preceding the complete arrest.

These findings indirectly indicate that the loss of CD31 provide neutrophils with an advantage during the adhesion steps. The “slow rolling” and “firm adhesion” steps are mediated by selectin and conformationally-opened integrins (Ley et al., 2007) thus we propose that CD31 may have a role in controlling the activation (conformation changes) of the integrins during neutrophil recruitment.

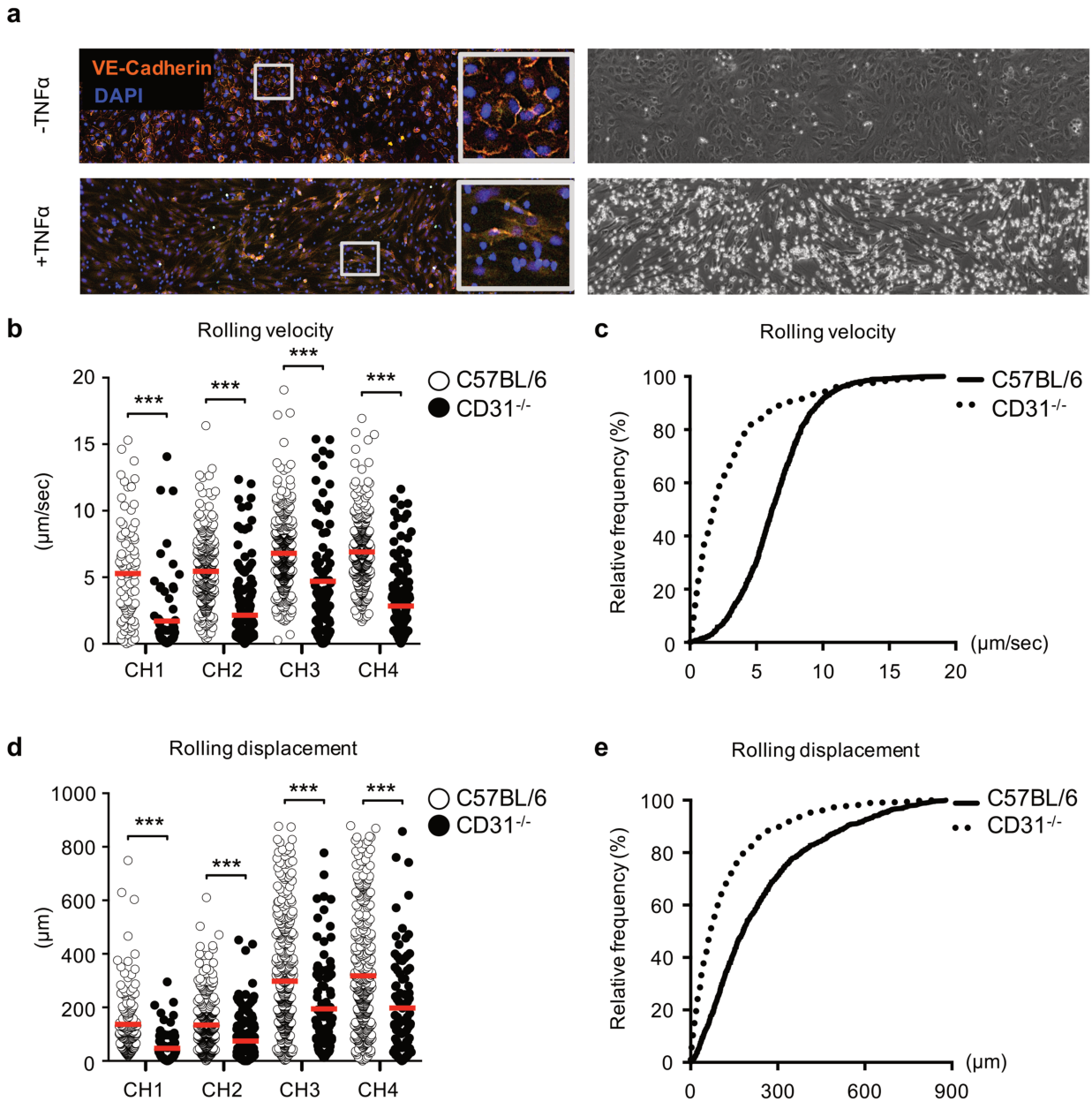

FIGURE 15. CD31$^{-/-}$ NEUTROPHILS EXHIBIT ENHANCED 'SLOW ROLLING' BEHAVIOR *IN VITRO*

(a) *Experimental setup to analyze neutrophil-endothelial cell-cell interactions under physiological flow conditions in vitro. Primary small intestinal microvascular endothelial cells derived from C57BL/6 mice (Cell Biologics #C57-6054) were seeded (10^6/channel) on fibronectin-coated Vena8® chips (Cellix #V8EP-800-120-02P10) and cultured for 48h under a 6.2 dynes/cm^2 pulsatile flow (Cellix Kima pump® system). Cells were then stimulated overnight with 10nM TNF-α in order to activate the EC signals necessary to allow the adhesion of neutrophils.* ***(b)*** *Neutrophils were*

purified from C57BL/6 WT or CD31$^{-/-}$ bone marrows with using a negative immunomagnetic selection kit (STEMCELL #19762), following to the manufacturer's instructions. Cells of the two genotypes were separately stained with distinct fluorescent probes (ThermoFisher CFSE #C34571 and Cell tracer violet #C34570) and then washed twice to discard residual extracellular dyes. Fluorescent WT and CD31$^{-/-}$ neutrophils were mixed 1:1 in the same cell suspension, in order to assess their rolling in a competitive manner. Neutrophils were allowed to run in 4 individual flow channels over the pre-activated endothelial cells during 5 minute and videos were acquired with a Zeiss Axiovert 200 M inverted microscope. In parallel conditions, the dyes used to trace the neutrophils purified by WT and CD31$^{-/-}$ mice were inversed, to ensure that fluorophores were not interfering with cell behavior. Rolling parameters were analyzed using an automated ImageJ Plugin (Trackmate) within each channel (CH1–CH4). Each point represents the velocity of one cell defined as its average speed during its tracking. ***(c)*** *The percentages of relative frequency distribution of pooled rolling velocities of WT and CD31$^{-/-}$ neutrophils are also shown.* ***(d)*** *Cellular displacement of each of the 4 channels (CH1 through toCH4) was calculated with the Trackmate Plugin and data are expressed as the travelled distance of each neutrophil, from the start to the end of its track.* ***(e)*** *Cumulative frequency distribution was calculated with Prism GraphPad software. The percentage of frequency distribution of all neutrophil tracks, by WT and CD31$^{-/-}$ neutrophils is shown and data are expressed as individual points and mean (red dash) of all points in each individual channel. p *<0.05 **<0.01 ***<0.001 (Unpaired Student's t-test).*

8.2.3 CD31 engagement by the peptide controls leukocyte-endothelial cells interactions in vivo

In vitro flow chambers are powerful experimental tools to investigate cell rolling under "physiological flow" but they cannot reproduce the complexity of vessels' structure nor the hemodynamics of the whole blood in the circulation.

To explore *in vivo* the role of CD31 in leukocyte adhesion within the systemic circulation, we performed intravital microscopy experiments in wild-type or CD31$^{-/-}$ mice. The mesenteric microcirculation was chosen as the anatomical site of investigation because the surgery procedure to prepare the small intestine is quick and easy. Indeed, as the only surgical

incision is along the *linea alba* (which does not contain blood vessels), there are no risks of bleeding and thus the state of basal inflammation is reduced compared to other preparations like the cremaster muscle or the skinfold chambers, for which outstanding surgical skills are required to obtain reproducible tissues preparations (Secklehner et al., 2017).

In order to study the early steps of adhesion, we followed leukocyte adhesion in real-time, by recording videos of the mesenteric venules under resting condition and after a topical application of ionomycin on the vessel. Among other dramatic signaling effects, ionomycin was chosen because it is able to instantaneously mobilize the Weibel-Palade bodies at the endothelial cell surface (Conte et al., 2015) allowing the exposure of high levels of P-Selectin on the vascular lumen (Harrison-Lavoie et al., 2006) and CXCL-1 (Oynebraten et al., 2004), both crucial to enable leukocyte slow-rolling.

As shown in **Figure 16**, ionomycin application induced a rapid retention of leukocytes on endothelial cells which increased three-fold from baseline after only 3 minutes. Interestingly, intravenous administration of the $CD31^{agonist}$ resulted in a dramatic reduction of WT leukocyte adhesion (292.3±4.91 vs 117.7±13.32 leukocytes per field at 3 minutes, **Figure 16a**) and an augmentation in rolling velocity (which passed from 4.97±1.50 µm/sec to 12.89±2.10 µm/sec, **Figure 16c**). The fact that this effect that was not observed in $CD31^{-/-}$ mice, corroborates the specificity of the CD31-derived peptide. Although we did not observe differences between WT an KO mice in terms of total number of adhering leukocytes, $CD31^{-/-}$ cells displayed a reduced rolling velocity (3,59±0.90 µm/sec vs 4.97±1.50 µm/sec), which confirmed the previous *in vitro* results.

In conclusion, we found that CD31 loss-of-function by genetic invalidation confers to neutrophils an enhanced capacity to adhere to endothelial cells, while the CD31 gain-of-function triggered by the peptide dramatically reduces rolling velocity and adhesion *in vivo*.

Although the comprehension of the mechanisms controlling the activation of the adhesion cascade during neutrophil recruitment have been incremented (Ley et al., 2007), little is known regarding the negative regulatory pathways. We propose that CD31 may play a key role in such a negative regulatory pathway thereby controlling neutrophil recruitment. Our data suggests that one the possible mechanisms of action of CD31 in this setting consists

in the establishment of a raised threshold for neutrophil adhesion on activated endothelial cells.

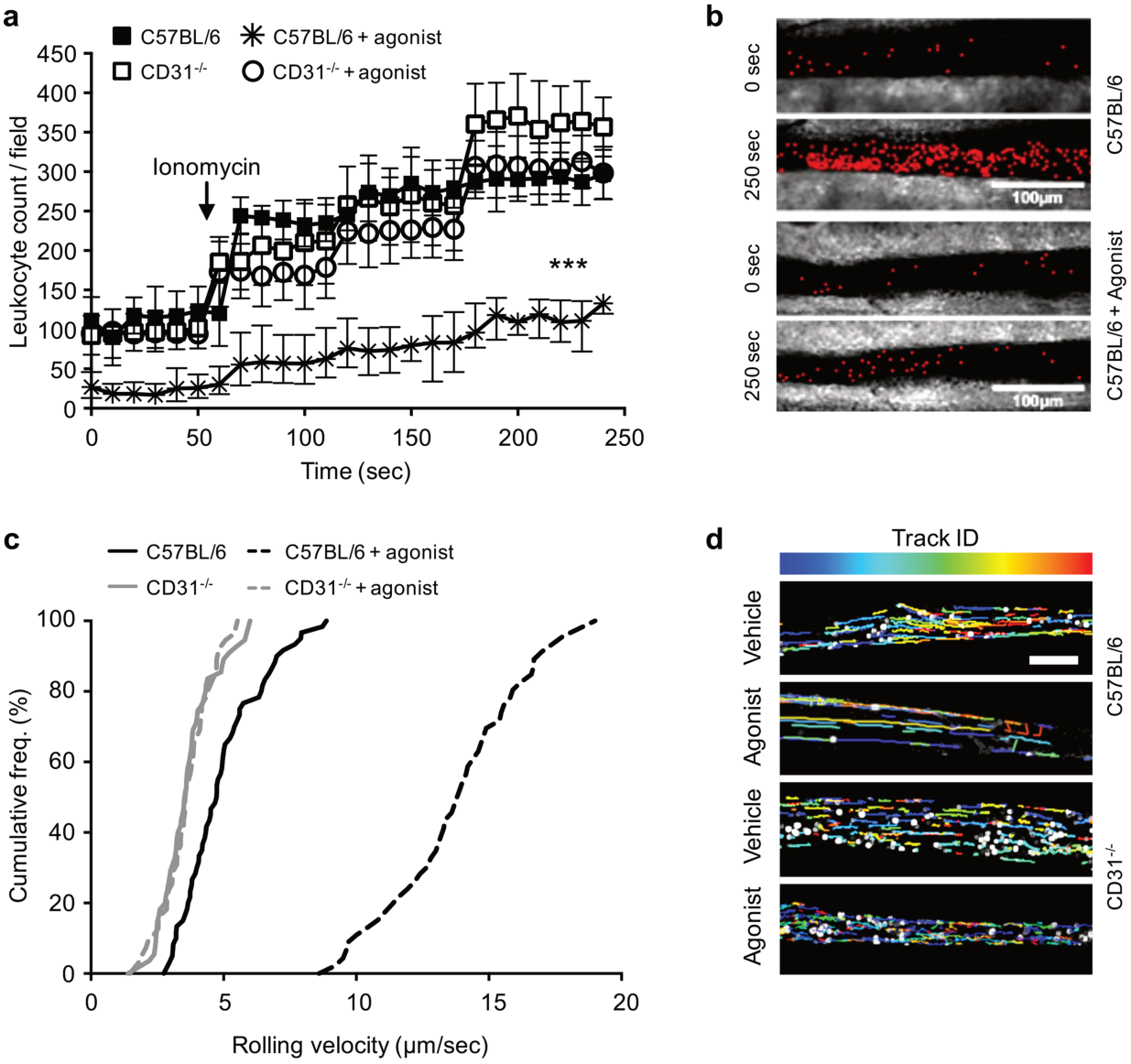

FIGURE 16. CD31 ENGAGEMENT CONTROLS LEUKOCYTE-ENDOTHELIAL CELL INTERACTIONS *IN VIVO*

C57BL/6 WT or CD31$^{-/-}$ mice (male, 8-week old) were anesthetized with an intraperitoneal injection of 100 mg/kg ketamine-HCL and 20 mg/kg xylazine. Anesthetized mice received an i.v. injection of rhodamine immediately before opening the abdominal cavity in order to stain blood leukocytes. The abdomen was opened, the small intestine was exteriorized and the mesenteric network

unfolded. Body temperature of the mice was kept at 37°C and surgically exposed tissue were kept moist with an isotonic buffered solution. Mice were subjected to intravital fluorescence video microscopy starting in resting conditions and continuing after local application of ionomycin (1µM) onto a segment of mesenteric venule. Some groups received 2,5 mg/kg of CD31^{agonist} intravenously before surgery in order to investigate the effect of CD31 engagement on Leukocyte-Endothelial cell interactions. Videos were performed with an upright fluorescence macroscope (MacroFluo®, Leica Microsystems) equipped with a thermostatic heating plate connected to a sCMOS camera (Orca-Flash-4.0, Hamamatsu Photonics). Images acquisition was performed using the Metamorph® software (Molecular Devices) and images post-processed with ImageJ® Software. ***(a)*** *Quantification of total leukocytes rolling fraction (including adhering cells) in the image field one minute before (basal recording) and 3 minutes after the local application of ionomycin. Data are expressed as mean ± SD. p *<0.05 **<0.01 ***<0.001 (Unpaired Student's t-test).* ***(b)*** *Representative images before and three minutes after a local application of ionomycin in C57BL/6 mice treated or not with the CD31 agonist, showing the recruitment of leukocytes onto the inflamed mesenteric venule segment.* ***(c)*** *Cumulative frequencies of rolling velocities of rhodamine-labelled leukocytes interacting with activated endothelial cells were calculated with a cell tracker plugin of ImageJ. Data represent the mean rolling velocity of n>100 cells pooled from 3 mice per group. For each mouse, recordings were performed on venules with similar calibers and surface areas (40-70µm).* ***(d)*** *Representative images of rolling displacement of cells in mesenteric venules of WT or CD31 KO mice treated or not with the CD31^{agonist} peptide (Scale bar 40µm). Cumulative frequency distribution was calculated with Prism GraphPad software.*

8.2.4 Neutrophil recruitment is accompanied by CD31 signaling, while its invalidation unexpectedly compromises cell accumulation at the inflammatory site

Leukocyte rolling and arrest within the vasculature ultimately lead to the breaching of the endothelial barrier opening the access for the leukocytes towards the site of inflammation (Nourshargh and Alon, 2014). This phenomenon, known as trans-endothelial migration (TEM), occurs principally between adjacent endothelial cells (paracellular route) or, less frequently, across the body of endothelium [transcellular route (Muller, 2011)]. Our previous

data supported a role for the CD31 in negatively regulating leukocyte adhesion on activated endothelial cells and we sought to study whether its absence had also an effect on neutrophil extravasation. For this purpose, we choose to work with the IL-1β-induced peritonitis experimental model, wherein the intraperitoneal injection of the inflammatory cytokine elicits a local recruitment of neutrophils. In this sterile peritonitis model, the inflammatory site – being a cavity – allows the cellular exudate to be easily harvested as a single cell suspension, which is therefore readily suitable for accurate quantitative/qualitative characterization by flow cytometry.

As shown in **Figure 17a**, the injection of IL-1β provoked a rapid systemic neutrophil mobilization in the circulating blood, which reached the plateau at two hours. In the basal condition, we could not detect any neutrophil within the peritoneal cavity, while, as soon as one hour after IL-1β injection, neutrophils (identified as $Ly6G^+$ cells) start to egress into the peritoneal cavity (**Figure 17b**). Interestingly, the kinetics of transmigration into the inflammatory fluid was not linear, but rather exponential after 2 hours, and peaked at 4 hours in wild-type mice. We measured various potential chemokines in the blood and peritoneal fluids of experimental mice and found that CXCL-1 dramatically increased at 4 hours post-IL1β, both in the blood and into the peritoneal cavity (**Figure 17d**). This has likely contributed to the mobilization of the neutrophils in the systemic circulation as well as their migration at the site of inflammation in the peritoneal cavity. Indeed, CXCL-1 is a chemokine specific for myeloid cells that has a potent neutrophil chemoattractant activity (Ritzman et al., 2010). We also evaluated the concentration of soluble CD31 in the plasma and we found that it rapidly increased after IL-1β injection (**Figure 17c**). Interestingly, soluble CD31 reached a plateau at two hours concomitantly with the peak of neutrophil systemic mobilization, whereas at four hours – when neutrophils have mostly egressed from the circulation and have reached the peritoneal cavity – it declines. It is therefore tempting to speculate that the increased soluble CD31 that we have detected in the circulating blood witnesses the shedding of CD31 that occurs during neutrophils TEM. In addition to the truncated form of CD31 that derives from activated leukocytes, another soluble form of CD31 that comprises all the 6 extracellular domains and the cytoplasmic tail is produced mostly by EC by the alternative splicing of the exon which encoded the transmembrane domain (Goldberger et al., 1994). Our test could not distinguish these two forms. However, considering that the *de novo* biosynthesis of CD31 takes about 3 hours (Goldberger et al., 1994), it is more likely

the increased plasma soluble CD31 that peaks at 2 hours after the induction of peritonitis derives from a proteolytic cleavage.

In order to explore the distribution of CD31 and whether the signaling motifs of CD31 were engaged during neutrophil transmigration in this setting, we performed *in situ* immunofluorescence microscopy on whole-mount preparations of the omentum. Indeed, the omentum has been proposed to be the major site for neutrophil extravasation into the peritoneal cavity in experimental peritonitis (Buscher et al., 2016; Fukatsu et al., 1996). As shown in **Figure 17e**, we observed faint or absent CD31 staining on the endothelium along the vessels "hotspots" where neutrophils extravasation could be observed (harrow heads). This finding, suggesting that the faint staining is due to the cleavage of CD31, could explain the parallel rise in soluble CD31 plasma concentration.

Remarkably, we found that neutrophils that were accomplishing trans-endothelial migration were positively stained with a monoclonal antibody specific for the phosphorylated CD31 ITIM motif (pY_{713}, red staining), allowing us to document for the first time that neutrophil's CD31 is functionally engaged during TEM. Interestingly, $Ly6G^+$ cells in close proximity with endothelial cells displayed the highest intensity for pY_{713} (**Figure 17f**). The latter observation can be significant, since neutrophils might indeed receive the most potent CD31-dependent cell signaling while crossing the endothelial cell junctions when one considers that (i) CD31 activation is mediated principally by trans-homophilic interaction with other cells (Ilan and Madri, 2003), and (ii) CD31 expression is ten-times higher at the intercellular junctions of endothelial cells than anywhere else in the organism (Lertkiatmongkol et al., 2016; Newman, 1994).

This urged us to analyze how the extravasation of CD31 knock-out neutrophils would proceed, with using the same experimental setup. Unexpectedly, the number of $Ly6G^+$ cells in the peritoneal exudate of $CD31^{-/-}$ mice at four hours was five-times less compared to wild-type mice ($0.5x10^6 \pm 0.2x10^6$ vs $2.4x10^6 \pm 0.5\ x10^6$; **Figure 17b**). Although these data are in agreement with what had already been described in the literature (Duncan et al., 1999; Thompson et al., 2001), they are in apparent contradiction with our previous results showing that neutrophil rolling phase is rather favored by the absence of CD31 (**Figure 16**). Indeed, we expected that an enhancement in the adhesion cascade, due to the lack of CD31, would have been followed by an improved neutrophil egression into the inflammatory site. The

reason why CD31$^{-/-}$ neutrophils failed to reach the peritoneal cavity was puzzling, since we did not observe any difference in neutrophil systemic mobilization compared with wild-type neutrophils (**Figure 17a**), neither a defect of CXCL-1 release in the blood or in the peritoneal cavity of CD31$^{-/-}$ mice (**Figure 17d**) that could explain this phenomenon. A difference in the expression of β_2-integrins could also be supposed, but flow cytometry characterization of the cellular exudate did not support this possibility since the level of CD11b mean fluorescence was the same at surface of wild-type and CD31$^{-/-}$ knock-out Ly6G^{+} cells (**Figure 17h**).

Considering that CD31 is highly-concentrated at the endothelial junctions (Albelda et al., 1991), and that we found that CD31 becomes phosphorylated during neutrophil recruitment, we sought to assess whether the absence of CD31 was compromising the process of trans-endothelial migration of neutrophils. Indeed, CD31-CD31 interactions between leukocyte and endothelial cell have been proposed to initiate the signaling pathway responsible for the calcium flux that is required for TEM (Muller, 2016). Nevertheless, we found that TEM was not impaired in CD31$^{-/-}$ mice, as documented by the fact that most of Ly6G^{+} cells could access the omental extravascular space at 4 hours after the induction of the peritonitis (**Figure 17g**). CD31 appears therefore to be dispensable for TEM itself, but it might however be important for the subsequent steps of neutrophil recruitment. Indeed, in CD31$^{-/-}$ omentum, several neutrophils were found to be tightly bound to the external side of the vessels, thereby reflecting a defect to detach from the basement membrane, in agreement with the function evoked by the authors that had first characterized CD31$^{-/-}$ mice (Duncan et al., 1999).

Interestingly, regardless of their number, the shape of CD31$^{-/-}$ neutrophils that reached the peritoneal cavity displayed atypical morphological side-scatter features (**Figure 17h**). Considering that the side-scattering is largely imposed by granularity and intracellular complexity (Marina et al., 2012), our observations suggest that the absence of CD31 deeply affected the cellular morphology of infiltrated neutrophils that have succeeded in detaching from the basement membrane and that have reached the peritoneal cavity.

Altogether, our data point at dual, and almost opposite, roles of CD31 during neutrophil extravasation: (i) a negative regulation of the adhesion of neutrophils on the luminal side of the vasculature, as revealed by the stronger adhesive contacts established by CD31$^{-/-}$ neutrophils on activated endothelial cells, and (ii) a positive role in promoting the detachment

from the basement membrane once the neutrophils have crossed the endothelial cell barrier, as revealed by the incapacity of $CD31^{-/-}$ neutrophils to detach from the external portion of the vessel and fully migrate toward the inflammatory site in the peritonitis model. Our data show that an intact and functional CD31 localizes at the uropod, where the integrins are in a closed conformation (**Figure 13c**), suggesting that the function of CD31 is necessary for the detachment of neutrophils. Indeed, uropod elongation has been demonstrated to be the final step for leukocyte detachment from the vessels *in vivo* (Hyun et al., 2012) and the fact that we found a deep change in their morphology of peritonitis-infiltrated $CD31^{-/-}$ neutrophils, suchlike they had lost part of their material, we next explored whether the absence of CD31 could affect the polarization/elongation of the uropod of neutrophils during their interactions on constituents of the basement membrane.

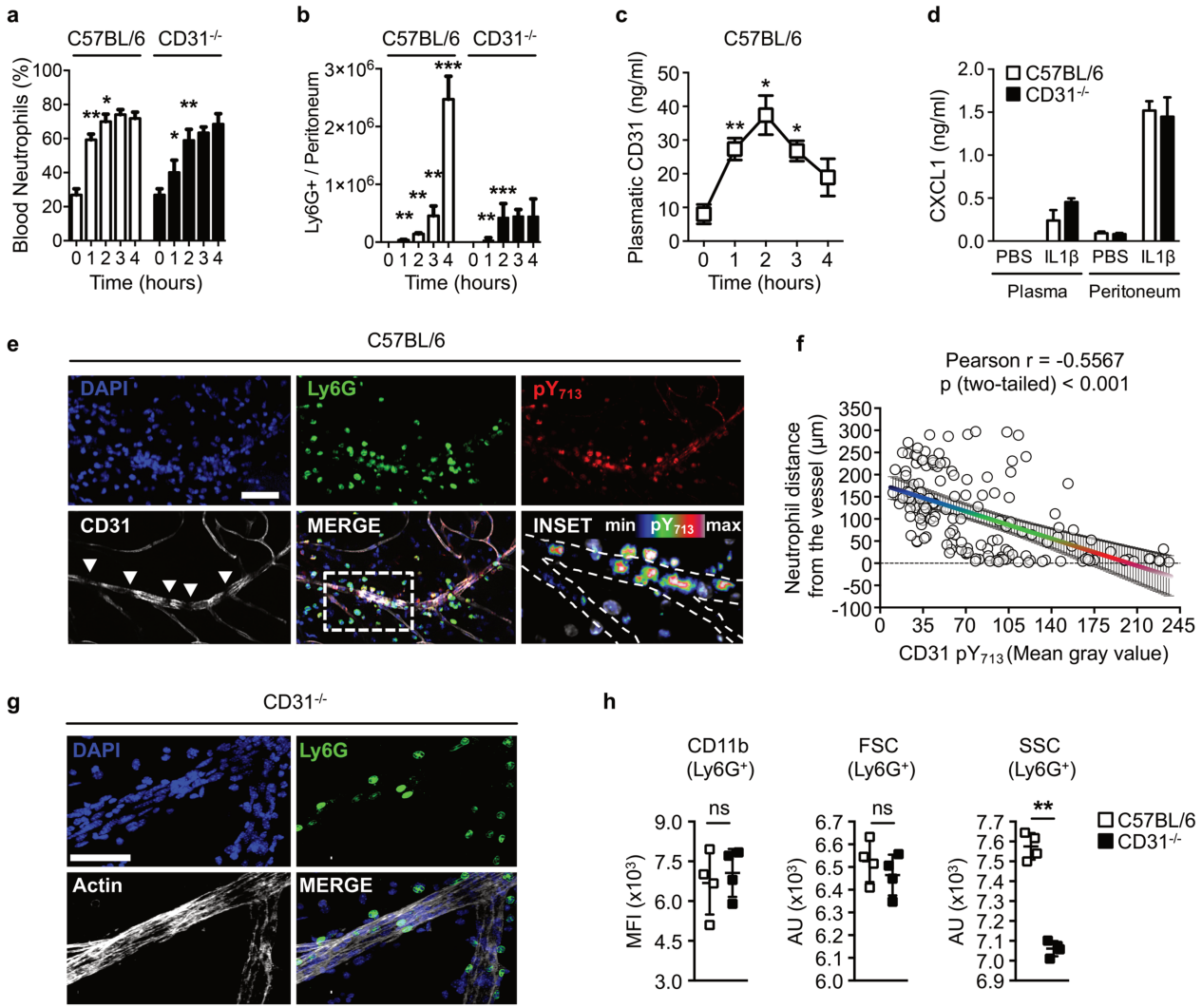

FIGURE 17. CD31$^{-/-}$ NEUTROPHILS ARE READILY MOBILIZED IN THE CIRCULATION BUT FAIL TO REACH OUT TO THE INFLAMMATORY SITE AFTER CROSSING THE VESSEL WALL

(a) *Peritonitis was induced in C57BL/6 and CD31$^{-/-}$ mice (9-13 week-old, n=4/group) by i.p. administration of 1ml containing 40ng of IL-1β (R&D 401) and blood neutrophil percentage was evaluated with an automated cell counter, during the 4 hours following the injection of IL-1β.* ***(b)*** *At each hour, mice were anesthetized and peritoneal cavity was washed with 5ml of PBS-EDTA (5mM) in order to recover cellular exudate. Cells were stained with monoclonal antibodies directed at CD45 (clone 30-F11), Ly6G (clone 1A8) and samples were analyzed by flow cytometry using an LSR II flow cytometer (BD Biosciences). Absolute cell count was determined using 123count eBeads (eBioscience 01-1234) according to the manufacturer's instructions.* ***(c)*** *At the same time points, plasmatic CD31 concentration was assessed using a custom cytometric magnetic bead-*

*based sandwich immunoassay. Data are expressed as mean ± SD. Statistical significance is indicated relative to previous time points. Unpaired Student's t-test *<0.05 **<0.01 ***<0.001. ns not statistically significant.* ***(d)*** *Plasma and cell-free peritoneal liquid of CD31$^{-/-}$ and wild-type C57BL/6 mice were collected at 4 hours after IL-1β injection and CXCL1 concentration was evaluated by ELISA (R&D #DY453).* ***(e)*** *Confocal microscopy of WT omental vessel at 4 hours after IL-1β injection. Omentum were dissected and fixed in 4%PFA for 1 hour at room temperature. Tissues were blocked and permeabilized 1 hour at room temperature with a solution containing 0.5% TritonX, 5% BSA and 0.1% fish gelatin. After extensive washes, samples were stained overnight at 4°C with purified monoclonal antibodies in PBS supplemented with 0.1% saponin. Detection was achieved using secondary f(ab')$_2$ antibodies coupled to fluorescent dyes (Cy3, A488, A647). Omentum were finally stained with DAPI and mounted with Prolong Gold. Z-stacks were taken with a Zeiss Axiovert 200 M inverted microscope equipped with an ApoTome module. Images are maximum intensity projections and show extravasating Ly6G-positive neutrophils (green, clone 1A8), CD31 (white, polyclonal R&D #AF3628), DAPI (blue) and the CD31 phosphorylated 713 tyrosine (pY$_{713}$ clone EPR8079, red). LUT colors refer to the pY$_{713}$ fluorescence intensity. Scale bar 50µm. (**f**) The intensity of CD31-pY713 was calculated in Ly6G-positive regions of interest (8-bit images, gray scale values 0-255) and plotted against the perpendicular distance of the corresponding neutrophil from the closest post-capillary venule. Pearson correlation and linear regression (showing 95% confidence interval) was performed using GraphPad Prism Software.* ***(g)*** *CD31$^{-/-}$ omentum were harvested at 4 hours after IL-1β injection and stained with Ly6G (green, clone 1A8), DAPI (blue) and phalloidin (white) as previously described. Scale bar 50µm.* ***(h)*** *Flow cytometry analysis of cells harvested in the peritoneal cavity 4 hours after IL-1β injection (AU arbitrary units, MFI median fluorescence intensity).*

8.2.5 CD31$^{-/-}$ neutrophils exhibit aberrant uropod polarization/elongation during migration on laminin in vitro

Laminins are major components of the basement membrane (Yousif et al., 2013) and best studied in regard of their relevance in the process of leukocytes extravasation (Wang et al., 2006). The preferred sites for extravasation for neutrophils are those characterized by Laminin α4 low expression at the level of postcapillary venules (Voisin et al., 2010),

indicating that intimate contacts established by the migrating neutrophils with the microvessel basement membrane are crucial for the correct trafficking of leukocytes that aim at reaching out to the inflammatory site.

The effect of CD31 on the polarization of $CD31^{-/-}$ neutrophils onto the constituents of the basement membrane was studied *in vitro* by immunofluorescence microscopy. Purified neutrophils from WT or $CD31^{-/-}$ mice were placed onto Laminin α4-coated surfaces, in the presence of CXCL1. Unfortunately, we could not find any conformation-specific antibody for studying integrins activation state of mouse cells. We therefore observed the distribution of talin and actin filaments within the cells, in order to evaluate the polarization state of mouse neutrophils.

As shown in **Figure 18a**, in wild type neutrophils the polymerized actin was largely localized at the lamellipodium, whereas talin was present at the opposite side (at the uropod). Talin is known to act as a bridge between the cytoskeleton and the exposed integrins (Calderwood et al., 2013) and the fact that talin is spatially far from F-actin at the cell rear, indicates that the integrins at the uropod of WT leukocytes are in a low-adhesive conformation state. In contrast, F-actin was concentrated along with talin also at the cellular rear of $CD31^{-/-}$ neutrophils, indicating a perturbation in the formation of the uropod in KO cells (**Figure 18a, b**). Moreover, we found that neutrophils lacking CD31 were more stretched and displayed elongated uropods compared to wild-type cells (**Figure 18d**), which may reflect an abnormal cellular locomotion in the absence of CD31.

We have previously shown in human neutrophils that phosphorylated CD31 localized at the uropod with the inositol phosphatase SHIP1, indicating that this phosphatase might be responsible for the downstream CD31 signaling. Interestingly, SHIP1 has been shown to functionally dissociate talin from integrins, thus shifting activated integrins back to their inactivated state (Dai et al., 2016). Moreover, our observations in $CD31^{-/-}$ cells were similar to those reported in neutrophils genetically invalidated for SHIP1, which displayed altered cellular morphology and abnormal polymerized actin also at the cellular rear (Mondal et al., 2012; Nishio et al., 2007). Therefore, we assessed the distribution of SHIP1 in WT and KO cells adhering to constituent of the basal membrane. Since CD44 has been documented to localize at the uropod during cellular migration, we used it to identify the cellular rear. We found that endogenous SHIP1 was preferentially localized at the detached uropod, together

with CD44, in CXCL1 activated wild-type neutrophils migrating on recombinant mouse Laminin α-4 (**Figure 18c**). At variance, in CD31$^{-/-}$ neutrophils, CD44 and SHIP1 were both distributed more evenly through the cell body. These findings confirmed that the uropod formation of neutrophils interacting with laminin is abnormal in the absence of CD31.

In order to be active, SHIP1 requires to be docked at the plasma membrane (Phee et al., 2000) where it needs to interact with the phosphorylated ITIM motifs of its molecular targets (Bruhns et al., 2000). In CD31$^{-/-}$ cells, the dysregulation of F-actin and talin organization might be dependent on defective SHIP1 recruitment at the uropod membrane, resulting into an abnormal adhesive phenotype. This could in turn explain their failure to detach from the vessel as observed *in vivo*. Our data hence ascribe a new role for CD31 which can act as a molecule regulating the uropod dynamics during neutrophil adhesion on Laminin α4.

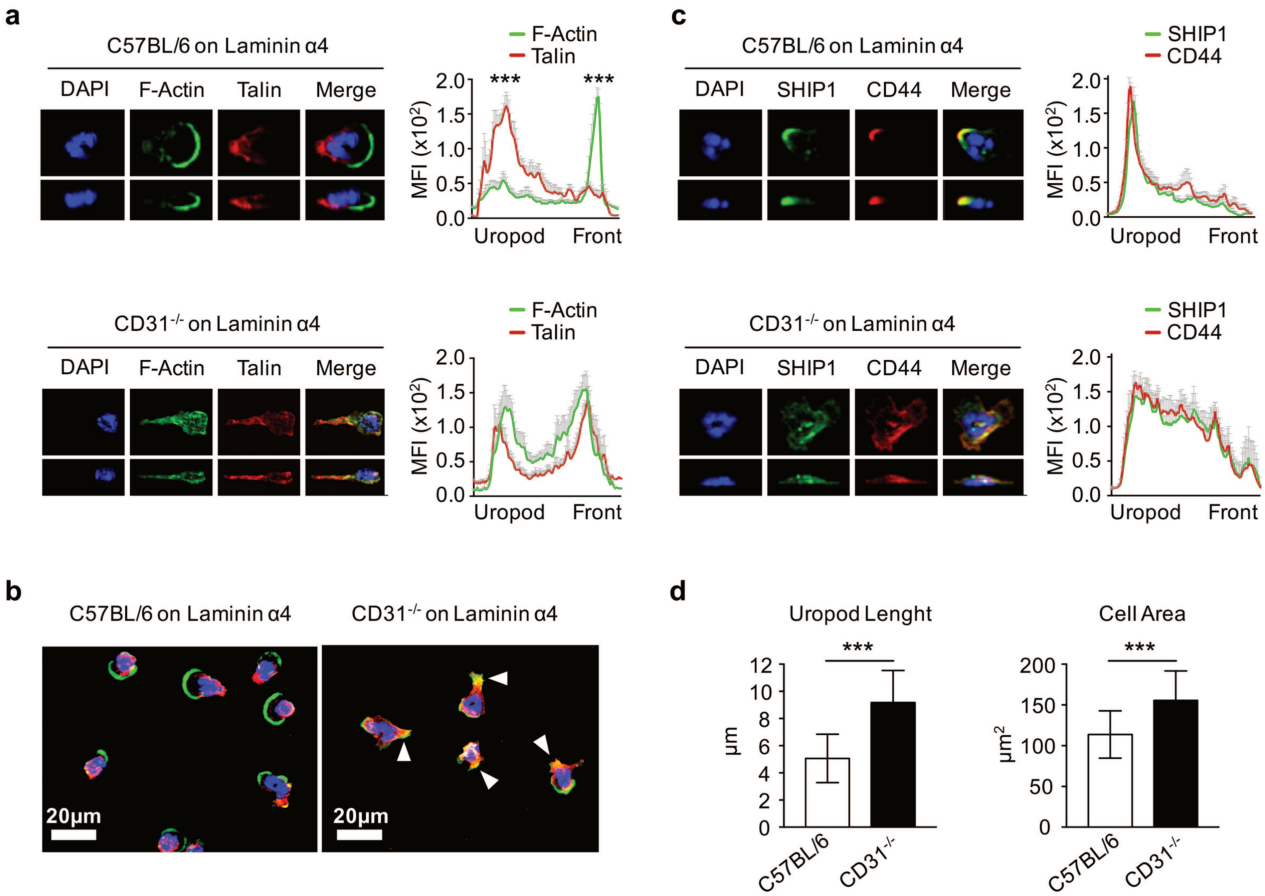

FIGURE 18. ANALYSIS OF CD31$^{-/-}$ NEUTROPHILS PHENOTYPE ON LAMININ

*Neutrophils prepared from C57BL/6 WT or CD31$^{-/-}$ mouse whole bone marrows were purified with a negative immunomagnetic selection kit according to the manufacturer's instructions (STEMCELL #19762). Cells were placed on recombinant mouse Laminin α4 (R&D #AF3837, overnight coating at 20µg/ml and blocked 1 hour with 1%BSA) and immobilized recombinant mouse CXCL1 (Biolegend #573702, 10ng/ml) for 5 minutes at 37°C. Cells were next fixed with 2%PFA for 10 minutes on ice and stained with antibodies. Cells were mounted in ProLong Gold and Z-stack images were taken with a Zeiss Axiovert 200 M inverted microscope equipped with an ApoTome module. 3D reconstructions of top and side view are shown. Quantification of mean fluorescence intensities (MFI, gray values range 0-255) of the indicated staining along the cell axis (mean ± SEM [SEM bars in grey color]; n > 8 cells/staining; statistical comparisons between the 20 first frontal and 20 last posterior measurement points) are shown. P *<0.05 **<0.01 ***<0.001 (Unpaired Student's t-test).* ***(a)***, ***(b)*** *Talin (Abcam, polyclonal #ab71333) and phalloidin (Thermo, #A22287) staining.* ***(c)*** *SHIP1 (clone PC1C) and CD44 (clone IM7) staining.* ***(d)*** *Quantification of uropod lengths of WT and CD31$^{-/-}$ neutrophils calculated as the distance from the backside of the nucleus to the end of the cellular tail. The area was calculated based on bright field images of the cells.*

8.2.6 *Defective motility of CD31$^{-/-}$ neutrophils is restored by pharmacological inhibition of integrin adhesiveness in vivo*

Leukocyte adhesion onto biological surfaces is mediated largely by integrins (Sorokin, 2010). Neutrophils that have successfully completed the rolling adhesion cascade and that have firmly adhered on endothelial cells, display integrins in their maximal adhesion state in order to resist to blood shear forces. Once they have crossed the endothelial cell barrier, leukocytes must detach from the vessel and move forward towards the static extravascular space. Neutrophils must therefore transit in two completely different microenvironments in a very short time and they likely should adapt their adhesive state in relation to the specific recruitment step. It is where the integrins might be tightly regulated.

We reasoned that, if the impaired migration in CD31$^{-/-}$ neutrophils resulted from a defective control of integrins adhesion on ECM ligands, reducing integrin interactions with the extracellular adhesive surfaces should improve neutrophil egress to the inflammatory site. To test this, we used different pharmacological strategies to dampen integrin adhesiveness so as to counteract the excessive neutrophil retention of CD31$^{-/-}$ neutrophils on BM/ECM components. As explained in **Figure 19a**, the pharmacological intervention was performed at two hours after the induction of inflammation, because this was the time point at which neutrophil systemic mobilization reached its plateau (**Figure 17a**) and at which leukocytes begin to transmigrate (**Figure 17b**). Furthermore, integrin inhibitors were injected intraperitoneally – rather than intravenously – in order to locally target cells that have already performed TEM, meanwhile minimizing the impact on intravascular leukocytes within the systemic circulation.

As a first integrin inhibitor, we used the Arginine-Glycine-Aspartic tripeptide (RGD). RGD is a common integrin cell adhesion motif displayed on the vast majority of ECM proteins including fibronectin, collagens and laminins (Wang et al., 2013). Indeed, nearly half of the integrins recognize this sequence (Ruoslahti, 1996). When RGD peptides are administered as soluble, they act as a decoy for integrins binding site, preventing leukocyte retention to ECM surfaces thereby promoting cellular forward movements (Mondal et al., 2012). As shown in **Figure 19b**, the RGD administration to wild type mice (at 2 hours after induction of inflammation) did not modify neutrophil recruitment to the peritoneal cavity. This indicates that the intraperitoneal RGD administration did not compromise cell migration to the tissue, conversely to the i.v. route, which has been shown to reduce leukocyte extravasation *in vivo* by inhibiting the rolling cascade (Sarangi et al., 2012).

Importantly, we found that the administration of RGD peptides restored neutrophil influx at the inflammatory site in mice lacking CD31, strongly indicating that the retention of CD31$^{-/-}$ neutrophils was due to an excessive integrin activation. Interestingly, transmigrated CD31$^{-/-}$ neutrophils treated with RGD displayed also higher side-scatter values (**Figure 19d**). The opposite phenomenon was indeed observed in **Figure 17g**, indicating that the morphological phenotype displayed by transmigrated KO neutrophils was likely due to excessive integrin-mediated adhesion.

RGD peptides are expected to interact with the majority of integrins, but leukocyte adhesion on constituent of the basement membrane and ECM proteins is reported to be dependent also by β_1-integrins (Gao and Issekutz, 1997). Moreover, neutrophils genetically invalidated for β_1-integrin reach the peritoneal cavity better than wild-type littermates (Sarangi et al., 2012), indicating that β_1-integrin as well might be a brake for leukocyte egression to the inflammatory site. Thus, we examined whether the migratory phenotype in $CD31^{-/-}$ mice was due to a defective control of the β_1 integrin adhesive state. As shown in **Figure 19b**, pharmacological inhibition of β_1-integrins re-conferred $CD31^{-/-}$ neutrophils with a normal migration phenotype, indicating that the restored motility observed with the RGD treatment was also due to β_1-integrins targeting.

Of note, treatment with the $CD31^{agonist}$ in wild type mice give opposite results depending on timing and way of administration. When injected systemically (i.v.), concomitantly with IL-1β, the peptide significantly reduced the egression of $Ly6G^+$ found in the peritoneum at two hours (**Figure 19c**), i.e. when neutrophils have almost finished the rolling phase and start to transmigrate. Conversely, the local (i.p.) injection at two hours – when leukocytes start to egress to the inflammatory site –, significantly enhanced neutrophils recruitment to the peritoneal cavity at four hours (**Figure 19b**). These findings demonstrate that CD31 is a key molecule involved in neutrophil integrin fine-tuning during their recruitment *in vivo* and its complex role lead to different outcomes depending on the step of leukocyte recruitment.

The observation that in WT mice the $CD31^{agonist}$ was able to improve neutrophil recruitment while the RGD peptide was not, can be possibly explained by the fact that the two molecules act with different mechanisms. The RGD peptide physically prevents leukocyte retention on ECM components, while the $CD31^{agonist}$ operates by activating the CD31 protein through which many signaling pathways may be affected.

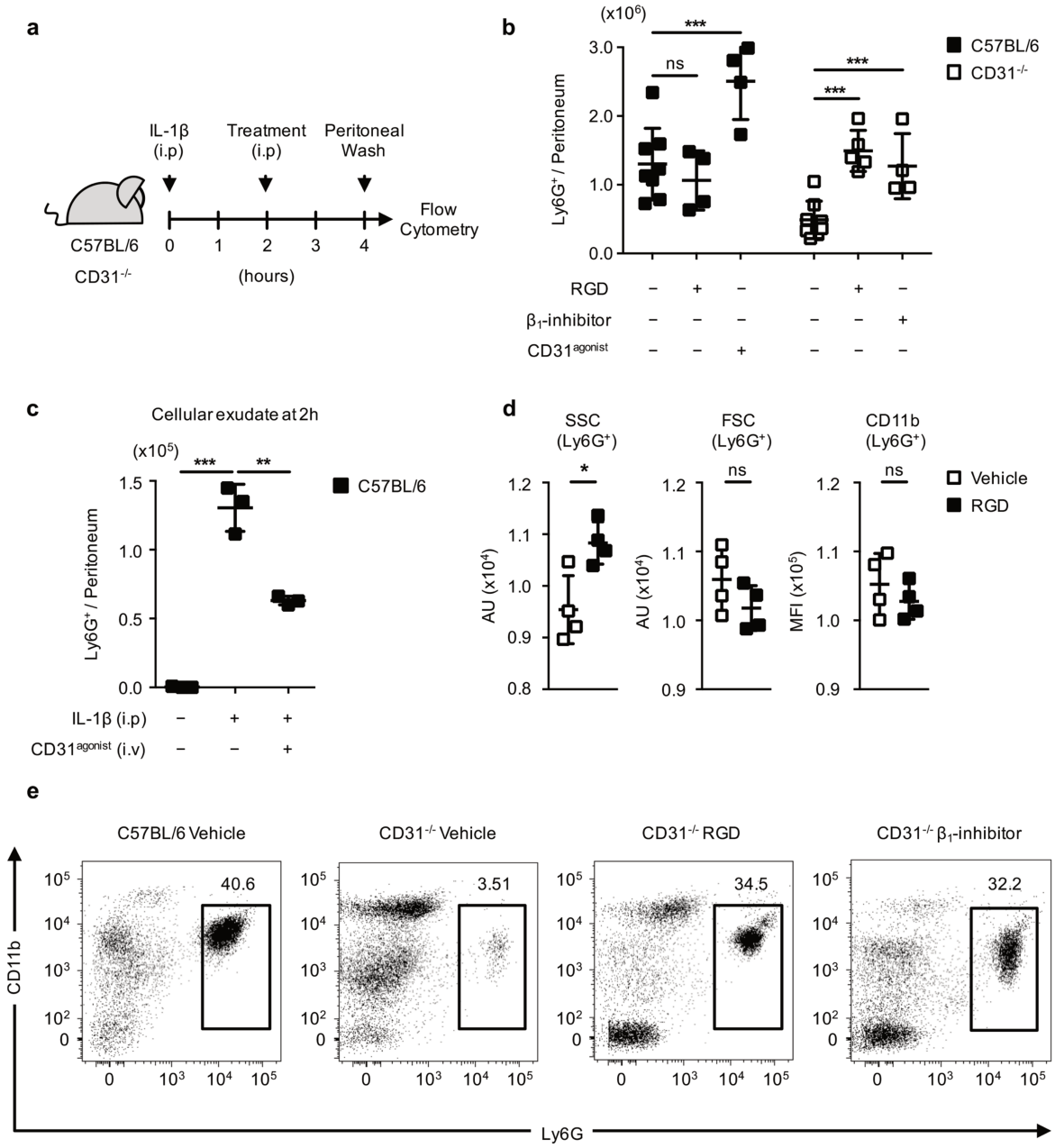

FIGURE 19. PHARMACOLOGICAL INTERVENTION ON NEUTROPHIL MOTILITY *IN VIVO*

(a) *Experimental design. C57BL/6 or CD31$^{-/-}$ mice (4-8/group) were injected with 1ml containing 40 ng of IL-1β i.p. to induce the peritonitis. After two hours, mice were injected intraperitoneally with vehicle, RGD peptides (Arg-Gly-Asp-Ser 10mg/kg, 460µM / 1ml / peritoneal cavity. Tocris #3498), β_1-inhibitor (BIO-5192 1µg/kg, 30µM / 1ml / peritoneal cavity. Tocris #5051) or CD31^{agonist} (2.5mg/kg, 50µM / 1ml / peritoneal cavity) depending on the experimental condition. At four hours,*

mice were sacrificed and peritoneal neutrophils were analyzed as described before. ***(b)*** *Quantification of cellular exudate at four hours. Neutrophils were identified as $CD45^+$, $CD11b^+$ and $Ly6G^+$ by flow-cytometry.* ***(c)*** *Sterile peritonitis was induced in C57BL/6 mice by the injection of IL-1β i.p with the concomitant intravenous administration with $CD31^{agonist}$ or vehicle. In this experiment, cellular exudate was harvester at two hours and characterized as usual by flow-cytometry.* ***(d)*** *Flow cytometry analysis of harvested cells at 4 hours in $CD31^{-/-}$ mice treated or not with RGD peptides. (AU arbitrary units, MFI median fluorescence intensity)* ***(e)*** *Dot plot representations of harvested peritoneal cells. Data are expressed as mean ± SD. Unpaired Student's t-test *<0.05 **<0.01 ***<0.001. ns not statistically significant.*

8.2.7 *CD31 engagement by the peptide favors neutrophil's uropod detachment from the basement membrane and cellular locomotion in the tissue*

Since the CD31 engagement by the peptide significantly enhanced WT neutrophil recruitment to the peritoneal cavity at 4 hours, we sought next to observe neutrophil behavior in living mice treated with the $CD31^{agonist}$. Among the established techniques to study cell trafficking *in vivo*, the direct observation of cells using multi-photon intravital microscopy (MP-IVM) is one of the most informative experimental approach (Hoover and Squier, 2013). The use of longer and more tissue-penetrating excitation wavelengths (>700nm) makes MP-IVM less damaging for biological samples and allows deeper analyses within the tissues. In addition, laser wavelengths used by this technology can take advantage of the intrinsic physical properties of the tissues – like the second harmonic generation (SHG) – in order to visualize the extracellular matrix without the use of any additional staining (Jiang et al., 2011). We choose to investigate inflammatory processes in the ear dermis, since it is richly vascularized, poorly affected by respiratory movements, no surgery preparation is required, and it is possible to perform image acquisition for long period of time in the same mouse. Finally, in order to study neutrophil behavior *in vivo*, we took advantage of the LysM-GFP mice strain, in which the intracellular expression of the green fluorescent protein is restricted specifically to myeloid cells (Faust et al., 2000).

As an initial step, we studied whether the CD31 gain-of-function with the peptide regulates neutrophil detachment from the vessel. As shown in **Figure 20a**, at one hour after the intradermal injection of IL-1β, GFP^+ leukocytes crawled within the vascular lumen of post-capillary venules of the ear dermis. In vehicle-treated mice, we confirmed previous findings demonstrating that extravasating leukocytes show delayed uropod detachment and become extremely elongated before disconnecting from the basement membrane (Hyun et al., 2012). Indeed, we observed that, once neutrophils completed the transmigration process, they went forward within the extravascular space, but the uropod remained attached at cellular rear to the outside edge of the vessel. Importantly, the administration of the $CD31^{agonist}$ induced an accelerated detachment, resulting in a very efficient release from the outside part of the vessel which favored fast and multiple neutrophils entries within the tissue compared to the control condition (**Figure 20b**). These data support our hypothesis that CD31 engagement across endothelial cell junctions may reduce integrin adhesiveness in order to allow an efficiently neutrophil detachment from inflamed vessels. The administration of the peptide might promote this process.

We sought next to investigate at later time points after the induction of the inflammation, the fate of extravasated neutrophils subjected or not to the peptide treatment. Interestingly, peptide-treated leukocytes moved faster at 3 hours (**Figure 20e** left panel) and displayed nearly half of the cellular length compared to the control groups (**Figure 20c**, **e** right panel), suggesting that cellular uropod is less adhesive on the ECM components. Moreover, they traveled a greater distance in the parenchyma (**Figure 20d, f**), indicating that the engagement of CD31 through endothelial cell junctions is important not only for the detachment from the basement membrane after the TEM, but also on late phases during which neutrophils travels within the tissue towards the inflammatory site.

Taken together, these results describe – at the single cell level – the fact that the sustained CD31 signaling triggered by the peptide enhanced neutrophil egression by controlling integrin assets during their late migration phase towards the inflammatory site (**Figure 19b**).

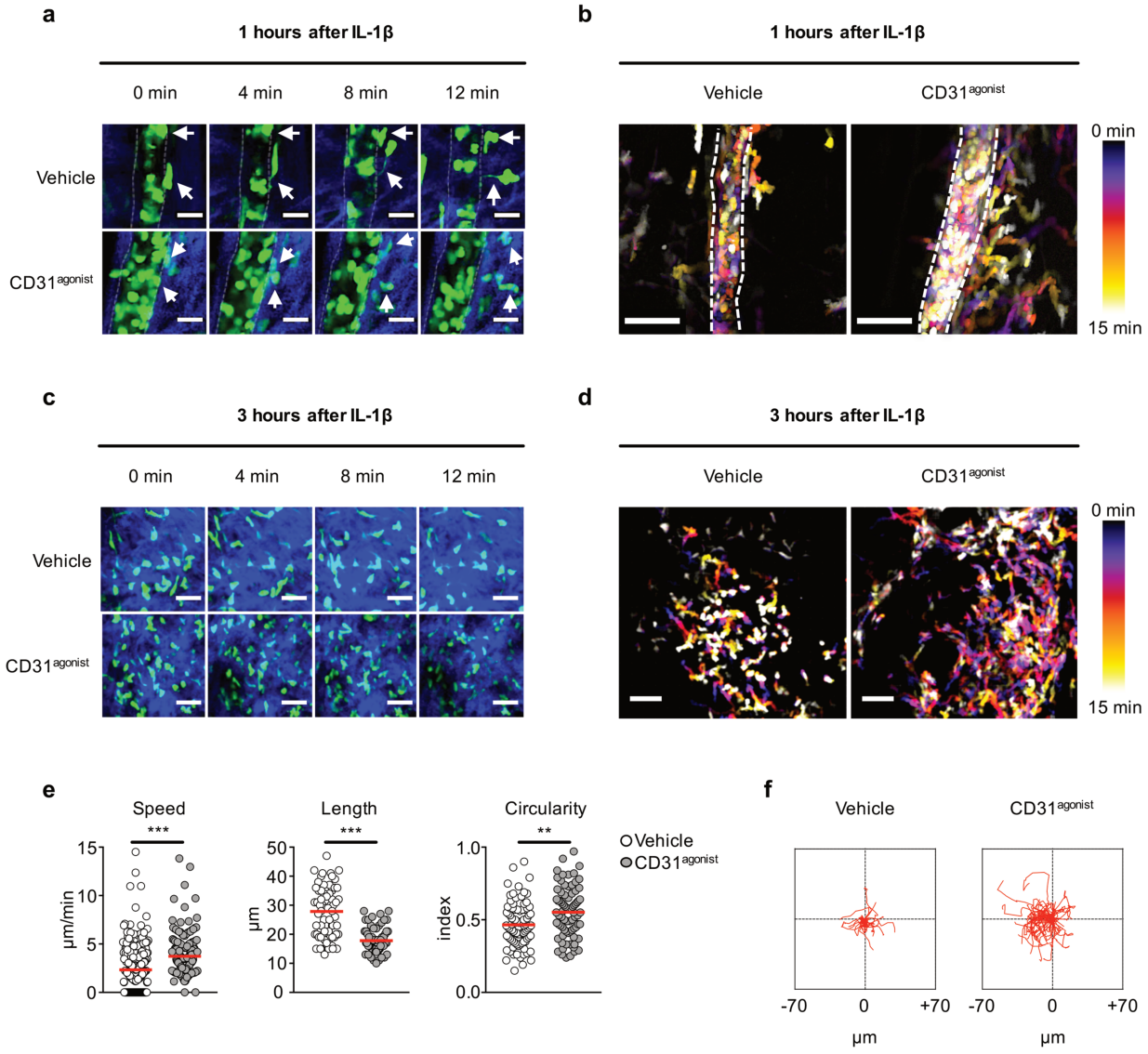

FIGURE 20. EFFECT OF CD31 ENGAGEMENT BY THE PEPTIDE DURING NEUTROPHILS RECRUITMENT *IN VIVO*

*LysM-GFP^{+} mice (males, 10 weeks old) were anaesthetized and placed on the imaging stage at 37°C. They were injected in the ear pinna with 10ng of IL-1β (R&D Systems #401-ML-005) in 2.5μl of PBS with or without the CD31^{agonist}. Mice were transferred immediately to the microscope stage and imaged for 15 to 20 minutes for each time point at an X-Y pixel resolution of 512 x 512. Multiphoton imaging was performed with a Zeiss LSM7 MP system equipped with both a 10x/0.3 NA air and 20x/1.0NA water-immersion objective lens (Zeiss) and a tunable titanium/ sapphire solid-state 2-photon excitation source (Chameleon Ultra II; Coherent Laser Group). (**a**) Time-lapse*

*images of post-capillary venules at one hour after IL-1β injection. Green color represents GFP$^+$ leukocytes and blue color the collagen fibers imaged with the secondary harmonic generation (SHG). Images are representative of two independent experiments. Scale bar 20µm. (**b**) Cell motion visualized by time color-coded superposition of frames. Scale bar 50µm. (**c**) Interstitial leukocytes at 3 hours after IL-1β injection. Scale bar 40µm. (**d**) Time color-coded superposition of frames at 3 hours. Scale bar 50µm. (**e**) Quantification of migratory speed and cell length of leukocytes at 3 hours after IL-1β injection was performed with an automated ImageJ Plugin (Trackmate). (**f**) Track plots of LysM-GFP$^+$ cells at 3 hours after IL-1β injection treated with vehicle (left) and treated with the CD31^{agonist} (right) normalized to the starting position. Data are expressed as mean showing all points. P *<0.05 **<0.01 ***<0.001 (Unpaired Student's t-test). n=60 cells from 2 independent mice per condition.*

8.2.8 Summary of Aim II section and graphical abstract

In the second part of the present work, we explored the contribution of the CD31 signaling pathway in the recruitment of neutrophils out of the vessels and towards the inflammatory sites during the acute phase of inflammation, using genetically-invalidated mice as well as a gain-of-function approach by the CD31^{agonist} administration.

Our first result indicated that CD31 might be involved in controlling integrin function at the uropod where it concentrates and gets activated in proximity of "closed" integrins. Remarkably, we found that CD31 negatively modulate neutrophil adhesion, as cells lacking the CD31 molecule rolled slowly on activated endothelial cells under flow conditions. On the contrary, upholding the CD31 signaling pathway in WT neutrophils with the CD31^{agonist} dramatically dampened their capacity to establish strong interactions with EC.

We proceeded to study the involvement of CD31 in the trans-endothelial migration process and their homing to the inflammatory site. We found that CD31 engagement in neutrophils during the TEM, was accompanied by the phosphorylation of its ITIM motif, indicating that CD31 molecular pathway is strongly involved during the aforementioned processes. Nevertheless, we were surprised to observe that the better adhesion of CD31$^{-/-}$ leucocytes

was unexpectedly followed by a lower recruitment within the inflammatory site, out of the vessel, *in vivo*. This phenotype became more puzzling when we did not found any difference in neutrophil mobilization into the systemic circulation neither an evident abnormality in TEM across the endothelial barrier. These observations highlighted an unforeseen complex role of CD31, since its involvement seems to lead to opposite consequences depending on the leukocyte recruitment steps. Intriguingly, we noticed that extravasated $CD31^{-/-}$ neutrophils were specifically retained at the outside face of the vessel and displayed an abnormal polarization phenotype when placed in contact with constituents of the vascular basement membrane. We demonstrated that the failure to reach the inflammatory site in *$CD31^{-/-}$* mice was due to their inability to correctly proceed to closing the uropod integrins, which therefore remain attached to the ECM after the TEM process. This hypothesis was supported by a competitive approach in which the application of decoy RGD peptides outside of the vessels was able to totally restore neutrophil efflux towards the peritoneal cavity. Finally, by the direct observation of leukocyte behavior by IV-MPM, we reported that CD31 promotes the uropod detachment thereby allowing an appropriate trafficking of leukocytes *in vivo*.

All together, these data suggest that CD31 works as an integrin regulator. It is endowed with a dual-role on migrating neutrophils, both supervising integrin activation for the adhesion within the lumen of the microvessels at the site of TEM and controlling uropod detachment on their way out of the vessel, after their crossing the endothelial barrier.

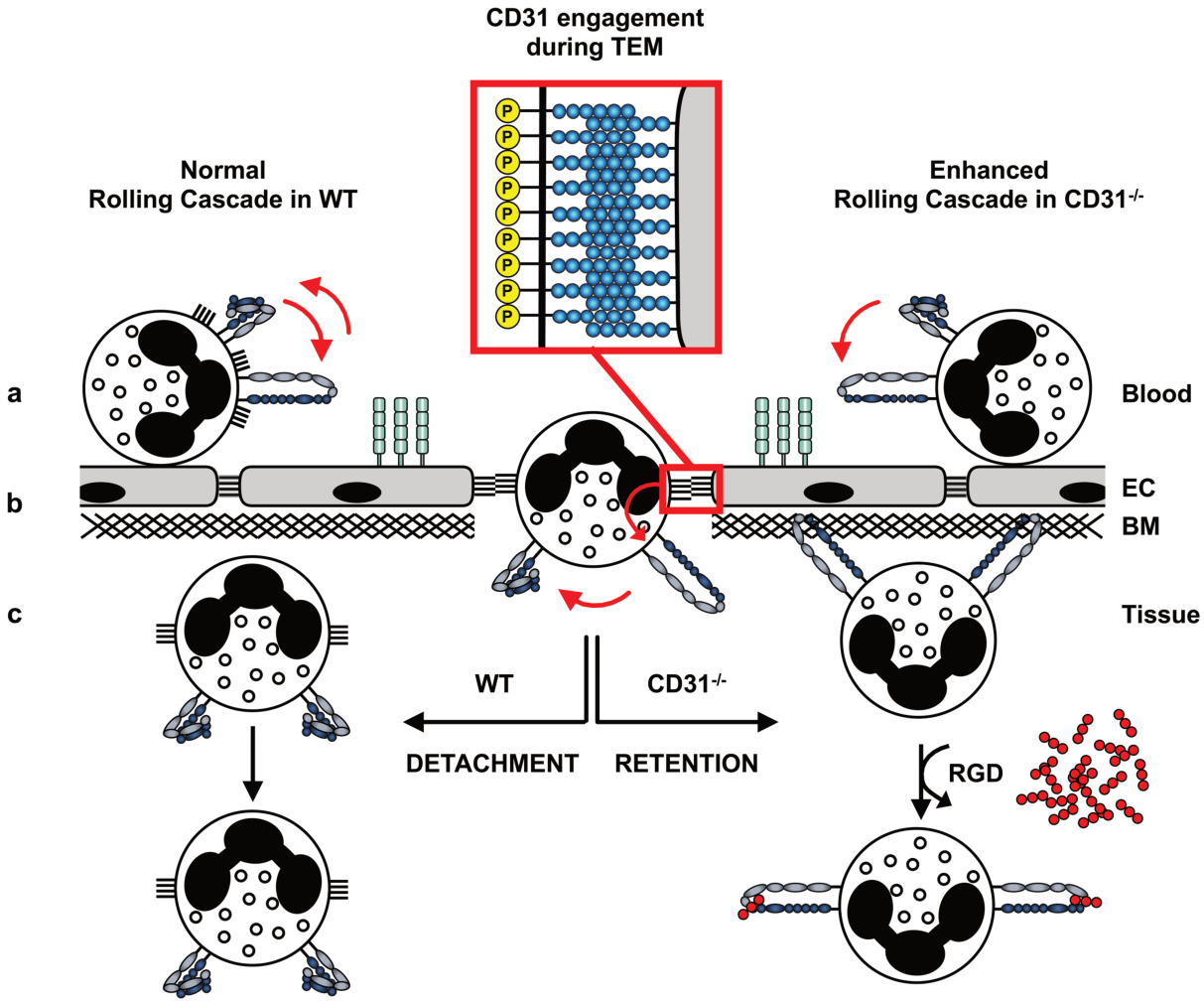

FIGURE 21. GRAPHICAL ABSTRACT OF AIM II SECTION

(a) *Neutrophil rolling and adhesion on activated endothelial cells is governed by the conformational changes of β_2-integrins within the vascular lumen. In CD31$^{-/-}$ mice, neutrophils exhibit an enhanced adhesion onto activated endothelial cells, suggesting that CD31 is involved in dampening integrin activity.* ***(b)*** *TEM across EC junctions results in CD31 trans-homophilic engagement which results in CD31 phosphorylation. We propose that this process is critical to close integrins during the final homing step of neutrophils into the inflammatory site.* ***(c)*** *The lack of CD31 anchor neutrophils to the outside of the vessel. Neutrophils can be released by soluble/decoy integrin ligands, indicating that the defective detachment phase in the absence of CD31 is related to an inappropriate control of the integrin activity.*

8.3 Aim III: CD31 and neutrophil activation

8.3.1 Context of Aim III section

Neutrophils play a crucial role in the first line of defense against noxious agents. Central to their function, is the ability to rapidly exit the circulation and migrate to the site of inflammation where they must recognize the nature of the danger in order to get activated and exert appropriately responses. To accomplish this important task, they express a large array of cell surface receptors, some of which are directly capable of recognition of microbial-associated structures and exert exquisitely "innate" functions, while others – such as Fc-receptors – are linked to the adaptive immune response. The interaction of these receptors with their cognate ligands, triggers neutrophil effector functions which is also referred as "activation". Because these effector functions are extremely potent and potentially harmful for the self, a tight molecular regulation is also mandatory in order to control the activation of neutrophils.

In this part of my work, we aimed at assessing whether CD31 could exert its regulatory function to modulate neutrophil activation. Indeed, many ITAM pathways and their kinase molecular effectors are involved in triggering neutrophil activation, while the ITIMs motifs within cytoplasmic tail of CD31, through their capacity to recruit phosphatases, could interfere with the activation signaling pathways.

The CD31 signaling pathway has already been described to control the ITAM-dependent activation by the Fc-Receptor CD32A [FcγRIIa, (Thai le et al., 2003)] and by the FcR common γ-chain (Lee et al., 2006) in human platelets. This prompted us to consider the possibility that CD31 may regulate the activation triggered by the immunoglobulin Fc receptors in neutrophils. Fc receptors are pivotal for triggering important neutrophil effector functions such as the antibody-mediated phagocytosis and the antibody-dependent cell-mediated cytotoxicity (Dallegri et al., 1983).

In the present section, I will present the experimental work that we have performed in order to study the role of the CD31 signaling pathway during Fc-receptor-mediated activation of human and murine neutrophils, *in vitro* and *in vivo*.

8.3.2 CD31 regulates CD32A-mediated neutrophil oxidative burst through SHIP1 pathway in human neutrophils

Antibody-dependent cell-mediated cytotoxicity (ADCC) critically relies on the Fc-receptor CD32A (Nagarajan et al., 2000) and it is no surprise that over-activation of the CD32A signaling pathway can cause ADCC-mediated tissue injury as exemplified in autoimmune diseases such as glomerulonephritis and rheumatoid arthritis. In these pathologies, both soluble and insoluble immune complexes provoke leukocyte activation, as indicated by the fact that neutrophils isolated from the synovial fluid of rheumatoid arthritis patients exhibits enhanced production of reactive oxygen species (Nurcombe et al., 1991). From a molecular point of view, the engagement of CD32A with immunoglobulins leads to FcR clustering that activates members of the Src kinase family. In turn, these tyrosine kinases trigger the phosphorylation of the cytoplasmic tail on the immunoreceptor tyrosine-based activation motif (ITAM) of CD32A (Rollet-Labelle et al., 2004) and this allows the recruitment of the spleen tyrosine kinase (Syk) by its tandem SH2 domains that starts an activation signaling pathway. The current molecular model states that ITAM-dependent kinase signaling can be regulated by counteracting pathways involving receptors that possess an immunoreceptor tyrosine-based inhibitory motif (ITIM) that, on the contrary, recruit phosphatases (Barrow and Trowsdale, 2006). CD31 being an ITIM-bearing molecule, we reasoned that its engagement could modulate CD32A activation of neutrophils. To test this hypothesis, we setup a series of in vitro experiments wherein the readout was the CD32A-mediated ROS production by human neutrophils.

As explained in **Figure 20a,** we used a protein G-coated solid surface in order to control the orientation of the immobilized antibody that we used to crosslink neutrophil CD32A. It is important to highlight that this choice was made in order to avoid the interaction, through the

Fc portion of the crosslinking antibody, with the other Fc-receptors, such as the ITIM-containing CD32B inhibitory receptor, that are also present on the neutrophil membrane. By forcing the Fc portion of the anti-CD32A antibody to bind on the protein G at the bottom of the well, we have ensured that the variable region of the crosslinking antibody CD32A was oriented to specifically target this Fc receptor at the surface of the neutrophils. As a readout for neutrophil activation we chose to evaluate the oxidative burst with a chemical substrate that becomes fluorescent upon oxidation (Oparka et al., 2016).

As shown in **Figure 22b**, the strategy we used to trigger the activation by CD32A engagement was specific, since ROS production in the "control isotype" condition was undetectable (the signal was at the same level as when the neutrophils were plated on the protein G-coated surface alone, in the absence of antibodies). Furthermore, in our setting, the activation was strictly dependent on an ITAM pathway, as demonstrated by the fact that pharmacological inhibition of the ITAM-associated kinase Syk completely abolished the CD32A-mediated neutrophil oxidative burst.

In this controlled, ITAM specific Fc receptor-mediated neutrophil activation setting, CD31 engagement by the $CD31^{agonist}$ dampened cellular activation in a dose-dependent manner, indicating that signals delivered by CD31 downregulate ROS production upon CD32A stimulation.

A stated before, CD31 does not possess intrinsic catalytic activities and needs to recruit SH2-containing phosphatases on its phosphorylated ITIM motifs to carry out its signaling functions (Ilan and Madri, 2003). The phosphatases described to interact with CD31 can be divided into two distinct subsets according to their enzymatic specificity. The first is composed by the tyrosine phosphatases SHP1 and SHP2, while the second belongs to the phosphatidylinositol phosphatases SHIP1. We reasoned that, if the CD31 signalization in the CD32A-induced neutrophil activation is mediated by one of these phosphatases, we would be able to abolish the $CD31^{agonist}$ effect by inhibiting the molecular partner responsible for CD31 downstream signalization.

In order to assess whether the phosphatases recruited by CD31 during Fc-receptor mediated neutrophil activation was a tyrosine phosphatase, we used the sodium stibogluconate (NaSG), which is reported to inhibit both SHP1 and SHP2 at the dose of 150μM (Pathak and Yi, 2001). As shown in **Figure 22c**, we confirmed that cell activation is

dependent on Syk and is inhibited by the peptide administration. Unexpectedly, NaSG did not impact on the effect of the CD31^{agonist} treatment, suggesting that CD31 downstream pathway does not rely on SHP1 or SHP2. We proceeded by investigating the possible role of phosphatidylinositol phosphatases SHIP1. Indeed, we found that the inhibition of SHIP1 inhibition alone by the compound 3AC resulted in a significant augmentation of the oxidative burst (**Figure 22d**), confirming that the metabolism of membrane lipids plays a fundamental role in controlling CD32A-neutrophil activation (Mondal et al., 2012). Importantly, the modulation of ROS production mediated by the CD31^{agonist} – even at the dose of 100µg/ml –, was completely abolished with the concomitant administration of 3AC.

These findings suggest that, in CD32A-activated human neutrophils, CD31 acts as a molecular platform to recruit SHIP1 in order to modulate neutrophils ROS production upon cellular activation.

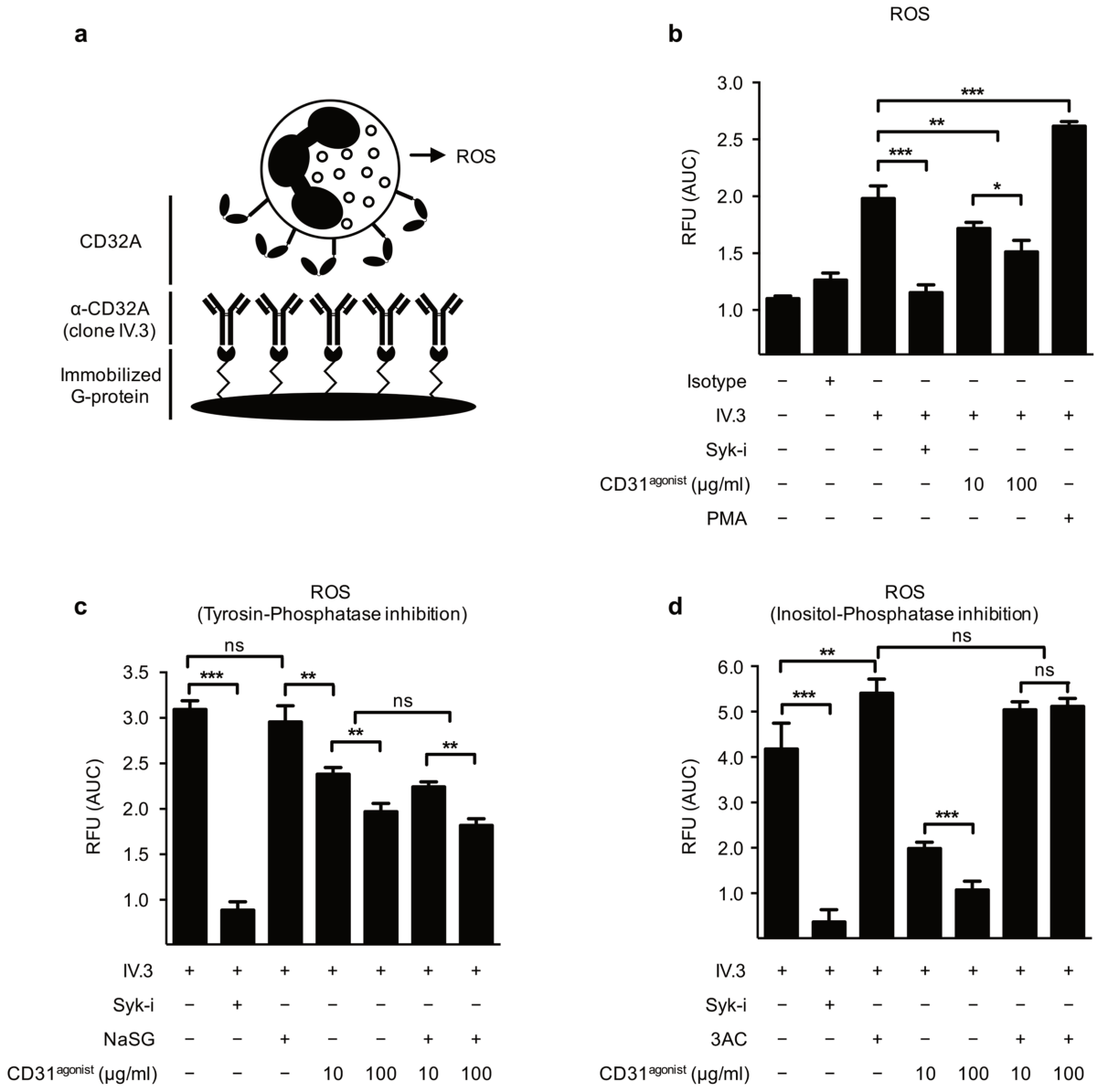

FIGURE 22. THE CD32A-DEPENDENT ROS PRODUCTION IS MODULATED BY THE CD31 SIGNALING PATHWAY

(a) *Experimental design. Protein G covalently-functionalized plates (Thermo #15157) were coated with 4µg/ml of αCD32A (clone IV.3, STEMCELL #60012) or with 4µg/ml of isotype control IgG2b, kappa (clone 27-35, BD #555740) overnight at 4°C. Purified human neutrophils (10^6/ml) were loaded with an intracellular ROS probe following manufacturer's instructions (CM-H2DCFDA, Thermo #C6827). Probe-loaded cells were next treated for 10 minutes at room temperature with the following compounds or a combination of them, depending on the experimental condition: Syk-*

inhibitor (BAY 61-3606, 150µM. Santa Cruz #202351), SHP1/2-inhibitor (NaSG, 150µM. Calbiochem #567565), SHIP1-inhibitor (3AC, 50µM. Calbiochem #565835) CD31^{agonist} (p8RI, 10µg/ml or 100µg/ml) and PMA (Phorbol 12-myristate 13-acetate, 50nM. Sigma #P1585). Neutrophils (100µl/well) were finally placed on functionalized plates and fluorescence was read at 494nm/524nm using an Infinite 200 PRO Microplate Reader (Tecan. Männedorf, Switzerland) at 37°C for 3 hours at 5 minute intervals. ***(b)*** *AUC values of ROS probe during 3 hours of neutrophil stimulation on αCD32A-coated wells or control conditions (Isotype-coated wells and uncoated wells) in the presence or not of the CD31^{agonist}.* ***(c)*** *CD31 modulation of Syk-dependent oxidative burst in the presence of the tyrosine phosphatase inhibitor NaSG or* ***(d)*** *in the presence of the phosphatidylinositol phosphatase SHIP1 inhibitor 3AC. Results are from 3 independent experiments with 3 different donors and each condition was performed in quadruplicate. Data are expressed as mean ± SD of the area under the curve (AUC) of relative fluorescence units (RFU) normalized on the control condition during the 3 hours of acquisition. P *<0.05 **<0.01 ***<0.001 (Unpaired Student's t-test).*

8.3.3 Neutrophil activation on immobilized immune complexes is modulated by CD31 in vivo

Immune complexes (IC)-mediated inflammation is a common mechanism in autoimmune diseases and several studies have suggested that IC-driven engagement of Fcγ receptors play a primary role in these pathologies (Nimmerjahn and Ravetch, 2008). In order to study the role of CD31 in neutrophil IC-driven activation *in vivo*, we choose an experimental model where the passive transfer of anti-glomerular basement membrane (GBM) immune serum causes glomerulonephritis (classified as a type-II hypersensitivity reaction). This model recapitulate the Goodpasture's syndrome in human patients (McAdoo and Pusey, 2017), which is a pathology characterized by the production of autoantibodies directed against the α-chain of type IV collagen of the basement membrane (Borza, 2007).

Since the glomerular endothelium is fenestrated, the antigen is directly accessible for autoantibodies and the i.v. administration of GBM-immune serum in mice readily causes the formation of insoluble IC *in situ* on the GBM. In these conditions, circulating FcγR-expressing

cells can also access the GBM and interact with the ICs in the lumen of the glomeruli capillaries. The intense neutrophils infiltration and local activation results in a damage of the endothelial barrier, the generation of edema, dysfunction of the glomerular filter and ultimately leads to kidney dysfunction.

In this experimental model, tissue injury has been confirmed to be dependent from the function of antibody receptors, since $Fc\gamma R^{-/-}$ mice were shown to be completely protected from the disease (Park et al., 1998), whereas the complement system-dependent tissue damages were reported to be negligible with high anti-GBM serum titers (Tipping et al., 1989). Moreover, the acute phase of the disease (2-6 hours after i.v. injection of the anti-GBM antibodies) is entirely mediated by circulating neutrophils (Schrijver et al., 1990) and specific pharmacological inhibition of MPO results in a complete protection from renal damages in the acute phase (Zheng et al., 2015). The role of neutrophils in IC-induced injury clearly illustrates how the molecular armament used to destroy noxious agents can also inflict severe damages to the tissue. Neutrophil-derived reactive oxygen species and proteases are particularly deleterious to host cells in these settings.

As shown in **Figure 23a**, the administration of the GBM-immune serum to both WT and $CD31^{-/-}$ mice resulted in a robust neutrophils mobilization in the systemic circulation compared to the group that received the control nonimmune serum ('Non-Immune Serum' group in which animals received the serum collected from the sheep without GBM immunization). As in the case of peritonitis (**Figure 17a**), we did not observe any difference between the two genotypes and the administration of the $CD31^{agonist}$ did not modify the initial phase of neutrophil mobilization either. As expected, the deposition of insoluble IC on the fenestrated glomerular endothelium resulted in local neutrophils recruitment (**Figure 23b**). It has been reported by MP-IVM, that the duration of leukocyte retention in the glomerulus was increased during the GBM-mediated GN (Devi et al., 2013) and this extended period of retention was suggested to be the cause of the neutrophil-dependent glomerular injury.

As shown in **Figure 23c**, $CD31^{-/-}$ mice displayed a greater extent of neutrophil infiltration [≥ 1 neutrophil was present in 70±8% of glomeruli analyzed (100-200 analyzed glomeruli per mouse, n=5/group) versus 58±5% in WT mice], while the $CD31^{agonist}$ treatment displayed no effect in $CD31^{-/-}$ mice. Conversely, administration of the peptide significantly reduced the number of $Ly6G^{+}$ cells per glomerular unit in the WT group: in these settings, the number of

neutrophil-infiltrated glomeruli was further reduced from 58± 5% to 28±10% (**Figure 23d**). The surface area of glomeruli, which reflects the local edema provoked by the vascular damages, measured in each group (**Figure 23e**), was perfectly correlated with the glomerular neutrophil recruitment.

Kidney function is essential for the homeostasis of the organism as it ensures the elimination a wide range of waste products and toxins from the blood. This task is accomplished by the kidney filtering units, called nephrons, which are large structures that contains the glomeruli. Glomeruli are the functional structures where plasma filtration occurs through the glomerular filter, which separates the blood from the primary urine. When the glomerular filter is intact, large molecules – like albumin – are not allowed to cross and hence not present in urines. We examined the presence of albumin in the urines in order to evaluate kidney dysfunction (Levey et al., 2015). Considering that urine dilution varies during the day, while creatinine is eliminated at constant rate in urines, we used the creatinine concentration as an internal control to normalize the albumin content.

As shown in **Figure 23f**, administration of the GBM-immune serum caused a 30-fold increase of the albumin/creatinine ratio (ACR) compared to the NIS group, thereby indicating that the glomerular filter was acutely (only 4 hours after serum injection) and severely damaged. Although $CD31^{-/-}$ mice displayed a worse ACR score as compared to the wild-type group (1331±457 vs 1048±264), it was not statistical significant (p=0.2). They may reach statistical significance by increasing the number of mice and/or by reducing the amount of immune serum administered. Indeed, the dose we used was so high that it could have provoked such devastating renal damages that could have masked the deleterious effect of the CD31 absence. On the other hand, WT mice that received the $CD31^{agonist}$ showed a significant improvement in the clinical score. This could be due to an effect of the CD31 signaling pathway on the regulation of neutrophil adhesion onto activated endothelial cells (as we shown previously in **Figure 15**, **Figure 16**) and/or on the regulation of Fcγ-receptor activation, as seen in the *in vitro* experiments described above.

In conclusion, these experiments demonstrate, by genetic invalidation and molecular intervention with the peptide, that CD31 is involved in controlling neutrophil recruitment and activation onto immobilized molecular complexes *in vivo*.

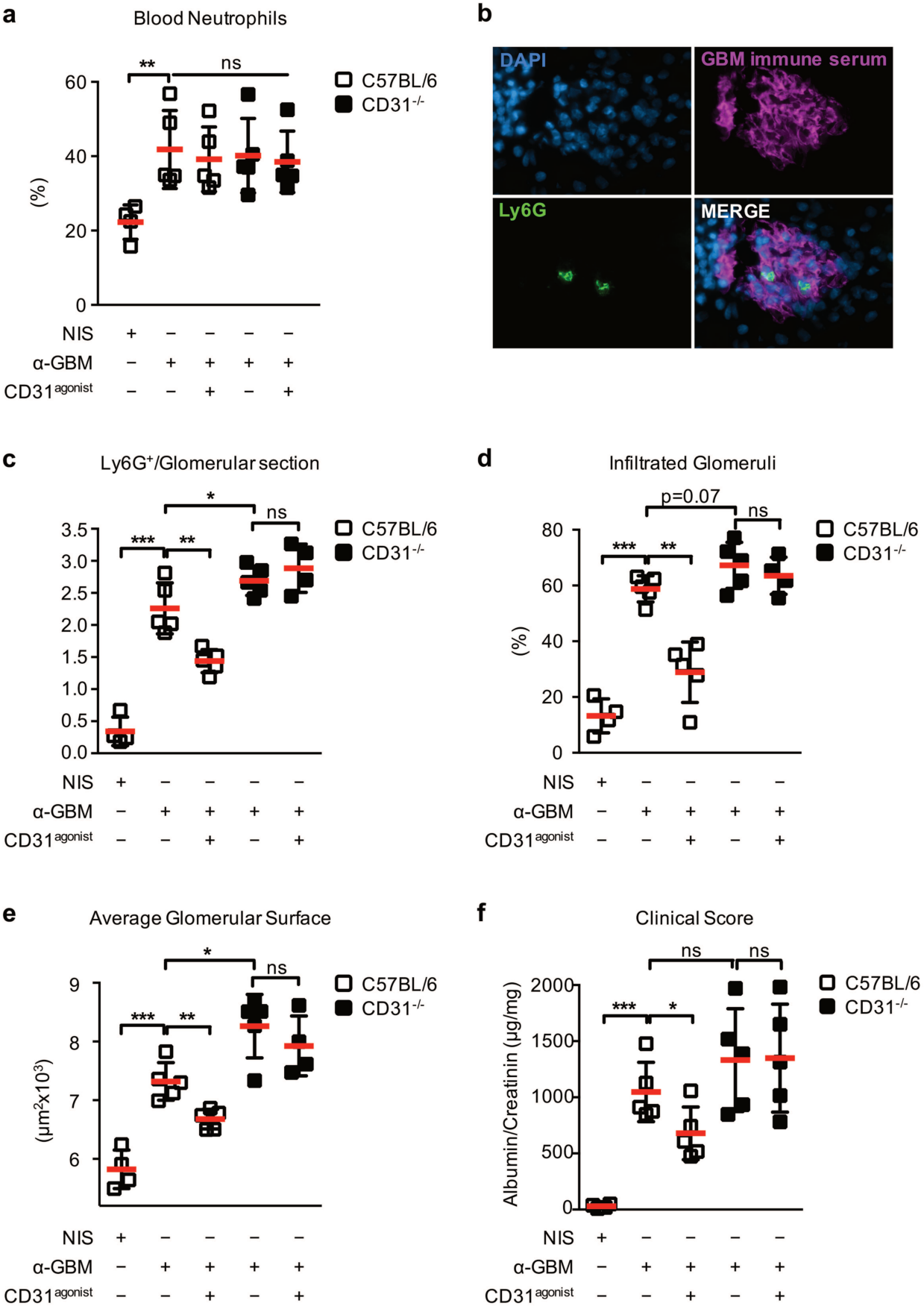
a
Blood Neutrophils
(%)
60
40
20
0
**
ns
C57BL/6
CD31-/-
NIS + – – – –
α-GBM – + + + +
CD31agonist – – + – +
b
DAPI
GBM immune serum
Ly6G
MERGE
c
Ly6G+/Glomerular section
3.5
3.0
2.5
2.0
1.5
1.0
0.5
0.0
*
ns
***
**
C57BL/6
CD31-/-
NIS + – – – –
α-GBM – + + + +
CD31agonist – – + – +
d
Infiltrated Glomeruli
(%)
80
60
40
20
0
p=0.07
ns
***
**
C57BL/6
CD31-/-
NIS + – – – –
α-GBM – + + + +
CD31agonist – – + – +
e
Average Glomerular Surface
(μm2x103)
9
8
7
6
*
ns
***
**
C57BL/6
CD31-/-
NIS + – – – –
α-GBM – + + + +
CD31agonist – – + – +
f
Clinical Score
Albumin/Creatinin (μg/mg)
2000
1500
1000
500
0
ns
ns
***
*
C57BL/6
CD31-/-
NIS + – – – –
α-GBM – + + + +
CD31agonist – – + – +

FIGURE 23. ROLE OF CD31 IN ANTIBODY-MEDIATED GLOMERULONEPHRITIS MOUSE MODEL

Experimental passive glomerulonephritis was induced in C57BL/6 or CD31$^{-/-}$ mice (males, 12-weeks-old, n=5/group) by intravenous administration of 100µl of anti-glomerular basement membrane immune serum (α-GBM, Probetex #PTX-001) or control non-immune serum. Some groups received concomitantly an i.v. administration of CD31^{agonist} at 2.5mg/Kg. ***(a)*** *At 4 hours after the induction of glomerulonephritis, blood was collected and the blood formula was determined with an automated cell counter, while plasma was stored at -80°C for further analysis.* ***(b)*** *At 4 hours, mouse kidneys were harvested and processed to obtain 8µm frozen-sections for IHC. Samples were stained with αLy6G antibody (clone 1A8) and αsheep-A647 to visualize anti-GBM immune deposits. A representative image of an infiltrated glomerulus is shown.* ***(c)*** *Each section was entirely acquired with the NanoZoomer 2.0-HT (Hamamatsu) digital slide scanner and individual TIFF images were processed by computer-assisted image analysis using the QWIN® program (Leica) and a custom macro was written to count the number of Ly6G$^+$ cells per glomerulus (the area of interest was determined by the GBM deposits and number of Ly6G positive cells was automatically counted). The same macro was also implemented to determine* ***(d)*** *the percentage of glomeruli infiltrated with at least one Ly6G$^+$ cell and* ***(e)*** *the mean glomerular surface area.* ***(f)*** *Renal damage was estimated by the albumin/creatinine ratio in urines collected at 4 hours. Albumin was quantified by ELISA (Bethyl Laboratories #E90-134) and creatinine levels were calculated by a colorimetric assay following manufacturer's instructions (R&D systems #KGE005). Data are expressed as mean ± SD. P *<0.05 **<0.01 ***<0.001 (Unpaired nonparametric Wilcoxon-Mann-Whitney test).*

8.3.4 *Injury triggered by αGBM-IC deposits is associated with CD31 shedding on glomerular endothelial cells*

In most tissues, the leukocyte response begins in post-capillary venules and the inflammatory stimuli that have instructed the recruiting leukocytes are generally located outside the blood vessels. A minimal initial neutrophil activation is required to adhere to and transmigrate the endothelial barrier, while their full activation occurs when they reach the

source of inflammation in the extravascular space. In the GBM GN model, on the contrary, the inflammatory stimuli are (so to speak) entrapped in the vessel wall, which becomes the target of immune effectors and hence the final destination for them.

CD31 trans-homophilic interactions – established by neutrophils and endothelial cells – are important to activate CD31 signalization (**Figure 17e**) and we know that the cleavage of the distal domains abolishes the CD31 functionality (**Figure 9** and **Figure 11**). Thus, we next evaluated the CD31 integrity (functionality) in the inflamed glomeruli. As shown in **Figure 24a** (left panel), glomerular endothelial cells were strongly positive for CD31 (yellow) in mice injected with the nonimmune serum (NIS), as expected, immune deposits were not detected. On the contrary, at four hours after the GBM-antiserum administration, *in situ* deposition of IC (violet) were accompanied by a diffuse and global loss of the glomerular CD31 staining (**Figure 24a** right panel).

This finding contrast with the observations we made in another model of acute inflammation, – the IL1β-induced peritonitis – in which the loss of extracellular CD31 on the inflamed endothelium (and neutrophils extravasation) occurred at discrete "hotspots" sites (**Figure 17e**). Contrariwise, in the GBM GN model, neutrophil recruitment is not performed on post-capillary venules, but, as explained above, on capillary endothelial cells. The passage in the capillaries of the glomeruli implies a greater "physical effort" for the neutrophils. Capillaries are about 8μm in diameter, considerably smaller than neutrophils (about 12μm) and therefore the latter must deform in order to squeeze all the way through the glomerular vascular network. This implies that interactions of the neutrophils with the IC deposits in the glomeruli is intimate and prolonged eventually resulting in a massive activation, which is extremely deleterious for EC and the glomerular filter. In this perspective, I propose that the diffuse (instead of spotty) loss of CD31 by EC in glomerulonephritis might also reflect a secondary, wider endothelial activation due to a bystander vascular damage inflicted by activated neutrophils.

As compared to concentration of soluble CD31 found in the plasma of control mice [4.1±1.5 ng/ml (**Figure 24b**)], values were dramatically (3-fold) increased in the group that received the GBM-immune serum (12.5±2.5 ng/ml; $p<0.001$ vs NIS). Considering that the biosynthesis of soluble CD31 by EC takes about 3 hours (Goldberger et al., 1994), these

findings strongly suggest that the loss of staining on glomerular EC is likely due to an active shedding process.

The administration of the peptide did not modify the amount of cleaved CD31 detected in the plasma (**Figure 24b**) but, as discussed in the previously (**Figure 11**), the peptide acts after (and requires) the cleavage of the CD31. It can only target those cells that have already engaged their native CD31 and does not bind on CD31 from resting cells. Therefore, it cannot prevent the initial activation and CD31 shedding, even though it could prevent a subsequent vague of activation and CD31 shedding. As expected, soluble CD31 was not detected in knockout mice, either by measure in the plasma (by our custom test based on the use of cytometric beads) in solubilized proteins from purified glomeruli [WB analysis (**Figure 24c**)].

Interestingly, we found the presence of endogenous (mouse) immunoglobulin deposits in the glomeruli of $CD31^{-/-}$ mice (**Figure 24c**) suggesting the possibility that an autoimmune IC-drive glomerulonephritis can occur in the absence of CD31, consistently with what has been reported by Wilkinson et al. (Wilkinson et al., 2002). The development of autoantibodies in $CD31^{-/-}$ mice has previously been observed and found to be related to a lowered activation threshold for B lymphocytes and the occurrence of a “spontaneous” hyper-responsive B-Cell activation with ageing. Indeed, the B-Cell Receptor (BCR) activation is also mediated by an ITAM/Syk-dependent signalization (Treanor, 2012) and it is tempting to speculate that the effect exerted by CD31 on FcγR/Syk-mediated activation that we have reported in neutrophils (**Figure 22**) could also account for the control of the signaling pathway downstream the BCR.

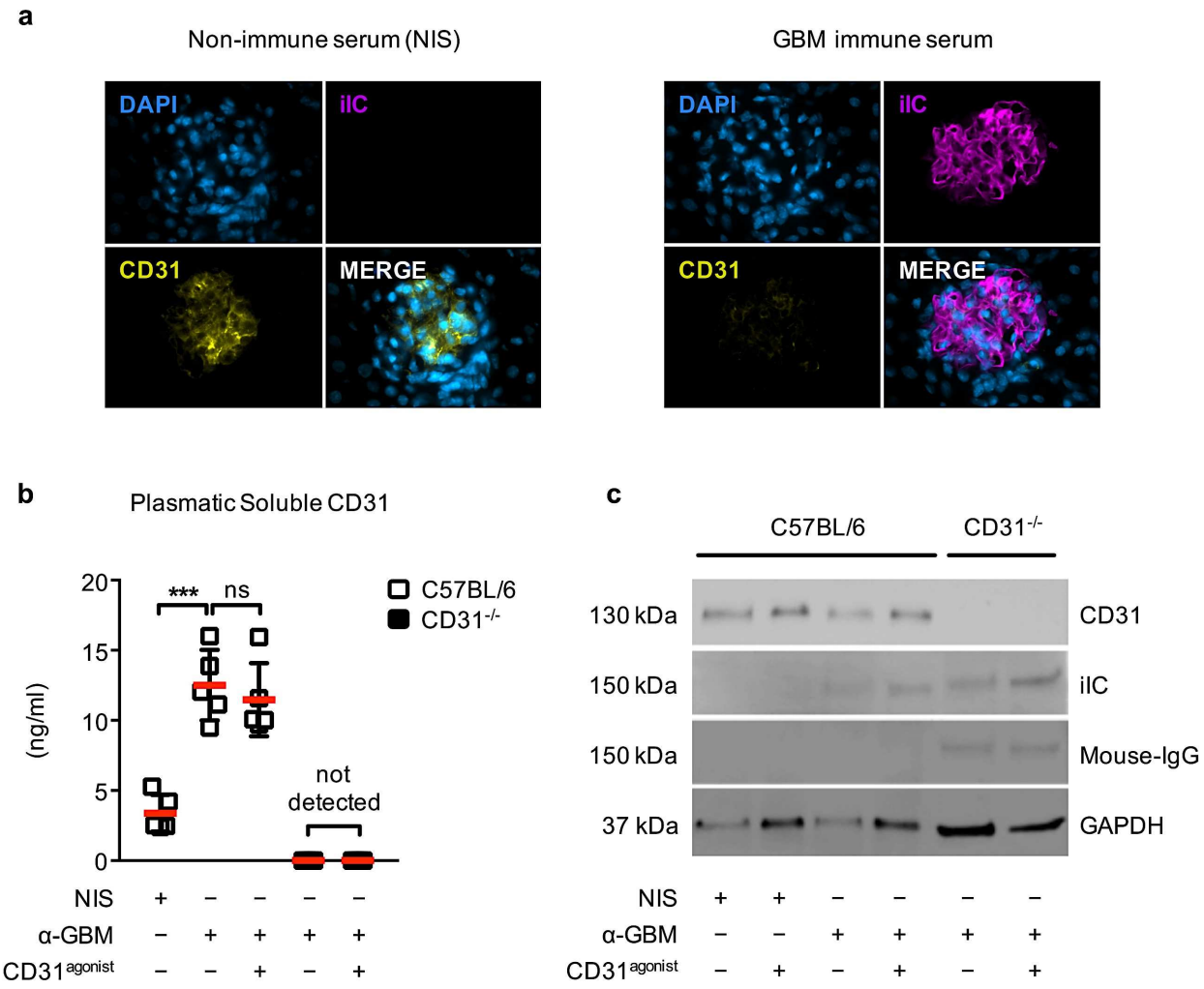

FIGURE 24. EVALUATION OF CD31 SHEDDING IN GBM GLOMERULONEPHRITIS

(a) *Frozen kidney sections (8µm thick) were stained for nuclei (Blue color, Hoechst), anti-GBM immune deposits (Violet color, α-goat) and for CD31 (Yellow color, clone 390). Z-stacks were taken with a Zeiss Axiovert 200 M inverted microscope equipped with an ApoTome module and images are shown as maximum intensity projections.* ***(b)*** *Plasma CD31 concentration was assessed by customized Luminex magnetic beads. Briefly, CD31 from EDTA-serum was captured with magnetic COOH beads (Bio Rad #MC10026-01) covalently immobilized with a polyclonal antibody directed against mouse CD31 (R&D #AF3628) with a custom conjugation kit (Bio Rad #171406001). After extensive washes, captured CD31 was revealed with a monoclonal antibody (MEC13.3) conjugated with PE. Fluorescence was read with the Luminex® 100/200™ system. Fluorescence was plotted against a standard curve obtained with recombinant mouse CD31 (R&D*

*#3628-PC) in order to determine CD31 concentrations. Data are expressed as mean ± SD. P *<0.05 **<0.01 ***<0.001 (Unpaired nonparametric Wilcoxon-Mann-Whitney test).* ***(c)*** *Kidneys were dissected and nephrons were purified using sequential sieving with metal meshes. Glomeruli were lysed in RIPA buffer and 20µg of total extracted proteins were separated by SDS-PAGE under reducing conditions. Proteins were blotted on a nitrocellulose membrane and stained with a polyclonal antibody directed against extracellular CD31 (Santa Cruz #sc8306), with a polyclonal antibody against sheep IgG (Thermo #A16041) or mouse IgG (Santa Cruz #sc-2005). GAPDH was used as an internal loading control.*

8.3.5 Neutrophils activation by IC drives an enhanced ROS production in the absence of CD31

A basal state of oxidative stress is constantly present in aerobic metabolism and has important roles in normal cell physiology. However, in pathological conditions, increased levels of oxidants might be relevant for the initiation and propagation of deleterious inflammatory processes. This is particularly evident for neutrophils that, once activated, can undergo a phenomenon called “respiratory burst” [for a recent review, see (El-Benna et al., 2016)]: a rapid, non-mitochondrial reduction of oxygen that forms highly-reactive oxygen species (ROS). ROS are essential to fight pathogens, as reflected by the fact that genetic defects of the NADPH oxidase results in a profound immunodeficiency and risk of infection in human patients (Holmes et al., 1967). Although pivotal for innate immunity, ROS cause damages to the host tissue in certain conditions. In the case of GBM glomerulonephritis model, the oxidative burst not only is directly toxic for the kidney, but ROS generated by FcγR-engagement recruit other neutrophils in loop, perpetuating the inflammatory process (Suzuki et al., 2003). Thus, we wanted next to characterize the molecular mechanisms of neutrophils activation by GBM-IC. As the immune complexes *in vivo* are formed by the deposition of antibodies on the basement membrane, we reproduced them *in vitro* by coating a Matrigel surface with the same GBM-immuneserum used in the murine model (**Figure 25a**). “Matrigel” is a solubilized basement membrane preparation extracted from a murine

sarcoma and contains the most important BM constituents, including Collagen IV, which is the autoantigen in the GBM GN disease (Borza, 2007).

As shown in **Figure 25b**, the interaction of purified neutrophils from WT mice with the αGBM-Matrigel immune complexes, provoked a rapid (≈25 minutes) increase of ROS production that reached the plateau at one hour. Conversely to the previous CD32A-crosslinking experiment (**Figure 22**), here we wanted to validate that neutrophil activation was actually supported by the Fc-receptor engagement and not by other interactions with ECM proteins. Blockade of Fc-receptors or Syk pharmacological inhibition (**Figure 25b, c**) completely inhibits the oxidative burst, indicating that neutrophil activation on GBM-IC strictly relies on ITAM-dependent Fc-receptor activation. Importantly, neutrophils lacking CD31 showed a prolonged oxidative burst, that reach its plateau after two hours (**Figure 25b**) and results in a significantly higher amount of released ROS compared to WT leukocytes (**Figure 25c**). Of note, the pharmacological inhibition of SHIP1 (the CD31 downstream phosphatase in this condition) in WT cells, provoked an overwhelming oxidative burst that was kinetically and quantitatively similar to that of $CD31^{-/-}$ neutrophils.

These findings suggest that neutrophil activation on GBM-IC is completely dependent on the FcR-ITAM axis and that CD31 is an important regulatory protein involved in controlling oxidative burst.

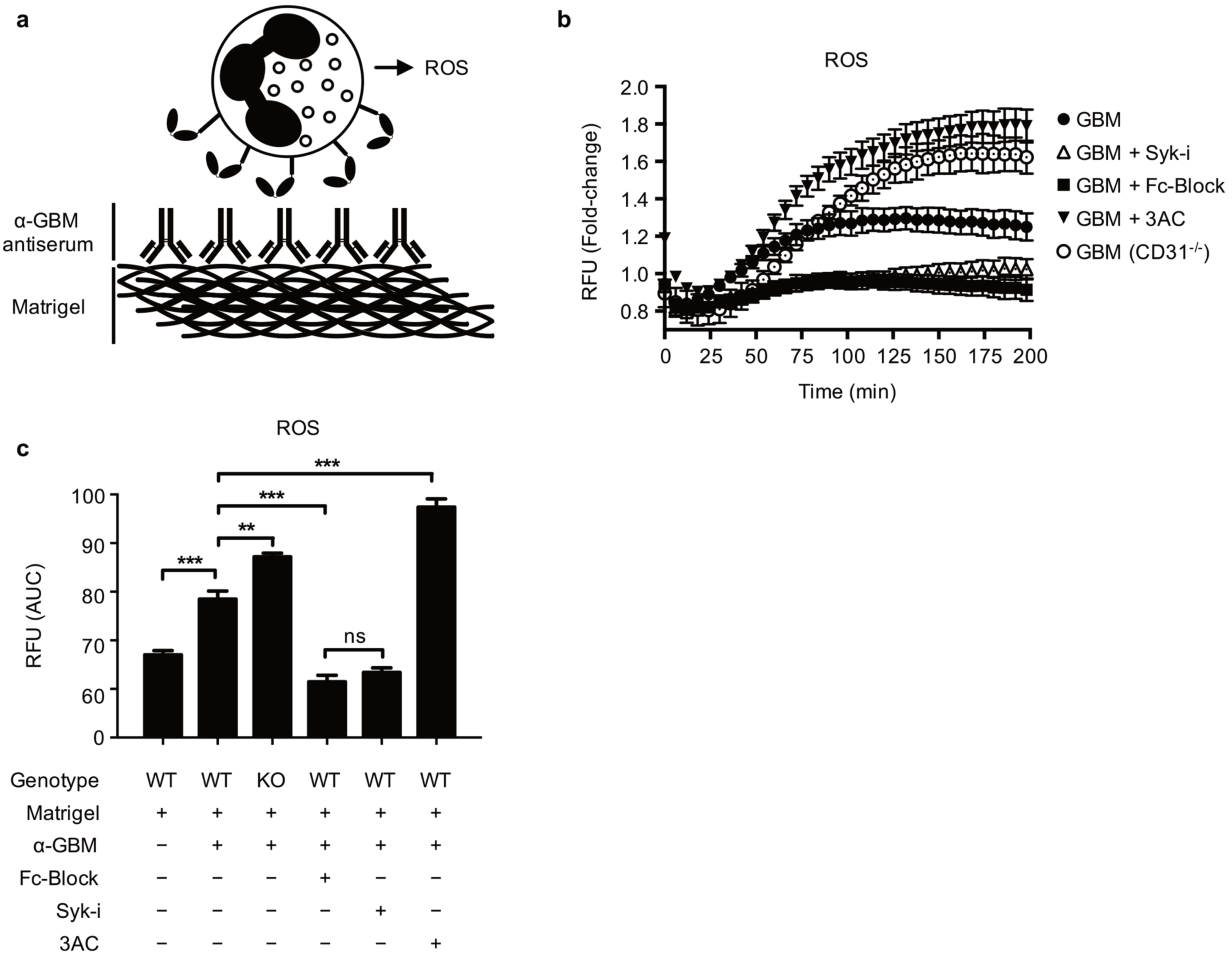

FIGURE 25. *IN VITRO* MOLECULAR CHARACTERIZATION OF αGBM-IC MEDIATED OXIDATIVE BURST IN MURINE NEUTROPHILS

(a) *Experimental design. 96-well plates were coated with 100µg/ml of Matrigel (Corning #354248) overnight at 4°C. Plates were next incubated with αGMB nephrotoxic serum (Probetex #PTX-001) or nonimmune serum at 1:10 dilution for 2 hours at 4°C. Purified murine neutrophils were purified as described previously and were loaded with an intracellular ROS probe following manufacturer's instructions (CM-H2DCFDA, Thermo #C6827). Probe-loaded cells (10^6/ml) were next treated for 10 minutes at room temperature with the following compounds: Fc-block (purified rat anti-mouse CD16/CD32, 2µg/ml. BD #553141), Syk-inhibitor (BAY 61-3606, 150µM. Santa Cruz #202351), SHIP1-inhibitor (3AC, 50µM. Calbiochem #565835). Neutrophils (100µl/well) were finally placed on functionalized plates and fluorescence was read at 494nm/524nm using an Infinite 200 PRO*

Microplate Reader (Tecan. Männedorf, Switzerland) at 37°C for 3 hours at 5 minute intervals. ***(b)*** *Real-time kinetics of fluorescent values during 3 hours of stimulation normalized to the Matrigel condition.* ***(c)*** *Normalized AUC values of ROS probe during 3 hours of neutrophil stimulation. Data are expressed as mean ± SD. P *<0.05 **<0.01 ***<0.001 (Unpaired t- test).*

8.3.6 *Upholding of the CD31 pathway by the peptide controls neutrophil ITAM-dependent protease degranulation in vitro and in vivo*

Neutrophils are professional phagocytic cells; their primary role is to engulf pathogens and dead/damaged eukaryotic cells in order to destroy them by intracellular respiratory burst or by fusion of endocytic vesicles with preformed granules. Phagocytosis is mediated by a number of receptors, among which Fc-receptors are the most extensively studied (Freeman and Grinstein, 2014). While the phagocytosis of ingestible particles (0.5-10µm) is safely managed by neutrophils, interaction with larger objects (i.e. fungal hyphae or asbestos fibers) might results in cytotoxic release before the phagosome is completely sealed (Donaldson et al., 2010; Schafer et al., 2014). This phenomenon is known as "frustrated" (or failed) phagocytosis and leads to the leakage of granule proteins into the extracellular spaces. In GBM glomerulonephritis, neutrophils are faced to antibodies that cover large surfaces area with which they enter in contact for prolonged time period (Devi et al., 2013). Confronted to the solid antibody-coated surface that they cannot engulf, they likely behave as when they are confronted to large foreign bodies. The resulting frustrated phagocytosis can be followed by intense neutrophil degranulation that can severely damage the host tissue (Henson, 1971).

In order to characterize these degranulation steps, we evaluated *ex vivo* the proteolytic activity in the kidneys of mice that had been subjected to the experimental passive glomerulonephritis. We used the *in situ* zymography, a unique technique that enables the localization of protease activity on histological samples by the addition of a substrate labeled with a quenched dye. The degradation of the substrate leads to the release of the quenched fluorescence, enabling the evaluation of the proteolytic activity with a

histological resolution (George and Johnson, 2010). Because the glomerulonephritis model that we used relies on anti-type IV collagen immunoreactivity (Borza, 2007), we investigated the protease activity directed against this collagen isoform. As shown in **Figure 26a**, we could not detect anti-collagen IV enzymatic activity in the kidneys of the mice that received the control serum. On the contrary, there was a massive digestion of the substrate in the tissues from mice injected with the anti-GBM serum, revealing the presence of a large amount of proteases. This intense proteolytic activity surely participates in the alteration of the GBM and contribute to explains the severe kidney dysfunction previously shown (**Figure 23f**). Thus, we sought to explore whether the protection seen in mice treated with the peptide might be explained also by a reduction of neutrophil degranulation. As shown in **Figure 26a** (bottom panels), the zymography performed on kidneys derived from mice treated with the CD31^{agonist} revealed a dramatic reduction of collagenase activity. This clearly demonstrates that the CD31 signaling pathway toughly limits the neutrophil activation *in vivo*.

We subsequently sought to characterize the molecular mechanisms controlling neutrophil degranulation on immobilized GBM-IC *in vitro*. We setup a real-time zymography experiment. As a readout, we used the elastase activity, a harmful protease stored in the azurophilic granules. Of note, azurophilc granules undergo limited exocytosis and they usually contribute to the intracellular degradation of microorganisms in the phagolysosome (Pham, 2006). Hence, we thought that the extracellular presence of elastase would likely reflect neutrophil frustrated phagocytosis. In support of this assumption, we failed to detect extracellular elastase activity in neutrophils challenged with the potent fMLP (in the initial experimental design, fMLP was supposed to be the positive control for degranulation). In striking contrast, the GBM-IC — mimicking the anti-collagen IV surface to which are confronted neutrophils in the glomerulonephritis model — induced the immediate (15 minutes) release of elastase in the supernatant (**Figure 26b**).

Neutrophil activation on GBM-IC, completely relied on the Fc-dependent ITAM pathway since the blockade of the Fc-receptor interaction on IC or the pharmacological inhibition of Syk, prevented elastase release (**Figure 26b, c**). Finally, treatment with the CD31^{agonist}

not only delayed degranulation (**Figure 26b**), but also weakened the amount of elastase release in the culture medium (**Figure 26c**).

Altogether, these results indicate that sustaining the CD31 signaling pathway with the agonist peptide can significantly reduce ITAM-mediated neutrophil degranulation — and the release of cytotoxic compounds — triggered by the detection of IC. As a result, this limits the collateral damages to the host tissue.

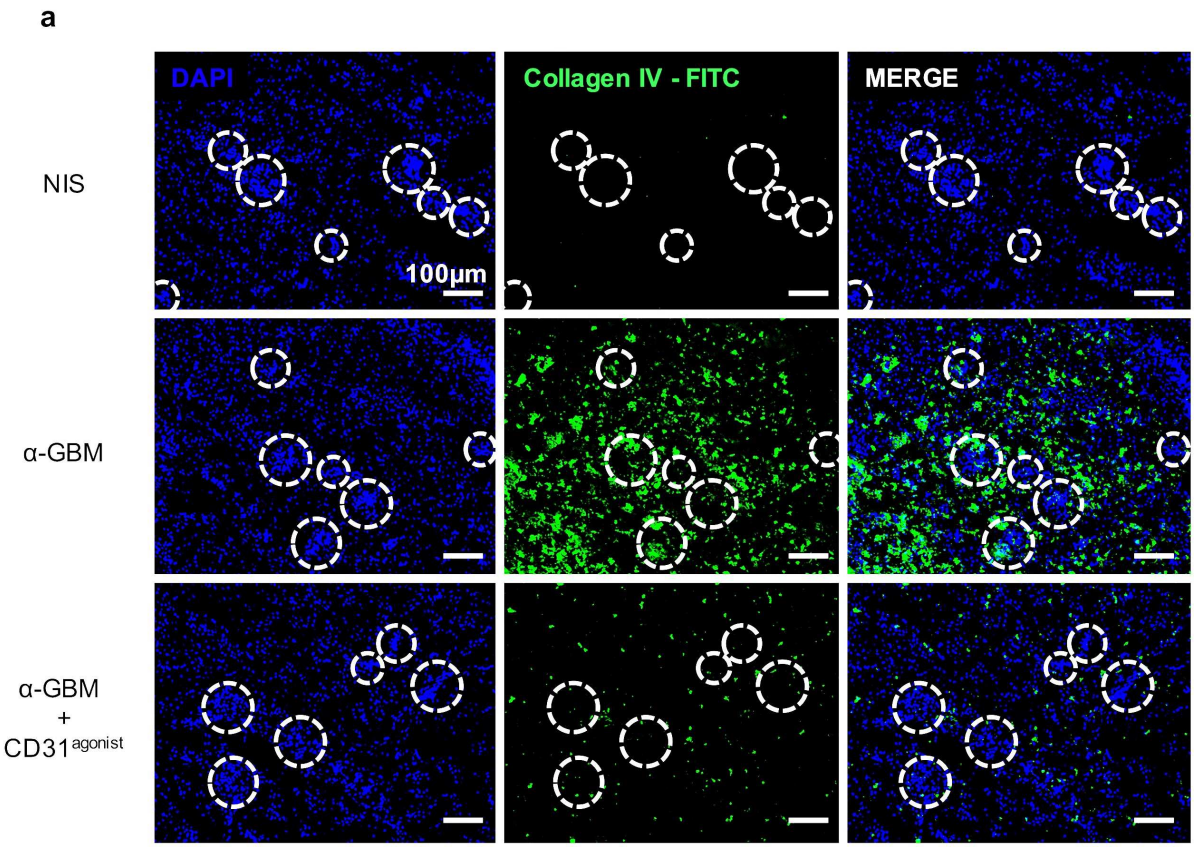
a
DAPI
Collagen IV - FITC
MERGE
NIS
100µm
α-GBM
α-GBM
+
CD31agonist
b
ELASTASE
RFU (Fold-change)
2.7
2.4
2.1
1.8
1.5
1.2
1.0
0
50
100
150
200
Time (min)
▽ MATRIGEL
◆ α-GBM+FcBlock
● α-GBM
○ α-GBM+Syk-i
✳ α-GBM+fMLP
□ α-GBM+CD31agonist
c
ELASTASE
AUC (RFU)
150
125
100
75
50
25
0
*
ns
***
***
**
Matrigel − + + + + + +
fMLP − − + − − − −
α-GBM − − − + + + +
Fc-Block − − − − + − −
Syk-i − − − − − + −
CD31agonist − − − − − − +

FIGURE 26. EVALUATION OF IC-DEPENDENT DEGRANULATION

(a) *In situ zymography was performed on kidney sections with the DQ™ IV collagenase assay kit (Life Technologies #D12052) following manufacturer's instructions. Briefly, 8µm frozen sections were incubated with DQ substrate for 3 hours at 37°C. Slides were washed extensively with PBS and fixed in 4% PFA. Samples were next stained with DAPI and mounted with ProLong Gold antifade. Images were taken at 20X magnification with a Zeiss Axiovert 200 M inverted microscope. Scale bar 100µm, glomeruli are highlighted with dotted white circles.* ***(b)*** *Real-time kinetics of neutrophil elastase activity. 96-multiwell plates were coated with GBM-IC as previously described and purified mouse neutrophils were loaded with DQ™ Elastin probe (20 µg/mL, Life technologies #e12056). Fluorescence was read at 490nm/525nm using an Infinite 200 PRO Microplate Reader (Tecan. Männedorf, Switzerland) at 37°C for 3 hours at 5 minute intervals.* ***(c)*** *Normalized AUC values of elastase probe during 3 hours of neutrophil stimulation. Data are expressed as mean ± SD. P *<0.05 **<0.01 ***<0.001 (Unpaired t- test).*

8.3.7 Summary of Aim III section and graphical abstract

In the third and final part of this work, we were interested in studying the molecular contribution of CD31 to neutrophil effector functions, focusing our attention on ITAM-dependent pathways. More precisely, we explored the hypothesis that CD31 ITIM pathway might regulate leukocyte Fcγ Receptor-mediated neutrophil activation. The interplay between these two molecules had previously been reported in human platelets (Thai le et al., 2003). We started with an *in vitro* test of oxidative burst and we found that upholding CD31 signaling with the agonist peptide decreased the production of reactive oxygen species specifically triggered by the CD32A-ITAM pathway. The inhibitory function exerted by CD31 in this condition was found to be dependent by the activation of the phosphatidylinositol 5'-phosphatase SHIP1, at variance with the inhibitory function of CD31 on other leukocytes, which were reported to depend on SH2-containing tyrosine phosphatases (Clement et al., 2014; Fornasa et al., 2010).

In order to evaluate the role of CD31 on effector functions of neutrophils *in vivo*, we setup model of anti-glomerular basement membrane glomerulonephritis by the passive transfer of a GBM-immune serum in mice. In this model, the glomerular capillary network become suddenly decorated with immune complexes directed against the underlying basement membrane. Since the glomerular EC are fenestrated, autoantibodies can have a direct access to their antigen within the lumen. As a consequence, neutrophils promptly interact with them in the vessels provoking the glomerulonephritis. We found that the administration of the GBM antiserum promptly caused an important blood neutrophilia and, as soon as four hours, glomeruli were massively infiltrated by neutrophils. Neutrophil recruitment and activation resulted in glomerular edema and degradation of local collagen, which was subsequently followed by severe kidney dysfunction. Intervention with the $CD31^{agonist}$ displayed no effect in mice lacking its molecular target, but resulted in a benefit for the clinical score in the wild-type group. This finding was indeed reflected by less neutrophil recruitment and activation on the IC. On the other hand, in $CD31^{-/-}$ mice all these parameters were exacerbated, indicating – by loss of function – that CD31 play an important immunomodulatory role in controlling neutrophil Fc-R activation also *in vivo*. Vascular damages in this pathology were found to be associated with an increase of plasmatic soluble CD31 and a concomitantly decrease of CD31 expression on glomerular endothelial cells. This process was likely to be dependent from a proteolytic mechanism and the peptide administration did not interfere with the shedding phase, indicating that it might act after it. From a functional point of view, we discovered that, besides inhibiting the oxidative burst, CD31 was also able to control specific granules (Collagenase) and the azurophilic granules (Elastase) release. IC-dependent degranulation of elastase was found to be a process mediated by ITAM pathway and the administration of the $CD31^{agonist}$ controlled it.

On the whole, these results provide evidences that the ITIM-bearing receptor CD31 is involved in controlling the ITAM-FcR activation in neutrophils. Pharmacological strategies able to target CD31 can be therefore represent an interesting therapeutic option to treat the acute phases of neutrophil-related inflammatory diseases.

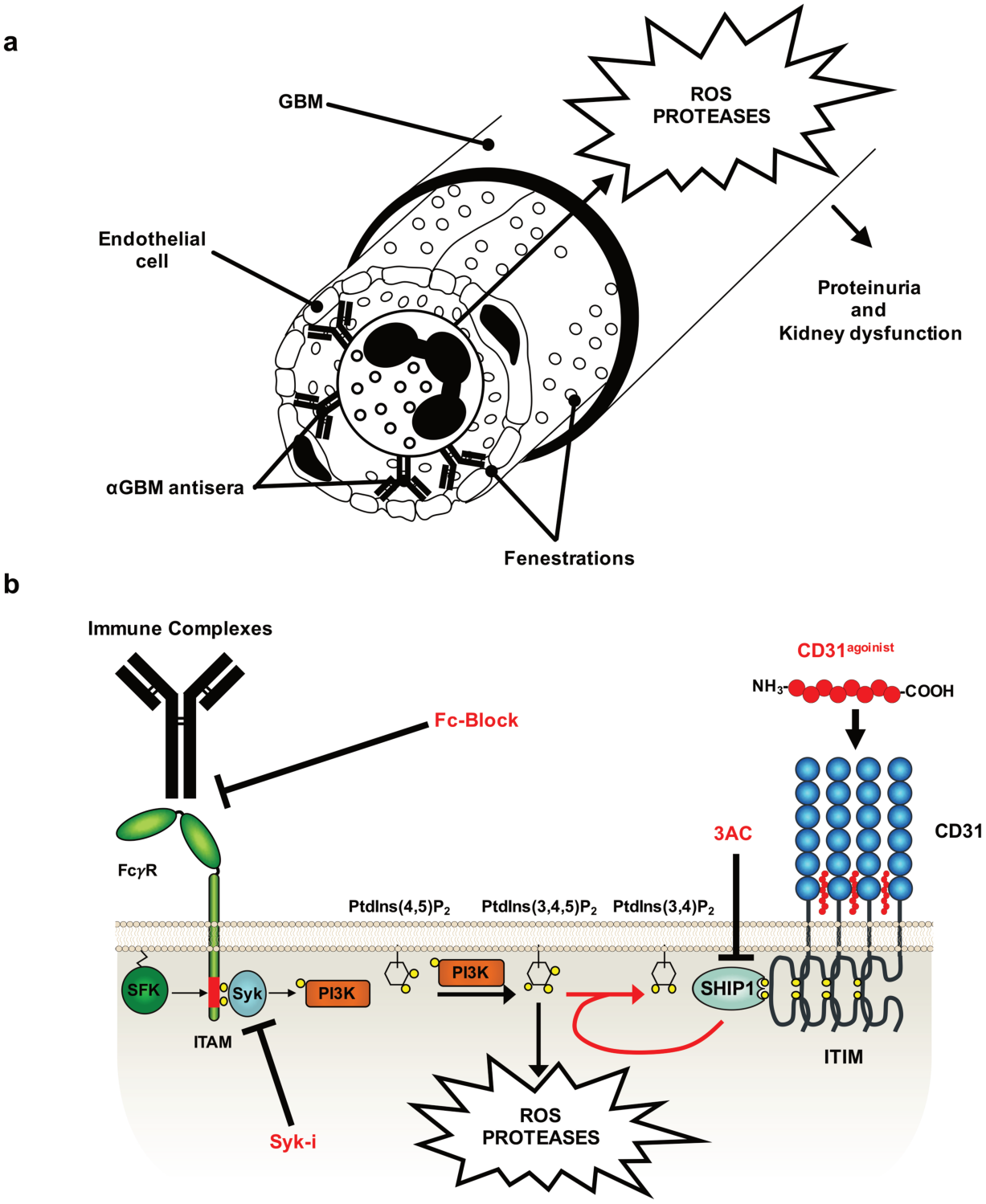

FIGURE 27. GRAPHICAL ABSTRACT OF AIM III SECTION

(a) *Administration of anti-Glomerular Basement Membrane immune serum (αGBM) results in immune complexes deposition within the glomerular lumen since the fenestrated endothelium give*

to antibodies direct access for the underlying glomerular basement membrane (GBM). Neutrophils interact with immune deposits with their Fc-receptors and release cytotoxic proteases and reactive oxygen species (ROS) within the lumen of glomerular capillaries. Activation of neutrophils cause severe damages to the tissue, which results in proteinuria and kidney dysfunction. ***(b)*** *From a molecular point of view, the engagement of Fc-receptors with immune complexes leads to the phosphorylation of its ITAM motif by members of the Src family kinase (SFK). Phosphorylated ITAM tyrosines are able to dock the Spleen Tyrosine Kinase (Syk) at the cellular membrane, which can in turn initiate an intracellular pathway that rely on the Phosphatidylinositol 3 Kinase (PI3K). The conversion of the Phosphatidylinositol (4,5) bisphosphate in Phosphatidylinositol (3,4,5) trisphosphate, trigger downstream events that lead to neutrophil activation. CD31 ITIM motif, in parallel, acts as a molecular platform for the recruitment of the SH2-containinh Phosphatidylinositol 5'-Phosphatase 1 (SHIP1) that convert PtdIns(3,4,5)P_3 in PtdIns(3,4)P_2, dampening the Fc-mediated activation. CD31$^{-/-}$ neutrophils displayed enhanced activation when interact with IC, while the use of CD31^{agonist} in WT mice reduce the severity of the disease.*

DISCUSSION

9 DISCUSSION

The function of circulating leukocytes requires that they exit the circulation and travel across peripheral tissues to reach the sites of acute inflammation. This is a very complex process and implies several steps, all requiring a tight orchestration, in order to be correctly accomplished. Indeed, although the immune cells are “the” essential component that endlessly protect host homeostasis against an immensity of noxious agents, their overwhelming or aberrant recruitment/activation to the inflammatory site can itself be the cause of life-threatening conditions. Throughout my thesis work, I focused my attention on neutrophils, as they represent the first – and in my opinion one of the most formidable – line of defense against pathogenic stimuli. Considered their powerful arsenal, understanding the mechanisms that control their trafficking and activation is hence important to prevent undesirable bystander damages to the host. My working hypothesis was that CD31, a trans-homophilic ITIM co-receptor constitutively expressed at the surface of circulating neutrophils – and of almost all the other cellular components that interact in the circulation – plays an important role in the regulation of the recruitment and activation of these leukocytes at sites of inflammation.

I found that, likewise on other leukocytes, the CD31 inhibitory signaling is rapidly disabled by a proteolytic cleavage after neutrophil activation. However, I demonstrated that an effective signal transmission can still occur by targeting the lingering CD31 fragment with using a CD31-derived homotypic peptide. With this regard, the experimental findings that I could obtain with the use of this $CD31^{agonist}$ peptide, pointed at an interesting and unique immunomodulatory strategy in which the intervention restored the physiological pathway mediated by CD31 in spite of its cleavage. Therefore, in order to study the contribution of CD31 in the steps required for neutrophil recruitment and activation, I could use a dual experimental approach: a “loss-of-function” strategy with using genetically-deficient mice, and a “gain-of-function” approach with the use of the agonist peptide. By using these opposites, but complementary strategies, I sought for coherent and reliable experimental results on which I could founded my thesis.

The experimental data I obtained throughout this work point at a double regulatory role of CD31 in controlling the adhesion and detachment phases of migrating neutrophils. This role

appeared to be important from the very first steps, under the flow forces opposed by the blood stream, trough to the migration in static conditions, when the cells needs to detach from external surface of vessel and move forward into the interstitial tissue through to their final destination, the site of tissue inflammation. The role of CD31 continues beyond the migration steps as we found that the CD31 ITIM pathway is also involved in setting the activation threshold for effector functions of neutrophils, upon the recognition of activating stimuli such as immobilized immune complexes.

In this section, I will try to discuss the principal findings of my work in a wider perspective, taking into account what is currently proposed in the literature. I will try also to consider the limitations of the experiments that I have performed and try to figure out what has yet to be done in order to address several additional questions that have raised from these experiments.

9.1 The puzzling role of CD31 in neutrophil adhesion

9.1.1 CD31 and the transendothelial migration

Almost 30 years have passed since CD31 was cloned (Newman et al., 1990), and the function of this protein in leukocyte adhesion is still matter of debate as different experimental settings have been giving (apparently) conflicting results. Early studies performed by Berman and coworkers (Berman and Muller, 1995; Berman et al., 1996) suggested that CD31 act as a β_2-integrings activator, a theory that has never been questioned. In those experiments, they found that the administration of an anti-CD31 mAb was able to drastically increase the adhesion of monocytes to fibroblast monolayers transfected with ICAM-1, a phenomenon that was inhibited with the concomitant administration of anti-CD18 antibodies. Although these results establish a clear link between CD31 and CD18 function, their interpretation can be dual and yield opposite conclusions: (i) the anti-CD31 monoclonal antibody, by ligating the receptor, may have acted as an agonist. As a consequence, the increased β_2-dependent adhesion would imply that CD31 is a positive regulator of integrins, as suggested by the authors; (ii) the antibody could have at

the contrary blocked the function of the receptor and act as an antagonist. In this case the interpretation would be that CD31 is negative regulator of integrins. In order to draw firm conclusion, it is necessary to evaluate the conformation (functional) state of integrins upon the CD31-targeted intervention. Nowadays we have at our disposal different reporter antibodies with which the functional state of the β_2-integrings can be directly assessed. By using this approach, we have shown that at the uropod of migrating neutrophils CD31 co-localized with close/inactive LFA-1 (**Figure 13c**) strongly suggesting that functional CD31 might indeed act to dampen adhesion, contrary to what has been hypothesized (Berman and Muller, 1995; Berman et al., 1996). The misinterpretation of these earlier studies has certainly been favored by the fact that, at the time of its cloning, CD31 has been assigned to the superfamily of Ig-like cell-adhesion-molecule (Newman PJ, Science 1990). This assumption was based on the structure of the extracellular portion of the molecule (presence of Ig like domains, suchlike in the known adhesion molecules at that time) and its dense presence at the EC cell-cell lateral borders. However, the relatively low (12.5 μM) dissociation constant of the homophilic CD31:CD31 interactions (Newton et al., 1999) could not support this hypothesis and indeed a few years later it was elegantly shown that a functional CD31 is involved contrariwise in cell-cell detachment, not in adhesion (Brown et al., 2002).

When anti-CD31 antibodies were injected *in vivo*, leukocytes were surprisingly found to be trapped between the EC layer and the basement membrane (Wakelin et al., 1996). These results were confirmed after the generation of CD31 knockout mice, since genetically invalidated leukocytes were also observed to be trapped at the edge of the vessel wall in a model of sterile peritonitis (Duncan et al., 1999). The fact that the intravenous administration of anti-CD31 antibodies recapitulate exactly the same phenotype of knockout mice, however, strongly suggests that those antibodies actually acted as antagonist for CD31, an observation that has never been taken in consideration so far. Furthermore, chimeric mice, in which only hematopoietic cells were deficient in CD31, also showed reduced neutrophil egression in the inflamed peritoneal cavity (Dangerfield et al., 2002), indicating that the trans-homophilic CD31:CD31 interactions between the endothelial cell and the leukocyte may be crucial for an effective recruitment into the tissue. The authors of this work proposed that $CD31^{-/-}$ leukocytes were trapped on the basement membrane due to a defective CD31-dependent upregulation of β_1-integrins which was likely necessary after the breaching of the

endothelial wall (Dangerfield et al., 2002). This interpretation is however challenged by more recent findings showing that neutrophils genetically-deficient for β_1-integrins do not display abnormalities in the TEM process and, on the contrary, their migration towards the inflammatory site was even four-time more efficient as compared to that of the WT littermates (Sarangi et al., 2012).

A major issue with the interpretations of these earlier studies may resides in the fact that the authors have not taken into account the complex behavior of neutrophils that move, including when they have to cross the vessel wall. The cell movements in general and the process of leukocytes transmigration in particular, indeed involve an iterative sequence of adhesion of the leukocyte at its front on endothelial cells (Ley et al., 2007), as well as its detachment at the opposite pole at the rear and out from the vascular wall (Hyun et al., 2012; Zen et al., 2011). In this context, a protein that promotes the adhesion is likely to favor the rolling and arresting phase but, concomitantly, it will hamper the dissociation of the rear membrane from the support, including from the uropod of transmigrating neutrophils once they reach the outside part of the vessel. In our work, we tried to study these two phases separately and also to distinguish the adhesion phase in flow conditions on endothelial cells within the blood vessel from the adhesion in static conditions on extracellular matrix, outside the vessels. This sequential approach enabled us to reveal a finely tuning contribution of CD31 in the TEM process that may have been overlooked in the previous works where the interpretation was based on final, global readouts. For instance, we observed that the intravenous administration of the $CD31^{agonist}$ in the systemic circulation dampened the recruitment of neutrophils into the inflamed peritoneal cavity (**Figure 19c**) reliably by inhibiting the rolling cascade (**Figure 16**), but when it was administrated in the peritoneal space, outside of the circulation, it strongly favored the egression of transmigrating neutrophils that became readily detectable into the inflammatory peritoneal fluid (**Figure 19b**). Indeed, our data suggest that this effect was related to an increased efficacy of the migrating neutrophils to detach from the vascular BM as observed by intravital multiphoton microscopy (**Figure 20**). In this regard, it will be interesting to observe by IVM the detachment of extravasating neutrophils also of $CD31^{-/-}$ mice, which has never been performed so far. Due to the current unavailability of a combined LysM-GFP/$CD31^{-/-}$ mouse strain, we could only study the effect of the CD31 agonist (gain-of-function) in CD31 WT LysM-GFP mice (in collaboration with Dr. P Maffia, Glasgow). To overcome this problem,

we plan to perform experiments in which CD31$^{-/-}$ neutrophils will be purified and labeled *ex vivo* prior to their injection in experimental mice. This approach will allow us to study directly, *in vivo* as we did for WT mice, the effect of the absence of CD31 on the detachment of the neutrophil uropod from the outside edge of the vessel and the interstitial locomotion.

One aspect that needs to be further investigated is the molecular nature of the interactions that transmigrated neutrophils establish with the sub-endothelial matrix. Indeed, early studies clearly demonstrated that PMNs from patients whose leukocytes congenitally lack CD11/CD18 β_2-integrins (i.e. LAD, leukocyte adhesion deficiency) exhibited a strong, but not total, reduction of adherence on laminin (Bohnsack, 1992). The same work was indeed the first to show that $\alpha_6\beta_1$ (VLA-6) was the integrin responsible for the β_2-independent adhesion of neutrophils to laminin. All these findings, however, point out at a major role for Mac1 in the interactions of neutrophils with laminin, whereas the role of β_1 integrins appears to be minor. This could possibly explain why Dangerfield and coworkers did not find additional inhibitory effect in neutrophils extravasation when they injected intravenously in CD31$^{-/-}$ mice anti-$\alpha_6\beta_1$ blocking antibodies (Dangerfield et al., 2002). With the same experimental approach used in this work, we plan to use specific integrin inhibitors in order to better dissect the role of each integrin type in the retention of the neutrophils on the basement membrane observed in CD31$^{-/-}$ mice. In my thesis, we focused on laminin as this is one of the most important component of the capillary and post-capillary vascular BM (Yousif et al., 2013), but the contribution of CD31 in modulating interaction on the others extracellular matrix components (fibronectin, collagens), as well as with NG2^{+} pericytes (Proebstl et al., 2012), remain to be investigated.

9.1.2 Role of CD31 during the rolling phase

The fact that phosphorylated CD31 localized at the uropod with β_2-integrins in a bent conformation (**Figure 13**) prompted us to investigate the role of CD31 in the adhesion cascade, as we hypothesized that CD31 may be involved in regulating integrin inside-out activation. We demonstrated that neutrophil lacking CD31, exhibited a slower rolling speed (**Figure 15**), whereas at the opposite the administration of the CD31^{agonist} dramatically

accelerated it (**Figure 16**). At the best of our knowledge, no work has previously investigated in depth the role of CD31 during the rolling phase of the adhesion cascade. The only reported information in this regard, come from Wakelin and coworkers, in a study of leukocyte transmigration during a sterile peritonitis in rats (Wakelin et al., 1996). They noticed that the injection of an anti-CD31 antibody blocked leukocyte passage through the basement membrane, but this treatment did not modify their rolling in the mesenteric microcirculation. A possible explanation of this discrepancy may come from the fact that they defined the "rolling" parameter as the count (i.e. the number) of cells that were visibly moving along the endothelium during the videomicroscopy recordings, but they did not quantify the speed of moving cells. Indeed, we neither have not found noticeable differences in terms of number of total rolling cells between WT and $CD31^{-/-}$ mice (**Figure 16a**), but the analysis of leukocyte speed revealed instead that $CD31^{-/-}$ cells moved slower compared to the control group (**Figure 16b**). The authors of the aforementioned work may have overlooked this phenomenon because the understanding of the steps involved in the adhesion cascade have considerably evolved only recently (Hogg et al., 2011). Another aspect that should be discussed, is the experimental approach that we used in order to study the adhesion cascade in the mesenteric microcirculation. It differs substantially from the common approach, which consists in regarding leukocytes rolling several hours after the experimental induction of inflammation in mice (Zarbock et al., 2008). The local stimulation with ionomycin allowed us to investigate the early dynamics of neutrophils' interaction with endothelial cells. This phenomenon is essentially mediated by the endothelial upregulation of P-selectin (Harrison-Lavoie et al., 2006), while at two hours after the administration of a pro-inflammatory cytokine (TNFα or IL-1β), the rolling is supported also by the *de-novo* expression of E-selectin (Zarbock et al., 2007). Evaluation of rolling velocity in these experimental conditions needs to be undoubtedly done, though purified $CD31^{-/-}$ neutrophils displayed enhanced slowly rolling also on endothelial cells treated overnight with TNFα in the flow chambers (**Figure 15b**), suggests that CD31 may have a role also on rolling on E-selectin.

Although we have evidences for an implication of CD31 in the adhesion cascade, the present work lack functional observations of integrin inside-out signaling in dynamic conditions. It will be interesting to study the expression of integrin activation epitopes – with different reporter antibodies – of neutrophil rolling in the presence or not of the $CD31^{agonist}$

peptide (Kuwano et al., 2010). In this experiment, neutrophils that activate integrins during the adhesion cascade could be labelled by using the appropriate fluorescent reporter antibody. Such dynamic experimental conditions would allow us to evaluate whether the $CD31^{agonist}$ administration can consistently modify the reactivity toward the NKI-L16 mAb, providing direct indications for CD31 involvement in integrin closing. Unfortunately, since reporter antibodies are only available for human integrins, this approach is not feasible to study the effect of CD31 deficiency *in vivo* (in mice).

Another important aspect that remains to be explored, is the signaling molecular partner responsible for the CD31-mediated control of neutrophil rolling velocity. For this purpose, I would evaluate the adhesion of neutrophils on activated EC in the presence or of specific SHP1/SHP2 or SHIP1 inhibitors together with the $CD31^{agonist}$. If the CD31 signaling depends on one of these phosphatases, the effect of the agonist peptide should be abolished by the specific chemical blocker. Alternatively, we could envisage to explore the effect of the $CD31^{agonist}$ administration on neutrophil rolling (by intravital microscopy) in mice genetically invalidated for the aforementioned phosphatases, but the interpretation of such results might be biased by possible compensatory mechanisms that might have occurred because of the genetic manipulation. We expect that neutrophils knocked-out for the responsible phosphatase would behave as $CD31^{-/-}$ neutrophils (**Figure 16**), i.e. they would be insensitive to the effect of the agonist peptide. Strikingly, it has already been reported that $SHP1^{-/-}$ leukocytes exhibit enhanced slow rolling and (like in $CD31^{-/-}$ mice) $SHP1^{-/-}$ neutrophils failed to emigrate to the inflammatory site (Stadtmann et al., 2015). Since SHP1 is a soluble enzyme already described to interact with CD31 (Hua et al., 1998), it would be extremely exciting to investigate whether CD31 may actually be its membrane-docking protein.

9.1.3 The complexity of CD31 and its functional domains

The generation of knockout mice provides a way to alter a specific gene in order to better discern its biological role. Although this is a powerful approach, the fact that the loss of expression is generated among all the cells of the organism, does not allow to discriminate its cell-specific effects. The function of CD31 has always been studied, including us in the

present work, by using the only available CD31$^{-/-}$ mouse strain, which is the same that was created almost 20 years ago by the insertion of a resistance marker in an essential codon of the protein (Duncan et al., 1999). This approach causes a premature stop codon resulting in the complete absence of the protein, extended to all the cells of the body. With this type of knockout mice, the only way to study cell-specific effects is to use specific cell preparation from total knockout mice and use them in WT mice. One of the few works that tried to evaluate the contribution of CD31 in different cell types used the bone marrow transplantation approach: only the hematopoietic system of chimeric mice was KO, whereas the endothelial cells remained WT (Dangerfield et al., 2002). Nevertheless, neither this strategy cannot distinguish between the different hematopoietic cells and several questions are still unanswered.

This is one of the main reason that prompted us to generate new CD31 KO mice with the cre-loxP system (Kos, 2004) by the insertion of two loxP sites at each side of the DNA segment that is meant to be deleted. This technology allows, by genetic cross with specific Cre recombinase transgenic mice, to create constitutive or inducible tissue-specific deletion of the protein so as to finely study the effect of the CD31 absence in all cell types in which is expressed. For example, by crossing the CD31 loxed around the exons 3/4 that we have generated (**Figure 28**) with platelet-specific Cre transgenic mice (for instance PF4-Cre, available in our laboratory) we plan to study whether the specifically absence of CD31 in platelets can modify the recruitment and activation of neutrophils since neutrophil-platelets interactions have recently emerged as being crucial to maintain the homeostasis in inflammatory-driven vascular damages (Gros et al., 2015).

In my thesis work, we demonstrated that the trans-endothelial migration was accompanied by the phosphorylation of the distal (Y_{713}) CD31 ITIM in neutrophils (**Figure 17e**). Nevertheless, we did not provide functional demonstration of the involvement of this signaling motif in the TEM process. For this purpose, we could use another CD31 loxed mouse that was generated in our laboratory driving the specific elimination of the exons encoding the ITIM motifs present in the mouse CD31 cytoplasmic tail (exons 13/14). With using these mice, the expression of the CD31 (the ectodomain as well as the cytoplasmic tail) is not affected, but the receptor cannot rely on it canonical signaling pathway.

Unfortunately, the backcrossing and expansion of these mice took more time than foreseen and suitable mice have become ready only recently, at the end of my PhD. It will be exciting to study whether the phenotype of retention on the basement membrane that we observed in CD31$^{-/-}$ mice in my thesis experiments, was actually due to a lack of the CD31-dependent signalization (CD31 exon 13/14 lox) or if the function of CD31 is barely resumed by its "adhesive" properties (no effect of the CD31 exon 13/14 lox and effect only seen with CD31 exon 3/4 lox, where the trans-homophilic ectodomain will be absent).

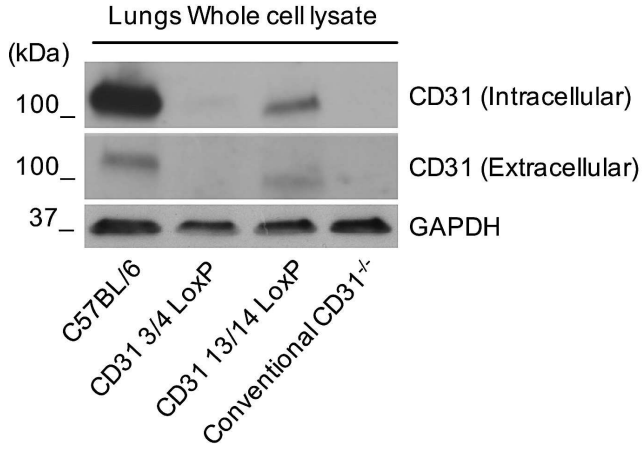

FIGURE 28. CHARACTERIZATION OF THE CD31$^{LOX/LOX}$ MICE STRAINS

Western blot analysis of lung homogenates coming from the different CD31 lox strains, after crossing with constitutive (CMV) Cre recombinase transgenic mice. The blot was revealed with an antibody reactive toward extracellular and intracellular epitope of CD31. 13/14 KO mice display a slightly decrease of CD31 molecular weight due to the loss of the cytoplasmic portion which contains the ITIM domains. "Conventional": the CD31$^{-/-}$ mice generated by Duncan et al. by the conventional homologous recombination technique.

9.1.4 Neutrophils are finally the good, the bad or the ugly?

Injured sites are accompanied by pain, redness, hotness, swelling and temporary loss of functions. These are indeed the cardinal signs of the acute phase of inflammation and are known since the dawn of time, although the underlying mechanisms have remained elusive for a long while. The dense presence of neutrophils at the site of acute inflammation has led to a paradigm stating that neutrophils are responsible for the inflammatory damage at sites of injury. As a shortcut, over the past decades, several clinical trials have attempted to disable mechanisms of neutrophil recruitment in the case of sterile-injury conditions [for a

review, see (Dirksen et al., 2007)]. However, despite a myriad of exciting results in preclinical studies in animal models, they were found disappointing to treat human patients. Monoclonal antibodies aimed to block β_2-integrins in clinical trials – like Rovelizumab [αCD11a (Faxon et al., 2002)] and Erlizumab [αCD18 (Baran et al., 2001)] – were ineffective to reduce the infarct size, while in another case patients started coughing up blood and later died (Dove, 2000).

In some cases, the failure of anti-adhesion therapies in the clinic may have resulted from problems in the trial design, such as the dosing and timing of treatment or the selection of patient populations and the clinical endpoints. Indeed, it should been considered that neutrophils start to adhere and activate into the circulation as soon as 30 minutes after the induction of the ischemic period in experimental models, while at one hour they have already extravasated into the tissue (Desilles et al., 2017). In the case of the αCD18 mAb, patients were enrolled into the clinical trials at <12 hours within the onset of symptoms associated with the myocardial infarction. In contrast with CD18-genetically deficient mice – in which β_2-integrins are absent from the beginning of the ischemic period – the therapeutic strategy mentioned above might have targeted neutrophils too late to produce a clinical benefit. With this regard, although some compromise in host defense against microorganisms is an expected consequence of inhibiting leukocyte trafficking in acute inflammatory conditions, the occurrence of rare infections with anti-integrin treatment (Yousry et al., 2006) has raised concerns about the perturbation of the immune system in chronic diseases.

Importantly, in light of recent advances, it is evident that the entry of neutrophils into injured sites and the ensuing acute inflammatory process, is the essential first step of wound healing (Jones et al., 2016). Thus, contrary to what proposed during the last ten years, avoiding the entry of neutrophils at injured sites would rather be deleterious for the long-term outcome. As an example, it has been recently shown that neutrophils' entry into acute infarcted myocardial tissue is crucial to orchestrate the post-myocardial infarction healing, as the local release of neutrophil gelatinase-associated lipocalin (NGAL) favors the switch of infiltrated macrophages towards a reparative phenotype (Horckmans et al., 2017). Indeed, the processes that lead to the origin (and the end) of the peculiar signs of post-injury inflammation are beginning to be well understood at a cellular and molecular level, as summarized in a recent review (Basil and Levy, 2016). For the innate immune response to

begin wound healing, neutrophils must promptly move to the injured site, where they do their task as long as needed (until the triggering stimulus is cleared) and then stop to be recruited in order to allows macrophages to finish clearing cellular debris and dead neutrophils, switch to a reparative phenotype to end the inflammatory phase and properly start restoring the tissue homeostasis. The coordinated mechanisms of neutrophils trafficking, activation and extinction are crucial for the good outcome of the healing process. If any of these neutrophils' states is not done properly, severe issues can ensue instead of tissue healing.

Rather than intervention aimed at the complete prevention of neutrophil trafficking, we therefore suggest that molecular agents able to sustain the physiologic control of neutrophil recruitment and activation, such as the CD31 co-signaling ITIM pathway, could be more fruitful to prevent pathogenic inflammatory conditions. This would be in line with the modern "biomimetic" vision of therapeutic agents, which aims at reproducing the physiologic regulatory mechanisms of the natural defense system instead of systematically suppressing them (van der Vlist et al., 2016). In this perspective, immunointerventions aimed at sustaining CD31 functionality might have a great place on the stage: the collective data in our laboratory indicate that they would leave alone resting leukocytes whereas they would efficiently prevent further activation of already acting neutrophils at inflammatory sites (Annex II) and, importantly, promote the progression of the healing cascade to the subsequent steps (Annex I).

9.2 Regulation of neutrophils activation by CD31 engagement

9.2.1 Interaction with Immune Complexes

Although neutrophils are of vital importance for the maintenance of host integrity against pathogens (van de Vijver et al., 2012), their deleterious role in inflammatory diseases is equally recognized and controlling neutrophil activation by pharmacological tools is increasingly becoming an attractive strategy (Segel et al., 2011). Likewise, the basic understanding of endogenous regulatory mechanisms can help the development of

strategies aimed to maintain their effector functions to an extend to be immunologically effective, but preventing at the same time an overwhelming and detrimental activation.

Activation of neutrophils through ICs plays a central role in the pathogenesis of several autoimmune inflammatory conditions. In these diseases, immune complexes not only can occur as circulating soluble ICs, but can be formed on extracellular solid surfaces and are thus immobilized (Salama et al., 2001). Neutrophils express various FcR receptors through which they can get activated and contribute to tissue inflammation via the release of soluble mediators that increase vascular permeability, promote further immune cell recruitment and can directly injury the host. Among the classes of human FcγRs, FcγRIIA (CD32A) is a potent activator of inflammation. It is expressed by myeloid cells and platelets and contains its own immunoreceptor tyrosine–based activation motif (ITAM) in the cytoplasmic tail, in contrast to other FcγRs that need to associate with the ITAM-bearing common Fcγ-chain as an adaptor to perform their signalization (Nimmerjahn and Ravetch, 2008). In the present work, we used the GBM glomerulonephritis as an experimental model to study *in vivo* the contribution of CD31 in modulating neutrophil activation by immobilized IC during the acute phase of the inflammatory condition (**Figure 23**) and have demonstrated that CD31 can reliably inhibit human CD32A-mediated neutrophil activation (**Figure 22**). Although we found a sharp kidney-protecting role for the use of the $CD31^{agonist}$ in this model (**Figure 23f**), it is important to consider that there is no CD32A orthologous in murine neutrophils (Bruhns, 2012). Indeed, no murine activating FcγRs possess intrinsically an ITAM motif and they completely depend on the association to the Fcγ-chain to transmit activation signals. To further support our hypothesis, it would be therefore interesting to investigate whether the protection exerted by the CD31 peptide *in vivo* can be replicated in a humanized mouse model in which the endogenous activating FcγRs are replaced by the human CD32A (Tsuboi et al., 2008). Nevertheless, our experiments mimicking the GBM IC on murine neutrophils *in vitro* (**Figure 25**) have shown that the activation cascade was dependent from FcγRs (as the blocking of those receptors maintain leukocytes in a resting state) and that it was mediated by an ITAM pathway (as Syk pharmacological inhibition completely avoid their activation).

Although we formally demonstrated that CD31 was involved in controlling both the oxidative burst (**Figure 25**) and neutrophil degranulation (**Figure 26**) on immobilized GBM IC *in vitro*,

the *in vivo* findings have to be carefully evaluated as other factors may contribute to explain the beneficial effects of the CD31^{agonist} peptide administration. In the second part of my thesis work we have studied the role of CD31 in the control of the adhesion and detachment of migrating neutrophils and, consistent with the hypothesis that CD31 reduces the adhesion and favors the detachment, we found that WT mice treated with the peptide have less neutrophils retained on the glomerular endothelium at four hours after the induction of the GN antiserum (**Figure 23c**, **d**). We cannot definitively conclude whether the CD31 role in this model is dependent exclusively in controlling FcγRs or by dampening at the same time the adhesion of neutrophil on immobilized ICs. It will be difficult distinguish this two phenomena, since the blockade of Mac1 (CD11b/CD18) in this model completely prevent the onset of the pathology by preventing the arrest of the neutrophils on the luminal side of the glomeruli (Devi et al., 2013), thus precluding the possibility to study the subsequent activation step. Moreover, the effect on β_2-integrins and on FcγRs in neutrophil activation could be combined and could more difficult to understand than one may believe. The engagement of β_2-integrins (especially Mac1), can itself positively support neutrophil activation on IC by sustaining specifically the CD32A antibody-dependent cell-mediated cytotoxicity (Liles et al., 1995; Zhou and Brown, 1994). FcRs indeed use signaling molecules associated with Mac-1 and crosstalk of both receptors are necessary for neutrophil activation and/or cytotoxic functions (Ortiz-Stern and Rosales, 2003; Tang et al., 1997).

In conclusion, the neutrophil modulation exerted by the CD31^{agonist} in the GBM GN model may be explained by both controlling the Fc-R pathway as well as integrin activation.

9.2.2 Control of the oxidative burst

Neutrophil activation can results in several effector function, among which, the oxidative burst is one of the most powerful to destroy pathogens (El-Benna et al., 2016). This is well illustrated by recurrence of life-threatening infections in patients affected the chronic granulomatous disease, a pathology due to congenital defects impacting on the oxidative burst process (Assari, 2006). When inappropriate however, the reactive oxygen species

unleashed in an oxidative burst response, can cause considerable collateral damages and are directly responsible for tissues injuries (Babior, 2000).

In the present work, we provided evidences indicating that, while the absence of CD31 resulted in an enhanced production of reactive oxygen species (**Figure 25**), upholding the CD31 molecular pathway reduced in a dose-response manner this specific neutrophil effector function (**Figure 22a**). Furthermore, we found that the CD31-mediated immunomodulation was dependent downstream by the phosphatidylinositol phosphatases SHIP1, as the pharmacological inhibition of its activity completely abolished the effect of the $CD31^{agonist}$ (**Figure 22d**). Although SHIP1 has been described to interact along with CD31 in a human myeloid cell line (Pumphrey et al., 1999), its direct association with CD31 in primary neutrophils has never been explored so far. It will be therefore important to study in deeper details the interaction between these two partners and assess whether the inhibitory functions driven by the peptide is correlated with an enhanced docking of SHIP1 to the CD31 ITIM motif by co-immunoprecipitation experiments. The fact that SHIP1 inhibition alone is associated with an augmented production of ROS by neutrophils activated on immobilized IC (**Figure 22d**), supports previous results indicating that this enzyme plays a central role in controlling FcR-mediated oxidative burst (Mondal et al., 2012). These findings also point at the metabolism of membrane lipid components as crucial for several neutrophil molecular pathways. Indeed, the production of PIP_3 by the phosphatidylinositol 3-kinase (PI3K) is one of the first molecular event in the signaling cascade triggered by the Fc-R ITAM pathway and PI3K inhibition with wortmannin completely abolishes neutrophil oxidative burst (Condliffe et al., 1998).

As depicted in the graphical abstract of the Aim II section, our current hypothesis is that CD31 would recruit SHIP1 at the cellular membrane where this enzyme would therefore reduce the local production of phosphatidylinositol(3,4,5)triphosphate (or PIP_3) by dephosphorylating the inositol ring in the 5' position. Reduced PIP_3 generation can consequently prevent further downstream activator signaling, notably the Bruton's tyrosine kinase (Bolland et al., 1998) and the Phospholipase Cγ (Scharenberg et al., 1998) pathways. These two enzymes are indeed recruited at the cellular membrane by the interaction between their PH (Pleckstrin homology) domain and the PIP_3. Once recruited on the membrane, PLCγ is responsible for the production of soluble IP_3 that, acting a second

messenger, induce the consequent release of Ca^{2+} from the endoplasmic reticulum stores into the cytoplasm (Putney and Tomita, 2012). In support of this, CD31 engagement has already been documented to be associated by a reduction of intracellular calcium in endothelial cells (Gurubhagavatula et al., 1998) and in T-lymphocytes (Newton-Nash and Newman, 1999). To evaluate this hypothesis, it will be important to assess by flow cytometry the calcium levels in activated neutrophil treated with the CD31 peptide or, in the same experimental settings, to study calcium flux in $CD31^{-/-}$ neutrophils challenged with IC.

The molecular machine implicated in the generation of reactive oxygen species in neutrophils is the NADPH oxidase (NOX). NOX is a multi-domain enzymatic complex that catalyze the reduction of molecular oxygen to superoxide anion (O_2^-), which is subsequently converted into the much more toxic hydrogen peroxide (H_2O_2) and – by the MPO – in hypochlorous acid. Under resting condition the different NOX constituents are segregated into the cytoplasm, but they are assembled at the membrane upon neutrophil activation (Panday et al., 2015). Of note, also the machinery assembly is largely dependent by the docking of its constituents at the membrane by the interaction of their PX (Phox Homology) domain on membrane's phospholipids (Xu et al., 2001). It will be interesting study the sub-cellular distribution of NOX components in order to investigate whether the absence of CD31 (or its functional engagement by the agonist peptide) can affect it.

In our experiments, we studied ROS production by using a chemical reporter derivate of the dichlorofluorescein (DCF), which become fluorescent upon oxidation by hydrogen peroxides (Rosenkranz et al., 1992). This is usually used as an indicator of a general oxidative stress and, however, the ROS molecular species with using this probe are quite unspecific as other free radicals – other than H_2O_2 – can oxidize it. Consequently, more specific tests should be done in order to study into details the contribution of CD31 in neutrophil-specific oxidative burst focusing also on the myeloperoxidase-dependent production of ROS.

9.2.3 Control of neutrophil degranulation

The other major neutrophil effector function explored in the present work was the extracellular release of antibiotic substances in the context of a sterile glomerulonephritis.

As presented in the introduction, one of the main feature of neutrophil is the segregation of its functional components into intracellular granules. These granules can be externalized and uncontrolled release into the extracellular environment is a common feature of many inflammatory disorders such as acute lung injury (Grommes and Soehnlein, 2011), rheumatoid arthritis (Wright et al., 2014) and septic shock (Sonego et al., 2016). Although granules mobilization and fusion with the cell membrane is a frequent mechanism in neutrophils effector functions, not all granules subtypes are supposed to release their content into the extracellular space. They are instead hierarchically discharged (secretory vesicles>gelatinase granules>specific granules), but azurophilic granules – due to their highly toxic content – are generally used to kill pathogens intracellularly. This was clear since almost 40 years, as the only experimental way to induce degranulation of azurophilic granules was to treat neutrophil with cytochalasin B (Bentwood and Henson, 1980). Cytochalasin B is an actin-depolymerization toxin that disrupt the neutrophils cortical actin (i.e. the actin shell just beneath the cell membrane), which is believed to act as a physical barrier that impede azurophilic granules to be exocyted (Jog et al., 2007). Therefore, it is not surprising that in our *in vitro* experiments neither the challenging with fMLP was able to induce the degranulation of the azurophilic elastase in murine neutrophils (**Figure 26b**). One of the few situations in which instead neutrophils release their antibiotic substances in the surrounding environment, is the case of a foreign object impossible to engulf. In the GBM GN, immune deposition is spread onto the entire luminal surface of the glomerular capillaries and neutrophils are therefore faced to ingest surfaces. We found indeed that immobilized GBM-IC were the only conditions able to induce a robust degranulation of azurophilic granules. Moreover, also this process was dependent of Fc-Receptors and their ITAM pathway (**Figure 26c**) and the administration of the $CD31^{agonist}$ peptide significantly reduced the release of elastase *in vitro* and the collagenase activity *in vivo* (**Figure 26a**). The role of neutrophil elastase in GBM GN is well known, as its pharmacological inhibition completely protected from proteinuria and glomerular degradation (Suzuki et al., 1998). It will be interesting to perform an *in situ* zymography also for elastase activity, to validate if the control of neutrophil frustrated phagocytosis by the $CD31^{agonist}$ is also a phenomenon that occur *in vivo* and that may contribute to explain the protection from kidney damages (**Figure 23f**). It will be difficult, also in this case, separate the contribution of CD31 in controlling neutrophils adhesion onto the IC, from the subsequent control of frustrated phagocytosis. It

is tempting to speculate that, since each phenomenon is strictly related to the other, the clinical benefit of targeting CD31 with the peptide would results in the control of both.

9.3 Shedding of CD31: implications and opportunities

9.3.1 CD31 cleavage

Proteolytic cleavage has emerged as a key mechanism in regulating the function of several receptors (Simon et al., 1995; Zen et al., 2013; Zen et al., 2011). The functionality of a given protein can indeed be affected by post-transcriptional modifications, by its compartmentalization or by its degradation. Considering the rapidity with which neutrophils exert their effector functions, it is not surprising that they may need to promptly adapt to a particular condition. Indeed, as explained in the introduction, they can rapidly upregulate the expression of a needed receptor by degranulation, while cleavage represents an equally effective way to get rid of another. This process concomitantly implies the loss of the original protein integrity, with the consequent release of its ectodomain. The truncated form of cleaved receptors often maintains biological activity, either by retaining its original function or by acquiring new ones. CD31 shedding was already found to occur in stimulated endothelial cells (Eugenin et al., 2006), platelets (Wong et al., 2004) and T cells (Fornasa et al., 2010), but its molecular reshaping in neutrophils has never been explored in details.

We performed a phenotypic analysis by flow cytometry on human neutrophils, since for human cells we dispose of several monoclonal antibodies directed against all the different ectodomains (Fornasa et al., 2010), which unfortunately is not the case for mouse samples. This strategy not only allowed us to discover that neutrophils invalidate CD31 functionality upon activation, but also to assert that is due to a shedding phenomenon. Indeed, as the domain 6 persist at the neutrophil surface even after 30 minutes of fMLP exposure, we can conclude that the molecule is not completely lost (**Figure 9a, c**). Moreover, by WB analysis of neutrophil membrane, the cleavage appeared to be performed at one specific site, since,

if not, we might have seen a protein smear rather than the appearance of a specific single band (**Figure 9e**). This experiment allowed us also to refine the cleavage site, as the molecular weight of the band – 29 kDa – corresponded to a sequence spanning from the C-terminal tail to the sixth (but not the fifth) domain. We conclude that circulating neutrophils express high level of CD31 in resting conditions, but they lose its expression after a strong cellular activation. However, whether CD31 expression on neutrophils is modified during (non-experimental) pathological conditions remains an unanswered question so far.

During the last period of my PhD I started the collection of blood samples coming from patients affected by vasculitis and lung transplantation. With this samples, I have planned to perform an in-depth flow-cytometry characterization of CD31 expression (D1/D6/Cytoplasmic) on peripheral blood neutrophils in correlation of activator markers (CD11b/CD66b/MPO/PR3). The gold-standard technique to isolate leukocytes from whole blood is to perform a Ficoll gradient and a consecutive congelation in DMSO at -80°. Collect neutrophil with a such method, however, is inadequate, as Ficoll is not suitable to isolate cells with a buoyant density superior to 1.077g/ml (as is the case of granulocytes), while the thawing process is not tolerated by living neutrophils. To overcome this problem, we have developed an alternative procedure that consist in fixing the whole blood – in order to not modify protein expression at the neutrophil surface – and lysing the red blood cell with a hypotonic buffer. Preparing samples in such way will allow us to reduce the bias of gradient centrifugation and to include neutrophil in our collection.

Another unaddressed question unexplored in this work, is the presence intracellular pool of CD31 in neutrophils granules. Indeed, even if preliminary, we may have indirect evidences of their presence. We have performed an experiment in which the shedding kinetics of CD31 was evaluated with neutrophils treated with cytochalasin B. As discussed previously, this compound is a fungal cell-permeable toxin that block actin polymerization (MacLean-Fletcher and Pollard, 1980) thereby paralyzing the cell, forcing neutrophil degranulation and preventing the intracellular recycling of membrane proteins by endocytosis (Bengtsson et al., 1991). As shown in **Figure 29**, after fMLP challenging we obtained a concomitantly increase of CD11b and a decrease of the distal CD31 domain (D1) as shown previously without the cytochalasin B treatment (**Figure 9a**). Surprisingly, we noticed also an augmentation of the signal reflecting the expression of CD31 6th domain, a finding that could

be explained by the externalization at the cellular surface of an intracellular pool of CD31. In the shedding kinetics without cytochalasin B, this phenomenon might be overlooked because of a dynamic recycling of membrane proteins, in a way that the absolute amount of CD31 at the cellular surface can result from a combination of protein shedding and *de novo* externalization of different pools.

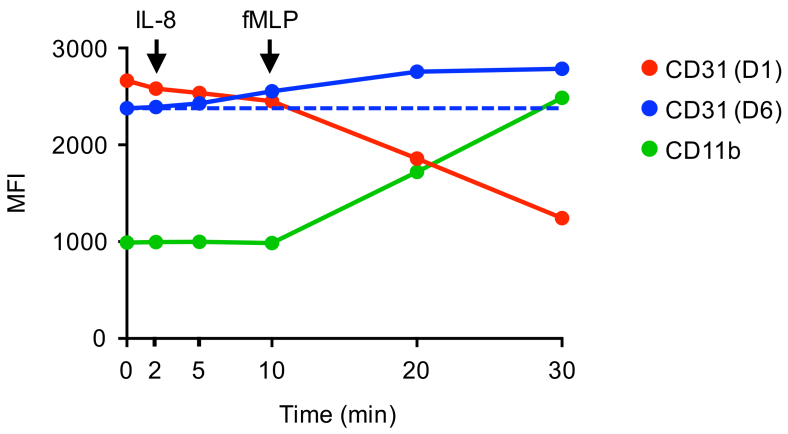

FIGURE 29. EVIDENCES FOR CD31 EXOCYTOSIS

Flow cytometry analysis of CD31 domains expression during activation of purified human neutrophils pre-incubated with cytochalasin B (2µM, SIGMA C6762).

In order to have definitive evidences for CD31 intracellular pools, it will be necessary to perform a nitrogen cavitation followed by density centrifugation so as to obtain a subcellular fractionation of the different neutrophil granules. This approach would allow us to determine not only whether neutrophils possess intracellular stocks of CD31, but also were they are located.

9.3.2 Who is the guilty?

The proteases responsible for CD31 cleavage, regardless of cell type, is still unknown. Although important to enrich the understanding of CD31 in neutrophil biology, I did not investigate the enzyme(s) implicated in CD31 shedding during my PhD. One systematic approach would envisage the evaluation of CD31 expression during the fMLP challenging with different protease inhibitor, or a combination of them if we may found a redundancy

(Zen et al., 2011). Neutrophils express an incredible wide range of proteases that include the family of matrix metalloproteases (MMPs) and the family of serine proteases (or "serprocidins") namely Neutrophil Elastase (NE), Cathepsin-G (CG) and Proteinase-3 (PR3). One clue to reduce the list of suspects, may come from another preliminary experiment in which I followed the kinetic of the CD31 first domain shedding in presence or absence of divalent cations. Chelators like EGTA and EDTA are indeed able to sequestrate Ca^{2+}, Mg^{2+}, Mn^{2+} and Zn^{2+}, which are mandatory for the catalytic activity of MMPs (Pelmenschikov and Siegbahn, 2002). As shown in **Figure 30**, fMLP stimulation of human neutrophils induce a cleavage of CD31 1st domain regardless whether the cells were in presence or in absence of chelators. This data suggests that MMPs may not be implicated in CD31 shedding, thus we should start investigating the role other proteases in this process.

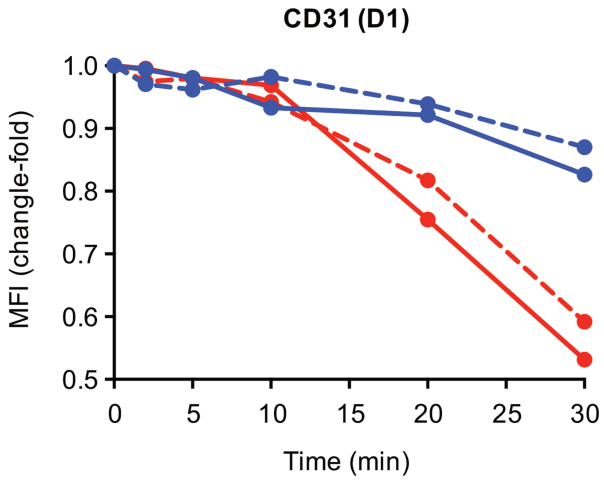

FIGURE 30. ROLE OF BIVALENT CATIONS ON CD31 DOMAIN 1 (D1) SHEDDING

Flow cytometry analysis of CD31 first domain expression in resting (blue lines) or activated (red lines) neutrophils in presence (dotted lines) or absence (continuous lines) of EGTA/EDTA reveals no differences in D1 shedding

Other unpublished experiments coming from our lab (by a previous PhD student, Giulia Fornasa) indicate that recombinant human neutrophil elastase and recombinant human cathepsin G are both able to cleave CD31 *in vitro* (**Figure 31**).

Nevertheless, it is important to consider that we were not able to induce the extracellular release of soluble neutrophil elastase not even with the potent fMLP stimulation (**Figure 26c**). Thus, the contribution of proteases stored in primary granules may play a role in CD31 shedding in specific situations (like frustrated phagocytosis). It is tempting to speculate that in such pathological situations, a release of these proteases could further participate to

CD31 cleavage and the resulting loss of CD31 functionality may contribute to a vicious circle of inflammation.

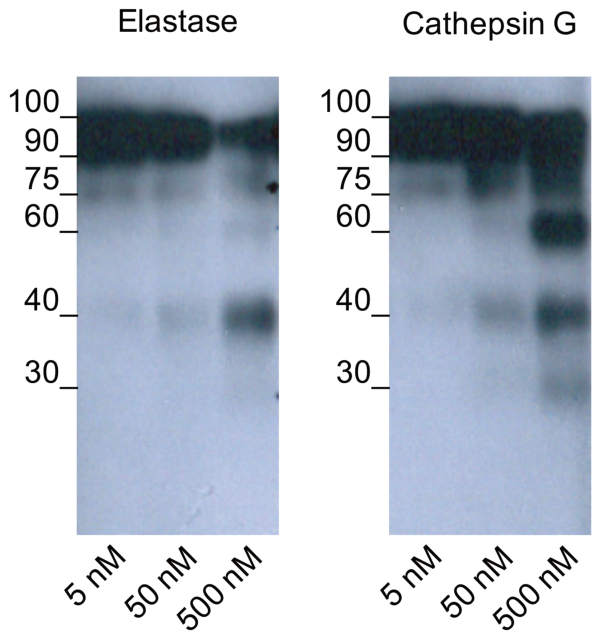

FIGURE 31. CLEAVAGE OF CD31 BY NE AND CG

Recombinant human Elastase and Cathepsin G were incubated at different doses (5, 50 and 500 nM) with recombinant human CD31 (1µg/ml) for 30 minutes at 37°C. Proteins were separated electrophoretically and blotted onto a nitrocellulose membrane. Membrane were revealed with a monoclonal antibody directed against CD31 domain 1 (clone JC70A). The band between 100 and 90 kDa correspond to the intact CD31 molecule, while band of 75, 60, 40 and 30 kDa are CD31 fragments.

An interesting clue comes from the mass spectrometry analysis of CD31 putative partners, when we noted that PR3 co-immunoprecipitate with CD31 in membrane protein preparations from human neutrophils (**Figure 12a**). The interactions found in these experiments needs to be validated by using other complementary techniques suchlike surface plasmon resonance (SPR), Western blotting or the Duolink® technology. PR3 is an intriguing candidate because, in contrast to the other serprocidins that are restricted to azurophilic granules, it is known to be present also in secretory vesicles and at the surface of resting neutrophils (Witko-Sarsat et al., 1999). Given the propensity of secretory vesicles to be readily mobilized at the membrane, it could likely explain the rapidity of CD31 cleavage. It should be taken into account, however, that membrane-bound PR3 have been shown to be catalytically inactive at the surface of resting neutrophil (Korkmaz et al., 2009), hence the contribution of this protease on CD31 cleavage must be carefully evaluated with appropriate experiments.

A mandatory aspect to consider is that the protease activity in an *in vitro* condition differs considerably from the complex environment of living organisms. Several endogenous anti-proteases are indeed present in both the circulation and (less) within the tissues, thus their role in controlling proteolytic processes has to be taken into account (Law et al., 2006).

Finally, in the case we succeed to find the enzyme implicated in CD31 degradation *in vitro*, it will be worthy to evaluate the presence of cleaved CD31 in the plasma (like we did in ***Figure 17*d**) of the corresponding knockout mice under neutrophil-mediated inflammatory conditions. These experiments could give a strong and complementary validating approach *in vivo*.

9.3.3 Plasma soluble CD31: a novel biomarker for neutrophil activation?

Our data demonstrated that the acute inflammation is accompanied with an increase of soluble plasmatic CD31 (**Figure 17d** and **Figure 24b**) and this phenomenon is likely to be dependent from a proteolytic cleavage.

In order to quantify the amount of soluble CD31 in murine plasma, we developed a customized CBA assay (Cytometric Bead Array). The principle of this technique is similar to an ELISA, with the exception that the capture antibody is immobilized on a magnetic bead (rather than a plastic surface) and the detection is made with a fluorescent antibody by flow cytometry (and not by chemiluminescence). Furthermore, compared to a classical ELISA, this test provides several advantages: (i) use of minimal sample volumes, (ii) possibility of multiplexing with other analytes, (iii) is less time-consuming, (iv) the fluorescence detection by cytometry allows an enhanced sensitivity and (v) each test can be replicated several times. Every single bead corresponds indeed at one single test unit (an ELISA well) and, as an example, the cytometric acquisition of 300 beads reliably correspond to 300 technical replicates of the same biological sample (Morgan et al., 2004). The measured fluorescence intensities coming from samples are finally interpolated with a standard curve made with recombinant mouse CD31. Nevertheless, since the capture antibody was polyclonal, we were not able to discriminate the cellular origin of cleaved CD31.

Indeed, we know that soluble CD31 can take origin from distinct cellular processes.

It can be:

(i) released under physiological condition by endothelial cells as a soluble molecule due to a splicing of the transmembrane portion encoding exon (Goldberger et al., 1994),

(ii) cleaved below the 6th domain by activated endothelial cells (Ilan et al., 2001) and platelets (patent WO 2013/152919),

(iii) cleaved below the 5th domain by lymphocytes (Fornasa et al., 2010) and neutrophils (**Figure 9**).

Given the complexity of the molecular forms that can be found in the plasma, a comprehensive strategy should envisage the simultaneous detection of all CD31 domains in order to determine the precise origin of the soluble CD31. Unfortunately, this is not possible nowadays for murine cells due to the lack of monoclonal antibodies directed against the 5th and 6th domain. Even though the loss of the glomerular positivity for CD31 in immunohistology definitely suggested a cleavage on endothelial cells (**Figure 24a**), the plasmatic dosage that we performed in mice cannot be conclusive regarding the molecular nature of shed CD31 in the systemic circulation (**Figure 24b**).

For human samples, however, several monoclonal antibodies have been purified and their epitope characterized. This is the reason why our laboratory has developed and patented (WO 2010/000756 A1) a CBA assay to study the CD31 shedding in human samples (**Figure 32**). The beads are covalently functionalized with a monoclonal antibody directed against the first domain of CD31 – thus permitting the capture of all CD31 molecular forms –, while different fluorescent-labelled antibodies enable the scanning and the discrimination of the domains present on the captured protein.

It will be interesting, therefore, to evaluate CD31 shedding in biological samples coming from patients affected by diseases in which the pathological role of neutrophils is established. Interesting pathologies associated with neutrophil activation would be rheumatoid arthritis (Wright et al., 2014), ischemia-reperfusion injury (Kettritz, 2012) and vasculitis (Schofield et al., 2013).

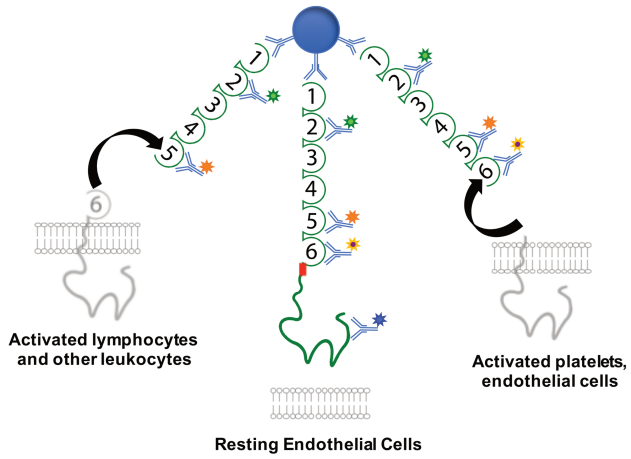

FIGURE 32. CBA ASSAY FOR THE DETECTION OF DIFFERENT CD31 SOLUBLE FORMS

Beads covalently-bound with anti-domain 1 can capture several forms of soluble CD31. Detection is performed with antibodies against different domains of CD31: shed by leukocytes and neutrophils ($D2^+/D5^+$), shed by platelets and activated EC ($D2^+/D5^+/D6^+$) and physiologically secreted by EC ($D2^+/D5^+/D6^+/Cyto^+$).

(Patent WO 2010/000756 A1)

9.3.4 Therapeutic perspectives

Our findings suggested that CD31 displays immunomodulatory properties on neutrophil and we have demonstrated that the agonist peptide we used is indeed able to specifically uphold CD31 functions on activated (but not resting) neutrophils (**Figure 11**). Indeed, the fact that activated neutrophils did not lost completely the expression of CD31 at the cellular surface, but leave intact the sixth domain (crucial for CD31 oligomerization), we hypothesized that cleaved CD31 was still able to function properly. Our results open up the possibility of developing a new drug for the treatment of acute inflammatory conditions, especially those that can lead tissue dysfunction or to chronic conditions. The unique characteristics of CD31 way of action and its modulation during neutrophil activation, make the lingering CD31 domain featured with unique therapeutic opportunities. Indeed, the main advantage of targeting CD31 is that the pharmacological strategy consists in reinforcing a physiological inhibitory pathway – lost in the pathologic condition – rather than performing a complete suppression of the cell population, regardless of the activation status, as it is currently achieved with using blocking antibodies (anti CD3 or anti-CD20, for instance). In support of this view, different studies were performed in animal models so as to target CD31 for treating inflammatory conditions with the use of both monoclonal antibodies (Ishikaw et al., 2002),

recombinant soluble CD31 (Groyer et al., 2007) or CD31-derived peptides (Clement et al., 2015; Fornasa et al., 2012).

Considered that our CD31^{agonist} peptide has physicochemical characteristics which make it suitable for in vivo applications (**Figure 10**), we have tested its therapeutic potential a pre-clinical experimental model of angiotensin-induced abdominal aortic dissection (Annex I, in preparation). This pathology is a life-threatening condition with a mortality of 50 % within the first 48 hours (Kurihara et al., 2012). Here, the outcome of tissue healing after the acute phase, essentially depends upon the resolution of the initial inflammatory which is mainly mediated by macrophages. Dr S. Delbosc, in our laboratory, has results indicating that the CD31^{agonist} peptide can impact on the phenotype switch of macrophages (*in vitro* and *in vivo*), promoting the their polarization towards a “reparatory” M2 phenotype, which is necessary for collagen deposition and effective tissue repair (Novak and Koh, 2013). When the peptide was used for a curative purpose in this model, we found a significant increase of collagen deposition in the lesions and an accelerated healing of the dissected aortic wall. These results are encouraging and we would like to translate the use of this peptide from the bench to the bedside for the clinical management of inflammatory diseases.

During my PhD, I also worked at another preclinical study aimed to target CD31 in a rat model of mesenteric ischemia-reperfusion injury (Annex II, under reviewing). Acute mesenteric ischemia is indeed a life-threatening condition in which the role of neutrophil activation is well established (Grootjans et al., 2010). Consistently, we found that the treatment with the CD31^{agonist} peptide protected the small bowel from the damages associated with the reperfusion as well as neutrophil activation locally (in the intestinal tissue) and in the systemic circulation. These results further confirm an immunomodulatory role of CD31 in neutrophil activation and open the possibility of developing a novel drug to treat the acute phase of a broad spectrum of inflammatory disease.

In conclusion, the results of the experiments performed during my thesis work uncover an unpredicted crucial role for CD31 in the control of neutrophil trafficking, by working as an integrin regulator and of neutrophil activation, by rising its threshold. Of note, our preclinical data point at a potential clinical application of our work, identifying CD31 agonists as therapeutic tools to control excessive neutrophil activation in pathologic inflammatory conditions.

BIBLIOGRAPHY

10 BIBLIOGRAPHY

Albelda, S.M., Muller, W.A., Buck, C.A., and Newman, P.J. (1991). Molecular and cellular properties of PECAM-1 (endoCAM/CD31): a novel vascular cell-cell adhesion molecule. J Cell Biol *114*, 1059-1068.

Anderson, D.C., and Springer, T.A. (1987). Leukocyte adhesion deficiency: an inherited defect in the Mac-1, LFA-1, and p150,95 glycoproteins. Annu Rev Med *38*, 175-194.

Assari, T. (2006). Chronic Granulomatous Disease; fundamental stages in our understanding of CGD. Med Immunol *5*, 4.

Athens, J.W., Raab, S.O., Haab, O.P., Mauer, A.M., Ashenbrucker, H., Cartwright, G.E., and Wintrobe, M.M. (1961). Leukokinetic studies. III. The distribution of granulocytes in the blood of normal subjects. J Clin Invest *40*, 159-164.

Babior, B.M. (2000). Phagocytes and oxidative stress. Am J Med *109*, 33-44.

Baran, K.W., Nguyen, M., McKendall, G.R., Lambrew, C.T., Dykstra, G., Palmeri, S.T., Gibbons, R.J., Borzak, S., Sobel, B.E., Gourlay, S.G., *et al*. (2001). Double-blind, randomized trial of an anti-CD18 antibody in conjunction with recombinant tissue plasminogen activator for acute myocardial infarction: limitation of myocardial infarction following thrombolysis in acute myocardial infarction (LIMIT AMI) study. Circulation *104*, 2778-2783.

Barrow, A.D., and Trowsdale, J. (2006). You say ITAM and I say ITIM, let's call the whole thing off: the ambiguity of immunoreceptor signalling. Eur J Immunol *36*, 1646-1653.

Basil, M.C., and Levy, B.D. (2016). Specialized pro-resolving mediators: endogenous regulators of infection and inflammation. Nat Rev Immunol *16*, 51-67.

Bauer, S., Abdgawad, M., Gunnarsson, L., Segelmark, M., Tapper, H., and Hellmark, T. (2007). Proteinase 3 and CD177 are expressed on the plasma membrane of the same subset of neutrophils. J Leukoc Biol *81*, 458-464.

Bayat, B., Werth, S., Sachs, U.J., Newman, D.K., Newman, P.J., and Santoso, S. (2010). Neutrophil transmigration mediated by the neutrophil-specific antigen CD177 is influenced by the endothelial S536N dimorphism of platelet endothelial cell adhesion molecule-1. J Immunol *184*, 3889-3896.

Bedard, K., and Krause, K.H. (2007). The NOX family of ROS-generating NADPH oxidases: physiology and pathophysiology. Physiol Rev *87*, 245-313.

Bengtsson, T., Dahlgren, C., Stendahl, O., and Andersson, T. (1991). Actin assembly and regulation of neutrophil function: effects of cytochalasin B and tetracaine on chemotactic peptide-induced O2- production and degranulation. J Leukoc Biol *49*, 236-244.

Bentwood, B.J., and Henson, P.M. (1980). The sequential release of granule constitutents from human neutrophils. J Immunol *124*, 855-862.

Bergom, C., Paddock, C., Gao, C., Holyst, T., Newman, D.K., and Newman, P.J. (2008). An alternatively spliced isoform of PECAM-1 is expressed at high levels in human and murine tissues, and suggests a novel role for the C-

terminus of PECAM-1 in cytoprotective signaling. J Cell Sci *121*, 1235-1242.

Berman, M.E., and Muller, W.A. (1995). Ligation of platelet/endothelial cell adhesion molecule 1 (PECAM-1/CD31) on monocytes and neutrophils increases binding capacity of leukocyte CR3 (CD11b/CD18). J Immunol *154*, 299-307.

Berman, M.E., Xie, Y., and Muller, W.A. (1996). Roles of platelet/endothelial cell adhesion molecule-1 (PECAM-1, CD31) in natural killer cell transendothelial migration and beta 2 integrin activation. J Immunol *156*, 1515-1524.

Biswas, P., Zhang, J., Schoenfeld, J.D., Schoenfeld, D., Gratzinger, D., Canosa, S., and Madri, J.A. (2005). Identification of the regions of PECAM-1 involved in beta- and gamma-catenin associations. Biochem Biophys Res Commun *329*, 1225-1233.

Bohnsack, J.F. (1992). CD11/CD18-independent neutrophil adherence to laminin is mediated by the integrin VLA-6. Blood *79*, 1545-1552.

Bohnsack, J.F., and Zhou, X.N. (1992). Divalent cation substitution reveals CD18- and very late antigen-dependent pathways that mediate human neutrophil adherence to fibronectin. J Immunol *149*, 1340-1347.

Bolland, S., Pearse, R.N., Kurosaki, T., and Ravetch, J.V. (1998). SHIP modulates immune receptor responses by regulating membrane association of Btk. Immunity *8*, 509-516.

Borregaard, N. (2010). Neutrophils, from marrow to microbes. Immunity *33*, 657-670.

Borregaard, N., Kjeldsen, L., Sengelov, H., Diamond, M.S., Springer, T.A., Anderson, H.C., Kishimoto, T.K., and Bainton, D.F. (1994). Changes in subcellular localization and surface expression of L-selectin, alkaline phosphatase, and Mac-1 in human neutrophils during stimulation with inflammatory mediators. J Leukoc Biol *56*, 80-87.

Borregaard, N., Miller, L.J., and Springer, T.A. (1987). Chemoattractant-regulated mobilization of a novel intracellular compartment in human neutrophils. Science *237*, 1204-1206.

Borza, D.B. (2007). Autoepitopes and alloepitopes of type IV collagen: role in the molecular pathogenesis of anti-GBM antibody glomerulonephritis. Nephron Exp Nephrol *106*, e37-43.

Branzk, N., Lubojemska, A., Hardison, S.E., Wang, Q., Gutierrez, M.G., Brown, G.D., and Papayannopoulos, V. (2014). Neutrophils sense microbe size and selectively release neutrophil extracellular traps in response to large pathogens. Nat Immunol *15*, 1017-1025.

Brinkmann, V., Reichard, U., Goosmann, C., Fauler, B., Uhlemann, Y., Weiss, D.S., Weinrauch, Y., and Zychlinsky, A. (2004). Neutrophil extracellular traps kill bacteria. Science *303*, 1532-1535.

Brown, D.A., and Rose, J.K. (1992). Sorting of GPI-anchored proteins to glycolipid-enriched membrane subdomains during transport to the apical cell surface. Cell *68*, 533-544.

Brown, S., Heinisch, I., Ross, E., Shaw, K., Buckley, C.D., and Savill, J. (2002). Apoptosis disables CD31-mediated cell detachment from phagocytes promoting binding and engulfment. Nature *418*, 200-203.

Bruhns, P. (2012). Properties of mouse and human IgG receptors and their contribution to disease models. Blood *119*, 5640-5649.

Bruhns, P., Vely, F., Malbec, O., Fridman, W.H., Vivier, E., and Daeron, M. (2000). Molecular basis of the recruitment of the SH2 domain-containing inositol 5-phosphatases SHIP1 and SHIP2 by fcgamma RIIB. J Biol Chem *275*, 37357-37364.

Buscher, K., Wang, H., Zhang, X., Striewski, P., Wirth, B., Saggu, G., Lutke-Enking, S., Mayadas, T.N., Ley, K., Sorokin, L., *et al.* (2016). Protection from septic peritonitis by rapid neutrophil recruitment through omental high endothelial venules. Nat Commun *7*, 10828.

Cai, T.Q., and Wright, S.D. (1996). Human leukocyte elastase is an endogenous ligand for the integrin CR3 (CD11b/CD18, Mac-1, alpha M beta 2) and modulates polymorphonuclear leukocyte adhesion. J Exp Med *184*, 1213-1223.

Calderwood, D.A., Campbell, I.D., and Critchley, D.R. (2013). Talins and kindlins: partners in integrin-mediated adhesion. Nat Rev Mol Cell Biol *14*, 503-517.

Campbell, I.D., and Humphries, M.J. (2011). Integrin structure, activation, and interactions. Cold Spring Harb Perspect Biol *3*.

Cao, M.Y., Huber, M., Beauchemin, N., Famiglietti, J., Albelda, S.M., and Veillette, A. (1998). Regulation of mouse PECAM-1 tyrosine phosphorylation by the Src and Csk families of protein-tyrosine kinases. J Biol Chem *273*, 15765-15772.

Carman, C.V., and Springer, T.A. (2004). A transmigratory cup in leukocyte diapedesis both through individual vascular endothelial cells and between them. J Cell Biol *167*, 377-388.

Carman, C.V., and Springer, T.A. (2008). Trans-cellular migration: cell-cell contacts get intimate. Curr Opin Cell Biol *20*, 533-540.

Cepinskas, G., Savickiene, J., Ionescu, C.V., and Kvietys, P.R. (2003). PMN transendothelial migration decreases nuclear NFkappaB in IL-1beta-activated endothelial cells: role of PECAM-1. J Cell Biol *161*, 641-651.

Chen, Y., Schlegel, P.G., Tran, N., Thompson, D., Zehnder, J.L., and Chao, N.J. (1997). Administration of a CD31-derived peptide delays the onset and significantly increases survival from lethal graft-versus-host disease. Blood *89*, 1452-1459.

Cheung, K., Ma, L., Wang, G., Coe, D., Ferro, R., Falasca, M., Buckley, C.D., Mauro, C., and Marelli-Berg, F.M. (2015). CD31 signals confer immune privilege to the vascular endothelium. Proc Natl Acad Sci U S A *112*, E5815-5824.

Cicmil, M., Thomas, J.M., Sage, T., Barry, F.A., Leduc, M., Bon, C., and Gibbins, J.M. (2000). Collagen, convulxin, and thrombin stimulate aggregation-independent tyrosine phosphorylation of CD31 in platelets. Evidence for the involvement of Src family kinases. J Biol Chem *275*, 27339-27347.

Clement, M., Fornasa, G., Guedj, K., Ben Mkaddem, S., Gaston, A.T., Khallou-Laschet, J., Morvan, M., Nicoletti, A., and Caligiuri, G. (2014). CD31 is a key coinhibitory receptor in the development of immunogenic dendritic cells. Proc Natl Acad Sci U S A *111*, E1101-1110.

Clement, M., Fornasa, G., Loyau, S., Morvan, M., Andreata, F., Guedj, K., Khallou-Laschet, J., Larghi, P., Le Roux, D., Bismuth, G., *et al.* (2015). Upholding the T cell immune-regulatory function of CD31 inhibits the formation of T/B immunological synapses in vitro and attenuates the development of experimental autoimmune arthritis in vivo. J Autoimmun *56*, 23-33.

Condliffe, A.M., Hawkins, P.T., Stephens, L.R., Haslett, C., and Chilvers, E.R. (1998). Priming of human neutrophil superoxide generation by tumour necrosis factor-alpha is signalled by enhanced phosphatidylinositol 3,4,5-trisphosphate but not inositol 1,4,5-trisphosphate accumulation. FEBS Lett *439*, 147-151.

Conte, I.L., Cookson, E., Hellen, N., Bierings, R., Mashanov, G., and Carter, T. (2015). Is there more than one way to unpack a Weibel-Palade body? Blood *126*, 2165-2167.

Critchley, D.R. (2009). Biochemical and structural properties of the integrin-associated cytoskeletal protein talin. Annu Rev Biophys *38*, 235-254.

Dai, B., Wu, P., Xue, F., Yang, R., Yu, Z., Dai, K., Ruan, C., Liu, G., Newman, P.J., and Gao, C. (2016). Integrin-alphaIIbbeta3-mediated outside-in signalling activates a negative feedback pathway to suppress platelet activation. Thromb Haemost *116*, 918-930.

Dallegri, F., Patrone, F., Holm, G., Gahrton, G., and Sacchetti, C. (1983). Neutrophil-mediated antibody-dependent cellular cytotoxicity against erythrocytes. Mechanisms of target cell destruction. Clin Exp Immunol *52*, 613-619.

Dangerfield, J., Larbi, K.Y., Huang, M.T., Dewar, A., and Nourshargh, S. (2002). PECAM-1 (CD31) homophilic interaction up-regulates alpha6beta1 on transmigrated neutrophils in vivo and plays a functional role in the ability of alpha6 integrins to mediate leukocyte migration through the perivascular basement membrane. J Exp Med *196*, 1201-1211.

Deaglio, S., Morra, M., Mallone, R., Ausiello, C.M., Prager, E., Garbarino, G., Dianzani, U., Stockinger, H., and Malavasi, F. (1998). Human CD38 (ADP-ribosyl cyclase) is a counter-receptor of CD31, an Ig superfamily member. J Immunol *160*, 395-402.

DeLisser, H.M., Christofidou-Solomidou, M., Strieter, R.M., Burdick, M.D., Robinson, C.S., Wexler, R.S., Kerr, J.S., Garlanda, C., Merwin, J.R., Madri, J.A., *et al.* (1997). Involvement of endothelial PECAM-1/CD31 in angiogenesis. Am J Pathol *151*, 671-677.

Desilles, J.P., Syvannarath, V., Ollivier, V., Journe, C., Delbosc, S., Ducroux, C., Boisseau, W., Louedec, L., Di Meglio, L., Loyau, S., *et al.* (2017). Exacerbation of Thromboinflammation by Hyperglycemia Precipitates Cerebral Infarct Growth and Hemorrhagic Transformation. Stroke *48*, 1932-1940.

Devi, S., Li, A., Westhorpe, C.L., Lo, C.Y., Abeynaike, L.D., Snelgrove, S.L., Hall, P., Ooi, J.D., Sobey, C.G., Kitching, A.R., *et al.* (2013). Multiphoton imaging reveals a new leukocyte recruitment paradigm in the glomerulus. Nat Med *19*, 107-112.

Diamond, M.S., Staunton, D.E., Marlin, S.D., and Springer, T.A. (1991). Binding of the integrin Mac-1 (CD11b/CD18) to the third immunoglobulin-like domain of ICAM-1 (CD54) and its regulation by glycosylation. Cell *65*, 961-971.

Dirksen, M.T., Laarman, G.J., Simoons, M.L., and Duncker, D.J. (2007). Reperfusion injury in humans: a review of clinical trials on reperfusion injury inhibitory strategies. Cardiovasc Res *74*, 343-355.

Donaldson, K., Murphy, F.A., Duffin, R., and Poland, C.A. (2010). Asbestos, carbon nanotubes and the pleural mesothelium: a review of the hypothesis regarding the role of long fibre retention in the parietal pleura, inflammation and mesothelioma. Part Fibre Toxicol *7*, 5.

Dove, A. (2000). CD18 trials disappoint again. Nat Biotechnol *18*, 817-818.

Du, X., Gu, M., Weisel, J.W., Nagaswami, C., Bennett, J.S., Bowditch, R., and Ginsberg, M.H. (1993). Long range propagation of conformational changes in integrin alpha IIb beta 3. J Biol Chem *268*, 23087-23092.

Duncan, G.S., Andrew, D.P., Takimoto, H., Kaufman, S.A., Yoshida, H., Spellberg, J., de la Pompa, J.L., Elia, A., Wakeham, A., Karan-

Tamir, B., *et al*. (1999). Genetic evidence for functional redundancy of Platelet/Endothelial cell adhesion molecule-1 (PECAM-1): CD31-deficient mice reveal PECAM-1-dependent and PECAM-1-independent functions. J Immunol *162*, 3022-3030.

El Benna, J., Hayem, G., Dang, P.M., Fay, M., Chollet-Martin, S., Elbim, C., Meyer, O., and Gougerot-Pocidalo, M.A. (2002). NADPH oxidase priming and p47phox phosphorylation in neutrophils from synovial fluid of patients with rheumatoid arthritis and spondylarthropathy. Inflammation *26*, 273-278.

El-Benna, J., Hurtado-Nedelec, M., Marzaioli, V., Marie, J.C., Gougerot-Pocidalo, M.A., and Dang, P.M. (2016). Priming of the neutrophil respiratory burst: role in host defense and inflammation. Immunol Rev *273*, 180-193.

Eugenin, E.A., Gamss, R., Buckner, C., Buono, D., Klein, R.S., Schoenbaum, E.E., Calderon, T.M., and Berman, J.W. (2006). Shedding of PECAM-1 during HIV infection: a potential role for soluble PECAM-1 in the pathogenesis of NeuroAIDS. J Leukoc Biol *79*, 444-452.

Faurschou, M., and Borregaard, N. (2003). Neutrophil granules and secretory vesicles in inflammation. Microbes Infect *5*, 1317-1327.

Faust, N., Varas, F., Kelly, L.M., Heck, S., and Graf, T. (2000). Insertion of enhanced green fluorescent protein into the lysozyme gene creates mice with green fluorescent granulocytes and macrophages. Blood *96*, 719-726.

Fawcett, J., Buckley, C., Holness, C.L., Bird, I.N., Spragg, J.H., Saunders, J., Harris, A., and Simmons, D.L. (1995). Mapping the homotypic binding sites in CD31 and the role of CD31 adhesion in the formation of interendothelial cell contacts. J Cell Biol *128*, 1229-1241.

Faxon, D.P., Gibbons, R.J., Chronos, N.A., Gurbel, P.A., Sheehan, F., and Investigators, H.-M. (2002). The effect of blockade of the CD11/CD18 integrin receptor on infarct size in patients with acute myocardial infarction treated with direct angioplasty: the results of the HALT-MI study. J Am Coll Cardiol *40*, 1199-1204.

Fensome, A., Cunningham, E., Prosser, S., Tan, S.K., Swigart, P., Thomas, G., Hsuan, J., and Cockcroft, S. (1996). ARF and PITP restore GTP gamma S-stimulated protein secretion from cytosol-depleted HL60 cells by promoting PIP2 synthesis. Curr Biol *6*, 730-738.

Ferrero, E., Ferrero, M.E., Pardi, R., and Zocchi, M.R. (1995). The platelet endothelial cell adhesion molecule-1 (PECAM1) contributes to endothelial barrier function. FEBS Lett *374*, 323-326.

Fish, K.N. (2009). Total internal reflection fluorescence (TIRF) microscopy. Curr Protoc Cytom *Chapter 12*, Unit12 18.

Fornasa, G., Clement, M., Groyer, E., Gaston, A.T., Khallou-Laschet, J., Morvan, M., Guedj, K., Kaveri, S.V., Tedgui, A., Michel, J.B., *et al*. (2012). A CD31-derived peptide prevents angiotensin II-induced atherosclerosis progression and aneurysm formation. Cardiovasc Res *94*, 30-37.

Fornasa, G., Groyer, E., Clement, M., Dimitrov, J., Compain, C., Gaston, A.T., Varthaman, A., Khallou-Laschet, J., Newman, D.K., Graff-Dubois, S., *et al*. (2010). TCR stimulation drives cleavage and shedding of the ITIM receptor CD31. J Immunol *184*, 5485-5492.

Freeman, S.A., and Grinstein, S. (2014). Phagocytosis: receptors, signal integration, and the cytoskeleton. Immunol Rev *262*, 193-215.

Fukatsu, K., Saito, H., Han, I., Yasuhara, H., Lin, M.T., Inoue, T., Furukawa, S., Inaba, T., Hashiguchi, Y., Matsuda, T., *et al*. (1996). The greater omentum is the primary site of neutrophil exudation in peritonitis. J Am Coll Surg *183*, 450-456.

Futosi, K., Fodor, S., and Mocsai, A. (2013). Reprint of Neutrophil cell surface receptors and their intracellular signal transduction pathways. Int Immunopharmacol *17*, 1185-1197.

Gao, J.X., and Issekutz, A.C. (1997). The beta 1 integrin, very late activation antigen-4 on human neutrophils can contribute to neutrophil migration through connective tissue fibroblast barriers. Immunology *90*, 448-454.

George, S.J., and Johnson, J.L. (2010). In situ zymography. Methods Mol Biol *622*, 271-277.

Goldberger, A., Middleton, K.A., Oliver, J.A., Paddock, C., Yan, H.C., DeLisser, H.M., Albelda, S.M., and Newman, P.J. (1994). Biosynthesis and processing of the cell adhesion molecule PECAM-1 includes production of a soluble form. J Biol Chem *269*, 17183-17191.

Goyert, S.M., Ferrero, E.M., Seremetis, S.V., Winchester, R.J., Silver, J., and Mattison, A.C. (1986). Biochemistry and expression of myelomonocytic antigens. J Immunol *137*, 3909-3914.

Graves, V., Gabig, T., McCarthy, L., Strour, E.F., Leemhuis, T., and English, D. (1992). Simultaneous mobilization of Mac-1 (CD11b/CD18) and formyl peptide chemoattractant receptors in human neutrophils. Blood *80*, 776-787.

Grommes, J., and Soehnlein, O. (2011). Contribution of neutrophils to acute lung injury. Mol Med *17*, 293-307.

Grootjans, J., Lenaerts, K., Derikx, J.P., Matthijsen, R.A., de Bruine, A.P., van Bijnen, A.A., van Dam, R.M., Dejong, C.H., and Buurman, W.A. (2010). Human intestinal ischemia-reperfusion-induced inflammation characterized: experiences from a new translational model. Am J Pathol *176*, 2283-2291.

Gros, A., Syvannarath, V., Lamrani, L., Ollivier, V., Loyau, S., Goerge, T., Nieswandt, B., Jandrot-Perrus, M., and Ho-Tin-Noe, B. (2015). Single platelets seal neutrophil-induced vascular breaches via GPVI during immune-complex-mediated inflammation in mice. Blood *126*, 1017-1026.

Groyer, E., Nicoletti, A., Ait-Oufella, H., Khallou-Laschet, J., Varthaman, A., Gaston, A.T., Thaunat, O., Kaveri, S.V., Blatny, R., Stockinger, H., *et al*. (2007). Atheroprotective effect of CD31 receptor globulin through enrichment of circulating regulatory T-cells. J Am Coll Cardiol *50*, 344-350.

Gurubhagavatula, I., Amrani, Y., Pratico, D., Ruberg, F.L., Albelda, S.M., and Panettieri, R.A., Jr. (1998). Engagement of human PECAM-1 (CD31) on human endothelial cells increases intracellular calcium ion concentration and stimulates prostacyclin release. J Clin Invest *101*, 212-222.

Halaby, D.M., Poupon, A., and Mornon, J. (1999). The immunoglobulin fold family: sequence analysis and 3D structure comparisons. Protein Eng *12*, 563-571.

Hallett, M.B., and Lloyds, D. (1995). Neutrophil priming: the cellular signals that say 'amber' but not 'green'. Immunol Today *16*, 264-268.

Hanna, S., and Etzioni, A. (2012). Leukocyte adhesion deficiencies. Ann N Y Acad Sci *1250*, 50-55.

Harrison-Lavoie, K.J., Michaux, G., Hewlett, L., Kaur, J., Hannah, M.J., Lui-Roberts, W.W., Norman, K.E., and Cutler, D.F. (2006). P-selectin and CD63 use different mechanisms for delivery to Weibel-Palade bodies. Traffic *7*, 647-662.

Henshall, T.L., Jones, K.L., Wilkinson, R., and Jackson, D.E. (2001). Src homology 2 domain-containing protein-tyrosine phosphatases, SHP-1 and SHP-2, are required for platelet endothelial cell adhesion molecule-1/CD31-mediated inhibitory signaling. J Immunol *166*, 3098-3106.

Henson, P.M. (1971). Interaction of cells with immune complexes: adherence, release of constituents, and tissue injury. J Exp Med *134*, 114s-135s.

Hind, L.E., Vincent, W.J., and Huttenlocher, A. (2016). Leading from the Back: The Role of the Uropod in Neutrophil Polarization and Migration. Dev Cell *38*, 161-169.

Hogg, N., Patzak, I., and Willenbrock, F. (2011). The insider's guide to leukocyte integrin signalling and function. Nat Rev Immunol *11*, 416-426.

Holmes, B., Page, A.R., and Good, R.A. (1967). Studies of the metabolic activity of leukocytes from patients with a genetic abnormality of phagocytic function. J Clin Invest *46*, 1422-1432.

Hoover, E.E., and Squier, J.A. (2013). Advances in multiphoton microscopy technology. Nat Photonics *7*, 93-101.

Horckmans, M., Ring, L., Duchene, J., Santovito, D., Schloss, M.J., Drechsler, M., Weber, C., Soehnlein, O., and Steffens, S. (2017). Neutrophils orchestrate post-myocardial infarction healing by polarizing macrophages towards a reparative phenotype. Eur Heart J *38*, 187-197.

Hsu, L.C., Enzler, T., Seita, J., Timmer, A.M., Lee, C.Y., Lai, T.Y., Yu, G.Y., Lai, L.C., Temkin, V., Sinzig, U., *et al*. (2011). IL-1beta-driven neutrophilia preserves antibacterial defense in the absence of the kinase IKKbeta. Nat Immunol *12*, 144-150.

Hua, C.T., Gamble, J.R., Vadas, M.A., and Jackson, D.E. (1998). Recruitment and activation of SHP-1 protein-tyrosine phosphatase by human platelet endothelial cell adhesion molecule-1 (PECAM-1). Identification of immunoreceptor tyrosine-based inhibitory motif-like binding motifs and substrates. J Biol Chem *273*, 28332-28340.

Hynes, R.O. (2002). Integrins: bidirectional, allosteric signaling machines. Cell *110*, 673-687.

Hyun, Y.M., Sumagin, R., Sarangi, P.P., Lomakina, E., Overstreet, M.G., Baker, C.M., Fowell, D.J., Waugh, R.E., Sarelius, I.H., and Kim, M. (2012). Uropod elongation is a common final step in leukocyte extravasation through inflamed vessels. J Exp Med *209*, 1349-1362.

Ilan, N., Cheung, L., Pinter, E., and Madri, J.A. (2000). Platelet-endothelial cell adhesion molecule-1 (CD31), a scaffolding molecule for selected catenin family members whose binding is mediated by different tyrosine and serine/threonine phosphorylation. J Biol Chem *275*, 21435-21443.

Ilan, N., and Madri, J.A. (2003). PECAM-1: old friend, new partners. Curr Opin Cell Biol *15*, 515-524.

Ilan, N., Mahooti, S., Rimm, D.L., and Madri, J.A. (1999). PECAM-1 (CD31) functions as a reservoir for and a modulator of tyrosine-phosphorylated beta-catenin. J Cell Sci *112 Pt 18*, 3005-3014.

Ilan, N., Mohsenin, A., Cheung, L., and Madri, J.A. (2001). PECAM-1 shedding during

apoptosis generates a membrane-anchored truncated molecule with unique signaling characteristics. FASEB J *15*, 362-372.

Ishikaw, J., Okada, Y., Bird, I.N., Jasani, B., Spragg, J.H., and Yamada, T. (2002). Use of anti-platelet-endothelial cell adhesion molecule-1 antibody in the control of disease progression in established collagen-induced arthritis in DBA/1J mice. Jpn J Pharmacol *88*, 332-340.

Jackson, D.E., Kupcho, K.R., and Newman, P.J. (1997). Characterization of phosphotyrosine binding motifs in the cytoplasmic domain of platelet/endothelial cell adhesion molecule-1 (PECAM-1) that are required for the cellular association and activation of the protein-tyrosine phosphatase, SHP-2. J Biol Chem *272*, 24868-24875.

Jerke, U., Marino, S.F., Daumke, O., and Kettritz, R. (2017). Characterization of the CD177 interaction with the ANCA antigen proteinase 3. Sci Rep *7*, 43328.

Jiang, X., Zhong, J., Liu, Y., Yu, H., Zhuo, S., and Chen, J. (2011). Two-photon fluorescence and second-harmonic generation imaging of collagen in human tissue based on multiphoton microscopy. Scanning *33*, 53-56.

Jog, N.R., Rane, M.J., Lominadze, G., Luerman, G.C., Ward, R.A., and McLeish, K.R. (2007). The actin cytoskeleton regulates exocytosis of all neutrophil granule subsets. Am J Physiol Cell Physiol *292*, C1690-1700.

Johansson, M.W., Patarroyo, M., Oberg, F., Siegbahn, A., and Nilsson, K. (1997). Myeloperoxidase mediates cell adhesion via the alpha M beta 2 integrin (Mac-1, CD11b/CD18). J Cell Sci *110 (Pt 9)*, 1133-1139.

Jones, H.R., Robb, C.T., Perretti, M., and Rossi, A.G. (2016). The role of neutrophils in inflammation resolution. Semin Immunol *28*, 137-145.

Kan, A., Mohamedali, A., Tan, S.H., Cheruku, H.R., Slapetova, I., Lee, L.Y., and Baker, M.S. (2013). An improved method for the detection and enrichment of low-abundant membrane and lipid raft-residing proteins. J Proteomics *79*, 299-304.

Kansas, G.S. (1996). Selectins and their ligands: current concepts and controversies. Blood *88*, 3259-3287.

Kettritz, R. (2012). How anti-neutrophil cytoplasmic autoantibodies activate neutrophils. Clin Exp Immunol *169*, 220-228.

Kinhult, J., Egesten, A., Benson, M., Uddman, R., and Cardell, L.O. (2003). Increased expression of surface activation markers on neutrophils following migration into the nasal lumen. Clin Exp Allergy *33*, 1141-1146.

Kirschbaum, N.E., Gumina, R.J., and Newman, P.J. (1994). Organization of the gene for human platelet/endothelial cell adhesion molecule-1 shows alternatively spliced isoforms and a functionally complex cytoplasmic domain. Blood *84*, 4028-4037.

Kolaczkowska, E., and Kubes, P. (2013). Neutrophil recruitment and function in health and inflammation. Nat Rev Immunol *13*, 159-175.

Korkmaz, B., Jaillet, J., Jourdan, M.L., Gauthier, A., Gauthier, F., and Attucci, S. (2009). Catalytic activity and inhibition of wegener antigen proteinase 3 on the cell surface of human polymorphonuclear neutrophils. J Biol Chem *284*, 19896-19902.

Kos, C.H. (2004). Cre/loxP system for generating tissue-specific knockout mouse models. Nutr Rev *62*, 243-246.

Kurihara, T., Shimizu-Hirota, R., Shimoda, M., Adachi, T., Shimizu, H., Weiss, S.J., Itoh, H., Hori, S., Aikawa, N., and Okada, Y. (2012). Neutrophil-derived matrix

metalloproteinase 9 triggers acute aortic dissection. Circulation *126*, 3070-3080.

Kuwano, Y., Spelten, O., Zhang, H., Ley, K., and Zarbock, A. (2010). Rolling on E- or P-selectin induces the extended but not high-affinity conformation of LFA-1 in neutrophils. Blood *116*, 617-624.

Lacy, P. (2006). Mechanisms of degranulation in neutrophils. Allergy Asthma Clin Immunol *2*, 98-108.

Law, R.H., Zhang, Q., McGowan, S., Buckle, A.M., Silverman, G.A., Wong, W., Rosado, C.J., Langendorf, C.G., Pike, R.N., Bird, P.I., *et al*. (2006). An overview of the serpin superfamily. Genome Biol *7*, 216.

Lee, F.A., van Lier, M., Relou, I.A., Foley, L., Akkerman, J.W., Heijnen, H.F., and Farndale, R.W. (2006). Lipid rafts facilitate the interaction of PECAM-1 with the glycoprotein VI-FcR gamma-chain complex in human platelets. J Biol Chem *281*, 39330-39338.

Lefort, C.T., Rossaint, J., Moser, M., Petrich, B.G., Zarbock, A., Monkley, S.J., Critchley, D.R., Ginsberg, M.H., Fassler, R., and Ley, K. (2012). Distinct roles for talin-1 and kindlin-3 in LFA-1 extension and affinity regulation. Blood *119*, 4275-4282.

Lertkiatmongkol, P., Paddock, C., Newman, D.K., Zhu, J., Thomas, M.J., and Newman, P.J. (2016). The Role of Sialylated Glycans in Human Platelet Endothelial Cell Adhesion Molecule 1 (PECAM-1)-mediated Trans Homophilic Interactions and Endothelial Cell Barrier Function. J Biol Chem *291*, 26216-26225.

Levey, A.S., Becker, C., and Inker, L.A. (2015). Glomerular filtration rate and albuminuria for detection and staging of acute and chronic kidney disease in adults: a systematic review. JAMA *313*, 837-846.

Ley, K., Laudanna, C., Cybulsky, M.I., and Nourshargh, S. (2007). Getting to the site of inflammation: the leukocyte adhesion cascade updated. Nat Rev Immunol *7*, 678-689.

Li, P., Li, M., Lindberg, M.R., Kennett, M.J., Xiong, N., and Wang, Y. (2010). PAD4 is essential for antibacterial innate immunity mediated by neutrophil extracellular traps. J Exp Med *207*, 1853-1862.

Liles, W.C., Ledbetter, J.A., Waltersdorph, A.W., and Klebanoff, S.J. (1995). Cross-linking of CD18 primes human neutrophils for activation of the respiratory burst in response to specific stimuli: implications for adhesion-dependent physiological responses in neutrophils. J Leukoc Biol *58*, 690-697.

Lim, K., Hyun, Y.M., Lambert-Emo, K., Capece, T., Bae, S., Miller, R., Topham, D.J., and Kim, M. (2015). Neutrophil trails guide influenza-specific CD8(+) T cells in the airways. Science *349*, aaa4352.

Lu, T.T., Barreuther, M., Davis, S., and Madri, J.A. (1997). Platelet endothelial cell adhesion molecule-1 is phosphorylatable by c-Src, binds Src-Src homology 2 domain, and exhibits immunoreceptor tyrosine-based activation motif-like properties. J Biol Chem *272*, 14442-14446.

Luo, B.H., Carman, C.V., and Springer, T.A. (2007). Structural basis of integrin regulation and signaling. Annu Rev Immunol *25*, 619-647.

MacLean-Fletcher, S., and Pollard, T.D. (1980). Mechanism of action of cytochalasin B on actin. Cell *20*, 329-341.

Mamdouh, Z., Chen, X., Pierini, L.M., Maxfield, F.R., and Muller, W.A. (2003). Targeted recycling of PECAM from endothelial surface-connected compartments during diapedesis. Nature *421*, 748-753.

Marelli-Berg, F.M., Clement, M., Mauro, C., and Caligiuri, G. (2013). An immunologist's guide to CD31 function in T-cells. J Cell Sci *126*, 2343-2352.

Marina, O.C., Sanders, C.K., and Mourant, J.R. (2012). Correlating light scattering with internal cellular structures. Biomed Opt Express *3*, 296-312.

Mauer, A.M., Athens, J.W., Ashenbrucker, H., Cartwright, G.E., and Wintrobe, M.M. (1960). Leukokinetic Studies. Ii. A Method for Labeling Granulocytes in Vitro with Radioactive Diisopropylfluorophosphate (Dfp). J Clin Invest *39*, 1481-1486.

McAdoo, S.P., and Pusey, C.D. (2017). Anti-Glomerular Basement Membrane Disease. Clin J Am Soc Nephrol.

McDonald, B., Pittman, K., Menezes, G.B., Hirota, S.A., Slaba, I., Waterhouse, C.C., Beck, P.L., Muruve, D.A., and Kubes, P. (2010). Intravascular danger signals guide neutrophils to sites of sterile inflammation. Science *330*, 362-366.

Middelhoven, P.J., Ager, A., Roos, D., and Verhoeven, A.J. (1997). Involvement of a metalloprotease in the shedding of human neutrophil Fc gammaRIIIB. FEBS Lett *414*, 14-18.

Millet, A., Martin, K.R., Bonnefoy, F., Saas, P., Mocek, J., Alkan, M., Terrier, B., Kerstein, A., Tamassia, N., Satyanarayanan, S.K., *et al*. (2015). Proteinase 3 on apoptotic cells disrupts immune silencing in autoimmune vasculitis. J Clin Invest *125*, 4107-4121.

Mollinedo, F., Calafat, J., Janssen, H., Martin-Martin, B., Canchado, J., Nabokina, S.M., and Gajate, C. (2006). Combinatorial SNARE complexes modulate the secretion of cytoplasmic granules in human neutrophils. J Immunol *177*, 2831-2841.

Mondal, S., Subramanian, K.K., Sakai, J., Bajrami, B., and Luo, H.R. (2012). Phosphoinositide lipid phosphatase SHIP1 and PTEN coordinate to regulate cell migration and adhesion. Mol Biol Cell *23*, 1219-1230.

Morgan, E., Varro, R., Sepulveda, H., Ember, J.A., Apgar, J., Wilson, J., Lowe, L., Chen, R., Shivraj, L., Agadir, A., *et al*. (2004). Cytometric bead array: a multiplexed assay platform with applications in various areas of biology. Clin Immunol *110*, 252-266.

Muller, W.A. (2011). Mechanisms of leukocyte transendothelial migration. Annu Rev Pathol *6*, 323-344.

Muller, W.A. (2013). Getting leukocytes to the site of inflammation. Vet Pathol *50*, 7-22.

Muller, W.A. (2016). Localized signals that regulate transendothelial migration. Curr Opin Immunol *38*, 24-29.

Nagarajan, S., Venkiteswaran, K., Anderson, M., Sayed, U., Zhu, C., and Selvaraj, P. (2000). Cell-specific, activation-dependent regulation of neutrophil CD32A ligand-binding function. Blood *95*, 1069-1077.

Nathan, C. (2006). Neutrophils and immunity: challenges and opportunities. Nat Rev Immunol *6*, 173-182.

Newman, D.K., Hamilton, C., and Newman, P.J. (2001). Inhibition of antigen-receptor signaling by Platelet Endothelial Cell Adhesion Molecule-1 (CD31) requires functional ITIMs, SHP-2, and p56(lck). Blood *97*, 2351-2357.

Newman, P.J. (1994). The role of PECAM-1 in vascular cell biology. Ann N Y Acad Sci *714*, 165-174.

Newman, P.J. (1999). Switched at birth: a new family for PECAM-1. J Clin Invest *103*, 5-9.

Newman, P.J., Berndt, M.C., Gorski, J., White, G.C., 2nd, Lyman, S., Paddock, C., and Muller, W.A. (1990). PECAM-1 (CD31) cloning and relation to adhesion molecules of the immunoglobulin gene superfamily. Science *247*, 1219-1222.

Newman, P.J., Hillery, C.A., Albrecht, R., Parise, L.V., Berndt, M.C., Mazurov, A.V., Dunlop, L.C., Zhang, J., and Rittenhouse, S.E. (1992). Activation-dependent changes in human platelet PECAM-1: phosphorylation, cytoskeletal association, and surface membrane redistribution. J Cell Biol *119*, 239-246.

Newman, P.J., and Newman, D.K. (2003). Signal transduction pathways mediated by PECAM-1: new roles for an old molecule in platelet and vascular cell biology. Arterioscler Thromb Vasc Biol *23*, 953-964.

Newton, J.P., Buckley, C.D., Jones, E.Y., and Simmons, D.L. (1997). Residues on both faces of the first immunoglobulin fold contribute to homophilic binding sites of PECAM-1/CD31. J Biol Chem *272*, 20555-20563.

Newton, J.P., Hunter, A.P., Simmons, D.L., Buckley, C.D., and Harvey, D.J. (1999). CD31 (PECAM-1) exists as a dimer and is heavily N-glycosylated. Biochem Biophys Res Commun *261*, 283-291.

Newton-Nash, D.K., and Newman, P.J. (1999). A new role for platelet-endothelial cell adhesion molecule-1 (CD31): inhibition of TCR-mediated signal transduction. J Immunol *163*, 682-688.

Nimmerjahn, F., and Ravetch, J.V. (2008). Fcgamma receptors as regulators of immune responses. Nat Rev Immunol *8*, 34-47.

Nishio, M., Watanabe, K., Sasaki, J., Taya, C., Takasuga, S., Iizuka, R., Balla, T., Yamazaki, M., Watanabe, H., Itoh, R., *et al*. (2007). Control of cell polarity and motility by the PtdIns(3,4,5)P3 phosphatase SHIP1. Nat Cell Biol *9*, 36-44.

Nourshargh, S., and Alon, R. (2014). Leukocyte migration into inflamed tissues. Immunity *41*, 694-707.

Novak, M.L., and Koh, T.J. (2013). Macrophage phenotypes during tissue repair. J Leukoc Biol *93*, 875-881.

Nurcombe, H.L., Bucknall, R.C., and Edwards, S.W. (1991). Neutrophils isolated from the synovial fluid of patients with rheumatoid arthritis: priming and activation in vivo. Ann Rheum Dis *50*, 147-153.

O'Toole, T.E., Katagiri, Y., Faull, R.J., Peter, K., Tamura, R., Quaranta, V., Loftus, J.C., Shattil, S.J., and Ginsberg, M.H. (1994). Integrin cytoplasmic domains mediate inside-out signal transduction. J Cell Biol *124*, 1047-1059.

Odin, J.A., Edberg, J.C., Painter, C.J., Kimberly, R.P., and Unkeless, J.C. (1991). Regulation of phagocytosis and [Ca2+]i flux by distinct regions of an Fc receptor. Science *254*, 1785-1788.

Ono, M., Bolland, S., Tempst, P., and Ravetch, J.V. (1996). Role of the inositol phosphatase SHIP in negative regulation of the immune system by the receptor Fc(gamma)RIIB. Nature *383*, 263-266.

Oparka, M., Walczak, J., Malinska, D., van Oppen, L.M., Szczepanowska, J., Koopman, W.J., and Wieckowski, M.R. (2016). Quantifying ROS levels using CM-H2DCFDA and HyPer. Methods *109*, 3-11.

Ortega-Gomez, A., Perretti, M., and Soehnlein, O. (2013). Resolution of inflammation: an integrated view. EMBO Mol Med *5*, 661-674.

Ortiz-Stern, A., and Rosales, C. (2003). Cross-talk between Fc receptors and integrins. Immunol Lett *90*, 137-143.

Oynebraten, I., Bakke, O., Brandtzaeg, P., Johansen, F.E., and Haraldsen, G. (2004). Rapid chemokine secretion from endothelial cells originates from 2 distinct compartments. Blood *104*, 314-320.

Paddock, C., Zhou, D., Lertkiatmongkol, P., Newman, P.J., and Zhu, J. (2016). Structural basis for PECAM-1 homophilic binding. Blood *127*, 1052-1061.

Panday, A., Sahoo, M.K., Osorio, D., and Batra, S. (2015). NADPH oxidases: an overview from structure to innate immunity-associated pathologies. Cell Mol Immunol *12*, 5-23.

Park, S.Y., Ueda, S., Ohno, H., Hamano, Y., Tanaka, M., Shiratori, T., Yamazaki, T., Arase, H., Arase, N., Karasawa, A., *et al*. (1998). Resistance of Fc receptor- deficient mice to fatal glomerulonephritis. J Clin Invest *102*, 1229-1238.

Pathak, M.K., and Yi, T. (2001). Sodium stibogluconate is a potent inhibitor of protein tyrosine phosphatases and augments cytokine responses in hemopoietic cell lines. J Immunol *167*, 3391-3397.

Patil, S., Newman, D.K., and Newman, P.J. (2001). Platelet endothelial cell adhesion molecule-1 serves as an inhibitory receptor that modulates platelet responses to collagen. Blood *97*, 1727-1732.

Pelmenschikov, V., and Siegbahn, P.E. (2002). Catalytic mechanism of matrix metalloproteinases: two-layered ONIOM study. Inorg Chem *41*, 5659-5666.

Peters, A.M. (1998). Just how big is the pulmonary granulocyte pool? Clin Sci (Lond) *94*, 7-19.

Pham, C.T. (2006). Neutrophil serine proteases: specific regulators of inflammation. Nat Rev Immunol *6*, 541-550.

Phee, H., Jacob, A., and Coggeshall, K.M. (2000). Enzymatic activity of the Src homology 2 domain-containing inositol phosphatase is regulated by a plasma membrane location. J Biol Chem *275*, 19090-19097.

Podolnikova, N.P., Podolnikov, A.V., Haas, T.A., Lishko, V.K., and Ugarova, T.P. (2015). Ligand recognition specificity of leukocyte integrin alphaMbeta2 (Mac-1, CD11b/CD18) and its functional consequences. Biochemistry *54*, 1408-1420.

Poon, I.K., Lucas, C.D., Rossi, A.G., and Ravichandran, K.S. (2014). Apoptotic cell clearance: basic biology and therapeutic potential. Nat Rev Immunol *14*, 166-180.

Proebstl, D., Voisin, M.B., Woodfin, A., Whiteford, J., D'Acquisto, F., Jones, G.E., Rowe, D., and Nourshargh, S. (2012). Pericytes support neutrophil subendothelial cell crawling and breaching of venular walls in vivo. J Exp Med *209*, 1219-1234.

Pumphrey, N.J., Taylor, V., Freeman, S., Douglas, M.R., Bradfield, P.F., Young, S.P., Lord, J.M., Wakelam, M.J., Bird, I.N., Salmon, M., *et al*. (1999). Differential association of cytoplasmic signalling molecules SHP-1, SHP-2, SHIP and phospholipase C-gamma1 with PECAM-1/CD31. FEBS Lett *450*, 77-83.

Putney, J.W., and Tomita, T. (2012). Phospholipase C signaling and calcium influx. Adv Biol Regul *52*, 152-164.

Raoof, M., Zhang, Q., Itagaki, K., and Hauser, C.J. (2010). Mitochondrial peptides are potent immune activators that activate human neutrophils via FPR-1. J Trauma *68*, 1328-1332; discussion 1332-1324.

Ritzman, A.M., Hughes-Hanks, J.M., Blaho, V.A., Wax, L.E., Mitchell, W.J., and Brown, C.R. (2010). The chemokine receptor CXCR2 ligand KC (CXCL1) mediates neutrophil recruitment and is critical for development of experimental Lyme arthritis and carditis. Infect Immun *78*, 4593-4600.

Rollet-Labelle, E., Marois, S., Barbeau, K., Malawista, S.E., and Naccache, P.H. (2004). Recruitment of the cross-linked opsonic receptor CD32A (FcgammaRIIA) to high-density detergent-resistant membrane domains in human neutrophils. Biochem J *381*, 919-928.

Romson, J.L., Hook, B.G., Kunkel, S.L., Abrams, G.D., Schork, M.A., and Lucchesi, B.R. (1983). Reduction of the extent of ischemic myocardial injury by neutrophil depletion in the dog. Circulation *67*, 1016-1023.

Rosenkranz, A.R., Schmaldienst, S., Stuhlmeier, K.M., Chen, W., Knapp, W., and Zlabinger, G.J. (1992). A microplate assay for the detection of oxidative products using 2',7'-dichlorofluorescin-diacetate. J Immunol Methods *156*, 39-45.

Ruoslahti, E. (1996). RGD and other recognition sequences for integrins. Annu Rev Cell Dev Biol *12*, 697-715.

Sachs, U.J., Andrei-Selmer, C.L., Maniar, A., Weiss, T., Paddock, C., Orlova, V.V., Choi, E.Y., Newman, P.J., Preissner, K.T., Chavakis, T., *et al*. (2007). The neutrophil-specific antigen CD177 is a counter-receptor for platelet endothelial cell adhesion molecule-1 (CD31). J Biol Chem *282*, 23603-23612.

Salama, A.D., Levy, J.B., Lightstone, L., and Pusey, C.D. (2001). Goodpasture's disease. Lancet *358*, 917-920.

Sarangi, P.P., Hyun, Y.M., Lerman, Y.V., Pietropaoli, A.P., and Kim, M. (2012). Role of beta1 integrin in tissue homing of neutrophils during sepsis. Shock *38*, 281-287.

Sardjono, C.T., Harbour, S.N., Yip, J.C., Paddock, C., Tridandapani, S., Newman, P.J., and Jackson, D.E. (2006). Palmitoylation at Cys595 is essential for PECAM-1 localisation into membrane microdomains and for efficient PECAM-1-mediated cytoprotection. Thromb Haemost *96*, 756-766.

Saverymuttu, S.H., Peters, A.M., Keshavarzian, A., Reavy, H.J., and Lavender, J.P. (1985). The kinetics of 111indium distribution following injection of 111indium labelled autologous granulocytes in man. Br J Haematol *61*, 675-685.

Schafer, K., Bain, J.M., Di Pietro, A., Gow, N.A., and Erwig, L.P. (2014). Hyphal growth of phagocytosed Fusarium oxysporum causes cell lysis and death of murine macrophages. PLoS One *9*, e101999.

Scharenberg, A.M., El-Hillal, O., Fruman, D.A., Beitz, L.O., Li, Z., Lin, S., Gout, I., Cantley, L.C., Rawlings, D.J., and Kinet, J.P. (1998). Phosphatidylinositol-3,4,5-trisphosphate (PtdIns-3,4,5-P3)/Tec kinase-dependent calcium signaling pathway: a target for SHIP-mediated inhibitory signals. EMBO J *17*, 1961-1972.

Schofield, Z.V., Woodruff, T.M., Halai, R., Wu, M.C., and Cooper, M.A. (2013). Neutrophils--a key component of ischemia-reperfusion injury. Shock *40*, 463-470.

Schrijver, G., Bogman, M.J., Assmann, K.J., de Waal, R.M., Robben, H.C., van Gasteren, H., and Koene, R.A. (1990). Anti-GBM nephritis in the mouse: role of granulocytes in the heterologous phase. Kidney Int *38*, 86-95.

Schwartzberg, P.L., Finkelstein, L.D., and Readinger, J.A. (2005). TEC-family kinases: regulators of T-helper-cell differentiation. Nat Rev Immunol *5*, 284-295.

Secklehner, J., Lo Celso, C., and Carlin, L.M. (2017). Intravital microscopy in historic and contemporary immunology. Immunol Cell Biol.

Segel, G.B., Halterman, M.W., and Lichtman, M.A. (2011). The paradox of the neutrophil's role in tissue injury. J Leukoc Biol *89*, 359-372.

Sengelov, H., Boulay, F., Kjeldsen, L., and Borregaard, N. (1994a). Subcellular localization and translocation of the receptor for N-formylmethionyl-leucyl-phenylalanine in human neutrophils. Biochem J *299 (Pt 2)*, 473-479.

Sengelov, H., Follin, P., Kjeldsen, L., Lollike, K., Dahlgren, C., and Borregaard, N. (1995). Mobilization of granules and secretory vesicles during in vivo exudation of human neutrophils. J Immunol *154*, 4157-4165.

Sengelov, H., Kjeldsen, L., Diamond, M.S., Springer, T.A., and Borregaard, N. (1993). Subcellular localization and dynamics of Mac-1 (alpha m beta 2) in human neutrophils. J Clin Invest *92*, 1467-1476.

Sengelov, H., Kjeldsen, L., Kroeze, W., Berger, M., and Borregaard, N. (1994b). Secretory vesicles are the intracellular reservoir of complement receptor 1 in human neutrophils. J Immunol *153*, 804-810.

Shaw, S.K., Bamba, P.S., Perkins, B.N., and Luscinskas, F.W. (2001). Real-time imaging of vascular endothelial-cadherin during leukocyte transmigration across endothelium. J Immunol *167*, 2323-2330.

Simon, S.I., Burns, A.R., Taylor, A.D., Gopalan, P.K., Lynam, E.B., Sklar, L.A., and Smith, C.W. (1995). L-selectin (CD62L) cross-linking signals neutrophil adhesive functions via the Mac-1 (CD11b/CD18) beta 2-integrin. J Immunol *155*, 1502-1514.

Simons, K., and Toomre, D. (2000). Lipid rafts and signal transduction. Nat Rev Mol Cell Biol *1*, 31-39.

Singbartl, K., Green, S.A., and Ley, K. (2000). Blocking P-selectin protects from ischemia/reperfusion-induced acute renal failure. FASEB J *14*, 48-54.

Sonego, F., Castanheira, F.V., Ferreira, R.G., Kanashiro, A., Leite, C.A., Nascimento, D.C., Colon, D.F., Borges Vde, F., Alves-Filho, J.C., and Cunha, F.Q. (2016). Paradoxical Roles of the Neutrophil in Sepsis: Protective and Deleterious. Front Immunol *7*, 155.

Sorokin, L. (2010). The impact of the extracellular matrix on inflammation. Nat Rev Immunol *10*, 712-723.

Stadtmann, A., Block, H., Volmering, S., Abram, C., Sohlbach, C., Boras, M., Lowell, C.A., and Zarbock, A. (2015). Cross-Talk between Shp1 and PIPKIgamma Controls Leukocyte Recruitment. J Immunol *195*, 1152-1161.

Stephens, P., Romer, J.T., Spitali, M., Shock, A., Ortlepp, S., Figdor, C.G., and Robinson, M.K. (1995). KIM127, an antibody that promotes adhesion, maps to a region of CD18 that includes cysteine-rich repeats. Cell Adhes Commun *3*, 375-384.

Stockinger, H., Schreiber, W., Majdic, O., Holter, W., Maurer, D., and Knapp, W. (1992). Phenotype of human T cells expressing CD31, a molecule of the immunoglobulin supergene family. Immunology *75*, 53-58.

Sugimoto, M.A., Vago, J.P., Teixeira, M.M., and Sousa, L.P. (2016). Annexin A1 and the Resolution of Inflammation: Modulation of Neutrophil Recruitment, Apoptosis, and Clearance. J Immunol Res *2016*, 8239258.

Sun, Q.H., DeLisser, H.M., Zukowski, M.M., Paddock, C., Albelda, S.M., and Newman, P.J. (1996). Individually distinct Ig homology

domains in PECAM-1 regulate homophilic binding and modulate receptor affinity. J Biol Chem *271*, 11090-11098.

Sundd, P., Pospieszalska, M.K., Cheung, L.S., Konstantopoulos, K., and Ley, K. (2011). Biomechanics of leukocyte rolling. Biorheology *48*, 1-35.

Suzuki, S., Gejyo, F., Kuroda, T., Kazama, J.J., Imai, N., Kimura, H., and Arakawa, M. (1998). Effects of a novel elastase inhibitor, ONO-5046, on nephrotoxic serum nephritis in rats. Kidney Int *53*, 1201-1208.

Suzuki, Y., Gomez-Guerrero, C., Shirato, I., Lopez-Franco, O., Gallego-Delgado, J., Sanjuan, G., Lazaro, A., Hernandez-Vargas, P., Okumura, K., Tomino, Y., *et al*. (2003). Pre-existing glomerular immune complexes induce polymorphonuclear cell recruitment through an Fc receptor-dependent respiratory burst: potential role in the perpetuation of immune nephritis. J Immunol *170*, 3243-3253.

Tang, T., Rosenkranz, A., Assmann, K.J., Goodman, M.J., Gutierrez-Ramos, J.C., Carroll, M.C., Cotran, R.S., and Mayadas, T.N. (1997). A role for Mac-1 (CDIIb/CD18) in immune complex-stimulated neutrophil function in vivo: Mac-1 deficiency abrogates sustained Fcgamma receptor-dependent neutrophil adhesion and complement-dependent proteinuria in acute glomerulonephritis. J Exp Med *186*, 1853-1863.

Thai le, M., Ashman, L.K., Harbour, S.N., Hogarth, P.M., and Jackson, D.E. (2003). Physical proximity and functional interplay of PECAM-1 with the Fc receptor Fc gamma RIIa on the platelet plasma membrane. Blood *102*, 3637-3645.

Thompson, R.D., Noble, K.E., Larbi, K.Y., Dewar, A., Duncan, G.S., Mak, T.W., and Nourshargh, S. (2001). Platelet-endothelial cell adhesion molecule-1 (PECAM-1)-deficient mice demonstrate a transient and cytokine-specific role for PECAM-1 in leukocyte migration through the perivascular basement membrane. Blood *97*, 1854-1860.

Tipping, P.G., Boyce, N.W., and Holdsworth, S.R. (1989). Relative contributions of chemo-attractant and terminal components of complement to anti-glomerular basement membrane (GBM) glomerulonephritis. Clin Exp Immunol *78*, 444-448.

Treanor, B. (2012). B-cell receptor: from resting state to activate. Immunology *136*, 21-27.

Tsuboi, N., Asano, K., Lauterbach, M., and Mayadas, T.N. (2008). Human neutrophil Fcgamma receptors initiate and play specialized nonredundant roles in antibody-mediated inflammatory diseases. Immunity *28*, 833-846.

Utgaard, J.O., Jahnsen, F.L., Bakka, A., Brandtzaeg, P., and Haraldsen, G. (1998). Rapid secretion of prestored interleukin 8 from Weibel-Palade bodies of microvascular endothelial cells. J Exp Med *188*, 1751-1756.

Van Acker, H., and Coenye, T. (2017). The Role of Reactive Oxygen Species in Antibiotic-Mediated Killing of Bacteria. Trends Microbiol *25*, 456-466.

van de Vijver, E., Maddalena, A., Sanal, O., Holland, S.M., Uzel, G., Madkaikar, M., de Boer, M., van Leeuwen, K., Koker, M.Y., Parvaneh, N., *et al*. (2012). Hematologically important mutations: leukocyte adhesion deficiency (first update). Blood Cells Mol Dis *48*, 53-61.

van der Vlist, M., Kuball, J., Radstake, T.R., and Meyaard, L. (2016). Immune checkpoints and rheumatic diseases: what can cancer immunotherapy teach us? Nat Rev Rheumatol *12*, 593-604.

Vestweber, D. (2015). How leukocytes cross the vascular endothelium. Nat Rev Immunol *15*, 692-704.

Voisin, M.B., Probstl, D., and Nourshargh, S. (2010). Venular basement membranes ubiquitously express matrix protein low-expression regions: characterization in multiple tissues and remodeling during inflammation. Am J Pathol *176*, 482-495.

Wakelin, M.W., Sanz, M.J., Dewar, A., Albelda, S.M., Larkin, S.W., Boughton-Smith, N., Williams, T.J., and Nourshargh, S. (1996). An anti-platelet-endothelial cell adhesion molecule-1 antibody inhibits leukocyte extravasation from mesenteric microvessels in vivo by blocking the passage through the basement membrane. J Exp Med *184*, 229-239.

Wang, F., Li, Y., Shen, Y., Wang, A., Wang, S., and Xie, T. (2013). The functions and applications of RGD in tumor therapy and tissue engineering. Int J Mol Sci *14*, 13447-13462.

Wang, J., Wu, Y., Hu, H., Wang, W., Lu, Y., Mao, H., Liu, X., Liu, Z., and Chen, B.G. (2011). Syk protein tyrosine kinase involves PECAM-1 signaling through tandem immunotyrosine inhibitory motifs in human THP-1 macrophages. Cell Immunol *272*, 39-44.

Wang, S., Voisin, M.B., Larbi, K.Y., Dangerfield, J., Scheiermann, C., Tran, M., Maxwell, P.H., Sorokin, L., and Nourshargh, S. (2006). Venular basement membranes contain specific matrix protein low expression regions that act as exit points for emigrating neutrophils. J Exp Med *203*, 1519-1532.

Wang, Y., Su, X., Sorenson, C.M., and Sheibani, N. (2003). Tissue-specific distributions of alternatively spliced human PECAM-1 isoforms. Am J Physiol Heart Circ Physiol *284*, H1008-1017.

Weinstock, M.T., Francis, J.N., Redman, J.S., and Kay, M.S. (2012). Protease-resistant peptide design-empowering nature's fragile warriors against HIV. Biopolymers *98*, 431-442.

Wengner, A.M., Pitchford, S.C., Furze, R.C., and Rankin, S.M. (2008). The coordinated action of G-CSF and ELR + CXC chemokines in neutrophil mobilization during acute inflammation. Blood *111*, 42-49.

Wilkinson, R., Lyons, A.B., Roberts, D., Wong, M.X., Bartley, P.A., and Jackson, D.E. (2002). Platelet endothelial cell adhesion molecule-1 (PECAM-1/CD31) acts as a regulator of B-cell development, B-cell antigen receptor (BCR)-mediated activation, and autoimmune disease. Blood *100*, 184-193.

Wipke, B.T., and Allen, P.M. (2001). Essential role of neutrophils in the initiation and progression of a murine model of rheumatoid arthritis. J Immunol *167*, 1601-1608.

Witko-Sarsat, V., Cramer, E.M., Hieblot, C., Guichard, J., Nusbaum, P., Lopez, S., Lesavre, P., and Halbwachs-Mecarelli, L. (1999). Presence of proteinase 3 in secretory vesicles: evidence of a novel, highly mobilizable intracellular pool distinct from azurophil granules. Blood *94*, 2487-2496.

Wong, M.X., Harbour, S.N., Wee, J.L., Lau, L.M., Andrews, R.K., and Jackson, D.E. (2004). Proteolytic cleavage of platelet endothelial cell adhesion molecule-1 (PECAM-1/CD31) is regulated by a calmodulin-binding motif. FEBS Lett *568*, 70-78.

Wong, M.X., Roberts, D., Bartley, P.A., and Jackson, D.E. (2002). Absence of platelet endothelial cell adhesion molecule-1 (CD31) leads to increased severity of local and systemic IgE-mediated anaphylaxis and modulation of mast cell activation. J Immunol *168*, 6455-6462.

Woodfin, A., Voisin, M.B., Beyrau, M., Colom, B., Caille, D., Diapouli, F.M., Nash, G.B., Chavakis, T., Albelda, S.M., Rainger, G.E., *et al*. (2011). The junctional adhesion molecule JAM-C regulates polarized transendothelial migration of neutrophils in vivo. Nat Immunol *12*, 761-769.

Wright, H.L., Moots, R.J., and Edwards, S.W. (2014). The multifactorial role of neutrophils in rheumatoid arthritis. Nat Rev Rheumatol *10*, 593-601.

Wu, Y., Stabach, P., Michaud, M., and Madri, J.A. (2005). Neutrophils lacking platelet-endothelial cell adhesion molecule-1 exhibit loss of directionality and motility in CXCR2-mediated chemotaxis. J Immunol *175*, 3484-3491.

Xie, J., Li, R., Kotovuori, P., Vermot-Desroches, C., Wijdenes, J., Arnaout, M.A., Nortamo, P., and Gahmberg, C.G. (1995). Intercellular adhesion molecule-2 (CD102) binds to the leukocyte integrin CD11b/CD18 through the A domain. J Immunol *155*, 3619-3628.

Xie, Y., and Muller, W.A. (1993). Molecular cloning and adhesive properties of murine platelet/endothelial cell adhesion molecule 1. Proc Natl Acad Sci U S A *90*, 5569-5573.

Xu, Y., Seet, L.F., Hanson, B., and Hong, W. (2001). The Phox homology (PX) domain, a new player in phosphoinositide signalling. Biochem J *360*, 513-530.

Yago, T., Petrich, B.G., Zhang, N., Liu, Z., Shao, B., Ginsberg, M.H., and McEver, R.P. (2015). Blocking neutrophil integrin activation prevents ischemia-reperfusion injury. J Exp Med *212*, 1267-1281.

Ye, X., McLean, M.A., and Sligar, S.G. (2016). Phosphatidylinositol 4,5-Bisphosphate Modulates the Affinity of Talin-1 for Phospholipid Bilayers and Activates Its Autoinhibited Form. Biochemistry *55*, 5038-5048.

Yousif, L.F., Di Russo, J., and Sorokin, L. (2013). Laminin isoforms in endothelial and perivascular basement membranes. Cell Adh Migr *7*, 101-110.

Yousry, T.A., Major, E.O., Ryschkewitsch, C., Fahle, G., Fischer, S., Hou, J., Curfman, B., Miszkiel, K., Mueller-Lenke, N., Sanchez, E., *et al*. (2006). Evaluation of patients treated with natalizumab for progressive multifocal leukoencephalopathy. N Engl J Med *354*, 924-933.

Yu, H.B., Zou, B.Y., Wang, X.L., and Li, M. (2016). Investigation of miscellaneous hERG inhibition in large diverse compound collection using automated patch-clamp assay. Acta Pharmacol Sin *37*, 111-123.

Zarbock, A., Abram, C.L., Hundt, M., Altman, A., Lowell, C.A., and Ley, K. (2008). PSGL-1 engagement by E-selectin signals through Src kinase Fgr and ITAM adapters DAP12 and FcR gamma to induce slow leukocyte rolling. J Exp Med *205*, 2339-2347.

Zarbock, A., Lowell, C.A., and Ley, K. (2007). Spleen tyrosine kinase Syk is necessary for E-selectin-induced alpha(L)beta(2) integrin-mediated rolling on intercellular adhesion molecule-1. Immunity *26*, 773-783.

Zehnder, J.L., Shatsky, M., Leung, L.L., Butcher, E.C., McGregor, J.L., and Levitt, L.J. (1995). Involvement of CD31 in lymphocyte-mediated immune responses: importance of the membrane-proximal immunoglobulin domain and identification of an inhibiting CD31 peptide. Blood *85*, 1282-1288.

Zen, K., Guo, Y., Bian, Z., Lv, Z., Zhu, D., Ohnishi, H., Matozaki, T., and Liu, Y. (2013). Inflammation-induced proteolytic processing of the SIRPalpha cytoplasmic ITIM in

neutrophils propagates a proinflammatory state. Nat Commun *4*, 2436.

Zen, K., Guo, Y.L., Li, L.M., Bian, Z., Zhang, C.Y., and Liu, Y. (2011). Cleavage of the CD11b extracellular domain by the leukocyte serprocidins is critical for neutrophil detachment during chemotaxis. Blood *117*, 4885-4894.

Zenaro, E., Pietronigro, E., Della Bianca, V., Piacentino, G., Marongiu, L., Budui, S., Turano, E., Rossi, B., Angiari, S., Dusi, S., *et al*. (2015). Neutrophils promote Alzheimer's disease-like pathology and cognitive decline via LFA-1 integrin. Nat Med *21*, 880-886.

Zhang, Y., Fonslow, B.R., Shan, B., Baek, M.C., and Yates, J.R., 3rd (2013). Protein analysis by shotgun/bottom-up proteomics. Chem Rev *113*, 2343-2394.

Zheng, W., Warner, R., Ruggeri, R., Su, C., Cortes, C., Skoura, A., Ward, J., Ahn, K., Kalgutkar, A., Sun, D., *et al*. (2015). PF-1355, a mechanism-based myeloperoxidase inhibitor, prevents immune complex vasculitis and anti-glomerular basement membrane glomerulonephritis. J Pharmacol Exp Ther *353*, 288-298.

Zhou, M.J., and Brown, E.J. (1994). CR3 (Mac-1, alpha M beta 2, CD11b/CD18) and Fc gamma RIII cooperate in generation of a neutrophil respiratory burst: requirement for Fc gamma RIII and tyrosine phosphorylation. J Cell Biol *125*, 1407-1416.

ANNEXES

11 ANNEX I

(In preparation)

A drug-suitable CD31 peptide favors reparative polarization of macrophages in vitro and aortic healing after acute dissection in vivo

Sandrine Delbosc[1], Kevin Guedj[1], Francesco Andreata[1], Marc Clement, Giulia Fornasa, Jamila Khallou-Laschet, Marion Morvan, Guillaume Even, Emanuele Procopio, Anh-Thu Gaston, Marie Le Borgne, Antonino Nicoletti and Giuseppina Caligiuri

[1] These authors contributed equally to the work

Structured Abstract

Background

Type B aortic dissection is a rare but life-threatening event and its management remains challenging due to lack of specific therapeutic agents aimed at favoring rapid tissue healing. We recently described a beneficial effect of a CD31 signaling in reducing the inflammatory response and prevent the occurrence of type B aortic dissection in apolipoprotein E knockout ($E^{-/-}$) mice subjected to chronic angiotensin (Ang) II-infusion.

Objectives

Develop a drug-suitable CD31 agonist peptide to promote healing of acute aortic dissection in a curative pre-clinical study.

Methods

The candidate peptide drug was selected by functional in vitro screening of a peptide library built from the parent 23-mer peptide. A retro-inverso sequence of the best hit, termed P8RI, passed ADME-tox analysis. Male 28-week old $E^{-/-}$ mice were implanted with Ang II-releasing pumps and were randomly assigned to receive P8RI (2.5 mg/kg/d) or the vehicle (PBS), starting from day 14 (n=20/group). Leukocyte infiltrate and healing features of dissected aortic segments were analyzed by histology and immunofluorescence. The direct effect of P8RI on pro-reparative macrophages was evaluated in vitro.

Results

P8RI treatment promoted the resolution of the intramural hematoma and the production of collagen in dissected aortas. These pro-healing effects were associated with reduced $iNOS^+$ $MMP9^+$ Arginase-II^+ and more Arginase-I^+ $CD68^+$ cells infiltrate, and the results of in vitro experiments showed that the peptide promotes the switch of pro-inflammatory macrophages towards the pro-reparative M2 phenotype.

Conclusions

CD31 signaling promotes the switch of macrophages from the pro-inflammatory to the reparative phenotype and favors the healing of experimental dissected aortas. Our data

suggest that periacute treatment with of the drug-suitable CD31 agonist peptide P8RI may improve the clinical management of Type B aortic dissection.

Introduction

Acute aortic dissection is a life-threatening disease with a mortality of 50 % within the first 48 hours. In the absence of involvement of the ascending aorta (type B aortic dissection), the clinical management is essentially medical and directed at reducing as much as possible the systemic blood pressure and heart frequency in order to limiting the propagation of the false lumen and hence restrain the end-organ damage and risk of rupture (Suzuki, 2014).

Due to the lack of specific therapeutic agents aimed at favoring rapid tissue healing, up to 30% of the patients requires a subsequent intervention because of aneurysmal expansion, progressive dissection, and other complications from the unresolved dissection process (Lumsden, 2008). Interestingly, the rate of recurrent events is independent of the treatment (open surgery, endovascular repair or aggressive anti-hypertensive treatment) and occurs more frequently in patients affected by connective tissue disorders (Isselbacher, 2016), highlighting the importance of an appropriate arterial healing process for the long-term prognosis.

The outcome of tissue healing after an acute injury essentially depends upon the resolution of the initial inflammatory phase and macrophages play a crucial role in this setting. Right after entering the wound, circulating monocytes contribute to the demolition phase by acquiring a pro-inflammatory phenotype but, for an appropriate tissue healing, they must exert a fundamental function consisting in the phagocytosis of apoptotic neutrophils and acquisition of a reparative phenotype (Mantovani, 2013). Importantly, recent work in this field suggest that if the wound contains blood-derived elements, as it is the case in dissected aortas, the switch from the proinflammatory to the reparative phenotype of the wound healing process may be consistently delayed and even remain unachieved (Sindrilaru, 2011).

The molecular mechanisms regulating the equilibrium between the different types of macrophages polarization in wound healing are not yet completely disclosed but a growing body of evidence suggests that macrophages are very plastic cells and that their phenotype strictly depends upon the balance between opposing outside-in signaling signaling

pathways downstream of the multiple surface receptors that can be engaged at the surface of active macrophages (Lawrence, 2011). Thus, the prevalence of stat1/IRF5 pathway leads to a pro-inflammatory (M1) phenotype and the switch towards the reparative (M2) phenotype that is needed for the resolution phase of tissue healing can only occur upon the repression of this pathway (Zhou, 2014). The uncoupling of the stat1/IRF5 pathway downstream of a activating receptor can be operated by tyrosine phosphatases, such as SHP-1, which can be recruited and activated by co-clustered ITIM bearing receptors, such as FCγRIIB and PD-1 (Boekhoudt, 2007; Yao, 2014).

CD31, widely used as an endothelial marker (Liu, 2012) is indeed an ITIM-bearing receptor (Newman, 1999) and may play a crucial role in the regulation of macrophage functions because, at variance with the other ITIM receptors, it is constitutively expressed by both macrophages and neutrophils and its trans-homophilic engagement is indispensable for efficiently engulfing dead neutrophils (Vernon-Wilson, 2007). The expression of an intact CD31 is also associated with anti-inflammatory and angiogenic macrophages (Kim, 2013). The latter, are essential hallmarks of the switch from pro-inflammatory to reparative macrophages (Roszer, 2015).

In apolipoprotein E knockout ($E^{-/-}$) mice subjected to chronic angiotensin (Ang) II-infusion model, an experimental model of abdominal aortic dissection (Trachet, 2015), the infiltration of macrophages at sites of aortic wounds is closely associated with the occurrence of dissection (Saraff, 2003) as well as with the subsequent aneurysmal transformation (Rateri, 2011). Interestingly, the administration of a synthetic peptide derived from CD31 and endowed with immunomodulatory properties (Zehnder, 1995; Chen, 1997) is able to target wound infiltrated macrophages and prevent the incidence of aortic dissection in this model (Fornasa, 2012). However, the peptide sequence used in these previous studies is not suitable as a drug for clinical use.

In order to evaluate the therapeutic potential of CD31 agonists in the clinical management of type B aortic dissection, we have developed a drug-suitable CD31 agonist peptide and evaluated its ability to promote healing of acute aortic dissection in a curative pre-clinical study.

Methods

Identification of a drug-suitable CD31 agonist peptide

In order to identify a drug-suitable CD31 peptide, we screened two peptide libraries "Truncation" library: offset=1, H-, -OH or both, n of peptides=94; and "Scanning" library: 8-mer, offset=1, n of peptides=30, derived from the human (NHASSVPRSKILTVRVILAPWKK) and mouse (SSMRTSPRSSTLAVRVFLAPWK) parent peptides (Mimotopes, Australia (full list and sequences in supplementary table 1). Functional screening of the peptide libraries was performed by assessing the expression of the activation marker CD69 on single mononuclear cell suspensions deriving from mouse spleen and from human peripheral venous blood (Caligiuri, 2013). Briefly, human peripheral blood mononuclear cells were stimulated for 48h in vitro using 2µg/ml of coated anti-Human CD3 (clone UCHT-1, R&D Systems) and soluble anti-Human CD28 (clone 37407, R&D Systems), in complete medium [RPMI 1640 Glutamax (Life technologies), 10-5 M ß-mercaptoethanol, 2 mM L-glutamine, 1X antibiotic/antimycotic solution (Gibco) and 10% decomplemented fetal calf serum (FCS, Biowest)]. Mouse spleens from OT-II mice (C57BL/6-Tg(TcraTcrb)425Cbn/Crl mice, from Charles River France Laboratories) were meshed through 70µm cell strainer (BD biosciences). After red blood cell lysis by hypotonic solution and several washes, single mononuclear cells were counted and plated (2x105cells/well) in round bottom 96-well plate, in complete medium for 48 hours, with 50 ng/ml of OVA peptide (329-337 epitope, from Anaspec). Peptides from the libraries were all diluted in PBS/0.1% of DMS and used at a final concentration of 50 µg/ml on both human and mouse mononuclear cells. The extent of cell activation of human (clone RPA-T4 coupled to APC) and mouse (clone GK1.5 coupled to APC) CD4+ T cells was analyzed by the mean fluorescence intensity obtained with PE anti-human (clone FN50) or anti-mouse (H1.2F3) CD69 antibodies by flow cytometry (all antibodies from BD Biosciences). ADME-Tox analysis was performed on the retro-inverso sequence of the best hit, termed P8RI. Potassium currents mediated by hERG (human ether-a-go-go related gene) channel were recorded with the conventional patch-clamp technique using the whole cell configuration on stably transfected HEK cells (Physiostim, Lautrec, France). Bacterial reverse mutation test was performed on Salmonella typhimurium TA 98 and TA 100 strains (CiToxLab, Evreux, FRANCE). Plasma concentrations of P8RI obtained after intravenous, oral and subcutaneous administration to C57BL6 mice were

used to determine its bioavailability and half-life (pharmacokinetic studies, Eurofins-ADME BIOANALYSES, Vergeze, FRANCE). In vivo toxicology was evaluated during a 14-day subcutaneous dose range study in C57BL6 mice (Centre de Recherches Biologiques, Baugy, FRANCE). Morbidity/mortality checks were performed twice daily. Clinical observations were performed before the first dosing and daily. Functional and neurobehavioural tests were performed before the first dosing, on D7 and on D14. Body weight was recorded at D-1, D1, D2, D5, D8, D11 and D14. Food consumption was measured weekly. Blood samples for hematology and clinical chemistry analysis were collected on D15. All animals were euthanized on D15. Kidneys, liver, heart and lungs were weighed, fixed and preserved at necropsy.

Angiotensin II infusion in ApoE$^{-/-}$ mice

Male, 28-week-old ApoE$^{-/-}$ mice (B6.129P2-Apoetm1Unc/Crl, Charles River France) were maintained on a regular chow diet under standard conditions. The experiments were repeated four times and included two groups of mice (n ≥10 mice/group) randomly assigned to receive daily a subcutaneous injection (50 µL) of either the peptide solution ('peptide' group, 2.5 mg/kg/day) or of the vehicle solution ('control' group). The treatment was started 14 days after the beginning of the angiotensin II (Sigma, #A9525) infusion (1 mg/kg/day), thus well after the occurrence of aortic dissection which occurs within the first 7 days (Saraff, 2003; Cao, 2010). At the end of the study, mice were euthanized by exsanguination under anaesthesia (i.p. injection of Ketamine-HCl 100 mg/kg and Xylazine 20 mg/kg, animals were considered as safely anaesthetized when no attempt to withdraw the limb after pressure could be observed). Blood was withdrawn from the right heart ventricle and collected in EDTA tubes for blood cell and plasma analysis. The heart and the aorta were dissected, photographed and mounted in cryomolds for further histomorphologic analysis on cryosections. All the investigations conformed to the Directive 2010/63/EU of the European Parliament and formal approval was granted by the Local Animal Ethics Committee (Comité d'éthique Bichat—Debré).

Histology

Detailed analysis was performed in aortas displaying evidence for the occurrence of an aortic dissection as detected by Perl's staining of iron deposits (≥70% of experimental mice in all experiments). Collagen qualitative analysis was performed on sequential cross

sections of the dissected aortic segments, after staining with picrosirius red and observation under polarized light observation. Digital images were acquired using AxioVision® and a Zeiss Axioobserver Z1 microscope. The extent of collagen deposition (brilliant red staining) was quantitatively assessed using a program developed in Quips language (Leica, Cambridge, UK).

Immunohistochemistry

Selected cryosections of aortic roots and abdominal aortas close to dissection sites were fixed for 10 minutes in parafolmadehyde (4% in PBS) and incubated with one of the following: rat anti-mouse CD68 (clone FA-11, Serotec), rat anti-mouse CD11b, (clone M1/70, Abcam), rat anti-mouse iNOS-FITC (clone 6/iNOS/NOS TypeII, BD biosciences), rabbit anti-mouse Arginase I (Sigma), biotinylated polyclonal goat anti-mouse MMP9, rat anti-mouse Perlecan (clone A7L6, Thermo Scientific), rat anti-mouse IRF5 (clone 903430, R&D Systems), mouse anti-human/mouse SMA (clone 1A4, Sigma, used with the M.O.M™ "Mouse-On-Mouse" basic kit, Vector Laboratories); Primary antibodies were revealed by fluorescently labelled (AlexaFluor® 488, Rhodamine or AlexaFluor®647) $F(ab')_2$ Fragment Affinity-Purified Antibodies® from Jackson ImmunoResearch Laboratories directed to mouse, rabbit or rat IgG, or alexaFluor®647 streptavidin (Invitrogen), as appropriate; Sections were counterstained with Hoechst and cover-mounted with Prolong Gold® anti-fade reagent (Invitrogen).

Analysis of mouse macrophages polarization, *in vitro*

Bone marrow-derived macrophages (BMDM) were prepared as previously described (Khallou-Laschet, 2010), from the femurs of 10 week-old WT (C57BL/6) and CD31 KO littermates (offspring of CD31+/- mice breeding) and were cultured for 24 hours in MEM medium (Invitrogen) supplemented with 10% FCS and 800 pg/mL Macrophage-Colony Stimulating Factor-1 (20% of a titrated L929 conditioned medium). Non-adherent cells were plated in 24-well plates (4x105 cells/well) for 7 days. For polarization studies, macrophages were stimulated overnight either with 100 ng/mL LPS (Sigma) and 100 U/mL IFN-γ (R&D System) in FCS-free medium to obtain inflammatory M1 macrophages or with 25 ng/mL interleukin-4 (IL-4, R&D System) to obtain alternative M2 macrophages. Non-polarized macrophages were maintained in complete medium.

The peptides were added during the polarization at a final concentration of 100 µg/ml. Culture supernatants were harvested for quantification of chemokines and cytokines, and cells were washed and lysed in TRIzol®. Total RNA was extracted and mRNA reverse transcription was performed using the iScript reverse transcriptase (Bio-rad). RT-qPCR was performed on a CFX 100 (Bio-Rad) cycler using the primers that are listed in the Supplementary table 2. We used 1ng of cDNA from each sample in a total volume of 22 µL that contained forward and reverse primers (250 nM) and SYBR Green Master Mix (Bio-Rad). The amplification program was the following: 1 cycle: 50°C, 2 min; 1 cycle: 95°C, 15 min; 50 cycles: 95°C, 40 s and 60°C, 1 min. Dissociation curves were analyzed at the end of the amplification, and the expression levels of the genes of interest were normalized to the expression of hypoxanthine-guanine phosphoribosyltransferase (HPRT).

Multiplex analysis of soluble molecules

Cell culture supernatants and plasma samples were subjected to multiplex analysis of 10 different soluble molecules (custom 10-plex set, R&D Systems, including TNFa, MCP-1, VEGF, IL-10, RANTES, MIP-1a, IL-23, IL-6, IP-10, MDC), following the manufacturer's instructions. Briefly, the different magnetic beads coupled with specific capture antibodies were mixed and incubated for 1 hour at room temperature with the individual biological samples. After several washes, a biotinylated detection antibody was added to the reaction. A streptavidin-phycoerythrin (streptavidin-PE) reporter complex was then added to reveal the biotinylated detection antibodies. PE fluorescence was then analyzed on a Bioplex-200® analyzer (Bio-Rad) and the concentration of the cytokines of interest was quantified using standard curves obtained with recombinant cytokines.

Statistical methods

The results are expressed as the means ± SEM. The differences between the groups were evaluated by one-way ANOVA with Fischer's post-hoc tests or by Mann-Whitney non-parametric tests, as appropriate. Any differences between groups were considered to be significant when the p value was <0.05. The analysis was performed with JMP® 6.0 Software (SAS Institute Inc., USA).

Results

Inflammatory M1 macrophages are involved in the AngII-induced aortic dissection

The sites of arterial wall dissection injury (detected as sites of elastin rupture) were consistently associated with the presence of macrophages, as detected by a densely rich CD68 positive area (Figure 1), further supporting the key role played by macrophages in the pathophysiology of aortic wall injury. Furthermore, the co-immunostaining of CD68 with iNOS and Arginase I revealed that most of these CD68 positive cells strongly express iNOS, whereas Arginase I was virtually absent in the area of these cells (Figure 1).

This result suggests that iNOS positive macrophages, which are described as the pro-inflammatory M1 macrophages, are actively involved in the pathologic processes associated with aortic dissection in this murine model.

The absence of CD31 signaling promotes the development M1-like macrophages

Since the CD31 signaling seems to influence the polarization of macrophages in vivo, we wanted to analyze its impact on macrophage polarization in vitro. To this purpose, bone marrow-derived macrophages were obtained from CD31 Wild Type (WT) and CD31 KO mice and polarized towards M1-like (LPS+IFNγ) or M2-like (IL-4) phenotypes.

We found that the M2-polarized macrophages from CD31 KO mice present a decrease in Arginase I expression, as compared with M2 macrophages from WT mice. Accordingly, the absence of CD31 signaling on M1 macrophages increases their expression of iNOS, as compared with macrophages from WT mice (Figure 2A).

Importantly, inflammatory cytokines produced by M1 macrophages, such as IL-6, MCP-1 and MIP1α were significantly overproduced under M1 polarization conditions in absence of CD31 expression. On the contrary, IL-4 secretion was reduced in absence of CD31 expression in M1 macrophages (Figure 2B).

These findings suggest that the absence of CD31 potentiates and accentuates the inflammatory phenotype in M1 polarization conditions, while the phenotype of M2 macrophages in M2 conditions is attenuated.

Identification of a drug-suitable CD31 agonist peptide

Because of its poor solubility in water (Figure 3A) the parent CD31 23-mer peptide was not suitable for further development as a candidate drug molecule for clinical use. In order to identify a drug-suitable CD31 agonist peptide we screened two peptide libraries derived from the human and mouse parent sequences. The best hit was found within the most proximal extracellular sequence of the CD31 molecule (aa 564-574, Figure 3B), which is highly conserved between the two species. Within this conserved sequence, we identified an 8-mer peptide (P8F, L-aminoacids, “forward” sequence) that was more readily soluble in water with minimal aggregated/degraded products (Figure 3C). The corresponding 8-mer retroinverso peptide (P8RI, D-aminoacids, inverse order sequence) displayed a very high water solubility and satisfying HPLC profile in saline solution (Figure 3D). P8F and P8RI peptides were as effective as the parent 23-mer peptide in reducing the extent of T-lymphocyte activation (data no shown) and we therefore chose the peptidase-resistant P8RI, for further development and preclinical studies in mice.

Since the parent peptide was biologically effective at 2.5mg/Kg subcutaneously in a previous study (Fornasa, 2010), we decided to use the same dose-range with this derived sequence. The calculated biodisponibility in the blood of a single injected subcutaneous dose of 50µg (2.5mg.Kg) is of 66% with a Cmax of 3.8 µg/ml detected 15 minutes after the subcutaneous injection (Supplementary Table 3). The injected peptide was detectable in the plasma up to 8 hours after its injection (Figure 1E), which supported the administration of the peptide daily.

In the perspective of pre-clinical studies and drug development, P8RI was subjected to ADME-tox analyses. As shown in Figure 1F, The IC 50 of the peptide doses on the hERG tail current amplitude was set at 150 µg/ml, which represents ≈40–fold the maximal detectable concentration of the drug in the plasma of mice having received the drug by a subcutaneous injection (Cmax). Of note, at the concentration of 5µg/ml, which is lower than the Cmax in the blood after a subcutaneous injection, the peptide has no effect on the tail amplitude of the potassium channel. The product is stable in solution for up to 100 days at room temperature. Bacterial reverse mutation test was completely negative both in non-metabolic and metabolic conditions on the Salmonella typhimurium TA 98 and TA 100. In order to assess the toxicology profile of P8RI in the curative daily treatment schedule, the

peptide was injected (2.5, 10 and 30mg/KG) or its vehicle to C57Bl6 mice (male, 20 week old, n=3/group) once a day by the subcutaneous route for 14 days in a 50µl volume of PBS. Mortality, food consumption, body weight and temperature, organ weight, biochemistry, hematology, and coagulation parameters were all normal in all treatment groups. No relevant clinical findings were recorded during the course of the study (data not shown).

CD31 peptide influences macrophages polarization towards M2 profile

We next wanted to assess whether activating CD31 signaling using the CD31 peptide would have an effect on the polarization of bone marrow-derived macrophage from WT mice. We found that the stimulation of in vitro-polarized macrophages by the CD31 peptide strongly increased the expression of Arginase I by M2 macrophages while it dramatically reduced the expression of M1 markers, such as iNOS and Arginase II by M1 macrophages (Figure 4C). Accordingly, the concentration of inflammatory cytokines produced by M1 macrophages under LPS stimulation was decreased upon stimulation with the CD31 peptide (IL-12, IL-6, TNF-α) whereas the concentration of IL-10 was increased (Figure 4D).

Altogether, those findings point out a critical involvement of CD31 signaling in macrophage polarization, and we believe that the regulatory properties of the CD31 molecule on macrophage are involved in tissue healing in the context of atherosclerosis and AngII-induced abdominal aortic dissection.

P8RI treatment promotes the healing of the dissected aortic wall through collagen production in the context of atherosclerosis and aneurysm formation

We therefore wondered whether, when used in a curative purpose, the peptide would have an effect on tissue repair in the context of aneurysms and atherosclerosis. Sirius red staining on transverse cryosection of AngII-induced aneurysms revealed that treatment with the CD31 peptide significantly increased the amount of collagen fibers, as compared to treatment with the control vehicle (Figure 5A). The extent of collagen deposition was not dependent on the amount of iron deposits, which appeared similarly abundant in the two groups. We also found that collagen deposition in atherosclerotic lesions in the aortic sinus was also significantly increased in CD31-peptide-treated mice, as compared to control mice (Figure 5B). These results indicate that CD31 peptide promote tissue repair in AngII-induced atherosclerosis and aneurysm formation through the production of collagen fibers.

CD31 peptide treatment is associated with the presence of “reparatory” M2-type macrophages in injured aortic walls.

We have previously shown that mouse macrophages are extremely plastic cells that can easily switch from a pro-inflammatory M1 phenotype towards a more “reparatory” M2 profile, depending on the signals they receive from their environment (Khallou-Laschet, 2010). We therefore evaluated whether the induction of aortic tissue repair by the CD31 peptide would be mediated through its effect on aortic macrophages polarization, endowing them with an M2-like profile.

To this end, we assessed the phenotype of tissue infiltrating macrophages on dissecting aneurysm deriving from CD31 peptide-treated mice as compared to control. As shown in Figure 6, the vast majority of CD68 positive macrophages co-expressed Arginase I — which is predominantly expressed by M2 macrophages — in tissue derived from CD31 peptide-treated mice whereas the presence of iNOS macrophages could only be detected in vehicle-treated mice.

Similarly, we found that most of the CD68-positive macrophages in the aortic sinus were also Arginase I-positive (M2) in CD31 peptide-treated mice as compared to control mice in which macrophages, which were instead positive for iNOS, presented an M1 phenotype.

These results strongly suggest that the CD31 peptide has an impact on the phenotype of macrophages, and that it promotes the polarization towards a “reparatory” M2 phenotype, which is known to provoke collagen deposition and further tissue repair.

Figures

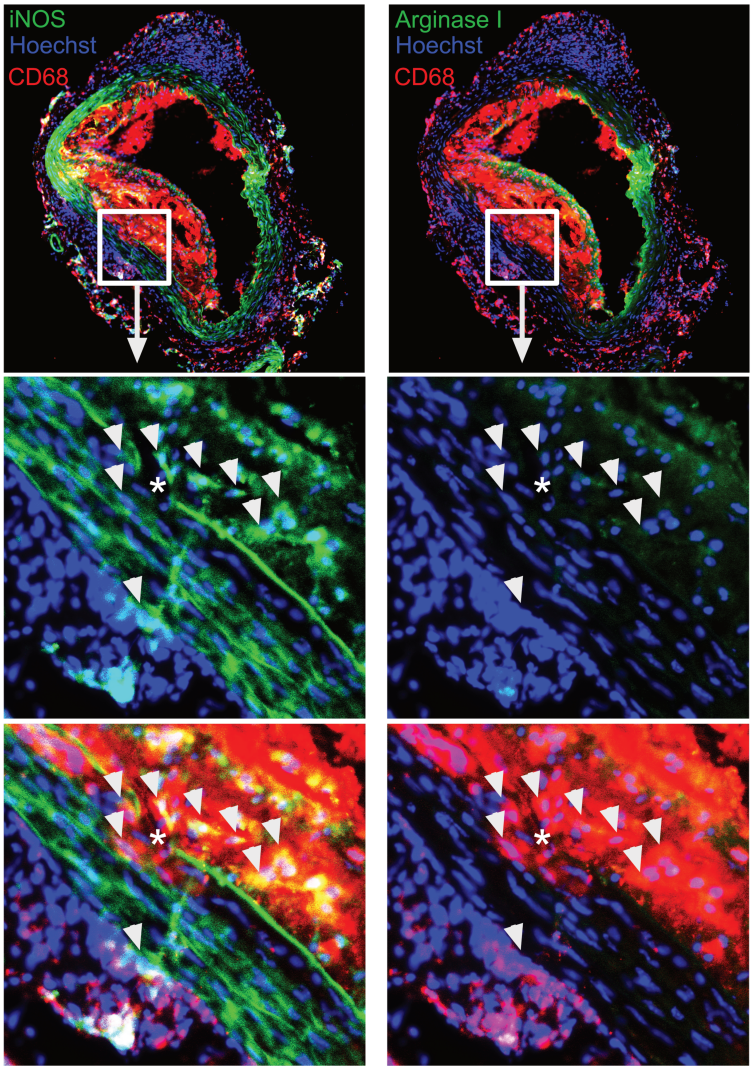

Figure 1. *Phenotype of macrophages at sites of arterial wall disruption. Cross-section of the abdominal aorta of a 28-week old male ApoE$^{-/-}$ mice. Sites of spontaneous elastin rupture (*) are infiltrated with CD68 positive (red staining) macrophages (white arrowheads). Co-immunostaining detected by green fluorescence of iNOS (left) or Arginase I (right) revealed that most wall rupture-associated macrophages display a pro-inflammatory, iNOS-positive /Arginase-negative phenotype.*

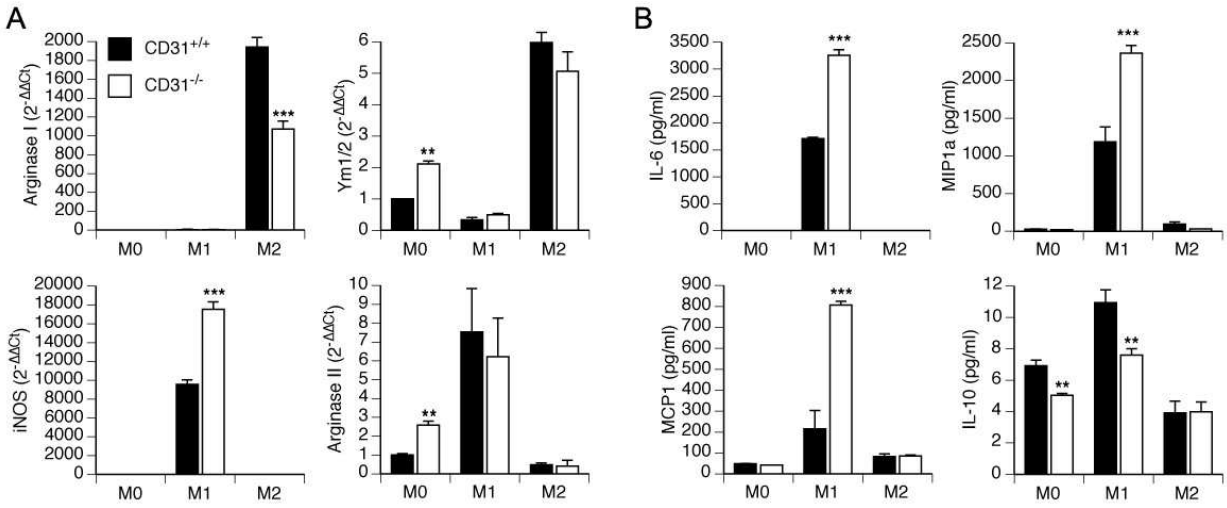

***Figure 2**. Impact of CD31 deficiency on macrophage polarization. BMDM from WT and CD31 KO mice were differentiated in vitro with M-CSF and subsequently polarized into M1 macrophages, with LPS and IFNg or into M2 macrophages, with IL-4. **A**. The genetic disruption of CD31 signalling was associated with a stronger expression of iNOS (M1 marker) on macrophages after LPS+IFNg stimulation. On the contrary, the expression of Arg I (M2 marker) in response to IL-4 was diminished in CD31 KO macrophages compared to WT. Hence, in absence of CD31 signalling, macrophages are prone to polarize into M1 cells whereas the expression of the CD31 favours the M2 polarization. **B**. Analysis of soluble cytokines released by the cultured macrophages in the supernatant showed that CD31 KO macrophages produced more IL-6, MCP-1 and IL-1b than WT macrophages after LPS+IFNg stimulation. On the contrary, the production of IL-4 by CD31 KO M2 macrophages was diminished as compared to WT macrophages. IL-10 production was reduced in M1 macrophages derived from CD31 KO mice but not in M2 cells*.

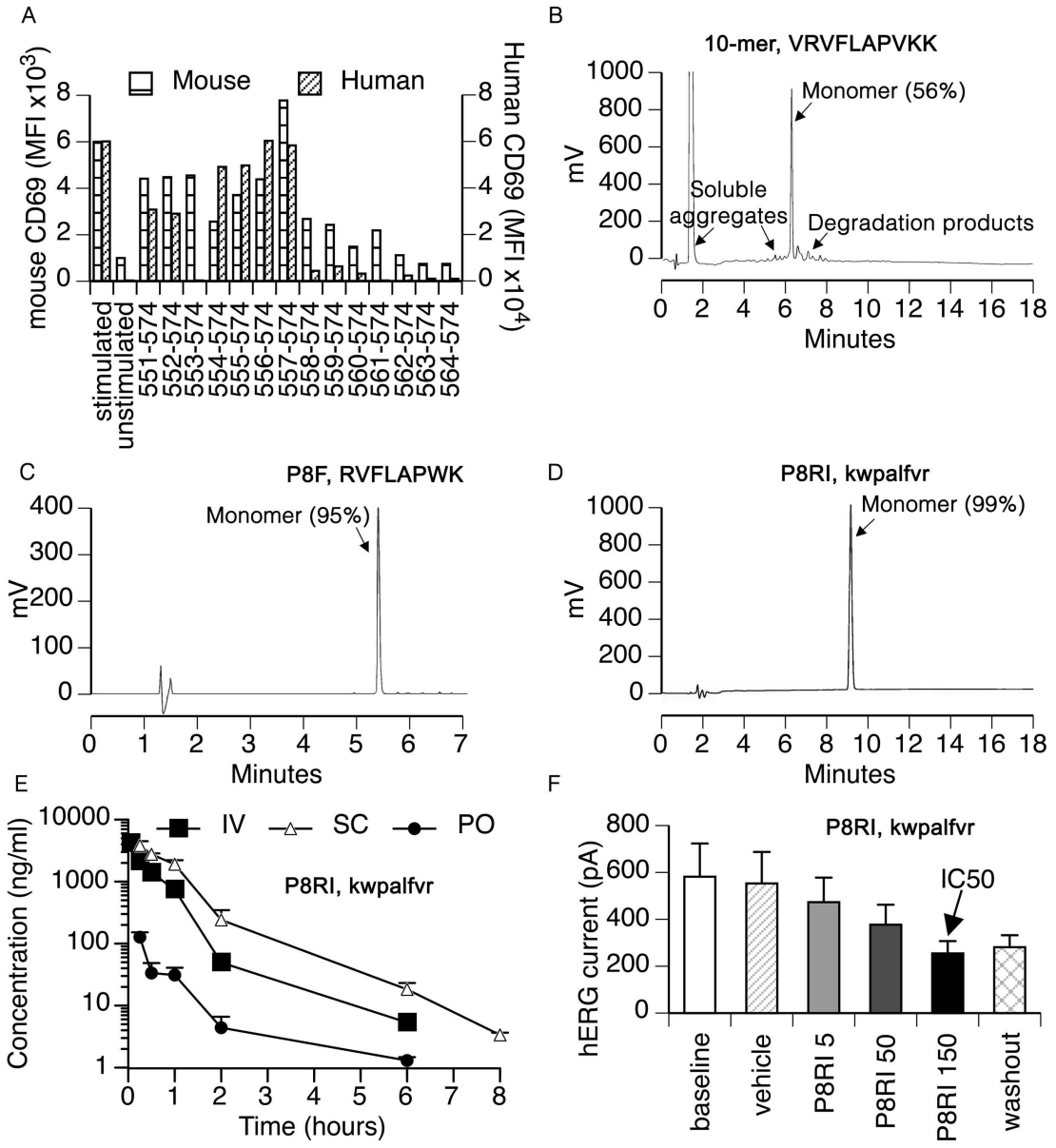

***Figure 3**. Identification and characterization of a drug-suitable CD31 agonist peptide. **A**. The best hit was selected from the "truncated" peptide library (see methods) on the basis of its ability to reduce both mouse and human leukocyte activation. The best hit following these criteria was a sequence spanning from mouse CD31 aa 564 to 574 (10-mer). **B**. HPLC analysis of the 10-mer peptide 564 to 574 selected in A showed a poor water solubility (56% monomer) and the presence of aggregates and debris of variable size. **C**. The 8-mer forward (P8F) sequence aa 565-573 from the "scanning" peptide, fully comprised within the 10-mer sequence, showed an excellent water solubility (95%). **D**. The corresponding retro-inverso aa 565-573 sequence (P8RI) showed an even greater solubility (99%). **E**. Pharmacokinetic analysis of P8RI after a bolus administration by intravenous (IV, 1 mg/Kg) or subcutaneous (SC, 2.5mg/Kg) injection, or an oral 2.5mg/Kg dose*

(per os, PO) in C57Bl/6 mice. ***F****. In vitro analysis of the hERG tail current amplitude on a stable cell line showed that the IC 50 of P8RI corresponded to the concentration of 150µM (x40 fold the AUC following subcutaneous injection of a 2.5mg/Kg dose in mice).*

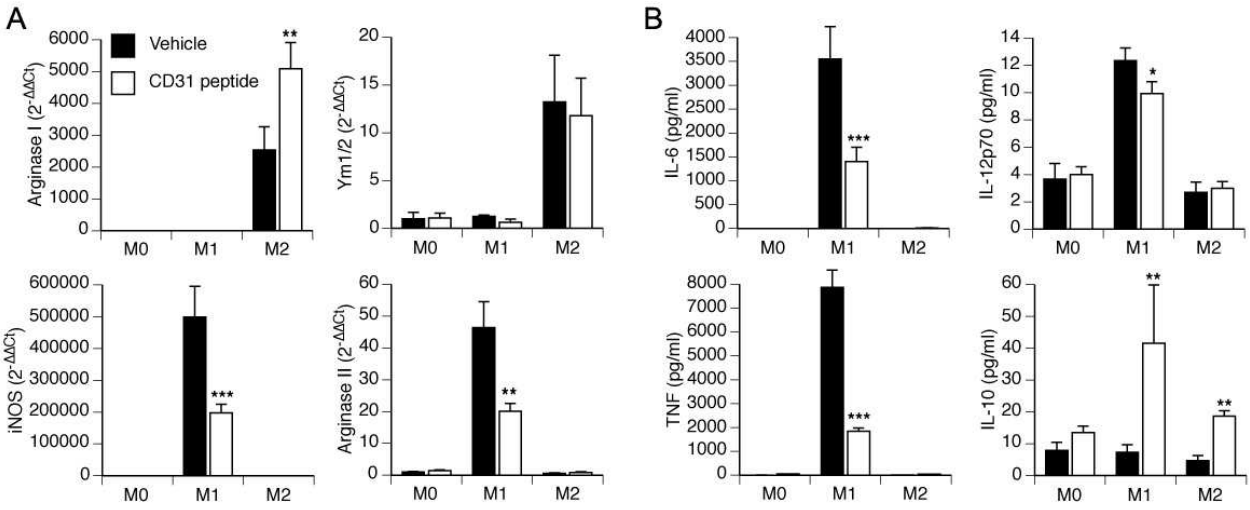

Figure 4*. Impact of the CD31 agonist peptide on macrophage polarization. BMDM from WT mice were differentiated in vitro with M-CSF and subsequently polarized into M1 macrophages, with LPS and IFNg or into M2 macrophages, with IL-4.* ***A****. The expression of M2-associated genes (Arginase I, Ym1/2) and M1-associated genes (iNOS, Arginase II) were assessed in the presence or absence of the CD31 agonist peptide.* ***B****. Analysis of soluble cytokines produced by M2 macrophages (IL-10) or M1 macrophages (IL-12, IL-6 and TNFα) were also evaluated.*

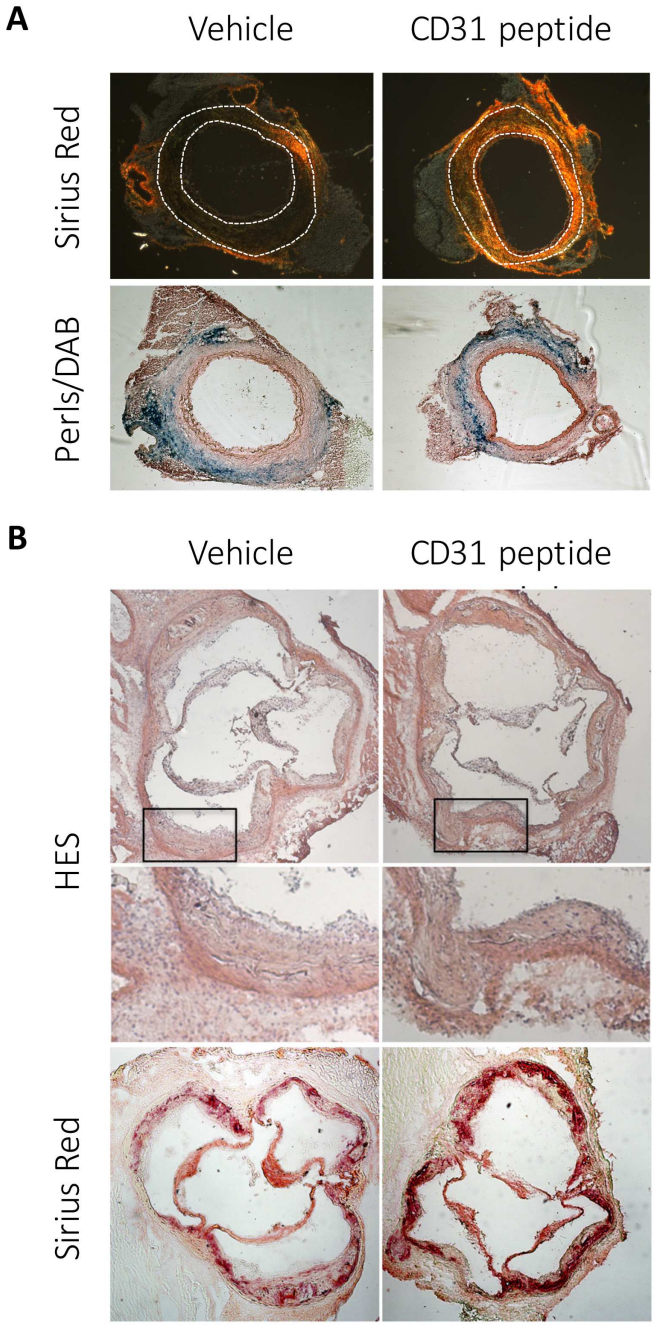

***Figure 5**. Evaluation of P8RI treatment on angiotensin II experimental aortic dissection and atherosclerosis in ApoE$^{-/-}$ mice. **A**. Representative images of abdominal aortic aneurysm staining of collagen (Sirius red) and iron deposits (Persl/DAB) in vehicle or CD31 peptide-treated mice. **B**. Micrographs of collagen deposition in aortic sinus.*

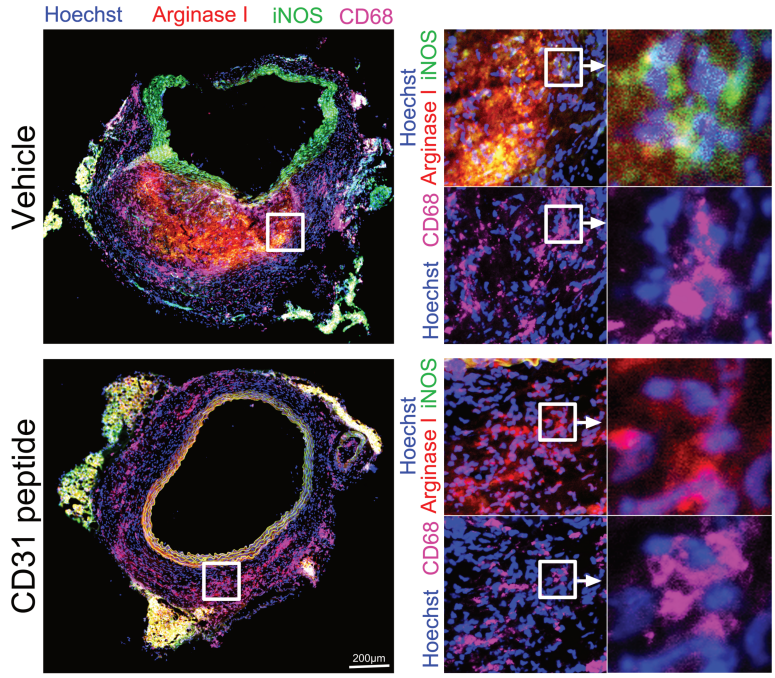

Figure 6. Phenotypic analysis of aortic wall-infiltrated macrophages in angiotensin II experimental aneurysm. Representative immunofluorescent cross-section micrographs of macrophages (CD68 positive cells, purple staining) M1-marker (iNOS, green staining) and M2-marker (Arginase I, red staining) in angiotensin II-induced aneurysm in mice treated with or without the CD31 peptide.

Bibliography

Benkirane, N., G. Guichard, M.H. Van Regenmortel, J.P. Briand, and S. Muller. 1995. Cross-reactivity of antibodies to retro-inverso peptidomimetics with the parent protein histone H3 and chromatin core particle. Specificity and kinetic rate-constant measurements. J Biol Chem 270:11921-11926.

Biswas, S.K., and A. Mantovani. 2010. Macrophage plasticity and interaction with lymphocyte subsets: cancer as a paradigm. Nat Immunol 11:889-896.

Boekhoudt, G.H., M.R. Frazier-Jessen, and G.M. Feldman. 2007. Immune complexes suppress IFN-gamma signaling by activation of the FcgammaRI pathway. J Leukoc Biol 81:1086-1092.

Fornasa, G., M. Clement, E. Groyer, A.T. Gaston, J. Khallou-Laschet, M. Morvan, K. Guedj, S.V. Kaveri, A. Tedgui, J.B. Michel, A. Nicoletti, and G. Caligiuri. 2012. A CD31-derived peptide prevents angiotensin II-induced atherosclerosis progression and aneurysm formation. Cardiovasc Res 94:30-37.

Fornasa, G., E. Groyer, M. Clement, J. Dimitrov, C. Compain, A.T. Gaston, A. Varthaman, J. Khallou-Laschet, D.K. Newman, S. Graff-Dubois, A. Nicoletti, and G. Caligiuri. 2010. TCR stimulation drives cleavage and shedding of the ITIM receptor CD31. J Immunol 184:5485-5492.

Hamill, O.P., A. Marty, E. Neher, B. Sakmann, and F.J. Sigworth. 1981. Improved patch-clamp techniques for high-resolution current recording from cells and cell-free membrane patches. Pflugers Arch 391:85-100.

Isselbacher, E.M., M.P. Bonaca, M. Di Eusanio, J. Froehlich, E. Bassone, U. Sechtem, R. Pyeritz, H. Patel, A. Khoynezhad, H.H. Eckstein, G. Jondeau, F. Ramponi, M. Abbasi, D. Montgomery, C.A. Nienaber, K. Eagle, M.E. Lindsay, and I. International Registry of Aortic Dissection. 2016. Recurrent Aortic Dissection: Observations From the International Registry of Aortic Dissection. Circulation 134:1013-1024.

Kim, O.H., G.H. Kang, H. Noh, J.Y. Cha, H.J. Lee, J.H. Yoon, M. Mamura, J.S. Nam, D.H. Lee, Y.A. Kim, Y.J. Park, H. Kim, and B.C. Oh. 2013. Proangiogenic TIE2(+)/CD31 (+) macrophages are the predominant population of tumor-associated macrophages infiltrating metastatic lymph nodes. Mol Cells 36:432-438.

Lawrence, T., and G. Natoli. 2011. Transcriptional regulation of macrophage polarization: enabling diversity with identity. Nat Rev Immunol 11:750-761.

Liu, L., and G.P. Shi. 2012. CD31: beyond a marker for endothelial cells. Cardiovasc Res 94:3-5.

Lumsden, A.B., and M.J. Reardon. 2008. Once dissected always dissected! Can stent grafts change the natural history of type B dissections?: a report from the International Registry of Acute Aortic Dissection. JACC Cardiovasc Interv 1:403-404.

Mantovani, A., S.K. Biswas, M.R. Galdiero, A. Sica, and M. Locati. 2013. Macrophage plasticity and polarization in tissue repair and remodelling. J Pathol 229:176-185.

Marelli-Berg, F.M., M. Clement, C. Mauro, and G. Caligiuri. 2013. An immunologist's guide to CD31 function in T-cells. J Cell Sci 126:2343-2352.

Newman, P.J. 1999. Switched at birth: a new family for PECAM-1. J Clin Invest 103:5-9.

Sindrilaru, A., T. Peters, S. Wieschalka, C. Baican, A. Baican, H. Peter, A. Hainzl, S. Schatz, Y. Qi, A. Schlecht, J.M. Weiss, M. Wlaschek, C. Sunderkotter, and K. Scharffetter-Kochanek. 2011. An unrestrained proinflammatory M1 macrophage population induced by iron impairs wound healing in humans and mice. J Clin Invest 121:985-997.

Suzuki, T., K.A. Eagle, E. Bossone, A. Ballotta, J.B. Froehlich, and E.M. Isselbacher. 2014a. Medical management in type B aortic dissection. Annals of Cardiothoracic Surgery 3:413-417.

Suzuki, T., K.A. Eagle, E. Bossone, A. Ballotta, J.B. Froehlich, and E.M. Isselbacher. 2014b. Medical management in type B aortic dissection. Ann Cardiothorac Surg 3:413-417.

Vernon-Wilson, E.F., F. Aurade, L. Tian, I.C. Rowe, M.J. Shipston, J. Savill, and S.B. Brown. 2007. CD31 delays phagocyte membrane repolarization to promote efficient binding of apoptotic cells. J Leukoc Biol 82:1278-1288.

Yang, T., D. Snyders, and D.M. Roden. 2001. Drug block of I(kr): model systems and relevance to human arrhythmias. J Cardiovasc Pharmacol 38:737-744.

Yao, A., F. Liu, K. Chen, L. Tang, L. Liu, K. Zhang, C. Yu, G. Bian, H. Guo, J. Zheng, P. Cheng, G. Ju, and J. Wang. 2014. Programmed death 1 deficiency induces the polarization of macrophages/microglia to the M1 phenotype after spinal cord injury in mice. Neurotherapeutics 11:636-650.

Zhou, D., C. Huang, Z. Lin, S. Zhan, L. Kong, C. Fang, and J. Li. 2014. Macrophage polarization and function with emphasis on the evolving roles of coordinated regulation of cellular signaling pathways. Cell Signal 26:192-197.

12 ANNEX II

(Under reviewing in Critical Care Medicine)

Peptide binding to cleaved CD31 dampens ischemia/reperfusion-induced intestinal injury

Thang Hoang Quoc[1], Alexandre Nuzzo[1,2], Liliane Louedec[1], Sandrine Delbosc[1], Francesco Andreata[1], Jamila Khallou-Laschet[1], Maksud Assadi[1,3], Philippe Montravers[3,4], Dan Longrois[1,3], Giuseppina Caligiuri[1], Antonino Nicoletti[1], Jean-Baptiste Michel[1], Alexy Tran-Dinh[1,3].*

[1] INSERM LVTS U1148, CHU Bichat Claude-Bernard, Paris, France

[2] Structure d'Urgences Vasculaires Intestinales (SURVI), CHU Beaujon, Clichy, France

[3] Département d'anesthésie-réanimation, CHU Bichat Claude-Bernard, Paris, France

[4] INSERM UMR 1152, CHU Bichat Claude-Bernard, Paris, France

ABSTRACT

Background: CD31 is a key transmembrane neutrophil immunoregulatory receptor. Mesenteric ischemia/reperfusion-induced neutrophil activation leads to a massive cleavage and shedding of the most extracellular domains of CD31 into plasma, enhancing the deleterious effect of neutrophil activation. We have evaluated the therapeutic potential of an engineered, drug-suitable synthetic octapeptide (P8RI), which restores the inhibitory intracellular signaling of cleaved CD31, in an experimental model of acute mesenteric ischemia/reperfusion.

Methods: Mesenteric ischemia/reperfusion (I/R) was induced in Wistar rats by superior mesenteric artery occlusion for 30 min followed by 4 h of reperfusion. Three groups of rats were compared: I/R + saline infusion (I/R controls group, n=20), I/R + P8RI infusion (P8RI group, n=20) and sham-operated rats + saline infusion (sham group, n=14). We assessed intestinal I/R injury by histology and biomarkers of neutrophil activation, cell death, bacterial translocation and CD31 cleavage. Mann-Whitney U-test, Student's t-test, two-way ANOVA and principal component analysis were used for statistical analysis.

Results: Compared to I/R controls, P8RI infusion significantly decreased intestinal ischemia/reperfusion injury (Chiu's score, $P=0.01$; epithelial area, $P=0.001$; intestinal bleeding, $P=0.0006$), neutrophil activation in plasma and intestinal wall (plasma matrix metalloproteinase-9, $P<0.001$; intestinal matrix metalloproteinase-9, $P=0.03$), cell death (plasma cell-free DNA, $P<0.05$), bacterial translocation (plasma Escherichia coli DNA, $P=0.04$) and CD31 cleavage ($P<0.0001$).

Conclusion: Binding of P8RI to cleaved CD31 reduced neutrophil activation and ischemia/reperfusion-induced intestinal injury. Drug-suitable P8RI is potentially a promising therapy in human acute mesenteric ischemia.

INTRODUCTION

Acute mesenteric ischemia is a life-threatening emergency with a high mortality rate, reaching 58% in intensive care unit patients[1]. It can lead to an overwhelming inflammatory response[2], bacterial translocation[3], digestive bleeding, intestinal necrosis, multiple organ failure[4] and death. There is no specific therapy targeting intestinal ischemia/reperfusion injury.

Neutrophils are key players in this pathology[5,6]. As in all leukocytes, the activation of neutrophils is tightly controlled by inhibitory co-receptors. Among the inhibitory receptors expressed by neutrophils, CD31 is a major target. Indeed, CD31 is a key leukocyte immunoregulatory receptor[7] and neutrophils are among the cells that express the highest number of CD31 molecules[8].

CD31 is a 130-kDa transmembrane glycoprotein receptor also expressed by the other leukocytes, platelets and endothelial cells. Transhomophilic engagement of CD31 raises the activation threshold of these cells via activation of SH2 tyrosine phosphatase[9]. When submitted to activating stimuli strong enough to overcome the activation threshold, cell activation is accompanied by the cleavage and shedding into plasma of most of the extracellular CD31, thereby interrupting the downstream cell signaling and leaving cell activation unharnessed[7]. It is of interest that after shedding, a short portion of the membrane-proximal extracellular sequence remains exposed at the cell surface. We recently engineered a drug-suitable synthetic octapeptide (termed P8RI), which is able to bind to this short portion and to restore the inhibitory intracellular signaling of cleaved CD31[10,11,12]. This peptide is derived from a parent sequence that has previously been successful as an in vivo therapeutic agent[13]. Herein, we have evaluated the therapeutic potential of P8RI, via a putative protective effect on neutrophil activation, in an experimental model of acute mesenteric ischemia/reperfusion.

MATERIALS AND METHODS

Procedures and animal care complied with principles formulated by the National Society for Medical Research (animal facility agreement: n° B75-18-03, experimentation authorization

n° 75-101, APAFiS#8724). Eight week-old male Wistar rats were purchased from Janvier laboratory.

Model of acute mesenteric ischemia/reperfusion

Rats were randomized into 3 groups: an ischemia/reperfusion (I/R) group treated with saline infusion (I/R controls, 20 rats), an ischemia/reperfusion group treated with P8RI infusion (P8RI group, 20 rats) and a sham-operated group (sham group, 20 rats).

Rat body temperature was maintained at 37.5°C by a heated surgical table. Non-fasting rats were anesthetized by intraperitoneal injection of 2 mg/kg of urethane. Cannulation of the right jugular vein and right carotid artery were performed for perfusion, blood sampling and arterial pressure measurements. After laparotomy, the superior mesenteric artery (SMA) was exposed but not occluded in the sham group. In the control and P8RI groups, the SMA was clamped. The clamp was removed after 30 min of ischemia, followed by 4 hours of reperfusion. A single 1 mg intravenous bolus of P8RI was administered 5 min before clamping SMA and was followed by a continuous perfusion at 1 mg/h until the end of reperfusion. The same procedure was performed for the control group, except for the infusion of P8RI, which was substituted by an equivalent volume of saline perfusion. The experimenter was blinded with regard to the treatment administered. Arterial blood pressure and diuresis were monitored throughout the experiment. Blood and peritoneal fluid were sampled in EDTA-tubes before the laparotomy and 30 min after clamping the SMA. Blood samples were also collected every hour during the reperfusion, and peritoneal fluid samples after 2 and 4 hours of reperfusion. Samples were centrifuged for 30 min at 16,000 g. Supernatants were used for assays. The small bowel was dissected out after rats were euthanized. The intestinal luminal content was collected for the quantification of intestinal bleeding. A mid-gut loop was resected and fixed in formalin and the remaining small bowel was homogenized. Homogenates were centrifuged for 30 min at 16,000 g and supernatants were used for assays.

Assessment of mesenteric ischemia/reperfusion-induced intestinal injury

Histological analysis of the intestinal mucosa

Highly glycosylated mucins and nuclei were stained respectively with Alcian blue and nuclear fast red on transverse paraffin-embedded sections of the small intestine in 7 rats

per group. Histological evaluation was performed using the grading system described by Chiu et al.[14], as described in the Supplemental Digital Content (Table E1).

Morphometric analysis of the small bowel

A morphometric evaluation of histological gut sections was performed using QWin software to determine the luminal area, epithelial and muscular layer areas, and the overall surface area in 7 rats per group, as described in the Supplemental Digital Content (see figure E1).

Intestinal bleeding

The intestinal bleeding was assessed by the quantification of heme concentration in the small intestine luminal content, using formic acid, in 7 rats per group, as described in the Supplemental Digital Content.

Neutrophil activation in the small bowel tissue

Neutrophil activation was assessed by the intestinal tissue concentrations of matrix metalloproteinase-9 (MMP-9) in 7 rats per group, using enzyme-linked immunosorbent assays, as described in the Supplemental Digital Content.

Assessment of mesenteric ischemia/reperfusion-induced neutrophil activation in plasma

Neutrophil activation in plasma was assessed by the plasma concentration of MMP-9 in 20 rats per group using an enzyme-linked immunosorbent assay, as described in the Supplemental Digital Content.

Assessment of mesenteric ischemia/reperfusion-induced cell death

Cell death was assessed by the plasma concentration of cell-free DNA in 20 rats per group using a Quant-it Picogreen dsDNA Reagent Kit (Invitrogen), as described in the Supplemental Digital Content.

Assessment of mesenteric ischemia/reperfusion-induced bacterial translocation

Bacterial translocation was assessed by the quantification of plasma DNA from Escherichia coli in 7 rats per group at 4 hours of reperfusion after the onset of mesenteric ischemia, using a real-time PCR technique, as described in Supplemental Digital Content.

Assessment of the cleavage and shedding of CD31 in plasma

The cleavage and shedding of CD31 into plasma was assessed by the assay of the soluble cleaved extracellular portion of CD31 in 7 rats per group using a cytometric bead array technology (CBA, BD). A polyclonal antibody targeting rat CD31 (R&D, #AF3628) and cross-linked to magnetic beads (MC10035-01, BioRad) was incubated with EDTA-plasma for 90 min at room temperature. Cleaved-circulating CD31 captured by the anti-CD31 cross-linked to beads was detected using a monoclonal antibody (clone TLD-3A12) coupled to phycoerythrin and incubated for 1 hour at room temperature. Median fluorescent intensity was analysed from 100 beads per sample (BioPlex 200 System, BioRad). A standard curve was obtained from serial dilutions of a recombinant mouse CD31 (R&D systems).

Statistical analysis

Quantitative data are expressed as medians with interquartile range (IQR) or means ± SEM. Mann-Whitney U-test, Student's t-test, two-way ANOVA with post-hoc multiple comparisons, Bonferroni test and Spearman correlation were performed as appropriate. Principal component analysis was performed to study how I/R conditions (controls, P8RI-treated and sham operated) impact the relationships (correlations) between the epithelial area, neutrophil activation, CD31 cleavage, intestinal bleeding, cell death and bacterial translocation.

RESULTS

No rats of any group died at the end of the 4 hours of reperfusion following mesenteric ischemia. Arterial blood pressure and diuresis were not significantly different between I/R controls, P8RI and sham groups (data not shown).

Effect of P8RI on mesenteric ischemia/reperfusion-induced intestinal injury

Histological analysis of the intestinal mucosa

I/R greatly increased the intestinal mucosa injury as assessed by Chiu's score compared to sham-operated rats (3[3-4] vs. 1[0-1] respectively, P=0.003), and P8RI administration significantly limited this injury compared to saline injection (2[1-2]) vs. 3 [3-4] respectively,

P=0.01). Indeed, Chiu's score was not significantly different between the P8RI and sham groups (2[1-2]) vs. 1[0-1] respectively, P=0.07). (Figure 1A).

Morphometric analysis of the small bowel

Morphometric analysis confirmed histological results by showing that I/R markedly decreased the small bowel epithelial area compared to sham-operated rats (90µm2 [71-116] vs. 192µm2 [154-219] respectively, P<0.0001). P8RI infusion limited the abrasion of the epithelial area compared to saline injection (146µm2 [140-179] vs. 90µm2 [71-116] respectively, P=0.001), but it remained significantly lower than in the sham group (192µm2 [154-219] in sham group, P=0.03 compared to P8RI group) (Figure 1B). The epithelial area was negatively correlated to the Chiu's score (r = - 0.72, p = 0.0002).

I/R also increased smooth muscle layer injury since morphometric analysis showed that its area was decreased compared to the sham group (36µm2 [33-40] vs. 50µm2 [45-63], respectively, P=0.0008). P8RI infusion failed to limit smooth muscle layer thinning (39µm2 [36-42] vs. 36µm2 [33-40] for saline injection, P=0.35). Indeed, the smooth muscle area remained significantly lower in the P8RI group than in the sham group (39µm2 [36-42] vs. 50µm2 [45-63] respectively, P=0.002).

Intestinal bleeding

I/R led to significantly more intestinal bleeding, as assessed by the luminal concentration of hemoglobin, which was significantly higher than in sham-operated rats (224µg/mg total protein [122-326] vs. 97µg/mg total protein [54-124] respectively, P=0.0006). P8RI administration greatly limited this bleeding as the hemoglobin concentration in the treated group was not significantly different from that in the sham group (99µg/mg total protein [89-141] in P8RI group, P=0.0006 compared to I/R controls; 97µg/mg total protein [54-124] in sham group, P=0.4 compared to P8RI group. (Figure 1C).

Cell death

Before laparotomy, the plasma concentration of cell-free DNA was similar in the 3 groups.

We found a significant overall effect of the treatment (P=0.007) and time (P=0.002) on the plasma concentration of cell-free DNA using a two-way ANOVA. After 4 hours of reperfusion following 30 min of ischemia, I/R significantly increased the plasma concentration of cell-

free DNA compared to sham-operated rats (1282 ± 133 ng/ml vs. 549 ± 86 ng/ml respectively, P<0.001). P8RI administration partially prevented this increase but levels remained significantly higher than in the sham group (989 ± 111 ng/ml in P8RI group, P<0.05 compared to I/R controls; 549 ± 86 ng/ml in sham group, P<0.05 compared to P8RI group). (Figure 1D).

Effect of P8RI on mesenteric ischemia/reperfusion-induced neutrophil activation

Neutrophil activation in the small bowel tissue

Neutrophil activation, assessed by the intestinal tissue concentration of MMP-9, was significantly higher in I/R controls than in sham-operated rats (5.6µg/mg total protein [0.9-12.7] vs. 1.4µg/mg total protein [1.2-2.0], respectively, P=0.03). P8RI administration significantly limited this intestinal MMP-9 increase as P8R1-treated rats presented MMP-9 levels similar to those of sham controls (1.3 µg/mg total protein [0.9-2.0] in P8RI group, P=0.03 compared to I/R controls; 1.4 µg/mg total protein [1.4-2.0] in sham group, P=0.78 compared to P8RI group) (Figure 2A).

Neutrophil activation in plasma

Before laparotomy, the plasma concentration of MMP-9 was similar in the 3 groups. We found a significant effect of the treatment (p = 0.0009) and time (P<0.0001) on the plasma MMP-9 concentration (two-way ANOVA). Plasma neutrophil activation assessed by the plasma concentration of MMP-9 was higher in the I/R controls than in the sham group just after ischemia (33.2 ng/ml [14.7-68.4] vs. 13.4 ng/ml [12.6-25.2] respectively, P<0.05) and at 2 hours (41.3 ng/ml [26.7-92.4] vs. 22.6 ng/ml [14.0-42.7] respectively, P<0.05), 3 hours (60.8 ng/ml [40.4-104.4] vs. 28.3 ng/ml [12.9-57.6] respectively, P<0.001) and 4 hours (69.6 ng/ml [39.8-132.8] vs. 25.3 ng/ml [12.6-41.0] respectively, p < 0.001) of reperfusion. P8RI administration limited plasma MMP-9 compared to saline injection at 3 hours (26.1 ng/ml [14.2-56.0] vs. 60.8 ng/ml [40.4-104.4] respectively, P< 0.001) and 4 hours (33.3 ng/ml [19.3-51.8] vs 69.6 ng/ml [39.8-132.8] respectively, P< 0.001) of reperfusion. Plasma neutrophil activation was not significantly different between the P8RI and sham groups (P> 0.05 after ischemia and after each time of reperfusion) (Figure 2B).

Effect of P8RI on mesenteric ischemia/reperfusion-induced bacterial translocation

Four hours of reperfusion after 30 min of ischemia tended to increase the plasma concentration of DNA from Escherichia coli (1/Ct value) compared to sham-operated rats (0.029[0.026-0.030] vs. 0.026[0-0.028] respectively, P=0.1). P8RI administration limited the bacterial translocation compared to saline injection (0.024[0.021-0.029] vs. 0.029[0.026-0.030] respectively, P=0.04) providing levels not significantly different from those of the sham group (0.024[0.021-0.029] vs. 0.026[0-0.028] respectively, P=0.56) (Figure 3).

Effect of P8RI on mesenteric ischemia/reperfusion-induced cleavage and shedding of CD31 into plasma.

Before laparotomy, the plasma concentration of soluble cleaved CD31 was similar in the 3 groups. We found a significant overall effect of the treatment (P<0.0001) but not of time (P =0.93) on this parameter. The cleavage and shedding of CD31 into plasma increased after 1 hour of reperfusion following mesenteric ischemia compared to sham-operated rats (24.3 ± 0.7 ng/ml vs. 18.7 ± 0.6 ng/ml respectively, P<0.001). P8RI infusion significantly limited this process at 1 hour (17.4 ± 0.9 ng/ml vs. 24.3 ± 0.7 ng/ml respectively, P<0.001), 2 hours (18.0 ± 1.1 ng/ml vs. 22.2 ± 0.9 respectively, P<0.05) and 4 hours (16.5 ± 1.2 ng/ml vs. 22.6 ± 1.5 ng/ml respectively, P<0.001) hours of reperfusion compared to saline injection. The plasma concentration of soluble cleaved CD31 was not significantly different between the P8RI and sham groups after ischemia and after each reperfusion time point (Figure 4).

Effect of P8RI on neutrophil activation, CD31 cleavage, intestinal bleeding, cell death, bacterial translocation and epithelial injury induced by mesenteric ischemia/reperfusion.

In P8RI, I/R controls and sham groups, principal component analysis showed a positive correlation between intestinal MMP-9, intestinal luminal hemoglobin, plasma cell-free DNA, plasma E coli DNA and plasma soluble cleaved CD31. On the contrary, epithelial area was strongly negatively correlated to these parameters (Figure 5A). Principal component analysis allowed the identification of a clustering of the sham and P8RI-treated groups, which were widely separated from I/R controls (Figure 5B). This result illustrates the major role of CD31 cleavage in neutrophil activation and ischemia/reperfusion-induced intestinal

injury, and may explain the protective effect of P8RI, which restores the immunoregulatory functions of cleaved CD31.

DISCUSSION

In this study, we demonstrated a protective effect of P8RI binding to cleaved CD31 in an experimental model of acute mesenteric ischemia/reperfusion. P8RI is a drug-suitable CD31-derived peptide that restores the inhibitory function of cleaved CD31 resulting from the activation of leukocytes, endothelial cells, and platelets. Thereby, P8RI reinstates vascular homeostasis[15].

P8RI infusion protected the intestinal mucosa from ischemia/reperfusion-induced injury as we observed a significant limitation in the abrasion of the villi and capillaries. This effect was mediated by the decrease in neutrophil activation, as assessed by MMP-9 release into the small bowel tissue and bloodstream. Rosario et al. have shown that the higher protease activity in the intestinal wall after a mesenteric ischemia/reperfusion episode originated from the infiltration of neutrophils and the release of MMP-9[16]. MMP-9 is the main protease stored in the tertiary granules of neutrophils, that at the occurrence can be mobilized under low chemotactic stimulation levels[17]. In addition, MMP9 is highly diffusible from the tissue to plasma[18]. MMP-9 activation is crucially involved in ischemia/reperfusion injury by modulating extracellular matrix turnover, by triggering inflammatory cell migration and pro-inflammatory mediator release and the stimulation of angiogenesis[19].

In contrast to the intestinal mucosa, we observed no protection against muscular layer injury by P8RI infusion. However, it has been shown that the neutrophil infiltration in the intestinal mucosa begins as early as 1 hour after ischemia/reperfusion, whereas it is delayed by 24 to 72 hours in the muscular layer[20]. This could explain why we failed to detect a protective effect on the muscular layer at 4 hours of reperfusion after 30 min of ischemia.

Cell-free DNA is a non-specific marker of tissue injury released into the bloodstream from necrotic cells[21], and is an independent predictor of mortality and sepsis in critically ill patients[22,23]. In human acute mesenteric ischemia/reperfusion, cell-free DNA is associated with the severity of bowel inflammation and necrosis[24]. Remarkably, we found that P8RI decreased the plasma concentration of cell-free DNA after mesenteric ischemia/reperfusion, indicating that P8RI significantly reduced intestinal tissue damage.

A basal circulating form of CD31 was detected in I/R controls, P8RI and sham groups. It has been shown that, in normal human plasma, there exists a soluble form of mature CD31 containing the cytoplasmic tail and reaching a concentration of 10 to 25 ng/ml, which is secreted only 48 hours after intracellular synthesis[25]. Thus, the soluble CD31 quantified here was more likely to result from the cleavage and shedding of CD31 after ischemia/reperfusion than to represent the mature form.

The cleavage of CD31 strongly correlated with the epithelial layer injury, neutrophil activation and cell death. It emphasizes the important role of CD31 in maintaining the integrity of intestinal mucosa. The protective effect of P8RI could be related to the inhibition of CD31 cleavage from neutrophils, thus decreasing their protease activity on the intestinal mucosa.

Bacterial translocation is a specific feature reflecting the loss of epithelial cell integrity after mesenteric ischemia/reperfusion and is a trigger of the systemic innate immune response and sepsis[26]. We found that P8RI decreased bacterial translocation as assessed by the detection of DNA from Escherichia coli in plasma using a real-time PCR technique, a more sensitive assay than bacterial blood cultures[27].

This study has several limitations. P8RI has not been tested for curative treatment, but it was useful to assess its protective role on a "controlled" mesenteric ischemia/reperfusion, a clinical condition encountered in repair of the descending aorta[28]. In addition, the cell type responsible for the shed CD31 in plasma was not determined. It may originate from tissue and/or blood neutrophils, and/or endothelial cells and/or platelets. In humans, the extracellular domain of CD31 is shed at different sites depending on the cellular origin (neutrophils, platelets or endothelial cells) and released in the circulation as a soluble form of CD31[29,30]. Our laboratory has developed a cytometric bead array technology to identify and quantify different soluble fractions of shed CD31 according to their cellular origin[31,32]. Unfortunately, this technology is not available for use in rats. Instead, we used a polyclonal antibody that targeted all forms of shed CD31 in plasma.

In conclusion, P8RI peptide binding to cleaved CD31 reduced neutrophil activation and ischemia/reperfusion-induced intestinal injury. Drug-suitable P8RI is potentially a promising therapy for preventing acute mesenteric consequences of ischemia/reperfusion.

FIGURES

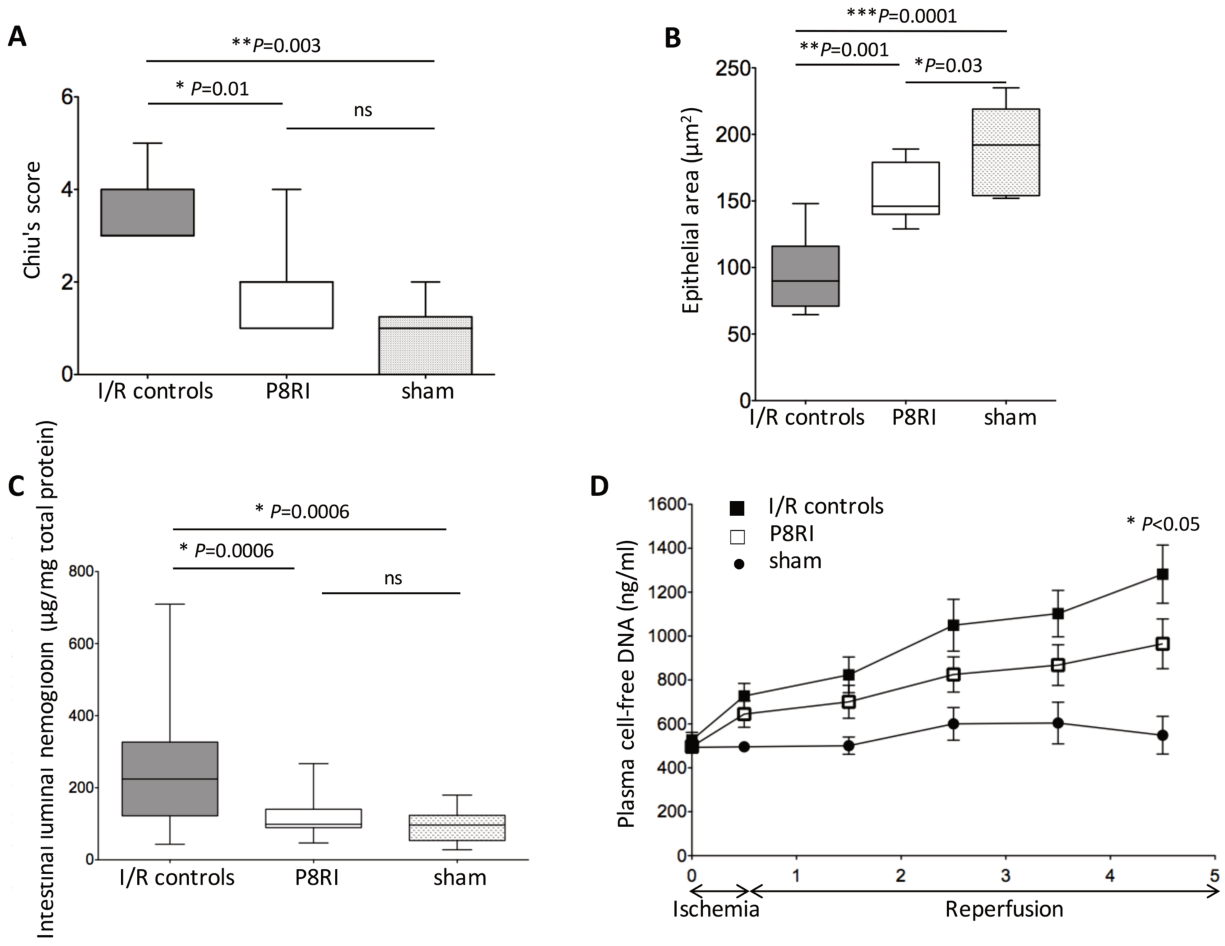

Figure 1: Effect of P8RI on mesenteric ischemia/reperfusion-induced intestinal injury.

Ischemia/reperfusion-induced intestinal injury was assessed by histological analysis using the Chiu's score that ranges from a normal mucosa (score=0) to a total mucosal necrosis (score=6), and morphometric analysis using Qwin software from scanned histological sections by a nanozoomer in I/R controls, P8RI and sham groups. (**A**) The Chiu's score of intestinal injury was lower in the P8RI group compared to I/R controls (*P=0.01). (**B**) The epithelial area was higher in the P8RI group than in I/R controls (*P=0.001). (**C**) The intestinal luminal hemoglobin concentration was lower in the P8RI group than in I/R controls (*P=0.0006). (**D**) Plasma cell-free DNA was used as a cell death marker. The plasma concentration of cell-free DNA was lower in the P8RI group than in I/R controls at 4 hours of reperfusion after mesenteric ischemia (*P<0.05).

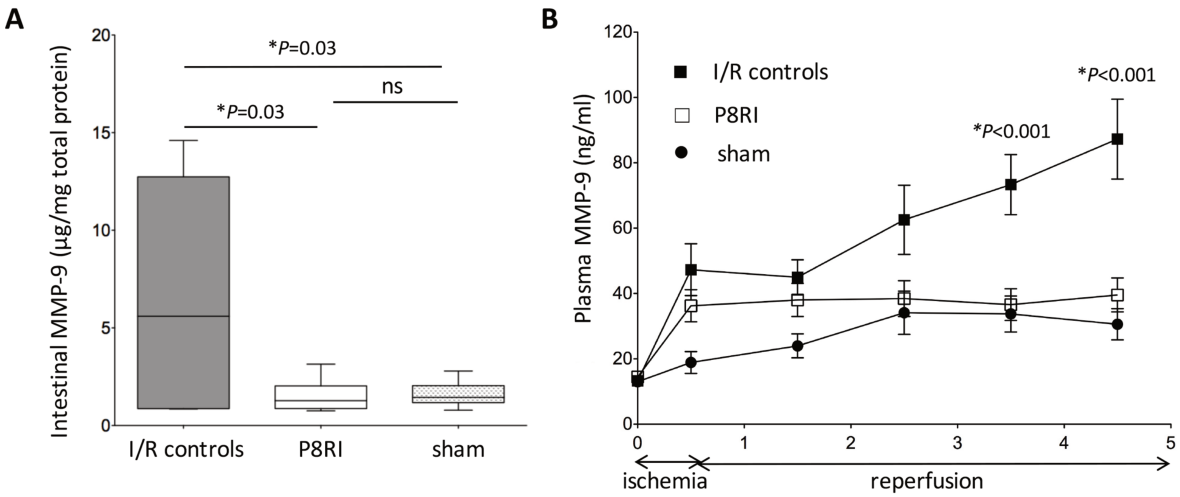

Figure 2: Effect of P8RI on mesenteric ischemia/reperfusion-induced neutrophil activation.

Mesenteric ischemia/reperfusion-induced neutrophil activation was assessed by the detection of MMP-9 in the small bowel tissue and plasma. (**A**) The concentration of MMP-9 in the intestinal tissue was lower in the P8RI group than in I/R controls (P=0.03). (**B**) The plasma concentration of MMP-9 was lower in the P8RI group than in I/R controls at 3 hours (*p< 0.001) and 4 hours (**P<0.001) of reperfusion after mesenteric ischemia. MMP-9: matrix metalloproteinase-9.

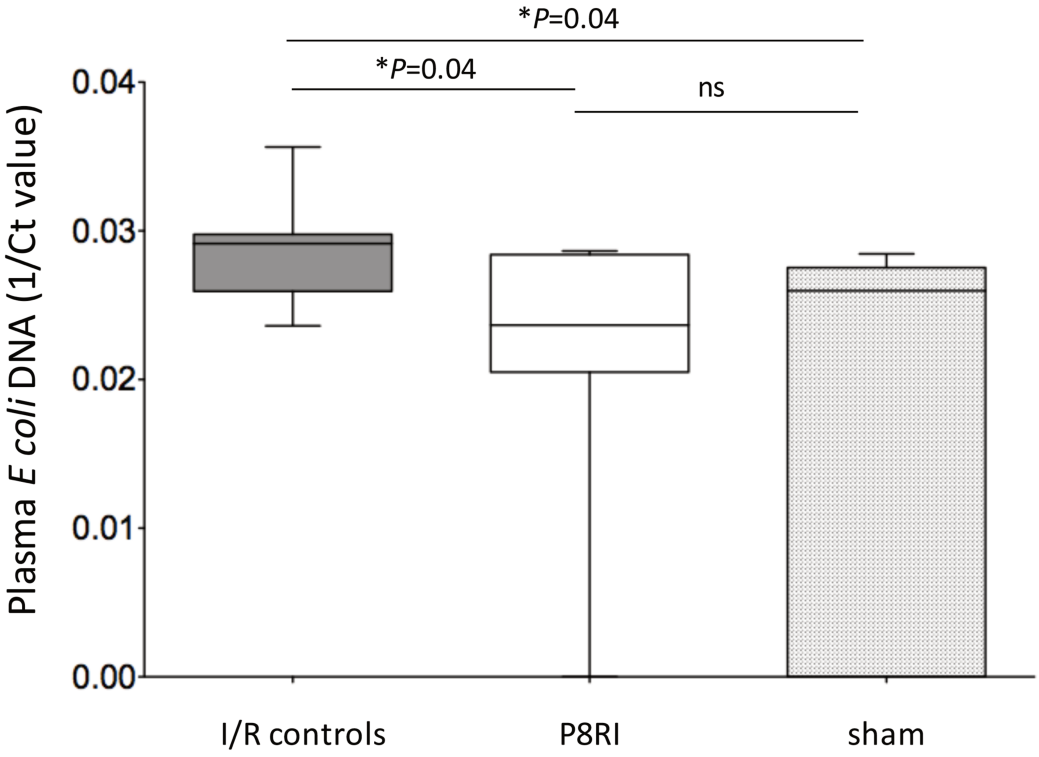

Figure 3. Effect of P8RI on mesenteric ischemia/reperfusion-induced bacterial translocation.

Bacterial translocation was assessed by the quantification of plasma DNA from Escherichia coli using real time PCR. Ct value represents the minimum number of cycles to detect plasma Escherichia coli DNA, and is inversely correlated to the quantity of plasma DNA from Escherichia coli. P8RI administration limited the plasma concentration of DNA from E coli compared to saline injection (*P=0.04).

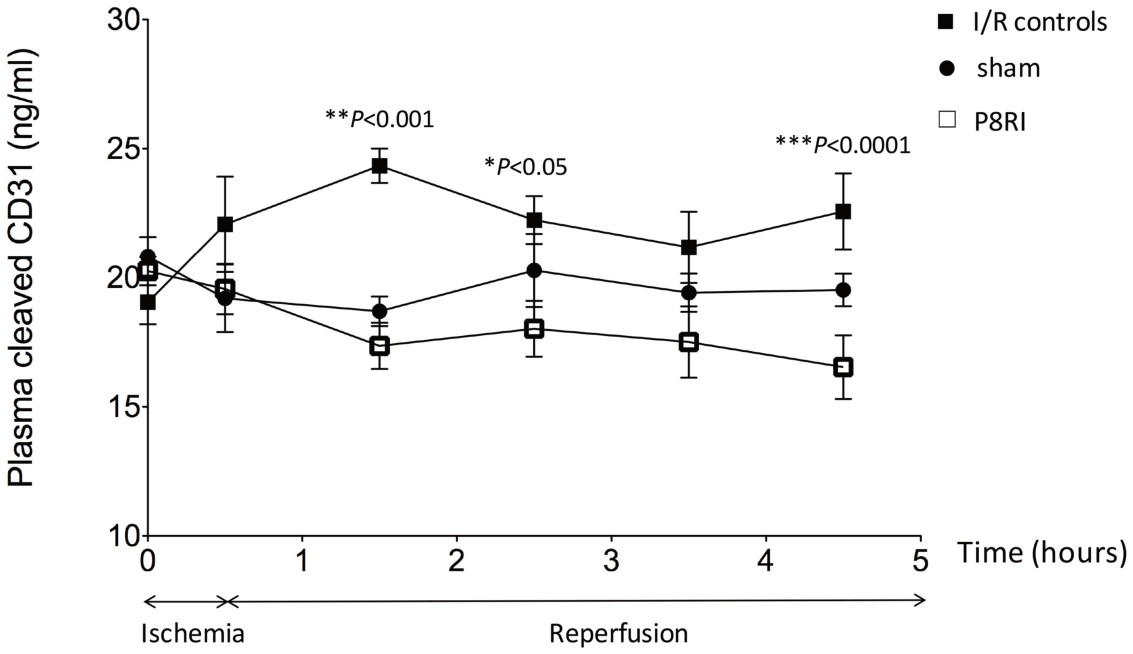

Figure 4: Effect of P8RI on mesenteric ischemia/reperfusion-induced cleavage and shedding of CD31 into plasma.

Cleavage and shedding of CD31 into plasma was assessed by the detection in plasma of the soluble cleaved extracellular portion of CD31. The concentration of soluble cleaved CD31 in plasma was lower in the P8RI group than in I/R controls at 1 hour (*P<0.001), 2 hours (**P<0.05) and 4 hours (***P<0.0001) of reperfusion after mesenteric ischemia

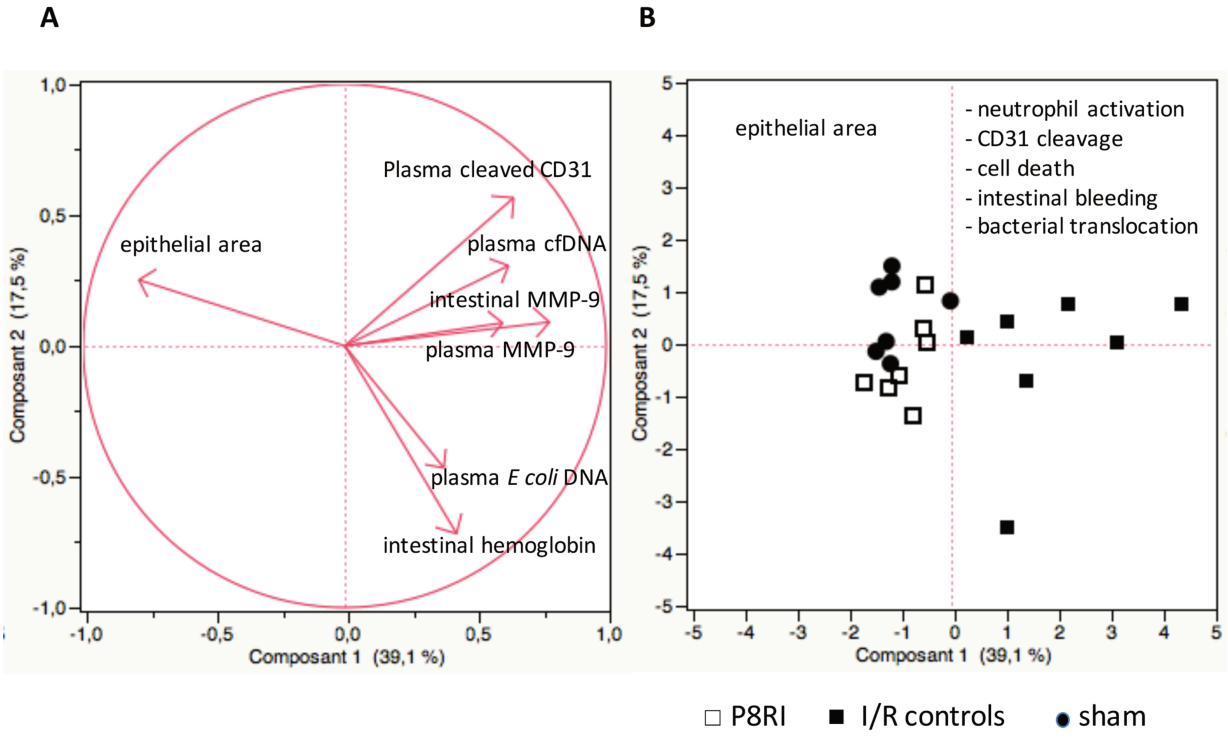

Figure 5: Principal component analysis demonstrated how CD31 engagement impacts ischemia injury biomarkers of neutrophil activation and consequences on small intestinal epithelium morphology.

(A) Principal component analysis showed positive correlations between intestinal MMP-9, plasma MMP-9, plasma cell-free DNA, intestinal luminal hemoglobin, plasma E coli DNA and plasma soluble cleaved CD31 in all groups. Conversely, epithelial area was strongly negatively correlated to these parameters. (B) Principal component analysis identified a clustering of the P8RI and sham groups, widely separated from I/R controls. MMP-9: matrix metalloproteinase-9, cfDNA: cell-free DNA

Supplemental Information

Table E1: Histological grading system: Chiu's score

Grade	Histological appearance
0	Normal
1	Subepithelial oedema, partial separation of apical cells
2	Epithelial cell sloughing from tips of villi
3	Progression of sloughing to base of villi
4	Partial mucosal necrosis of lamina propria
5	Total mucosal necrosis

Figure E1: Morphometric analysis of the intestinal wall.

Histological gut sections were scanned (slide scanner, Hamamatsu Nanozoomer) (A) and analysed using a custom QWin software (B). The luminal area (in blue) was defined by thresholding the space inside the intestinal ring whose external border was limited by the epithelium. The muscular layer (in red) was defined as extending from the basal side of the epithelial layer to the external border of the intestinal ring. The epithelial layer (in green) was defined as the area contained between the lumen and muscular layer.

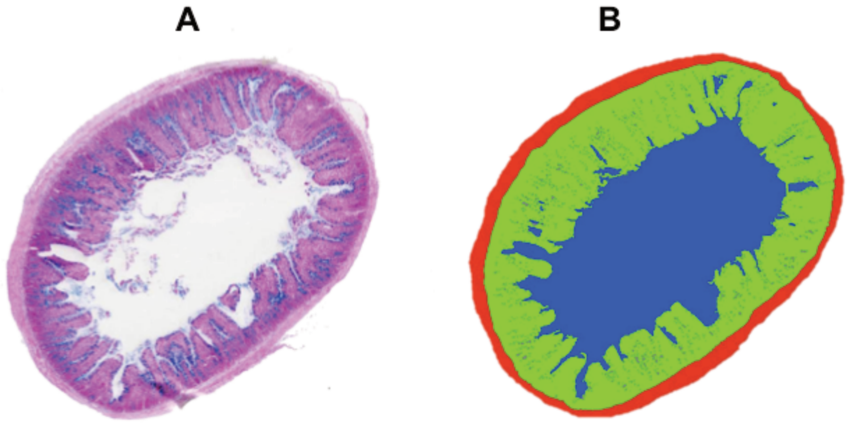

Assessment of intestinal bleeding

The degree of intestinal bleeding was assessed by quantification of the heme content in the luminal content of the small intestine. This luminal content was homogenized in distilled water and centrifuged for 30min at 16,000g. The heme content, used as a surrogate estimation of the luminal hemoglobin, was assessed by addition of formic acid to the supernatant and monitoring the optical density at a wavelength of 405nm (33). The heme content was normalized to the total protein concentration of the luminal content measured by colorimetric protein quantification (BCA protein assay kit, Sigma).

Assessment of neutrophil activation in the small bowel tissue.

The intestinal tissue was homogenized (TissuLyser, Quiagen) and extracted using RIPA buffer. The extract was centrifuged for 30min at 16,000g and the supernatant was used for assays. Total protein concentration in the supernatant was measured using a BCA protein assay kit (Sigma). Intestinal matrix metalloproteinase-9 (MMP-9) was used as a marker of intestinal tissue neutrophil activation. The intestinal tissue concentration of MMP-9 was determined using an enzyme-linked immunosorbent assay for rat (rat total MMP-9 DuoSet ELISA kit, R&D systems). The capture antibody was coated on 96-well half area microplates. A blocking buffer solution was used to block the remaining protein binding sites before incubating the supernatant obtained from centrifugation of the small bowel homogenate. The detection antibody was adjusted for the double antibody sandwich enzyme-linked immunosorbent assay protocol. Streptavidine and color reagent (R&D systems) were used

for the detection of the antigen-antibody reaction. The absorbance was analyzed at a wavelength of 450nm using a Tecan monochromator plate reader.

Assessment of cell death

Plasma cell-free DNA concentration was determined using the Quant-it Picogreen dsDNA Reagent Kit (Invitrogen). The lambda DNA standard and 10 µL of the sample were diluted in TE buffer before the addition of 100 µL Picogreen dsDNA reagent. After mixing, fluorescence was measured using a micro-plate reader (excitation 480nm, emission 520nm).

Assessment of bacterial translocation

Bacterial translocation was assessed by the quantification of genomic DNA from Escherichia coli in plasma. The technique used real time PCR (CFX96TM Real Time System, BioRad). DNA extractions were performed using 20µL of a dilution buffer and 0.5µL of a DNA release additive (Phire Tissu Direct PCR Master Mix, Thermo). After incubation at room temperature (5min), plasma was denatured at 98°C (2min) and centrifuged at 16,000 g (5min). One microliter of the supernatant was used to perform a real-time PCR with Escherichia coli's specific primers (Eurogentec). The amplification was programmed for a first cycle at 50°C (2min), a second cycle at 95°C (15min), 50 cycles at 95°C (40sec) and a last cycle at 60°C (1min). The Ct value represented the number of cycles at which a sufficient quantity of amplified DNA had accumulated to yield a detectable fluorescence signal in plasma. The plasma concentration of Escherichia coli DNA was proportional to the inverse of the Ct value (1/Ct value).

References

1. Leone M, Bechis C, Baumstarck K, et al.: Outcome of acute mesenteric ischemia in the intensive care unit: a retrospective, multicenter study of 780 cases. Intensive Care Med 2015; 41:667–676
2. Grootjans J, Lenaerts K, Derikx JPM, et al.: Human intestinal ischemia-reperfusion-induced inflammation characterized: experiences from a new translational model. Am J Pathol 2010; 176:2283–2291
3. Hebra A, Hong J, McGowan KL, et al.: Bacterial translocation in mesenteric ischemia-reperfusion injury: is dysfunctional motility the link? J Pediatr Surg 1994; 29:280–285; discussion 285–287
4. Landow L, Andersen LW: Splanchnic ischaemia and its role in multiple organ failure. Acta Anaesthesiol Scand 1994; 38:626–639
5. Sisley AC, Desai T, Harig JM, et al.: Neutrophil depletion attenuates human intestinal reperfusion injury. J Surg Res 1994; 57:192–196
6. Hernandez LA, Grisham MB, Twohig B, et al.: Role of neutrophils in ischemia-reperfusion-induced microvascular injury. Am J Physiol 1987; 253:H699–703
7. Marelli-Berg FM, Clement M, Mauro C, et al.: An immunologist's guide to CD31 function in T-cells. J Cell Sci 2013; 126:2343–2352
8. Newman PJ: The role of PECAM-1 in vascular cell biology. Ann N Y Acad Sci 1994; 714:165–174
9. Newman PJ, Newman DK: Signal transduction pathways mediated by PECAM-1: new roles for an old molecule in platelet and vascular cell biology. Arterioscler Thromb Vasc Biol 2003; 23:953–964
10. Caligiuri G, Nicoletti A, Michel J-B: CD31shed agonists for use in the prevention and/or treatment of reperfusion injury. EP16305311, submitted on March 2016
11. Caligiuri G, Nicoletti A: Use of CD31 peptides in the treatment of thrombotic and autoimmune disorders. WO 2010/000741 (PCT/EP2009/058188). 2015
12. Caligiuri G, Nicoletti A: Improved CD31 peptides. WO 2013/190014 (PCT/EP2013/062806). 2013
13. Chen Y, Schlegel PG, Tran N, et al.: Administration of a CD31-derived peptide delays the onset and significantly increases survival from lethal graft-versus-host disease. Blood 1997; 89:1452–1459
14. Chiu CJ, McArdle AH, Brown R, et al.: Intestinal mucosal lesion in low-flow states. I. A morphological, hemodynamic, and metabolic reappraisal. Arch Surg Chic Ill 1960 1970; 101:478–483
15. Fornasa G, Clement M, Groyer E, et al.: A CD31-derived peptide prevents angiotensin II-induced atherosclerosis progression and aneurysm formation. Cardiovasc Res 2012; 94:30–37
16. Rosário HS, Waldo SW, Becker SA, et al.: Pancreatic trypsin increases matrix metalloproteinase-9 accumulation and activation during acute intestinal ischemia-reperfusion in the rat. Am J Pathol 2004; 164:1707–1716
17. Borregaard N, Cowland JB: Granules of the human neutrophilic polymorphonuclear leukocyte. Blood 1997; 89:3503–3521
18. Borges LF, Touat Z, Leclercq A, et al.: Tissue diffusion and retention of metalloproteinases in ascending aortic aneurysms and dissections. Hum Pathol 2009; 40:306–313

19. Dejonckheere E, Vandenbroucke RE, Libert C: Matrix metalloproteinases as drug targets in ischemia/reperfusion injury. Drug Discov Today 2011; 16:762–778
20. Pontell L, Sharma P, Rivera LR, et al.: Damaging effects of ischemia/reperfusion on intestinal muscle. Cell Tissue Res 2011; 343:411–419
21. Jahr S, Hentze H, Englisch S, et al.: DNA fragments in the blood plasma of cancer patients: quantitations and evidence for their origin from apoptotic and necrotic cells. Cancer Res 2001; 61:1659–1665
22. Saukkonen K, Lakkisto P, Varpula M, et al.: Association of cell-free plasma DNA with hospital mortality and organ dysfunction in intensive care unit patients. Intensive Care Med 2007; 33:1624–1627
23. Rhodes A, Wort SJ, Thomas H, et al.: Plasma DNA concentration as a predictor of mortality and sepsis in critically ill patients. Crit Care Lond Engl 2006; 10:R60
24. Arnalich F, Maldifassi MC, Ciria E, et al.: Association of cell-free plasma DNA with perioperative mortality in patients with suspected acute mesenteric ischemia. Clin Chim Acta Int J Clin Chem 2010; 411:1269–1274
25. Goldberger A, Middleton KA, Oliver JA, et al.: Biosynthesis and processing of the cell adhesion molecule PECAM-1 includes production of a soluble form. J Biol Chem 1994; 269:17183–17191
26. MacFie J, O'Boyle C, Mitchell CJ, et al.: Gut origin of sepsis: a prospective study investigating associations between bacterial translocation, gastric microflora, and septic morbidity. Gut 1999; 45:223–228
27. Balzan S, de Almeida Quadros C, de Cleva R, et al.: Bacterial translocation: overview of mechanisms and clinical impact. J Gastroenterol Hepatol 2007; 22:464–471
28. Achouh PE, Madsen K, Miller CC, et al.: Gastrointestinal complications after descending thoracic and thoracoabdominal aortic repairs: a 14-year experience. J Vasc Surg 2006; 44:442–446
29. Wang SZ, Smith PK, Lovejoy M, et al.: Shedding of L-selectin and PECAM-1 and upregulation of Mac-1 and ICAM-1 on neutrophils in RSV bronchiolitis. Am J Physiol 1998; 275:L983–989
30. Naganuma Y, Satoh K, Yi Q, et al.: Cleavage of platelet endothelial cell adhesion molecule-1 (PECAM-1) in platelets exposed to high shear stress. J Thromb Haemost JTH 2004; 2:1998–2008
31. Caligiuri G, Nicoletti A: Detection of shed CD31, diagnosis of atherothrombosis and autoimmune disorders, and methods for analyzing signaling pathways. WO 2010/000756 (PCT/EP2009/058220). 2010
32. Caligiuri G, Nicoletti A: Detection of platelet-derived CD31. WO2013152919 (PCT/EP2013/055489). 2013
33. Garrick LM, Sharma VS, McDonald MJ, et al.: Rat haemoglobin heterogeneity. Two structurally distinct alpha chains and functional behaviour of selected components. Biochem J 1975; 149:245–258

13 ANNEX III

(Under reviewing in Journal of Clinical Investigation)

Vascular sequestration of donor-specific antibodies and endothelial chimerism protect pancreatic islet grafts from humoral rejection

Chien-Chia Chen[1], Eric Pouliquen[2], Alexis Broisat[3], Francesco Andreata[4], Maud Racapé[5], Patrick Bruneval[5], Laurence Kessler[6], Mitra Ahmadi[3], Sandrine Bacot[3], Carole Saison- Delaplace[1,2], Marina Marcaud[2], Jean-Paul Duong Van Huyen[5], Alexandre Loupy[5, 7], Thierry Berney[8], Emmanuel Morelon[1, 2, 9], Meng Kun Tsai[10], Marie-Nathalie Kolopp-Sarda[11], Alice Koenig[1], Virginie Mathias[12], Stéphanie Ducreux[12], Catherine Ghezzi[3], Valerie Dubois[12], Antonino Nicoletti[4], Thierry Defrance[1], Olivier Thaunat[1, 2, 9], *

1. French National Institute of Health and Medical Research (Inserm) Unit 1111, Lyon, France;
2. Edouard Herriot University Hospital, Department of Transplantation, Nephrology and Clinical Immunology, Lyon, France;
3. French National Institute of Health and Medical Research (Inserm) Unit 1039, Grenoble, France; Bioclinical Radiopharmaceutical laboratory, Joseph Fourier University (Grenoble 1), Grenoble, France;
4. French National Institute of Health and Medical Research (Inserm) Unit 1148, Laboratory of Vascular Translational Science, F-75018, Paris, France;
5. Paris Translational Research Centre for Organ Transplantation, Paris Descartes University, Paris, France;
6. Department of Diabetology, University Hospital, Strasbourg, France; Federation of Translational Medicine of Strasbourg, University of Strasbourg, Strasbourg, France;
7. Department of Kidney Transplantation, Necker Hospital, Assitance Publique-Hôpitaux de Paris, Paris, France;
8. Departement of Surgery, Islet Isolation, and Transplantation Center, Geneva University Hospitals, Geneva, Switzerland;
9. Lyon Est Medical Faculty, Claude Bernard University (Lyon 1), Lyon, France;
10. Department of Surgery, National Taiwan University Hospital and National Taiwan University, College of Medicine, Taipei, Taiwan;
11. Lyon-Sud University Hospital, Laboratory of Immunology, Lyon, France;
12. French National Blood Service (EFS), HLA Laboratory, Lyon, France;

* Correspondence to:
Olivier Thaunat MD, PhD
CIRI – INSERM U1111 - Université Lyon 1 21 Avenue Tony Garnier
69365 Lyon cedex 07, France
email: olivier.thaunat@inserm.fr

Abstract

Islet grafting restores endogenous insulin production in type 1 diabetic patients but long-term outcome remains disappointing due to the destruction of allogeneic islets by recipients' adaptive immune system. In solid organ transplantation, humoral rejection is recognized as the first cause of transplant failure. However, the observation of a cohort of 27 islet graft recipients revealed that the rate of graft attrition was not accelerated by appearance of donor- specific anti-HLA antibodies (DSA), suggesting that islet graft may be resistant to humoral rejection.

Murine experimental models showed that, while DSA bind to allogeneic targets expressed by islet cells and can readily induce their destruction in vitro, passive transfer of DSA did not impact islet graft survival in vivo. Live imaging studies using fluorescent and radiolabelled DSA, demonstrated that DSA were sequestrated in recipients' circulation and unable to reach endocrine cells of grafted islets. Heart transplantation model confirmed that endothelial cells were the only accessible targets for DSA, which induced the development of typical microvascular lesions in allogeneic transplants. Interestingly, the vasculature of allogeneic islet grafts exposed to DSA was devoid of histological lesions. This was due to the fact that re-establishment of blood-flow in grafted islets occurs through sprouting of capillaries from recipient's origin. We concluded that endothelial chimerism combines with vascular sequestration of DSA explains islet graft resistance to humoral rejection. Beyond the field of islet grafting, the reduced concentrations in immunoglobulin in interstitial tissue, confirmed in transplanted patients, may have important implications for biotherapies such as vaccines and monoclonal antibodies.

Introduction

Type 1 diabetes is one of the most prevalent chronic diseases of childhood. Epidemiologic studies have estimated that ~70,000 new cases are diagnosed every year and that the incidence of the disease increases annually by 2-5 % worldwide.

Type 1 diabetes is caused by an autoimmune-mediated destruction of pancreatic β cells, one of the 4 major types of cells present in the islets of Langerhans. β cells are unique cells in the pancreas that synthesize and secrete insulin, a key hormone for regulating glucose levels. β cells destruction therefore results in life-long dependence on exogenous insulin. Despite advances in insulin formulations, insulin delivery systems, and glucose monitoring, less than one-third of patients meet clinical care targets needed to prevent secondary end-organ complications such as retinal, renal, and neurological diseases[1].

Interestingly, early rodent experiments have demonstrated that islets of Langerhans (in which β cells represent 65-80% of the cells) can be isolated from pancreas exocrine component and grafted into a diabetic mouse[2]. Advances in pancreatic islet isolation and refinement of immunosuppressive protocols allowed to obtain the first patient achieving insulin independence in 1990[3]. In contrast to intensive insulin regimens and insulin pumps, pancreatic islet grafting allows restoring endogenous insulin secretion, which efficiently prevents, halts, or reverses the development or progression of secondary diabetes complications[4,5]. Unfortunately, islet function decreases over time such that by 3 years post- transplant, less than 50% of the recipients remain insulin independent[6].

Identifying the causes of progressive attrition of grafted islets appears as a necessary step to improve long-term results. Involvement of recipient's immune system is strongly supported by the observation that graft function is more resilient in autografts than allografts[7]. Alloimmune response drives rejection through two distinct effector arms: antibodies and cytotoxic T-cells. Donor-specific antibodies (DSA) are increasingly recognized as the prime cause of solid organ transplant failure[8,9]. As solid organ recipients, islet allograft recipients also develop DSA[10–12], however the impact of DSA on islet graft function remains unclear. Indeed, the few studies that have investigated whether DSA generation correlated with decreased islet graft survival have reached conflicting conclusions[10–13].

Here, we describe the results of a translational study demonstrating that allogeneic islets are resistant to DSA-mediated rejection. Although DSA can destroy islet cells in vitro, the decline of islet graft function was not accelerated in patients that developed DSA. Using murine experimental models, we demonstrate that the resistance of allogeneic islets to humoral rejection is explained by the combination of i) vascular sequestration of DSA, which are unable to access the allogeneic β cells in vivo and ii) the fact that unlike vascularization of transplanted organs (which comes from the donor), islet graft vascularization develops from the recipient.

Results

DSA do not accelerate pancreatic islet graft attrition in the clinic

In order to evaluate the impact of DSA on islet graft survival, we undertook a retrospective multicentric study. The medical files of all patients successfully grafted with allogeneic islets within the GRAGIL consortium between 2000 and 2013 were reviewed. Twenty-seven recipients had sufficient available clinical and biological material to be retrospectively analyzed.

The β-score[14] which integrates insulin requirements, C-peptide secretion, and glycemic control, was used to monitor the pancreatic islet graft function of the cohort longitudinally. As expected, β cell function decreased regularly over the follow-up period as reflected by the slope of linear regression (-0.5 β-score point per year; Figure 1A).

Among these 27 patients, 4 developed DSA while on immunosuppressive therapy with functional islet grafts. The rate of islet graft attrition of these 4 recipients with DSA was remarkably similar to the rate of islet graft attrition of patients without DSA (DSA vs no DSA: -0.53 vs -0.51, β-score point per year; Figure 1B).

Although the low number of patients and the correlative nature of the study did not allow drawing definitive conclusions, these results suggested that, in contrast with solid organ transplants, grafted islets are resistant to humoral rejection.

Murine model of intra-hepatic pancreatic islet grafting recapitulates the clinical findings

Wild type C57BL/6 (H-2b) mice were rendered diabetic by administration of intraperitoneal injection of streptozotocin. Diabetic mice were used as recipients of purified pancreatic islets (Figure 2A), which were injected in the portal vein as to mimic the grafting procedure used in the clinic (Figure 2B). Pancreatic islet morphology was assessed in the liver of syngeneic recipient mice 50 days post-grafting. Morphologically intact islets were found scattered within hepatic parenchyma, close to blood vessels of the portal tract (Figure 2C).

Grafted mice normalized their glycaemia within 4 days (Figure 2D). Wild type C57BL/6 (H- 2b) mice tolerated syngeneic islet grafts, as demonstrated by the fact that they remained euglycemic until the end of follow-up (Figure 2D). CBA islets (H-2k) triggered an allogeneic response in recipient mice, as reflected by the generation of DSA, which were detected in recipients' circulation and could be quantified using a customized flow cross match assay (Figure 2E). Recipient's allogeneic response led to the destruction of grafted islets as shown by return to hyperglycemia within 15 days (syngeneic vs allogeneic islets survival: p=0.0008, Log Rank test; Figure 2D).

In contrast with wild type animals, C57BL/6 RAG2 KO mice, which lack T and B cells but have a functional innate immune system, did not reject CBA islet grafts (Figure 2F). These results highlighted the central role of adaptive immunity in islet graft rejection and indicated that our model could be used to evaluate separately the impact of the two effector arms of adaptive immune system: i.e. antibodies and T cells.

In line with the latter idea, purified T cells were first transferred to C57BL/6 RAG2 KO recipients, which led to prompt rejection of allogeneic CBA islets, despite the absence of DSA. These data established that T cell-mediated response is sufficient to reject an allogeneic islet graft.

The impact of the sole recipient’s humoral alloimmune response on islet graft survival was then evaluated using passive transfer of DSA. Intravenous (IV) infusions of pooled immune sera were started 15 days after grafting procedure to mimic the clinical situation of patients developing de novo DSA. The amount of immune sera infused was set as to match the peak of DSA with the median value of DSA concentration observed in wild type C57BL/6 islet recipients (Figure 2E). The frequency

of immune sera infusions (every 72 hours) was set to keep the titer of circulating DSA close to the median value of DSA concentration observed in wild type C57BL/6 islet recipients (Figure 2E). In contrast with recipients transferred with purified T cells, mice transferred with DSA maintained normal glycaemia for all the follow- up period (Figure 2F) despite the fact that grafted islets did express donors' H-2 molecules (Figure 2G). This finding is reminiscent of our observation made in the clinic and raises the question of why grafted islets are resistant to DSA-mediated destruction.

Recipients' humoral response can destroy allogeneic islets in vitro

Antibody-mediated rejection is widely recognized as the first cause of failure for transplanted organs[8,9], including pancreas[15,16]. Beyond the mere quantity (i.e. the titer) of DSA, several recent clinical studies have highlighted the importance of the "quality" of DSA (i.e. the nature of heavy chain isotypes[17] and the ability for DSA to activate the complement cascade[18,19]). A first possibility to explain the lack of deleterious impact of DSA on grafted islets is that the nature of the alloimmune humoral response triggered by a graft might differ from that triggered by a transplant. To test this hypothesis, DSA responses of wild type C57BL/6 mice receiving either a CBA islet graft or a CBA heart transplant were compared. Although the peak of DSA titer was less heterogeneous and significantly higher after heart transplantation (heart vs islet: 1059±210 vs 25±11 µg/ml, $p<0.0001$, Mann Whitney test; Figure 2E), the spectra of heavy chain isotypes of DSA generated in response to a graft and a transplant were remarkably similar (Figure 2H), as was the ability for the two kinds of sensitized sera to destroy the cellular targets in a complement-dependent lymphocytotoxicity test in vitro (Figure 2I). Of note, a DSA titer of 3.2 µg/ml (equivalent to the median value observed in wild type C57BL/6 islet recipients and used in transfer experiments, Figure 2E) was sufficient to destroy 100% of allogeneic lymphocytes in vitro (Figure 2I). Finally this DSA titer was also sufficient to promote the destruction of 75% of allogeneic islet cells used as targets in a complement-dependent cytotoxicity assay in vitro (Figure 2J).

These results suggest that the lower DSA titers are likely not the sole explanation to the resistance of grafted islets to humoral rejection.

Optimizing experimental model to explore the mechanisms of islet graft resistance to DSA-mediated rejection in vivo

Intra-portal injection of pancreatic islets leads to their dissemination in liver parenchyma, which precludes direct in vivo observation of grafted islets and makes impossible their retrieval for analysis (Figure 2C). To facilitate the identification of the mechanisms underlying islet graft resistance to DSA-mediated rejection in vivo, we relied on an alternative, well validated model of islet grafting[20,21], where purified pancreatic islets are placed under the capsule of recipient's left kidney (Figure 3A).

Of note in this model, left nephrectomy (i.e. islet graft removal) at the end of follow-up period offers the unique opportunity to confirm the function of the graft and to rule out that glycemic control is due to neogenesis of insulin-producing β cells in native pancreas. Graft morphology analysis, performed 50 days after the procedure, showed large insulin-producing endocrine aggregates connected to cortical kidney vascularization (Figure 3B).

The subcapsular model of islet grafting recapitulated all the observations made when pancreatic islets were injected into the portal vein. Briefly: wild type C57BL/6 mice tolerated syngeneic islet grafts (Figure 3C). CBA islets were rejected by wild type C57BL/6 recipients (syngeneic vs allogeneic islet survival: $p<0.0001$, Log Rank test; Figure 3C), who generated DSA during the rejection process (Figure 3D). Finally, C57BL/6 RAG2 KO recipients did not reject CBA allogeneic islets (Figure 3E), even when they were infused twice weekly with DSA-containing immune sera (Figure 3E).

The use of immune sera represented another limitation to dissect the mechanisms underlying the resistance of grafted islets to humoral rejection. The heterogeneity of humoral responses generated by recipient mice (Figure 2E and 3D) made indeed complex the standardization of DSA transfer experiments. Although we made important efforts to ensure that each recipient received similar amount of DSA (Figure 2E and 3D), it was difficult to control the stability of the "quality" (i.e. spectrum of heavy chain isotypes and ability to activate the complement) of the different batches of pooled immune sera. Immune sera also represented a limitation to track DSA in vivo. The use of a commercially available purified mouse anti-H-2k monoclonal antibody (mAb) allowed overcoming these technical hurdles. The HB13 mAb, a mouse IgG2a directed against H-2Kk and Dk major histocompatibility complex class I molecules, was chosen for its ability to promote antibody-mediated rejection lesions in H-2k heart transplants 22. In vitro, HB13 displayed comparable ability as pooled immune sera from wild type C57BL/6 islet recipients to trigger complement-dependent lymphocytotoxicity (Figure 3F). However, since HB13 was slightly less efficient than pooled immune sera to induce allogeneic islet cell destruction in vitro (Figure 3G), we set the amount of HB13 transferred IV as to obtain a peak ~ a log higher than the median value of DSA concentration observed in wild type C57BL/6 islet recipients (Figure 3H). Infusion were performed IV every 72 hours to ensure that the titer of HB13 stayed above the median value of DSA concentration observed in wild type C57BL/6 islet recipients (Figure 3H). Similar to passive transfer of immune sera, IV infusions of HB13 did not show any impact on CBA islet graft survival in C57BL/6 RAG2 KO recipients (Figure 3I).

<u>DSA do not induce microvascular lesions to pancreatic islet graft in vivo</u>

C57BL/6 RAG2 KO mice were used as recipients of either subcapsular CBA pancreatic islets or a CBA heart transplant. HB13 or PBS was infused IV twice weekly to recipient mice for 30 days and

grafts/transplants were harvested for histological analysis. PBS did not induce significant histological changes to heart transplants and islet grafts. Heart transplants exposed to DSA showed, as previously reported[22,23], leukocyte margination in dilated capillaries (Figure 4A), which is typical of humoral rejection[24,25]. In contrast, pancreatic islet grafts exposed to DSA in vivo were devoid of such microvascular lesions (Figure 4A). Immunohistochemistry confirmed that, in contrast with heart transplants and despite the fact that they had similar density of microvessels, grafted islets did not develop endothelial turgidity, complement activation, or leukocyte infiltration upon DSA exposure (Figure 4B). Electron microscopy analyses further confirmed the integrity of both endothelial and endocrine cells of grafted islets exposed to DSA in vivo (Figure 4C).

Endothelial chimerism protects grafted islets from DSA-induced vascular lesions in vivo

In contrast with transplantation, where perfusion is immediately reestablished by surgical reconnection of arterial and venous vessels of the organ to recipient's circulation, the restoration of blood flow to grafted islets involves angiogenesis[26–30]. We postulated that this difference might explain the resistance of islet graft vasculature to the deleterious impact of DSA.

Syngeneic (C57BL/6, H-2b) or allogeneic (CBA, H-2k) hearts were transplanted to C57BL/6 RAG2 KO recipients. Four weeks after transplantation, the heart transplants were harvested and, following enzymatic digestion, the origin of hematopoietic (CD45+ CD31-), stromal (CD45- CD31-), and endothelial cells (CD45- CD31+) was assessed by H-2k expression using flow cytometry (Figure 5A). As expected, the endothelial cells of heart transplants were all from donor origin (Figure 5A). The same conclusion was reached when the same approach was applied to freshly isolated islets (Figure 5B).

Using the subcapsular model in C57BL/6 RAG2 KO recipients, we were able to micro-dissect grafted islets, which allowed performing the analysis at various time points (Figure 5C). Even in the absence of rejection in these immunocompromised recipients, a progressive replacement of donor endothelial cells by endothelial cells from recipient origin was observed within grafted islets (Figure 5D). Donor endothelial cells indeed represented less than 1/3 of intra-islet endothelial cells 6 weeks post-grafting. Since recipient endothelial cells do not express donor-specific allogeneic targets, the establishment of this endothelial chimerism therefore explains the lack of microvascular lesions in pancreatic islet grafts exposed to DSA. Endothelial cells of pancreatic islets are not directly responsible for graft function (i.e. the maintenance of recipient's glycemic balance) that depends on the production of insulin by CD45- CD31- endocrine cells. In contrast with endothelial cells, endocrine cells of CBA islet grafts expressed H-2k 6 weeks post-grafting in C57BL/6 RAG2 KO recipients (Figure 5E), demonstrating that they were of donor origin. While the expression of allogeneic targets should make endocrine cells sensitive to DSA-mediated destruction, the lack of

impact of DSA transfers on islet graft function (Figure 2F and 3E) instead demonstrates that endocrine cells are resistant to humoral rejection.

Increasing the expression of allogeneic targets on endocrine cells do not break islet graft resistance to humoral rejection in vivo

A first possible explanation to explain the lack of sensitivity of graft endocrine cells to DSA was that these cells expressed significantly less allogeneic targets than endothelial cells (MFI of H-2k staining of endocrine vs endothelial cells: 2762±2573 vs 59215±43506, p=0.012, t- test). In vitro exposure of dissociated islet cells to 0.5 ng/ml interferon gamma (IFN- γ) boosted the level of expression of MHC molecules (MFI of H-2k staining before vs after IFN-γ: 5271±21932 vs 53535±53515, p<0.0001, t-test; Supplementary Figure 3A). As expected, increasing the expression of allogeneic targets on dissociated islet cells made them more susceptible to DSA-mediated destruction in vitro (% of live cells without vs with IFN- γ: 48.7±4.9 vs 5.7±0.4, p<0.05, one-way ANOVA; Supplementary Figure 3B). Similar findings were made when the experiments were conducted specifically with an insulin-producing β cell line (Supplementary Figure 3C and 3D).

To determine whether increasing the expression of allogeneic targets on endocrine cells would be sufficient to break islet graft resistance to DSA in vivo, we relied on previously published works, which had reported that administration of polyinosinic:polycytidylic acid (poly I:C) to mice increased IFN-γ serum level up to a concentration of 1 ng/ml 31, similar to what we used for in vitro experiments. While intraperitoneal administration of 100 µg poly I:C reliably boosted MHC-I expression on pancreatic endocrine cells in vivo (MFI of H-2k staining without vs with poly I:C: 2633±15306 vs 55077±54026, p<0.0001, t-test; Supplementary Figure 3E), co-injection of poly I:C with DSA did not increase the sensitivity of CBA pancreatic islet grafts to humoral rejection (Figure 5F). These results indicate that the level of expression of allogeneic targets is not a key parameter explaining islet graft resistance to DSA-mediated rejection in vivo.

Vascular sequestration of DSA protects islet grafts from humoral rejection in vivo

The impossibility for circulating DSA to reach the allogeneic targets expressed by endocrine cells could be another explanation for in vivo resistance of islet grafts to humoral rejection. Immunoglobulins are indeed massive polar proteins, which may limit their ability to diffuse outside the vascular bed. In line with this theory was the observation that DSA-mediated lesions in transfer experiments were exclusively concentrated in the vasculature of heart transplants (Figure 4A and 4B). HB13 and an IgG2a κ isotype control mAb were conjugated with small fluorescent tags that allowed in vivo tracking of labeled immunoglobulins. In vivo video-microscopy of mesenteric vasculature of C57BL/6 mice revealed that, following IV injection of DyLight 633-labeled isotype

control mAb, fluorescent mAb were only detected within blood vessels. Only a local application of histamine, an organic nitrogenous mediator known to increase vascular permeability[32], resulted in progressive diffusion of the fluorescent mAb in the surrounding interstitial tissue.

In vivo video-microscopy was then used to monitor the distribution of fluorescence within grafted pancreatic islets. DyLight 488-conjugated HB13 and DyLight 633-conjugated isotype control mAb were coinjected IV to C57BL/6 RAG2 KO recipients. Under baseline conditions, both fluorescent mAb were only detected in the blood vasculature of grafted islets (Figure 6A). Application of histamine solution on grafted islets induced the diffusion of both fluorescent mAbs within the interstitial tissue of islet grafts (Figure 6B). While DyLight 633 signal progressively faded as isotype control mAb was washed away by lymph flow, DyLight 488 fluorescence remained stable, demonstrating that following extravasation from the circulation, DSA were able to bind to allogeneic targets expressed by endocrine islet cells (Figure 6B).

Although these findings supported the theory of a vascular sequestration of DSA, in vivo video-microscopy did not allow extending the tracking of mAb beyond few hours. To rule out the existence of a slow diffusion of DSA within grafted islets, we conducted a second set of experiments, where DSA was labeled with a gamma-radioactive isotope of iodine-125 (HB13-^{125}I). HB13-^{125}I was injected IV to C57BL/6 RAG2 KO mice and the radioactive signal was kinetically assessed over 72 hours using SPECT/CT-imaging (Figure 6C). HB13-^{125}I was only detected in the blood vasculature of the animals (Figure 6C). To further confirm the very limited ability of DSA to diffuse outside the vascular bed, we directly measured the radioactive signal emitted by various tissues of C57BL/6 RAG2 KO mice, 72H post IV injection of HB13-^{125}I. In line with previous data, HB13-^{125}I signal was almost entirely detected in the vascular system (i.e. spleen and blood; Figure 6D). Analyzing more precisely which fraction of the blood was containing the radioactive signal, we observed that HB13-^{125}I was in plasma rather than in cellular fraction, ruling out the possibility that vascular sequestration of DSA was the consequence of immunoglobulin binding to Fc receptors of peripheral blood mononuclear cells (Figure 6D). Finally, HB13-^{125}I was injected IV to C57BL/6 RAG2 KO recipient of either an islet graft or a heart transplant. While CBA heart displayed an increased radioactive signal as compared with control syngeneic heart (Figure 6E), islet to blood ratios were similar for CBA and C57BL/6 islet grafts, thereby demonstrating that allogeneic stromal cells from the graft are inaccessible targets for DSA.

<u>Vascular sequestration of DSA and complement components in transplanted patients</u>

In an attempt to validate the vascular sequestration of DSA in the clinic, we compared the composition of 32-paired plasma and lymph samples from recently transplanted renal recipients. Lymph samples, obtained from surgical drainage, were used as surrogates for interstitial fluid. SDS-

PAGE analyses revealed that plasma contained significantly more proteins than lymph (Figure 7A). This difference was more pronounced for high molecular weight proteins, i.e. proteins whose molecular weight was > 80 Kda (Figure 7A). Accordingly, lymph/plasma protein ratio inversely correlated with molecular weight in a linear regression model ($p<0.0001$; Figure 7A).

In line with these findings, lymph concentration of immunoglobulins G (IgG), whose molecular weight is 150 Kda, was only 1/3 of plasma concentration (plasma vs lymph: 7.85±1.94 vs 2.67±1.06 g/l, $p<0.0001$, paired t-test; Figure 7B). Seven patients from the cohort were sensitized against allogeneic human leukocyte antigen (HLA) molecules non- expressed by their renal allograft, which offered the opportunity to specifically evaluate the diffusion of anti-HLA antibodies in tissues. Of the 72 distinct anti-HLA antibody specificities detected in these 7 plasma samples (52 anti-HLA II and 20 anti-HLA I), 56 (78%) were also present in paired lymph samples but at lower titers (Figure 7C). Comparison of DSA titers for paired plasma and lymph samples, showed a positive correlation in linear regression model ($p<0.0001$; Figure 7D). Of the 16 anti-HLA specificities that were missing in the lymph, 9 (56%) were directed against HLA I, and 7 (44%) against HLA II. All 7 patients had at least 1 (range: 1 to 4) anti-HLA specificity missing in lymph repertoire. One patient had anti-HLA antibodies only in the circulation.

Several recent clinical studies have highlighted the importance of the classical complement cascade in the pathophysiology of DSA-mediated rejection[17–19]. The binding of C1q to DSA complexed with alloantigens initiates the cascade, which results in the assembly of the classical pathway C3 convertase. The latter cleaves C3 into C3a, a potent proinflammatory mediator that causes leukocyte recruitment, and C3b leading to the formation of membrane attack complexes. Interestingly C1q and C3 are both large proteins, whose molecular weights (respectively 400 and 186 Kda) exceed the molecular weight of IgG. Accordingly, these two activators of the classical complement cascade had even lower lymph/plasma concentration ratios than that of IgG (IgG vs C3 vs C1q: 0.35±0.11 vs 0.24±0.11 vs 0.22±0.10, $p<0.0001$, one-way ANOVA; Figure 7E).

These findings indicated that in human large proteins, including antibodies and activators of the complement cascade have limited ability to diffuse outside the vascular bed. Importantly, it shall be noted that vascular sequestration of large proteins is likely underestimated in our analyses because lymph samples were obtained from surgical drainages that were contaminated with trace of blood (as assessed by the presence of red blood cells: 123.103±203.103/mm3).

Discussion

Pancreatic islet grafting represents an attractive therapeutic alternative to pancreas transplantation for type I diabetic patients. Analyzing a cohort of 27 pancreatic islet graft recipients we observed that, although these patients can generate antibodies against donor- specific HLA molecules, DSA

appearance did not correlate with a shorten islet graft survival. This finding is in striking contradiction with the situation of solid organ transplantation[8,9], including pancreas transplantation[15,16], in which DSA-mediated rejection is unanimously recognized as the first cause of failure.

Using murine experimental models of pancreatic islet grafting, we identified several synergizing factors that explain islet graft resistance to humoral rejection. First, although DSA generated in response to allogeneic islet graft had the same characteristics (heavy chain isotypes, ability to activate complement...etc) as DSA generated in response to solid organ transplant, DSA titers were consistently lower in graft recipients. A second contributing factor is that graft endocrine cells expressed constitutively low levels of allogeneic targets (i.e. donor MHC molecules). These two factors are however insufficient to solely explain islet graft resistance to humoral rejection since i) immune sera from islet graft recipients efficiently destroyed allogeneic islet cells in vitro, and ii) increasing MHC expression on islet cells failed to break the resistance of islet grafts to DSA in vivo. Instead we conclude that the resistance of allogeneic islets to humoral rejection is mainly the synergistic consequence of i) the vascular sequestration of DSA and complement activators that restrains the deleterious impact of recipient's humoral response to the allogeneic targets expressed by the vasculature, and ii) the fact that islet graft vascularization developed mostly from the recipient. Graft indeed differs from transplant inasmuch as no vascular anastomosis is performed at the time of the surgical procedure. Re-establishment of islet blood-flow, which is critical for survival and function of grafted islets, occurs through sprouting of capillaries from recipient's origin[26–28]. Although some donor endothelial cells persist and can be integrated within newly formed microvessels[29,30], they only represent a minor fraction of graft endothelial cells. The lack of accessible allogeneic targets on vasculature explains why grafts do not develop DSA- mediated microvascular lesions that characterize humoral rejection. However, in our experimental study passive transfer of DSA was only started 15 days after the grafting procedure to mimic de novo DSA generation. It is therefore possible that starting DSA transfer earlier, i.e. at a time when grafted islets still contain a high proportion of allogeneic endothelial cells[33], might allow DSA to have deleterious impact on the graft. In fact, the variation of graft sensitivity to DSA due to dynamic changes in the origin of vascular bed has been proposed more than 30 years ago in a model of xenogeneic skin graft[34].

What could be the consequences of our findings in the clinic? The inexorable decline of islet graft function over time currently represents a major challenge in the field. Several lines of evidence indicate that, like in solid organ transplantation, recipient's alloimmune response is a major contributor to islet graft loss[7,35]. However, in contrary with transplanted organs, for which cellular rejection represents a marginal cause of graft loss[36], our data instead indicate that cellular rejection is both necessary and sufficient for the destruction of grafted islets. This conclusion is in line with previously published works[37,38] and carries important clinical implications. In solid organ

transplantation, histological examination represents the gold standard for the diagnosis of cellular rejection. In contrast, in clinical islet grafting, liver biopsies have not entered clinical routine for the monitoring of rejection. Indeed, only 5 to 10 g of purified pancreatic islets are injected in the portal vein of the recipient, leading to their dissemination within the 1.5 kg of liver parenchyma. As a consequence, the chance for a percutaneous needle biopsy to sample an islet is estimated below 5/1000. Although several techniques have been developed to monitor anti-HLA reactivity of peripheral blood lymphocytes[39–41], these surrogate approaches all imply the realization of labor-intensive and complex in vitro assays precluding their use in routine. Hence, rather than the treatment, it is the diagnosis of cellular rejection that seems to represents the main hurdle to the improvement of islet graft survival. To differentiate into DSA-producing plasma cells, B cells need to receive the help of follicular helper T cells. DSA appearance in the circulation, which can be easily monitored[42], therefore reflects the activation status of recipient's allogeneic T cells. It is therefore conceivable that DSA, although devoid of direct pathogenic effect on grafted islets, could be valuable biomarkers for the diagnosis of T cell-mediated rejection (like autoantibodies in type I diabetes[43]). In line with this idea, two recent clinical studies have established that DSA monitoring reliably identified islet graft recipients with the higher risk for rapid graft failure[12,13]. DSA monitoring could therefore be used to guide initiation of rejection treatment in islet recipients. The validity of this concept has been nicely illustrated by the recent report that an islet graft recipient, who experienced a decline in graft function concomitant with the appearance of circulating DSA, experienced a favorable outcome after intensification of immunosuppression[44]. Interestingly, this patient received anti-CD20 monoclonal antibody, which efficiently depleted B cells but had little impact on DSA titer and repertoire[45]. The beneficial effect of anti-CD20 treatment was therefore likely due to its impact on antigen-independent B cell roles[46]. Another therapeutic option would be to directly target alloreactive T cells using anti-CD3 mAb. This therapy, which has already proved successful to restore immune tolerance to self-antigens in Type 1 diabetes[47,48], could also be effective in the setting of graft rejection. Supporting this idea a study has demonstrated that a short low-dose course with anti-CD3 mAb started at the time of effector T cell priming to alloantigens, induced permanent acceptance of fully mismatched pancreatic islet grafts in a murine experimental model[49]. The beneficial effect of anti-CD3 mAb could be due to the fact that, while anti-CD3 mAb promoted the apoptosis of activated alloreactive T cells, regulatory T cells were spared from anti-CD3-induced depletion[49,50].

Finally, our study could also have more general implications in immunology. Our data indeed indicates that the reduced concentrations in several key components of the humoral response make interstitial tissue resistant to antibody-mediated lesions. This theory fits with seminal clinical observations made in the field of solid organ transplantation, in which humoral rejection was first named "vascular" rejection because most histologic damages were concentrated in the vasculature

of the transplants[51]. Physiologically, vascular sequestration of antibodies could contribute to the maintenance of immune tolerance in the presence of autoreactive B cell clones, which have repeatedly been observed in the humoral repertoire of healthy subjects[52]. It is also tempting to speculate that the difficulty for the immune system to transfer sufficient amount of antibody from the circulation to the site of tissue damage has been a driving evolutionary force for lymphoid neogenesis: the process by which ectopic “tertiary lymphoid organs” appear within chronically inflamed tissues[53], including rejected grafts[54], and serve as a site of local antibody generation[54–57]. Lastly, vascular sequestration of immunoglobulins and complement activators likely represents an important obstacle to the efficiency of biotherapies such as vaccines and monoclonal antibodies. Increasing vascular permeability of targeted tissue might represent an interesting approach to increase the therapeutic efficiency of these approaches. Supporting this concept, a recent experimental study has demonstrated that mice which have developed antibody against herpes simplex virus type 2 after vaccination, failed to survive to a new challenge with the virus in the absence of CD4+ T cells. The authors demonstrated that CD4+ T cells were indeed necessary to enable antibody delivery to the sites of infection by secreting IFN-γ and enhancing microvascular permeability 58.

Materials and Methods

Clinical studies

To determine the impact of DSA on islet graft survival, we retrospectively reviewed the medical files of all patients that received an islet graft between 2000 and 2013 within the GRAGIL (Groupe Rhin-Rhône-Alpes-Genève pour la Transplantation d'Ilots de Langerhans) Swiss-French multicenter network. Inclusion criteria were: i) successful islet grafting defined as insulin-independence post-procedure for ≥2 years, ii) availability of biological material for analysis of DSA response (HLA typing of donor and recipient, plus exhaustive annual sera samples). Twenty-seven patients were identified (characteristics of the cohort are presented in Supplementary Table 1), among which 4 developed de novo DSA, all during the first year post-grafting. Islet graft function was monitored longitudinally using the ß-score, a validated composite score that integrates insulin requirements, C-peptide secretion and glycemic control[14].

To compare the concentrations of different proteins in plasma and lymph we enrolled 32 consecutive patients, who underwent kidney transplantation in Lyon University Hospital. Seven of these patients had preformed anti-HLA antibodies that were not directed to the donor. Lymph was obtained when surgical drain was withdrawn (post-operative day 3-7). On the same day, plasma was collected from routine blood examination.

All patients gave informed consent for scientific analysis of the samples.

Comparison of lymph and plasma

For SDS page analysis, 1 µl of plasma or lymph sample was mixed with 19 µl of loading buffer LDS (Invitrogen, Saint Aubin, France) and run on a Bolt® 4–12% Bis-Tris gel (ThermoScientific, Saint Aubin, France) in MOPS buffer (ThermoScientific). Proteins were stained with Bio-safe Coomassie stain (Bio-Rad, Marnes-la-Coquette, France) according to the manufacturer's instructions.
The concentration of IgG and C3 were measured by immunonephelometry assay with BN ProSpec® (Siemens, Marburg, Germany) and C1q by Radial Immunodiffusion assays, kit for human complement functional assays (The Binding Site, Birmingham, UK).

Detection and characterization of anti-HLA antibodies

Centralized analyses were performed in a blinded fashion by a single trained immunobiologist (V.D.) at the French National Blood Service (EFS, Lyon, France).
Sera and lymph samples were analyzed using Single Antigen Flow Beads (Lifecodes Single Antigen [LSA] class I and class II; Immucor, Norcross, GA). The mean fluorescence intensity (MFI) was measured on a LABscan 100 (One Lambda, Canoga Park, CA).

Animals

Wild type C57BL/6 (H-2b, CD45.2), C57BL/6 Ly5.1 (H-2b, CD45.1) and CBA (H-2k) mice aged 8-15 weeks were purchased from Charles River Laboratories (Saint Germain sur l'Arbresle, France). RAG2 Knock Out mice on C57BL/6 background were obtained from CDTA (Cryopreservation Distribution Typage et Archivage animal, Orléans, France). All mice were maintained under EOPS (Exemption of Specific Pathogenic Organisms) condition in our animal facility: Plateau de Biologie Expérimentale de la Souris (http://www.sfr- biosciences.fr/plateformes/animal-sciences/AniRA-PBES; Lyon, France).
All experimental protocols were approved by the local ethical committee (CECCAPP).

Experimental murine models

Heterotopic heart transplantations were performed as in the literature[59].
Diabetes was induced by a single intraperitoneal injection of streptozotocin (170mg/kg). Recipient mice were considered diabetic if fasting glycaemia was measured >350mg/dL. Blood glucose level was monitored twice a week with FreeStyle Optium glucometer (Abbott, Rungis, France).
For pancreatic islets isolation, collagenase type XI 2mg (Sigma-Aldrich, Saint Quentin Fallavier, France) dissolved in 2ml Hank's solution was perfused into the pancreas of donor animal by cannulating the common bile duct. The pancreas was then removed and incubated at 37oC for 12 minutes. Islets were isolated by gradient density with Histopaque 1077.

After isolation, islet equivalents (IEQ) were either injected into the portal vein of the recipient (550 IEQ/recipient) or placed in the subcapsular space of left kidney (250 IEQ/recipient).

Adoptive transfer of T lymphocytes

For isolation of T lymphocytes, splenocytes from allosensitized C57BL/6 Ly5.1 mice were stained with phycoerythrin (PE)-conjugated antibodies against CD19 (1D3), B220 (RA3- 6B4), CD11b (M1/70), CD11c (HL3), NK-1.1 (PK136), Ter119/Erythroid cells (TER-119), CD117 (2B8) (1/200, all from BD Biosciences, Le Pont de Claix, France) and peridinin- chlorophyll protein (PerCP)-conjugated antibody against Thy1.2 (53-2.1) (BioLegend, London, United Kingdom).

After staining, cells were negatively separated by LD magnetic columns with anti-PE Microbeads labeling (Miltenyi Biotec, Paris, France). The separated cell suspensions underwent cell sorting by using a FACS Aria cell sorter (BD Biosciences). Five million purified T lymphocytes were transferred intravenously (IV) to C57BL/6 RAG2 KO mice.

Passive transfer of DSA

Transferred DSA were either polyclonal (immune sera) or monoclonal (clone HB13 directed against H-2Kk and Dk; BioXcell, West Lebanon, USA).

A single batch of immune serum was used for a given experiment. Each batch was prepared by pooling the serum of 6 C57BL/6 mice sensitized against H-2k. DSA titer was estimated for every batch using a custom flow cross match assay and a standard curve derived from known concentrations of HB13 (Supplementary Figure 1).

DSA were passively transferred to recipients by retro-orbital injection until the end of follow- up. The amount of DSA transferred and the frequency of infusions was set to ensure that the titer of circulating DSA remained stable and similar to the median value observed in wild type recipients grafted with allogeneic islets.

Flow cytometry

Fresh islets were dissociated by trypsin (0.05%)-EDTA (0.02%) solution (Sigma-Aldrich). Islet grafts collected from subcapsular space of kidney were dispersed by mixture of dispase (0.8mg/ml)/collagenase P (0.2mg/ml) and 0.1mg/ml DNAase (all from Roche, Meylan, France). Heart transplants harvested from recipient were digested by 500 unit/ml collagenase type II (Worthington, Lakewood, NJ) and 1 mg/ml collagenase/dispase (Roche).

Single cell suspensions were incubated with a blocking anti-mouse Fc receptor antibody (clone 2.4G2) for 20 minutes at 4°C and then with relevant fluorescent monoclonal antibodies: CD31 (clone MEC 13.3, 1/200, BD biosciences), CD19 (clone 1D3, 1/200, BD biosciences), H-2Dk (clone 36-7-5, 1/200, BD biosciences), kappa light chain (clone 187.1, 1/50, BD biosciences), IgG3 (clone R40-82, 1/200, BD biosciences), IgG/IgM (polyclonal, 1/200, BD biosciences), CD45 (clone 30-F11,

1/400, BioLegend), IgG1 (clone LO-MG1-2, 1/200, Zymed, South San Francisco, CA) and IgG2b (polyclonal, 1/200, SouthernBiotech, Brimingham, AL)) for 10 minutes at 4°C. Before acquisition, 0.1µg/ml 4',6-diamidino-2- phenylindole (DAPI) was added to the cell suspension to stain dead cells. Samples acquisitions were made on a LSR II flow cytometer (BD Biosciences) and analyses were performed with FlowJo software version 10.0.8r1 (Tree Star Inc, Ashland, OR).

In vitro cytotoxicity assay

For in vitro cytotoxicity assay, CBA splenocytes, CBA islet cell suspensions or the H-2k restricted ßTC-tet cell line 60, were incubated with immune serum or HB13 mAb for 1 hour at 4°C. When indicated, target cells were pre-cultured 24 hours in 0.5ng/ml interferon-γ (INF-γ, Peprotech, Neuilly sur Seine, France) to enhance MHC class I expression.

After washing of excess antibody, rabbit complement (Cedarlane, Burlington, USA) was added at 1/16 dilution for one hour at 37°C.

Dead cells were stained with DAPI and the percentage of viable cells was evaluated by flow cytometry. Survival rate is normalized on the results observed when cells were incubated with complement alone.

Pathological analyses

For analysis of H-2 expression by pancreatic islet cells, fresh islets isolated from C57BL/6 (H-2b) or CBA (H-2k) mice were embedded in Tissue-Tek OCT (Sakura Finetek, Villeneuve d'Ascq, France) and frozen in liquid nitrogen. Eight µm-thick cryosections were incubated for 20 minutes at 20°C with goat serum and then with 100µg/ml anti-H-2k mAb (clone HB13) overnight at 4°C. Sections were washed and then incubated with 20µg/mL AF488-conjugated goat anti-mouse IgG2a (Invitrogen) for 1h at 4°C. DAPI 1µg/ml was added to the sections to stain cell nuclei. Images were taken at 20X magnification by Zeiss Axioimager Z1 (Zeiss, Marly le Roi, France) and acquired by software Metamorph version 7.8.13.0 (Molecular Devices LLC, Sunnyvale, CA). Images analysis was performed by ImageJ (NIH). Pathological analyses of grafted islets were made as follow. After euthanasia of mouse, followed by evacuation of blood by 40ml PBS infusion via abdominal aorta with incision of inferior vena cava, vessel painting was performed by infusing 300µg wheat-germ agglutinin conjugated with Alexa Fluo 488 (16µg/ml, Invitrogen) into abdominal aorta and then 4% paraformaldehyde (PFA) for fixation. Organs containing grafted islets (liver for model #1 or kidney for model #2) were harvested and 400µm-thick slices of fresh tissue were prepared with a vibratome. Tissue slices were postfixed in 4% PFA and permeated with 2% Triton-X 100 for 2 hours at 20°C. Afterwards, slices were incubated in 10% goat serum for blocking, followed by primary antibody incubation: polyclonal guinea pig anti-insulin antibody (1/50, Dako, Les Ulis, France) overnight at 20°C. Goat anti-guinea pig IgG secondary antibody conjugated with AF647 (1/200, Invitrogen) was then used to reveal insulin-positive cells for 6 hours at 20°C. Nuclei were stained with 1µg/ml DAPI

for 1 hour at 20°C before applying specimens to slide and then immersed in the optical clearing solution RapidClear 1.52 (SunJin Lab, HsinChu, Taiwan). Images were taken at 5X magnification by Zeiss Axioimager Z1 and 20X magnification by LSM800 confocal microscope (Zeiss) with acquisition by software ZEN version 2.1 (Zeiss). Image analysis was performed by ImageJ.

For histological assessment of DSA-mediated lesions, heart transplants or left kidney (containing grafted islets) were harvested 30 days after the beginning of DSA transfer, fixed in 4% buffered formalin for 24h and embedded in paraffin for hematoxylin and eosin stain and immunohistochemistry. Immunohistochemistry sections was performed as in the literature 61. Briefly, after antigen retrieval by heating in citrate buffer, the following primary antibodies were used: anti-mouse CD31 (1/50; Dianova, Hamburg, Germany), anti-C4d (1/50; DB Biotech, Kosice, Slovakia), and anti-mouse CD68 (1/200; AbD Serotec, Kidlington, UK) to stain respectively endothelial cells, C4d complement fraction, and macrophages. Sections were then revealed by Vectastain ABC HRP Kit (Vector, Peterborough, UK). The intensity of the staining was graded semi-quantitatively (0 to 5) by a trained pathologist (P.B.). Transmission electron microscopy of left kidney (containing grafted islets) was performed as in the literature62.

Intravital microscopy

Mice were anesthetized by ketamine/xylene injection. Abdominal midline incision was made to pull the small intestine out or left flank incision was made to push left kidney out. Mesenteric vessels or left kidney (containing grafted islets) were exposed under upright fluorescence macroscope (MacroFluo, Leica Microsystems, Nanterre, France) equipped with a thermostatic plate and a 5X objective, which was connected to a sCMOS camera (Orca- Flash-4.0, Hamamatsu Photonics, Hamamatsu, Japan), and images were acquired by Metamorph and processed by ImageJ. HB13 mAb labeled with DyLight 488 Fast Conjugation Kit (Abcam, Paris, France) and isotype control (mouse IgG2a kappa, BioLegend) labeled with DyLight 633 Fast Conjugation Kit (Abcam) were infused simultaneously by retro-orbital injection. When indicated 2µl of histamine (100nM) was applied on the optical field.

Nuclear imaging

HB13-^{125}I was prepared using a direct iodination procedure with Iodogen® reagent (PerkimElmer, Waltham, USA) as oxidant. Briefly, 37 MBq of ^{125}I were added to 20 µg of HB13 in phosphate buffer (50mM) and the mixture was then transferred into a precoated IODOGEN®. The reaction was allowed to proceed at room temperature for 15 minutes. Radioiodinated HB13 was then purified through a Micro-spin G-25 size-exclusion column. Dynamic single photon emission computed tomography (SPECT)/computed tomography (CT) acquisitions were performed immediately, 24, 48 and 72 hours following an intravenous injection of 22.0 ± 3.6 MBq of HB13-^{125}I.

Following SPECT/CT imaging, transplanted heart and recipient kidney were harvested along with major organs. Tissue samples were weighed and their radioactivity was determined by gamma-well counting. The results were expressed as a percentage of injected dose per gram of tissue (%ID/g). Recipients' kidneys were then frozen, and 40µm-thick cryosections were obtained for autoradiographic imaging. Regions of interest were drawn in order to determine graft uptake. Transplanted heart and islet graft uptake were corrected to native heart or blood activity respectively.

Statistical analyses

For each data set, mean±standard deviation (SD) was calculated and was presented in the Results section of the main text. For graphical presentation of the same data sets, box plots were generated, using Prism software (Version 6.01; GraphPad Software Inc., La Jolla, CA), which present the entire data set distribution. The center line in the boxes shows the medians; box limits indicate the 25th and 75th percentiles, whiskers indicate the minimal and maximal values.

Sample size was determined on the basis of local ethical committees and previous experiments in the lab. Thus the sample size was not calculated as to ensure adequate statistical power to detect hypothesized effect sizes.

Differences between groups were evaluated (as indicated in relevant figure legends) by: Mann-Whitney test, paired t-test, one-way ANOVA followed by a Tukey's post hoc test, or by two-way ANOVA followed by a Sidak's post hoc test, according to the size of the groups and the distribution of the variable.

The differences between the groups were considered statistically significant for $p < 0.05$ and were reported with asterisk symbols (*: $p<0.05$; **: $p<0.01$; ***: $p<0.001$; ****: $p<0.0001$).

Authors' Contributions:

CCC and OT conceived and designed the experiments. CCC, EP, AB, FA, MR, PB, MA, SB, CSD, MM, MNKS, AK, VM, and SD performed the experiments. CCC, EP, AB, FA, MR, PB, VD, AN, and OT analyzed the data. LK, JPDvH, AL, TB, EM, MKT, CG contributed to reagents. CCC and OT wrote the paper; AL, TB, MKT, AK, EM, and TD contributed to the discussion.

Figure legends

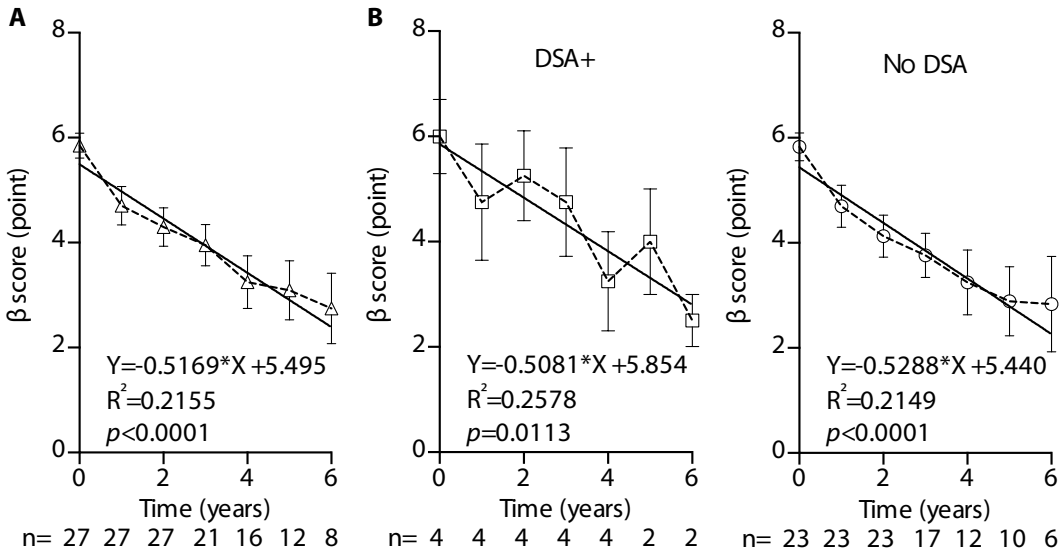

Figure 1: DSA did not impact pancreatic islet graft function

Pancreatic islet graft function of 27 patients was assessed every year using the ß score (mean±SD). Linear regression was used to estimate the relation between time and pancreatic islet graft function. **A**. The slope of regression line indicated the rate of islet graft attrition in the cohort. **B**. Four patients developed de novo donor-specific anti-HLA antibodies (DSA), all in the first year post-grafting. The rate of pancreatic islet graft attrition was estimated for the 4 patients with DSA (left: DSA+) and the remaining 23 patients without DSA (right: No DSA).

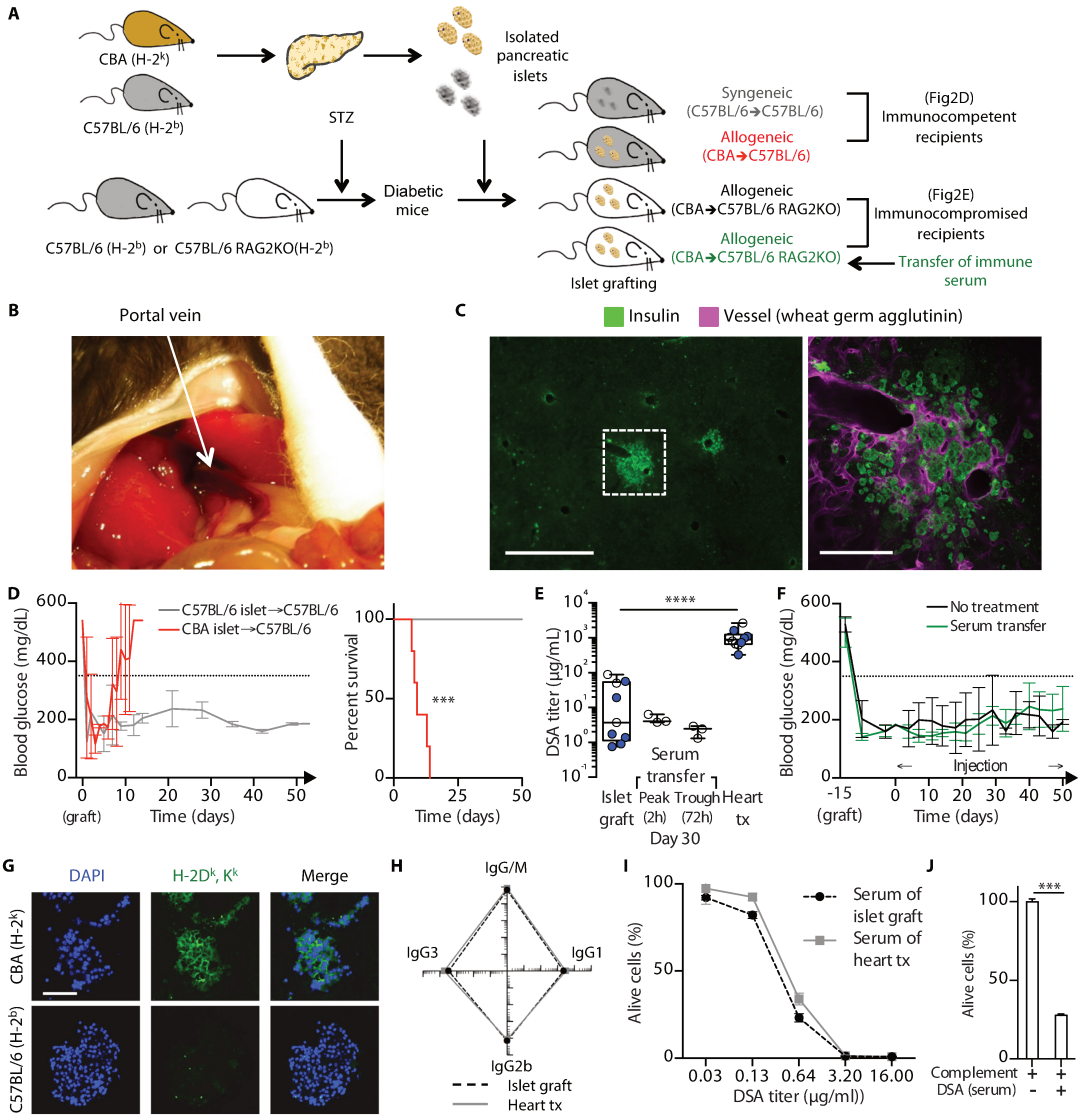

Figure 2: Experimental model recapitulates clinical findings

A. Pancreatic Islets from CBA (H-2k) or C57BL/6 (H-2b) mice were grafted to C57BL/6 (H- 2b) or C57BL/6 RAG2 KO (H-2b) recipients, which created 3 distinct donor/recipient combinations: syngeneic (C57BL/6=>C57BL/6, grey), allogeneic (CBA=>C57BL/6, red) and allogeneic in immunocompromised recipients (CBA=>C57BL/6 RAG2KO, black). In the 4th experimental group (green), immune serum was passively transferred to C57BL/6 RAG2 KO recipients grafted with CBA islets. **B**. View of the operative site exposing the portal vein of recipient (white arrow), in which purified islets were injected as to mimic the clinical procedure. **C**. Left: representative finding of immunofluorescence analyses performed 50 days after intraportal injection of syngeneic islets (scale bar=500µm). Right: magnification of the white dashed square shown on left thumbnail (scale bar=100µm). **D**. Left: blood glucose level was measured twice weekly in wild type C57BL/6 recipients to monitor islet graft function. Evolution of glycemia (mean±SD) is shown for C57BL/6 (syngeneic, grey) and CBA (allogeneic, red) grafts. Islet graft loss was defined by fasting glycaemia > 350 mg/dl (dashed line). Right: survival curves for C57BL/6 (syngeneic, grey) and CBA (allogeneic, red)

grafts are compared. ***: p=0.0008; Log Rank test. **E**. Flow cytometry cross match technique (described in Supplementary Figure 1) was used to quantify circulating DSA generated by wild type C57BL/6 recipients in response to a CBA heart transplant or an intraportal CBA islet graft. Individual values measured at the peak of humoral alloimmune response of 2 independent experiments (white and blue symbols) are shown. ****: p<0.0001; Mann Whitney test. The same technique was applied to monitor the peak and trough level of circulating DSA 30 days after starting passive IV transfer of immune serum. **F**. Blood glucose level was measured twice weekly in C57BL/6 RAG2 KO recipients of an intraportal CBA islet graft. Evolution of glycemia (mean±SD) is shown for recipients transferred (green) or not (black) with immune serum. **G**. H-2k expression was assessed on CBA (H-2k, upper row) and C57BL/6 (H-2b, lower row) freshly isolated pancreatic islets (scale bar=100µm). **H**. Heavy chain isotype repertoire of DSA generated by wild type C57BL/6 recipients in response to a CBA heart transplant (grey) or an intraportal CBA islet graft (dashed black) were compared. DSA of different isotypes were quantified by flow cytometry, values are expressed in MFI (mean±SD). **I. & J**. The cytotoxic potential of immune serum was evaluated in vitro using complement-dependent cytotoxic assay. I. Cytotoxic potential of immune serum of wild type C57BL/6 recipients sensitized with either a CBA heart transplant (grey) or an intraportal CBA islet graft (black dashed) were compared. J. The cytotoxic potential of the immune sera used for in vivo transfer experiments was assessed on CBA pancreatic islet cell suspension in vitro. ***: p<0.001, one-way ANOVA.

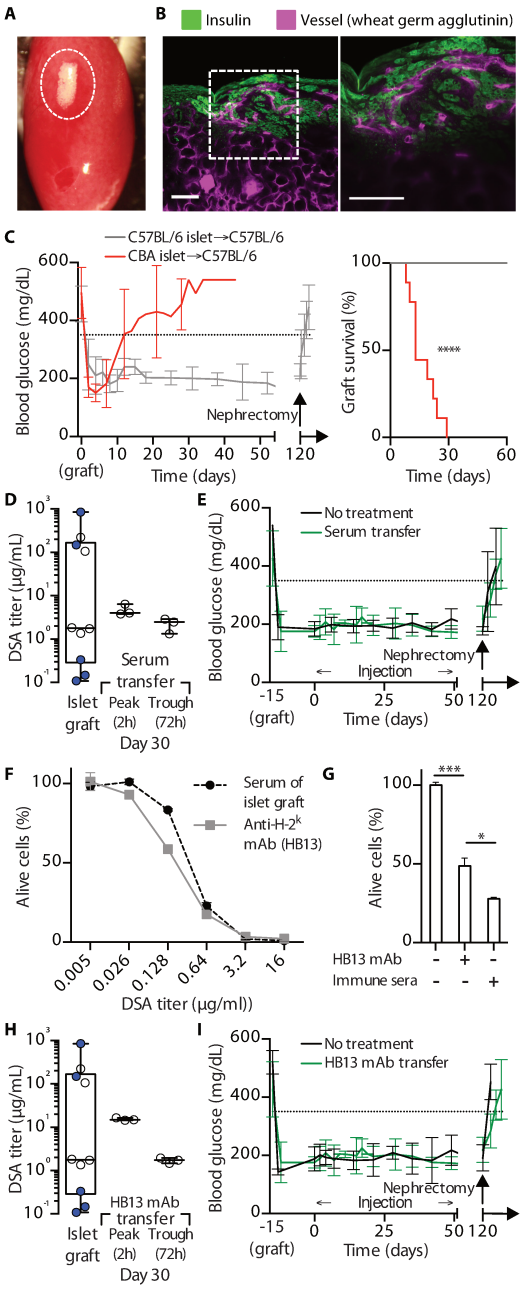

Figure 3: Optimization of experimental model

A. Post-operative view showing pancreatic islets (dashed white circle) grafted under the left kidney capsule of recipient. **B**. Left: representative finding of immunofluorescence analyses performed 50 days after subcapsular grafting of syngeneic islets (scale bar=100µm). Right: magnification of the white dashed square shown on left thumbnail (scale bar=100µm). **C**. Left: blood glucose level was measured twice weekly in wild type C57BL/6 recipients to monitor islet graft function. Evolution of glycemia (mean±SD) is shown for C57BL/6 (syngeneic, grey) and CBA (allogeneic, red) subcapsular islet grafts. Islet graft loss was defined by fasting glycaemia > 350 mg/dl (dashed line). Nephrectomy was performed at 120 days to confirm grafted islet function. Right: survival curves for C57BL/6 (syngeneic, grey) and CBA (allogeneic, red) subcapsular

islet grafts were compared. ****: p<0.0001 Log Rank test. **D**. Flow cytometry cross match technique was used to quantify circulating DSA generated by wild type C57BL/6 recipients in response to a CBA subcapsular islet graft. Individual values measured at the peak of humoral alloimmune response of 2 independent experiments (white and blue symbols) are shown. The same technique was applied to monitor the peak and trough level of circulating DSA 30 days after starting passive IV transfer of immune serum. **E**. Blood glucose level was measured twice weekly in C57BL/6 RAG2 KO mice grafted under the kidney capsule with CBA pancreatic islets. Evolution of glycaemia (mean±SD) is shown for recipients transferred (green) or not (black) with DSA. **F. & G**. The cytotoxic potential of immune serum was evaluated in vitro using complement- dependent cytotoxic assay. F. Cytotoxic potential of immune serum of wild type C57BL/6 recipients sensitized with a CBA islet graft (black dashed) and anti-H-2k mAb (clone HB13)

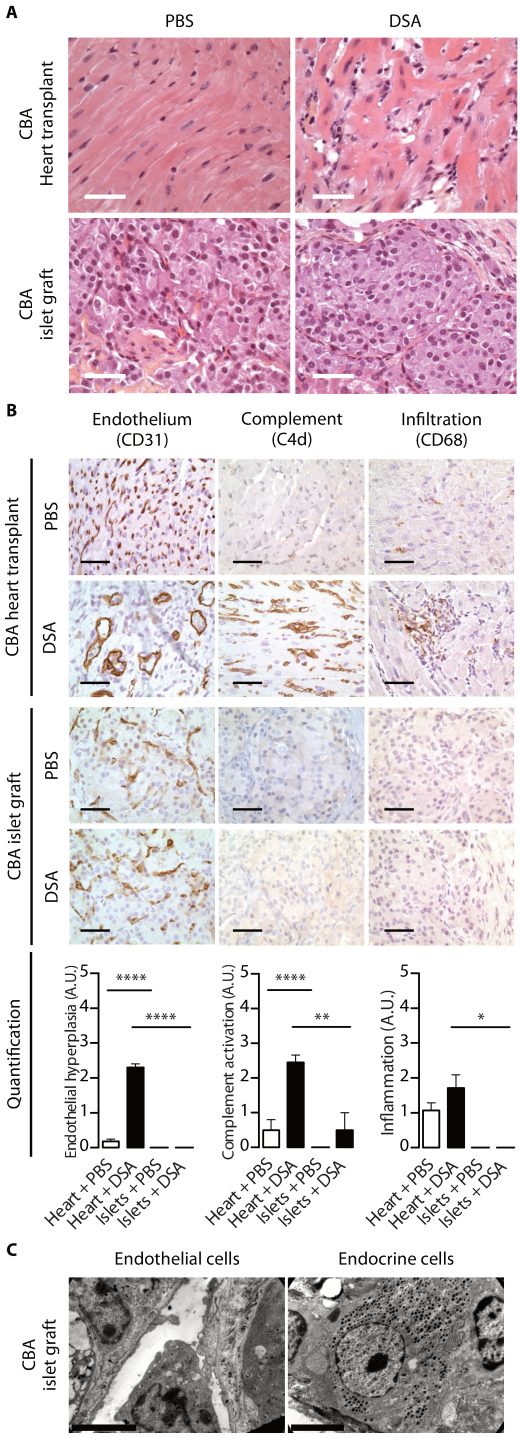

Figure 4: Histological evaluation of DSA-mediated lesions

C57BL/6 RAG2 KO mice were used as recipients of either a CBA subcapsular islet graft or a CBA heart transplant. HB13 or PBS was infused IV twice weekly to recipient mice for 30 days and grafts/transplants were harvested for histological analysis. **A**. Representative findings of hematoxylin and eosin stain are shown for the 4 experimental groups (scale bar=50µm). **B**. Immunohistochemistry was performed to evaluate the morphology of microvasculature (CD31), classical complement pathway activation (C4d), and

infiltration of macrophages (CD68). Representative findings are shown for the 4 experimental groups (scale bar=50µm). A trained pathologist graded intensity of each elementary lesion on a semi-quantitative scale (1-5). Mean±SD of the 4 experimental groups were compared. *: p<0.05, **: p<0.01, ***: p<0.001, and **** p<0.0001; two-way ANOVA. **C**. Transmission electron microscopy was used to assess the ultrastructural integrity of the endothelial (left) and the endocrine (right) cells of CBA islet grafts, 30 days after the beginning of HB13 transfer (scale bar=3µm).

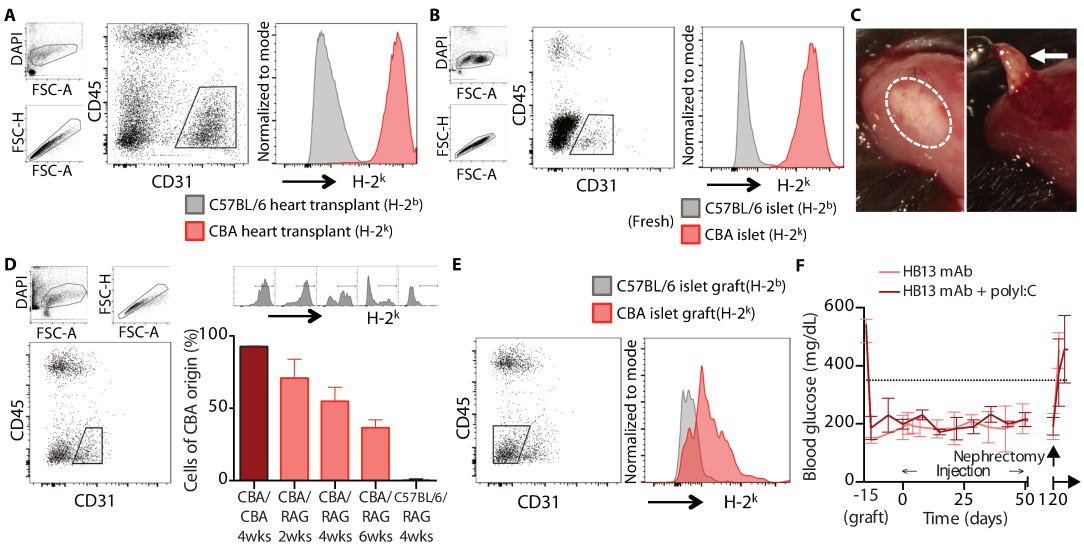

Figure 5: Endothelial chimerism in grafted islets

Each panel shows representative findings of 2 independent experiments. **A**. C57BL/6 (grey) or CBA (red) heart was transplanted to C57BL/6 RAG2 KO recipients. Four weeks after transplantation, single cell suspension was prepared by enzymatic digestion of the transplant and H-2k expression of CD45- CD31+ endothelial cells was assessed by flow cytometry. **B**. The same approach was used to analyze H-2k expression of endothelial cells of freshly isolated C57BL/6 (grey) or CBA (red) islets. **C**. Subcapsular implantation made possible the retrieval of grafted islets: operative views of islet graft before (left, white dashed circle), and during (right, white arrow) microdissection. **D. & E**. C57BL/6 islets were transplanted to C57BL/6 RAG2 KO recipient (grey) and CBA islets were grafted either to CBA (dark red) or C57BL/6 RAG2 KO recipient (light red). D. Grafted islets were microdissected at indicated time points and the proportion of endothelial cells from CBA origin (i.e. H-2k positive) was assessed by flow cytometry. E. The proportion of endocrine cells (CD45- CD31-) from CBA origin (H-2k positive) was assessed in C57BL/6 (grey) and CBA (red) islets 6 weeks after grafting in C57BL/6 RAG2 KO recipient. **F**. Blood glucose level was measured twice weekly in C57BL/6 RAG2 KO mice grafted under the kidney capsule with CBA pancreatic islets. Evolution of glycemia (mean±SD) is shown for recipients transferred with DSA alone (HB13 mAb, pink) or in association with polyI:C (dark red). Nephrectomy was performed at 120 days to confirm grafted islet function.

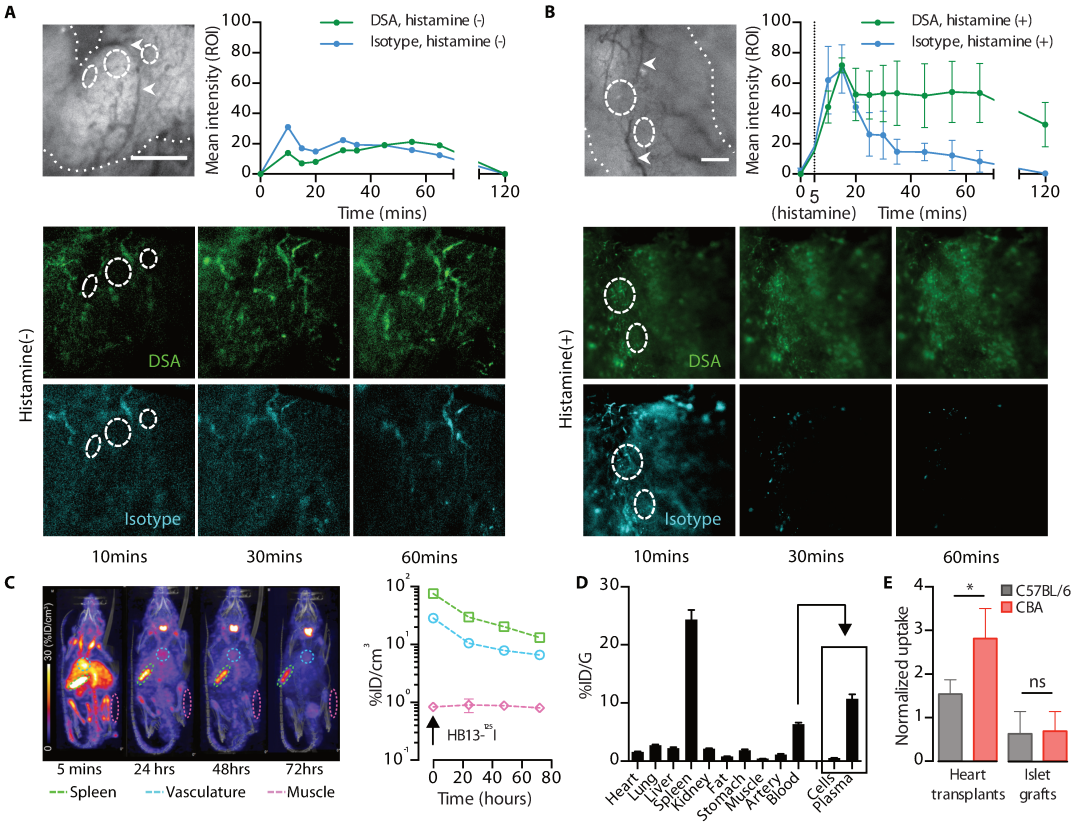

Figure 6: Vascular sequestration of DSA

A. C57BL/6 RAG2 KO mice were used as recipients of a CBA subcapsular islet graft. Fluorescently labeled DSA (HB13, green) and IgG2A isotype control (cyan) were infused simultaneously IV to recipient mice. Time-lapse intravital microscopy was used to monitor the intensity of DSA and isotype control fluorescence in several regions of interest (ROI). Upper left: representative bright field image showing the outer limit of islet graft (white dotted line) and the localization of the ROI (white dashed circles), which were positioned outside islet graft vasculature (white arrow heads). Scale bar=150µm. Upper right: mean intensity of fluorescence in ROI was recorded from the time of mAb injection and was used as a surrogate for mAb diffusion in graft interstitium (Mean±SD). Lower rows: representative images of intravital microscopy showing vascular sequestration of DSA (upper row) and isotype control (lower row). **B**. The same experiment was conducted as in A. except that histamine was locally applied on islet graft 5 minutes after the beginning of the recording. **C**. The biodistribution of IV transferred iodinated HB13 (HB13-^{125}I) was kinetically assessed in C57BL/6 RAG2 KO mice over 72 hours using SPECT/CT-imaging. Left panel: representative images of SPECT analyses taken 5 minutes, 24, 48 and 72 hours post-injection. Right panel: Evolution of the intensity of radioactive signals remaining in the circulation (spleen, green; blood, blue) or extravagating in control tissue (muscle, purple) over time. **D**. Quantification of radioactive signal in various tissues of C57BL/6 RAG2KO mice, measured 72 hours post IV injection of HB13-^{125}I. **E**. Quantification of radioactive signal (mean±SD) measured in the graft 72 hours post IV injection of HB13-^{125}I. C57BL/6 RAG2KO recipients were transplanted with syngeneic (C57BL/6, H-2b; grey) or allogeneic (CBA, H-2k; red)

hearts or grafted with syngeneic (C57BL/6, H-2b; grey) or allogeneic (CBA, H-2k; red) islets. *: p<0.05, one-way ANOVA.

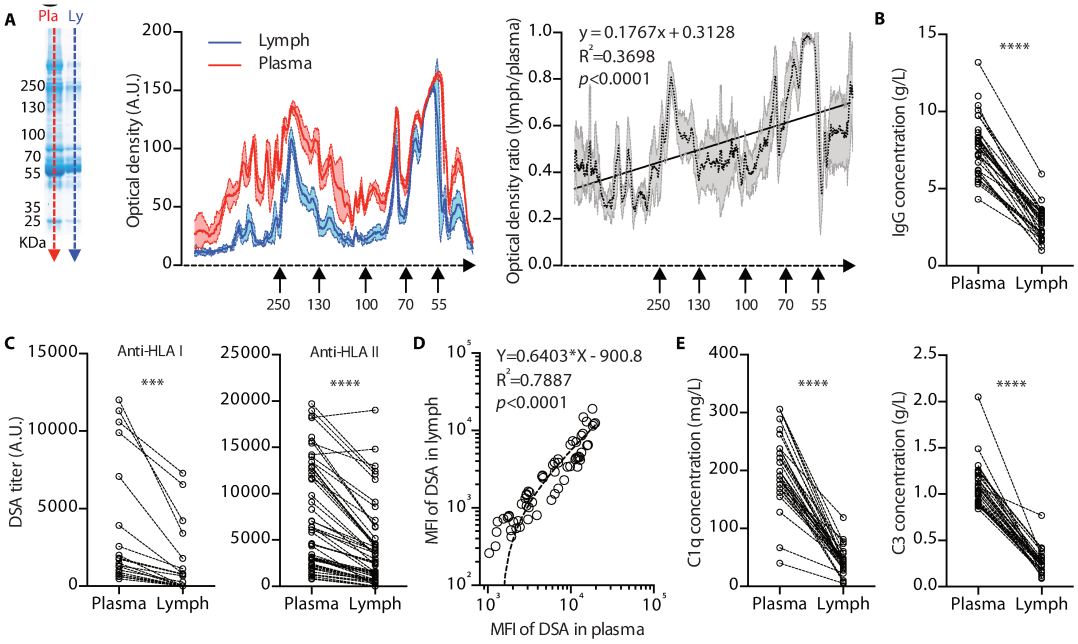

Figure 7: Vascular sequestration of DSA and complement components in transplanted patients

A. Comparison of protein content of paired plasma (Pla, red) and lymph (Ly, blue) samples. Left: Protein were separated by SDS-PAGE and stained with Coomassie blue. Representative example of SDS-PAGE gel is shown. Middle: Densitometric analysis of proteins was used to quantify the amount of proteins resolved by SDS-PAGE gels (Mean±SD). Right: Linear regression was used to determine the relation between the molecular weight of a protein and its ability to diffuse outside the vasculature. **B.** Comparison of IgG content of paired plasma and lymph samples. ****: p<0.0001; paired t- test**. C.** Comparison of DSA content of paired plasma and lymph samples. MFI measured in solid phase assay (left: anti-HLA I, right: anti-HLA II) was used as a surrogate for DSA titer for each anti-HLA specificity. ***: p=0.0003, ****: p<0.0001; paired t-test. **D.** Linear regression was used to determine the relation between plasma and lymph titer for each anti-HLA specificity. **E**. Comparison of the content in complement fractions C1q (left) and C3 (right) of paired plasma and lymph samples. ****: p<0.0001; paired t-test.

References

1. Miller, K. M. et al. Current state of type 1 diabetes treatment in the U.S.: updated data from the T1D Exchange clinic registry. Diabetes Care 38, 971–978 (2015).

2. Kemp, C. B., Knight, M. J., Scharp, D. W., Lacy, P. E. & Ballinger, W. F. Transplantation of isolated pancreatic islets into the portal vein of diabetic rats. Nature 244, 447 (1973).

3. Scharp, D. W. et al. Insulin independence after islet transplantation into type I diabetic patient. Diabetes 39, 515–518 (1990).

4. Fioretto, P., Steffes, M. W., Sutherland, D. E., Goetz, F. C. & Mauer, M. Reversal of lesions of diabetic nephropathy after pancreas transplantation. N. Engl. J. Med. 339, 69– 75 (1998).

5. Kennedy, W. R., Navarro, X., Goetz, F. C., Sutherland, D. E. & Najarian, J. S. Effects of pancreatic transplantation on diabetic neuropathy. N. Engl. J. Med. 322, 1031–1037 (1990).

6. Barton, F. B. et al. Improvement in outcomes of clinical islet transplantation: 1999-2010. Diabetes Care 35, 1436–1445 (2012).

7. Sutherland, D. E. R. et al. Islet autotransplant outcomes after total pancreatectomy: a contrast to islet allograft outcomes. Transplantation 86, 1799–1802 (2008).

8. Pouliquen, E. et al. Recent advances in renal transplantation: antibody-mediated rejection takes center stage. F1000prime Rep. 7, 51 (2015).

9. Sellarés, J. et al. Understanding the causes of kidney transplant failure: the dominant role of antibody-mediated rejection and nonadherence. Am. J. Transplant. Off. J. Am. Soc. Transplant. Am. Soc. Transpl. Surg. 12, 388–399 (2012).`

10. Pouliquen, E. et al. Anti-Donor HLA Antibody Response After Pancreatic Islet Grafting: Characteristics, Risk Factors, and Impact on Graft Function. Am. J. Transplant. Off. J. Am. Soc. Transplant. Am. Soc. Transpl. Surg. (2016). doi:10.1111/ajt.13936

11. Chaigne, B. et al. Immunogenicity of anti-HLA antibodies in pancreas and islet transplantation. Cell Transplant. (2016). doi:10.3727/096368916X691673

12. Brooks, A. M. S. et al. De Novo Donor-Specific HLA Antibodies Are Associated With Rapid Loss of Graft Function Following Islet Transplantation in Type 1 Diabetes. Am. J. Transplant. Off. J. Am. Soc. Transplant. Am. Soc. Transpl. Surg. 15, 3239–3246 (2015).

13. Piemonti, L. et al. Alloantibody and autoantibody monitoring predicts islet transplantation outcome in human type 1 diabetes. Diabetes 62, 1656–1664 (2013).

14. Ryan, E. A. et al. Beta-score: an assessment of beta-cell function after islet transplantation. Diabetes Care 28, 343–347 (2005).

15. Cantarovich, D. et al. Posttransplant donor-specific anti-HLA antibodies negatively impact pancreas transplantation outcome. Am. J. Transplant. 11, 2737–2746 (2011).

16. Mittal, S., Page, S. L., Friend, P. J., Sharples, E. J. & Fuggle, S. V. De novo donor- specific HLA antibodies: biomarkers of pancreas transplant failure. Am. J. Transplant. 14, 1664–1671 (2014).
17. Lefaucheur, C. et al. IgG Donor-Specific Anti-Human HLA Antibody Subclasses and Kidney Allograft Antibody-Mediated Injury. J. Am. Soc. Nephrol. JASN 27, 293–304 (2016).
18. Sicard, A. et al. Detection of C3d-binding donor-specific anti-HLA antibodies at diagnosis of humoral rejection predicts renal graft loss. J. Am. Soc. Nephrol. JASN 26, 457–467 (2015).
19. Loupy, A. et al. Complement-binding anti-HLA antibodies and kidney-allograft survival. N. Engl. J. Med. 369, 1215–1226 (2013).
20. Citro, A., Cantarelli, E. & Piemonti, L. Anti-inflammatory strategies to enhance islet engraftment and survival. Curr. Diab. Rep. 13, 733–744 (2013).
21. Merani, S., Toso, C., Emamaullee, J. & Shapiro, A. M. J. Optimal implantation site for pancreatic islet transplantation. Br. J. Surg. 95, 1449–1461 (2008).
22. Hirohashi, T. et al. A novel pathway of chronic allograft rejection mediated by NK cells and alloantibody. Am. J. Transplant. 12, 313–321 (2012).
23. Jindra, P. T., Jin, Y.-P., Rozengurt, E. & Reed, E. F. HLA class I antibody-mediated endothelial cell proliferation via the mTOR pathway. J. Immunol. Baltim. Md 1950 180, 2357–2366 (2008).
24. Farkash, E. A. & Colvin, R. B. Diagnostic challenges in chronic antibody-mediated rejection. Nat. Rev. Nephrol. 8, 255–257 (2012).
25. Haas, M. et al. Banff 2013 meeting report: inclusion of c4d-negative antibody-mediated rejection and antibody-associated arterial lesions. Am. J. Transplant. Off. J. Am. Soc. Transplant. Am. Soc. Transpl. Surg. 14, 272–283 (2014).
26. Nyqvist, D. et al. Donor islet endothelial cells in pancreatic islet revascularization. Diabetes 60, 2571–2577 (2011).
27. Henriksnäs, J. et al. Markedly decreased blood perfusion of pancreatic islets transplanted intraportally into the liver: disruption of islet integrity necessary for islet revascularization. Diabetes 61, 665–673 (2012).
28.Vajkoczy, P. et al. Histogenesis and ultrastructure of pancreatic islet graft microvasculature. Evidence for graft revascularization by endothelial cells of host origin. Am. J. Pathol. 146, 1397–1405 (1995).
29. Brissova, M. et al. Intraislet endothelial cells contribute to revascularization of transplanted pancreatic islets. Diabetes 53, 1318–1325 (2004).
30. Linn, T. et al. Angiogenic capacity of endothelial cells in islets of Langerhans. FASEB J. 17, 881–883 (2003).

31.Fujimoto, C., Nakagawa, Y., Ohara, K. & Takahashi, H. Polyriboinosinic polyribocytidylic acid [poly(I:C)]/TLR3 signaling allows class I processing of exogenous protein and induction of HIV-specific CD8+ cytotoxic T lymphocytes. Int. Immunol. 16, 55–63 (2004).

32. Mikelis, C. M. et al. RhoA and ROCK mediate histamine-induced vascular leakage and anaphylactic shock. Nat. Commun. 6, 6725 (2015).

33. Bosco, D. et al. Unique arrangement of alpha- and beta-cells in human islets of Langerhans. Diabetes 59, 1202–1210 (2010).

34. Jooste, S. V., Colvin, R. B., Soper, W. D. & Winn, H. J. The vascular bed as the primary target in the destruction of skin grafts by antiserum. I. Resistance of freshly placed xenografts of skin to antiserum. J. Exp. Med. 154, 1319–1331 (1981).

35. Okitsu, T., Bartlett, S. T., Hadley, G. A., Drachenberg, C. B. & Farney, A. C. Recurrent autoimmunity accelerates destruction of minor and major histoincompatible islet grafts in nonobese diabetic (NOD) mice. Am. J. Transplant. Off. J. Am. Soc. Transplant. Am. Soc. Transpl. Surg. 1, 138–145 (2001).

36. Halloran, P. F. et al. Disappearance of T Cell-Mediated Rejection Despite Continued Antibody-Mediated Rejection in Late Kidney Transplant Recipients. J. Am. Soc. Nephrol. JASN 26, 1711–1720 (2015).

37. Huurman, V. a. L. et al. Immune responses against islet allografts during tapering of immunosuppression--a pilot study in 5 subjects. Clin. Exp. Immunol. 169, 190–198 (2012).

38. Benda, B., Karlsson-Parra, A., Ridderstad, A. & Korsgren, O. Xenograft rejection of porcine islet-like cell clusters in immunoglobulin- or Fc-receptor gamma-deficient mice. Transplantation 62, 1207–1211 (1996).

39. Van Kampen, C. A. et al. Alloreactivity against repeated HLA mismatches of sequential islet grafts transplanted in non-uremic type 1 diabetes patients. Transplantation 80, 118– 126 (2005).

40. Heidt, S. et al. A NOVel ELISPOT assay to quantify HLA-specific B cells in HLA- immunized individuals. Am. J. Transplant. Off. J. Am. Soc. Transplant. Am. Soc. Transpl. Surg. 12, 1469–1478 (2012).

41. Breman, E. et al. HLA monomers as a tool to monitor indirect allorecognition. Transplantation 97, 1119–1127 (2014).

42. Gebel, H. M. & Bray, R. A. HLA antibody detection with solid phase assays: great expectations or expectations too great? Am. J. Transplant. Off. J. Am. Soc. Transplant. Am. Soc. Transpl. Surg. 14, 1964–1975 (2014).

43. Roep, B. O. Insulitis Revisited. Diabetes 65, 545–547 (2016).

44. Kessler, L. et al. Evidence for humoral rejection of a pancreatic islet graft and rescue with rituximab and IV immunoglobulin therapy. Am. J. Transplant. 9, 1961–1966 (2009).

45. Sautenet, B. et al. One-year Results of the Effects of Rituximab on Acute Antibody- Mediated Rejection in Renal Transplantation: RITUX ERAH, a Multicenter Double-blind Randomized Placebo-controlled Trial. Transplantation 100, 391–399 (2016).
46. Thaunat, O., Morelon, E. & Defrance, T. Am'B'valent: anti-CD20 antibodies unravel the dual role of B cells in immunopathogenesis. Blood 116, 515–521 (2010).
47. Herold, K. C. et al. Anti-CD3 monoclonal antibody in new-onset type 1 diabetes mellitus. N. Engl. J. Med. 346, 1692–1698 (2002).
48. Keymeulen, B. et al. Insulin needs after CD3-antibody therapy in new-onset type 1 diabetes. N. Engl. J. Med. 352, 2598–2608 (2005).
49. You, S. et al. Induction of allograft tolerance by monoclonal CD3 antibodies: a matter of timing. Am. J. Transplant. Off. J. Am. Soc. Transplant. Am. Soc. Transpl. Surg. 12, 2909– 2919 (2012).
50. Penaranda, C., Tang, Q. & Bluestone, J. A. Anti-CD3 therapy promotes tolerance by selectively depleting pathogenic cells while preserving regulatory T cells. J. Immunol. Baltim. Md 1950 187, 2015–2022 (2011).
51. Colvin, R. B. & Smith, R. N. Antibody-mediated organ-allograft rejection. Nat. Rev. Immunol. 5, 807–817 (2005).
52. Wardemann, H. et al. Predominant autoantibody production by early human B cell precursors. Science 301, 1374–1377 (2003).
53. Kratz, A., Campos-Neto, A., Hanson, M. S. & Ruddle, N. H. Chronic inflammation caused by lymphotoxin is lymphoid neogenesis. J. Exp. Med. 183, 1461–1472 (1996).
54. Thaunat, O. et al. Lymphoid neogenesis in chronic rejection: evidence for a local humoral alloimmune response. Proc. Natl. Acad. Sci. U. S. A. 102, 14723–14728 (2005).
55. Thaunat, O. et al. Chronic rejection triggers the development of an aggressive intragraft immune response through recapitulation of lymphoid organogenesis. J. Immunol. 185, 717–728 (2010).
56. Thaunat, O. et al. A stepwise breakdown of B-cell tolerance occurs within renal allografts during chronic rejection. Kidney Int. 81, 207–219 (2012).
57. Thaunat, O. et al. Immune responses elicited in tertiary lymphoid tissues display distinctive features. PloS One 5, e11398 (2010).
58. Iijima, N. & Iwasaki, A. Access of protective antiviral antibody to neuronal tissues requires CD4 T-cell help. Nature 533, 552–556 (2016).
59. Chen, Z. H. A technique of cervical heterotopic heart transplantation in mice. Transplantation 52, 1099–1101 (1991).

60. Efrat, S., Fusco-DeMane, D., Lemberg, H., al Emran, O. & Wang, X. Conditional transformation of a pancreatic beta-cell line derived from transgenic mice expressing a tetracycline-regulated oncogene. Proc. Natl. Acad. Sci. U. S. A. 92, 3576–3580 (1995).
61. Bruneval, P. et al. Mesangial expansion associated with glomerular endothelial cell activation and macrophage recruitment is developing in hyperlipidaemic apoE null mice. Nephrol. Dial. Transplant. Off. Publ. Eur. Dial. Transpl. Assoc. - Eur. Ren. Assoc. 17, 2099–2107 (2002).
62. Duong Van Huyen, J. P. et al. GDF15 triggers homeostatic proliferation of acid-secreting collecting duct cells. J. Am. Soc. Nephrol. JASN 19, 1965–1974 (2008).
63. Altman, N. & Krzywinski, M. Simple linear regression. Nat. Methods 12, 999–1000 (2015).